DISS. ETH Nr. 20707

Supersymmetric Higgs Self-Couplings: Two-Loop Corrections

Abhandlung
zur Erlangung des Titels

Doktor der Wissenschaften

der

ETH Zürich

vorgelegt von

Mathias Brucherseifer

MSc ETH Physik, ETH Zürich

geboren am 13.03.1985

von Deutschland

Angenommen auf Antrag von

Prof. Dr. Charalampos Anastasiou, Referent

PD Dr. Michael Spira, Korreferent

2012

Zusammenfassung

In dieser Arbeit präsentieren wir die Berechnung von Zwei-Schleifen-Korrekturen $\mathcal{O}(\alpha_s\alpha_t + \alpha_t^2)$ zu neutralen Higgs Selbstkopplungen in der reellen minimal-supersymmetrischen Erweiterung des Standard Modells. Hierbei kennzeichnet α_s die starke Kopplung und α_t ist proportional zur Top-Yukawa Kopplung im Quadrat. Diese Berechnung benutzt den Zugang des effektiven Potentials, welcher äquivalent ist zur kompletten diagrammatischen Rechnung im Limes verschwindender äusserer Viererimpulse. Die Renormierung der Higgs Selbstkopplungen wird in zwei verschiedenen Schemas durchgeführt, nämlich im $\overline{\text{DR}}$ und im On-Shell Schema. Die numerische Analyse zeigt, dass die Korrekturen im $\overline{\text{DR}}$ Schema, ausgewertet an einer zentralen Skala von $M_{\text{SUSY}}/2$, klein sind. Die Zwei-Schleifen-Korrekturen reduzieren die Grösse der theoretischen Unsicherheiten in den meisten Regionen des Parameterraums auf unter $\mathcal{O}(5\%)$. Die strahlungskorrigierten effektiven Kopplungen können benutzt werden, um den Higgs Sektor und den Mechanismus der Elektroschwachen Symmetriebrechung an heutigen und zukünftigen Teilchenbeschleunigerexperimenten zu testen.

Abstract

We present a calculation of the two-loop $\mathcal{O}(\alpha_s\alpha_t+\alpha_t^2)$ radiative corrections to neutral Higgs self-couplings in the real minimal supersymmetric extension of the standard model. The strong coupling is denoted by α_s and α_t is proportional to the top-Yukawa coupling squared. This calculation is performed with the effective potential method, providing results that are equivalent to the full diagrammatic calculation in the limit of vanishing external momenta. We renormalize the Higgs self-couplings in the $\overline{\text{DR}}$ and in the on-shell scheme. The numerical results for the self-couplings show that the corrections are small in the $\overline{\text{DR}}$ scheme at a central renormalization scale of $M_{\text{SUSY}}/2$. The two-loop corrections reduce the size of the theoretical uncertainties in most regions of parameter space below $\mathcal{O}(5\%)$. These loop-corrected effective couplings can be used at present and future colliders to test the Higgs sector and the mechanism of electroweak symmetry breaking in the minimal supersymmetric standard model.

Contents

Chapter 1

Introduction

On the fourth of July 2012 the two major experiments at the *Large Hadron Collider (LHC)*, Atlas and CMS, announced the discovery of a new bosonic particle with a mass of $125-126$ GeV [1]. All properties of this resonance, measured so far, are compatible with a *Standard Model (SM)* Higgs boson. The Higgs boson plays a crucial role in the SM, as well as in various of its extensions. First of all it is the only particle in the SM that has not yet been experimentally confirmed and the Higgs mass is the only undetermined parameter left in the SM. Moreover, if it has spin 0, it would be the only fundamental scalar in the theory. In the SM the Higgs boson induces the mechanism of *ElectroWeak Symmetry Breaking (EWSB)* that gives mass to the all other SM particles. Besides, it is crucial for the theoretical consistency of the SM. It is fair to say that the experimental verification of the Higgs particle as the origin of EWSB would be one of the biggest experimental and theoretical achievements in high energy physics.
To ascertain, whether the new found resonance at the LHC is compatible with the properties of the SM Higgs boson, one has to measure its couplings to all other particles in the theory. The couplings of the Higgs boson to the other SM particles have to be proportional to their masses. However there are also self-couplings of the Higgs boson following from the Higgs potential, which encode all the relevant information about the mechanism of EWSB. Measuring Higgs self-couplings is therefore essential in order to elucidate the mechanism that gives mass to all other particles in the SM.
EWSB is introduced ad-hoc in the SM, there is no explanation what its origin is. The *Minimal Supersymmetric extension of the SM (MSSM)* provides an elegant explanation of EWSB, inducing it naturally by radiative corrections. In the MSSM the Higgs sector consists of five physical bosons and the self-couplings of these determine the MSSM Higgs potential responsible for EWSB. In order to ascertain whether the measured data is compatible with the self-couplings of a SM Higgs boson or the MSSM Higgs bosons, precise theory predictions are necessary. In this work we will show how two-loop radiative corrections to effective Higgs self-couplings in the real MSSM are calculated and what the numerical size of these corrections is.
This thesis is organized as follows. In chapter 1 we first briefly discuss the SM and its problems. We then give an overview of the idea of supersymmetry and its formulation before we turn to the MSSM. We will discuss the basic structure of the MSSM, focusing on the topics relevant for this work, especially on the tree-level Higgs sector. This serves as a preparation for the second chapter, where we explain how two-loop corrections are implemented.
This calculation is performed in the framework of the effective potential, which will be introduced in the beginning of chapter 2. The following subsections are devoted to the technical details in the determination of the leading two-loop contributions to the effective potential. We will first review the calculation of the two-loop corrections to the Higgs masses before we discuss the self-couplings, since the result of the former are needed to evaluate the latter. In the last part of chapter 2 we will explain in detail how the Higgs masses and self-couplings are renormalized in order to get finite physical results.

The third chapter deals with the numerical evaluation of the Higgs masses and self-couplings. First we explain how we determine consistent numerical input parameters in two different renormalization schemes. Then we review the numerical results for the Higgs masses and investigate how different choices of parameters alter the result. Last but not least we present numerical results for all trilinear and two quartic Higgs self-couplings in two benchmark scenarios including the theoretical uncertainties.
In chapter 4 we summarize and give an outlook on possible extensions of this work. Finally in the appendix we present all analytic formulae necessary to reproduce our results. Moreover the calculation of the one-loop effective potential is explained in great detail and the calculations of the relevant two-loop potentials are outlined. The bibliography section in the end contains references to the relevant literature.

1.1 The Standard Model of Particle Physics

The Standard Model [2] of particle physics describes the electromagnetic, weak and the strong interactions of all known subatomic particles. The SM has been developed during the mid to late 20th century and since then its predictions have been confirmed experimentally with tremendous success. Theoretically the interactions of subatomic particles are described by a *Quantum Field Theory (QFT)* with local gauge symmetries. The SM is a non-abelian $U(1)_Y \times SU(2)_L \times SU(3)_C$ gauge theory, which is spontaneously broken to a $U(1)_{em} \times SU(3)_C$ gauge theory in order to give mass to the electroweak gauge bosons. The particle content can be classified into fermionic matter particles, namely leptons and quarks and force carriers, the gauge bosons. Moreover for spontaneous symmetry breaking a scalar particle, often referred to as the Higgs boson, is needed.
The interactions of the quarks and leptons are fixed by their representations in the gauge groups. Quarks have color charge and they are therefore affected by the strong interaction, whereas leptons are $SU(3)_C$ singlets. All fermions are charged under $SU(2)_L$ and the $U(1)_Y$ gauge symmetries. The former $SU(2)_L$ acts only on left-handed particles, violating the chiral symmetry and thus prohibiting mass-terms for the fermions. All SM fermions exist in three versions, called families, which can only be distinguished by their masses. The fact that the fermions do have masses already tells us that the $SU(2)_L$ symmetry has to be broken.
Gauge bosons mediate the forces dictated by the symmetries. Their number and properties are completely fixed by the gauge groups. In particular the preserved symmetries demand that all gauge bosons have to be massless. There are eight massless gauge bosons mediating the strong force, called *gluons* g, three massive weak gauge bosons, the $W^{\pm}$- and Z-boson and one electromagnetic gauge boson, the *photon* γ.

1.1.1 Electroweak Symmetry Breaking in the SM

In order to generate mass for the $W^{\pm}$- and Z-bosons, we need to break the electroweak symmetry. In the SM this is achieved by introducing one complex scalar doublet, whose neutral component acquires a real *Vacuum Expectation Value (VEV)* and thus spontaneously breaks[1] the electroweak symmetry $SU(2)_L \times U(1)_Y \to U(1)_{em}$. The gauge theory corresponding to the remaining $U(1)_{em}$-symmetry is called *Quantum Electro Dynamics (QED)*, mediated by a massless photon. *Spontaneous symmetry breaking (SSB)* is always connected to the appearance of massless Goldstone bosons, which become the longitudinal Degrees Of Freedom (DOF) of the massive $W^{\pm}$- and Z-bosons. After EWSB only one DOF of the complex scalar doublet remains, corresponding to a real scalar physical particle, the Higgs boson. This mechanism is usually called *Higgs mechanism*, although many other people were also involved in this development [4–6].

[1] The term spontaneous symmetry breaking is actually misleading. All fields in the theory remain symmetric under gauge transformations. After fixing the gauge (usually the SM is formulated in the *unitary* gauge) the vacuum is not invariant under the symmetry and therefore expanding around the ground state *hides* the symmetry. The term *hidden symmetry* is sometimes used and is more appropriate [3].

The VEV of the Higgs bosons can also induce mass to the SM fermions through Yukawa couplings. Moreover the Higgs particle restores the unitarity of the theory. It can even be proven under mild technical assumptions that the only way to maintain perturbative unitarity in a non-abelian gauge theory with massive gauge bosons up to arbitrary high energies is by introducing a scalar sector[2] in the theory, with couplings exactly fixed as in the Higgs mechanism [7]. The Higgs sector is therefore essential for the theoretical consistence of the SM.

1.1.2 Problems of the SM

The SM is a consistent theory describing most of the subatomic phenomena, without any of its predictions ever being disproved[3]. One could therefore be tempted to call it a "theory of nearly everything". Still there a number of phenomena that are not described by the SM. Moreover there are some theoretical caveats.

- **Gravity:** The only fundamental force that is not included in the SM is gravity. All quantum field theoretical descriptions of gravity so far are not renormalizable and thus not consistent.
- **Dark energy:** The quantum vacuum of the SM is not consistent with the expansion of the universe usually believed to be caused by dark energy.
- **Dark matter:** Various phenomena in the universe are described by *Dark Matter (DM)*, which is matter interacting only very weakly with ordinary matter via the SM forces. However, it is massive and therefore its gravitational effects alter the dynamics of the universe. The SM particles cannot account for all the DM in the universe[4].
- **Neutrino masses and neutrino oscillations:** In the SM neutrinos are massless and therefore they cannot describe neutrino oscillations.
- **Strong CP problem:** There are natural terms in the Quantum Chromo Dynamical (QCD) Lagrangian that are able to break the *Charge conjugation and Parity (CP)*-symmetry. These terms, however, have to be extremely small to match the experimental data. Because there is no symmetry in the SM protecting these terms, unnatural fine-tuning is needed.
- **Unification:** There are still 19 parameters in the SM. Reduction of the number of parameters and gauge couplings is theoretically very appealing.
- **Origin of EWSB:** EWSB is introduced ad-hoc in the SM. A complete theory should have an explanation about the origin of EWSB.
- **Three families:** The SM cannot explain why there are three families of quarks and leptons. Moreover it does not explain where the hierarchy between the Yukawa couplings originates from.
- **Hierarchy problem:** The large hierarchy between the electroweak scale and the Planck scale results in huge radiative corrections for scalar particles in the SM. Absorbing these corrections into renormalization constants requires unnatural fine tuning.

In order to solve all or some of these problems the SM has to be extended. The supersymmetric SM is one particular extension among many others. However, it is the most studied and it is able to solve a lot of these problems. We will first take a closer look at the hierarchy problem and explain the idea of how to solve it by supersymmetry.

[2] The number of complex doublets is not fixed, however, the minimality principle of the SM sets this number to one.

[3] The only direct observation contradicting the SM are neutrino oscillations, which require neutrinos to have mass. By adding sterile right-handed neutrinos to the SM, neutrinos acquire a mass. This introduces 8 new parameters to the SM, but the theory is still consistent.

[4] Massive neutrinos could account for some of the DM in the universe. However, light neutrinos cannot be responsible for the structure formation in the early universe.

1.1.3 The Hierarchy Problem

The hierarchy problem of the SM arises when we want to embed the SM in some larger theory, e.g. a *Grand Unified Theory (GUT)* or some theory of gravity at the Planck scale. In this sense it is not a problem of the SM alone, but it arises at the moment where we introduce a cutoff in energy Λ_{UV} above which new phenomena occur. Scalar particles are highly sensitive to the Ultra-Violet (UV) physics scale Λ_{UV}. When we calculate loop-corrections to the Higgs boson mass, for example from a fermion, coupling to the Higgs boson via $-\lambda_f H \bar{f} f$ (see Figure 1.1), we obtain a quadratic divergence in the cutoff scale Λ_{UV}.

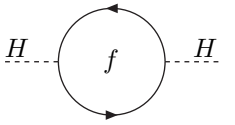

$$\Rightarrow \Delta m_H^2 = -\frac{|\lambda_f|^2}{8\pi^2}\left[\Lambda_{\mathrm{UV}}^2 - 3m_f^2 \log\frac{\Lambda_{\mathrm{UV}}^2+m_f^2}{m_f^2} + \cdots\right]$$

Figure 1.1: Correction to the Higgs boson mass due to a fermion f.

This divergence has to be absorbed in a counter term $(m_H^{phys})^2 = (m_H^0)^2 + \Delta m_H^2 - \delta m_H^2$. To obtain a Higgs mass at around the electroweak scale $\Lambda_{\mathrm{EW}} \sim \mathcal{O}(100\mathrm{GeV})$ we have to introduce a huge fine-tuning of about 28 digits for a cutoff scale $\Lambda_{\mathrm{UV}} \sim \mathcal{O}(10^{16}\mathrm{GeV})$. Note that fermions and massless[5] gauge bosons are not sensitive to UV physics, because the former are protected by the chiral symmetry and the latter are protected by the gauge symmetry.

Solution: Suppose there are two additional scalar degrees of freedom ϕ_L and ϕ_R in the SM coupling to the Higgs sector via

$$\mathcal{L}_{Scalar} = -\frac{\lambda}{2}H^2(|\phi_L|^2 + |\phi_R|^2) - H(\mu_L|\phi_L|^2 + \mu_R|\phi_R|^2) - m_L^2|\phi_L|^2 - m_R^2|\phi_R|^2. \tag{1.1.1}$$

There are two additional diagrams contributing to the Higgs self-energy The last diagram in Figure 1.2

Figure 1.2: Correction to the Higgs boson mass due to a fermion f and two scalars ϕ_R and ϕ_L.

yields a quadratic divergence in Λ_{UV}. However, with the opposite sign compared to the fermions. The contribution to the Higgs mass from the scalar diagrams is

$$\Delta m_H^2|_{Scalar} = \frac{1}{16\pi^2}\left[2\lambda\Lambda_{\mathrm{UV}}^2 - \left(\lambda m_L^2 + \mu_L^2\right)\log\frac{\Lambda_{\mathrm{UV}}^2+m_L^2}{m_L^2} - \left(\lambda m_R^2 + \mu_R^2\right)\log\frac{\Lambda_{\mathrm{UV}}^2+m_R^2}{m_R^2}\right] \tag{1.1.2}$$

If we choose

$$\lambda = |\lambda_f|^2 \tag{1.1.3}$$

we cancel the quadratic divergence in Λ_{UV}. Moreover if we also impose

$$m_f = m_L = m_R, \qquad \mu_L^2 = \mu_R^2 = 2\lambda m_f^2 \tag{1.1.4}$$

[5]The would-be Goldstone bosons, i.e. the longitudinal DOF of the massive gauge bosons are also affected by quadratic divergences.

we also cancel the logarithms arising in the Higgs mass corrections. Unbroken Supersymmetry exactly fulfills both relations Eqs. (1.1.3, 1.1.4) and is therefore much more stable w.r.t. radiative corrections.

1.2 Supersymmetry

SUperSYmmetry (SUSY) has been developed in the beginning of the 1970's mainly for mathematical and aesthetic reasons [9, 10]. In this section we will first describe the historical development of SUSY and later apply SUSY-theories to particle physics phenomenology.
SUSY links particles of different spin, i.e. it transforms bosons into fermions and vice versa. The generator Q of SUSY transformations must be an anticommuting spinor

$$Q|Boson\rangle = |Fermion\rangle, \qquad Q|Fermion\rangle = |Boson\rangle. \tag{1.2.1}$$

Since this generator is fermionic, it is obvious that SUSY is a space-time symmetry. Putting such a symmetry into a QFT framework is quite difficult because it has to be consistent with Poincaré and Lorentz invariance, where the latter contains basically the definition of spin. Moreover the *Coleman-Mandula theorem* [8] served as a no-go theorem for symmetries beyond the Poincaré and the internal gauge symmetries. This theorem however, assumes that the symmetry generators obey a Lie Algebra. The SUSY generators Q, however, are fermionic, i.e. they obey anticommutation relations. In the early 1970's the idea for SUSY was first brought up in string theories [9], which back then were an attempt to describe the strong interaction. Later in the 1970's $N = 1$ SUSY was developed [10] without drawing much interest at first. Only in 1973 when the first SUSY field theories in four dimensions were constructed [11] the subject attracted a lot of attention. Haag, Lopuszanski and Sohnius one year later showed that SUSY is the only possible extension of space-time symmetries of particle interactions and the SUSY generators Q (and their hermitian conjugate $\bar{Q}$) have to satisfy the following commutation and anticommutation relations of a *graded Lie algebra* [12]

$$\{Q, \bar{Q}\} = P^\mu \sigma_\mu, \qquad \{Q, Q\} = \{\bar{Q}, \bar{Q}\} = 0, \qquad [P^\mu, Q] = [P^\mu, \bar{Q}] = 0 \tag{1.2.2}$$

where P^μ is the four-momentum generator of space-time translations. Subsequent work stated that SUSY theories have a better high energy behavior, exploiting the cancellation of fermionic and bosonic loops. In particular the non-renormalization theorems [13] were theoretically very appealing.
We will restrict our further analysis here to $N = 1$ SUSY, where N is the number of SUSY generators, i.e. number of distinct $(Q, \bar{Q})$-pairs. This means that for a renormalizable gauge theory (all fields have spin ≤ 1) there are only two possible kinds of supermultiplets[6]: A *chiral* supermultiplet consists of a Weyl fermion and a complex scalar, whereas a *vector* supermultiplet consists of a spin-1 vector boson and a spin-$\frac{1}{2}$ Weyl fermion. From Eq. (1.2.2) it also follows that all states in a supermultiplet must have the same mass. Moreover the number of fermionic and bosonic DOF in a supersymmetric theory must be equal.

1.2.1 Superfield and Superspace Formalism

To introduce SUSY in a formal and mathematical way, the notion of superfields and superspace is a very elegant tool. In order to implement SUSY in a 4-dimensional field theory, we introduce the supercoordinates $(x^\mu, \theta, \bar{\theta})$, which span the superspace. Here x^μ is just the ordinary four component space-time vector and θ, $\bar{\theta}$ are spinorial coordinates spanning the fermionic subspace of superspace. They obey $\theta\theta = -2\theta_1\theta_2$ and $\bar{\theta}\bar{\theta} = 2\bar{\theta}^{\dot{1}}\bar{\theta}^{\dot{2}}$. An infinitesimal transformation on the superspace can be given in terms of two component anticommuting spinor parameters ε and $\bar{\varepsilon}$

$$z \equiv (x^\mu, \theta, \bar{\theta}) \to (x^\mu - i\theta\sigma^\mu\bar{\varepsilon} + i\varepsilon\sigma^\mu\bar{\theta}, \theta + \varepsilon, \bar{\theta} + \bar{\varepsilon}). \tag{1.2.3}$$

[6] A supermultiplet consists of the fermionic and bosonic superpartners connected by the SUSY transformations Eq. (1.2.1).

Any function on the superspace can be easily expanded in θ and $\bar{\theta}$, because any spinorial coordinate with power higher than two vanishes, i.e. $\theta^n = 0$ and $\bar{\theta}^n = 0$, for $n > 2$. The most general scalar superfield with spin ≤ 1 on superspace is

$$\mathcal{F}(z) = f(x) + \theta\xi(x) + \bar{\theta}\bar{\chi}(x) + \theta\theta M(x) + \bar{\theta}\bar{\theta}N(x) + \theta\sigma^\mu\bar{\theta}A_\mu(x) + \theta\theta\bar{\theta}\bar{\lambda}(x) + \bar{\theta}\bar{\theta}\theta\zeta(x) + \theta\theta\bar{\theta}\bar{\theta}D(x), \quad (1.2.4)$$

where $f(x), F(x), N(x), D(x)$ denote scalar fields, $\xi(x), \zeta(x)$ are left-handed Weyl spinor fields, $\bar{\chi}(x), \bar{\lambda}(x)$ right-handed Weyl spinor fields and $A_\mu(x)$ is a complex vector field. This means that $\mathcal{F}$ has 16 bosonic and 16 fermionic DOF. By applying a superspace transformation Eq. (1.2.3) to the expanded superfield $\mathcal{F}(z)$ we see that the D-component (the coefficient of the $\theta\theta\bar{\theta}\bar{\theta}$-term) of the superfield transforms by a four divergence, which will be discarded as any surface term. Any D-term in a Lagrangian is therefore supersymmetric. Linear combinations and products of superfields are again superfields, i.e. superfields form a linear representations of the SUSY algebra.
This representation of the SUSY algebra is reducible. The field content of the irreducible representations corresponds exactly to the supermultiplets introduced in section 1.2. It is convenient to introduce the complex coordinate $y = x - i\theta\sigma^\mu\bar{\theta}$. The *chiral superfield* (also called left chiral) Φ has a simple form expressed in this complex coordinate

$$\Phi(y, \theta) = \phi(y) + \theta\xi(y) + \theta\theta F(y), \quad (1.2.5)$$

where ϕ is a complex scalar, ξ is a left-handed Weyl spinor and F denotes an auxiliary complex scalar field. The *anti-chiral superfield* (also called right chiral) $\Phi^\dagger$, expressed in the hermitian conjugate of the complex coordinate, reads

$$\Phi^\dagger(\bar{y}, \bar{\theta}) = \phi^\star(\bar{y}) + \bar{\theta}\bar{\xi}(\bar{y}) + \bar{\theta}\bar{\theta}F^\star(\bar{y}), \quad (1.2.6)$$

where $\phi^\star$ is a complex scalar, $\bar{\xi}$ is a right-handed Weyl spinor and $F^\star$ is an auxiliary complex scalar field. Note that the F-component of a chiral superfield transforms into itself plus a space-time derivative. Hence, any F-term in the Lagrangian density leads to a SUSY-invariant action when surface terms can be discarded.
The *vector superfield* $V(x^\mu, \theta, \bar{\theta})$ is defined to be hermitian

$$V^\dagger = V. \quad (1.2.7)$$

This means that $\Phi\Phi^\dagger$ and $\Phi + \Phi^\dagger$ are vector superfields. We can thus define a supergauge transformation by

$$V \to V + i\Lambda - i\Lambda^\dagger, \quad (1.2.8)$$

where Λ and $\Lambda^\dagger$ are chiral and anti-chiral superfields respectively. In the *Wess-Zumino* gauge, the vector superfield has the following form

$$V_{WZ} = \theta\sigma^\mu\bar{\theta}A_\mu(x) + \theta\theta\bar{\theta}\bar{\lambda}(x) + \bar{\theta}\bar{\theta}\theta\zeta(x) + \theta\theta\bar{\theta}\bar{\theta}D(x), \quad (1.2.9)$$

where A_μ is a complex vector, λ and $\bar{\lambda}$ are left- and right-handed Weyl spinors and D is an auxiliary field, without a kinetic term. It can therefore be eliminated using its equation of motion.

1.2.2 Constructing Supersymmetric Lagrangians

To construct supersymmetric Lagrangians, we use the fact that the D-term always transforms by a four divergence. Moreover the F-term is supersymmetric for any combination of chiral fields only. Renormalizability demands that the mass dimension of the operators in the Lagrangian is not more than four.

Chiral Superfield Lagrangian: A general renormalizable supersymmetric Lorentz invariant Lagrangian density, involving only polynomials of chiral superfields, is therefore

$$\mathcal{L}_{\text{chiral}} = \left[\Phi_i \Phi_i^\dagger\right]_D + \left[\mathcal{W}(\Phi_i) + h.c.\right]_F , \tag{1.2.10}$$

$$\mathcal{W}(\Phi_i) = h_i \Phi_i + \frac{1}{2} m_{ij} \Phi_i \Phi_j + \frac{1}{3!} f_{ijk} \Phi_i \Phi_j \Phi_k, \tag{1.2.11}$$

where we sum over the repeated indices i, j, k and the subscripts D and F mean that we single out the corresponding terms, which survive after integrating out the Grassmann variables. The superpotential is then replaced by the same function of the scalar field ϕ only, i.e. $\mathcal{W}(\Phi_i) \to \mathcal{W}(\phi_i)$. The first term in the Lagrangian Eq. (1.2.10) is a vector superfield. The second term is a polynomial in the chiral fields consisting of the *superpotential* $\mathcal{W}$, defined in Eq. (1.2.11) plus its hermitian conjugate. Note that for SUSY invariance the superpotential has to be analytic (or holomorphic). We can now express the Lagrangian in terms of component fields. Using the equations of motion for the auxiliary fields F and $F^\star$

$$F_i = -\frac{\partial \mathcal{W}^\dagger}{\partial \phi_i^\dagger} = -h_i^\star - m_{ij}^\star \phi_j^\star - \frac{1}{2} f_{ijk}^\star \phi_j^\star \phi_k^\star, \qquad F_i^\star = -\frac{\partial \mathcal{W}}{\partial \phi_i} = -h_i - m_{ij} \phi_j - \frac{1}{2} f_{ijk} \phi_j \phi_k, \tag{1.2.12}$$

we arrive at

$$\mathcal{L}_{\text{chiral}} = \mathcal{L}_{\text{kin}} + \mathcal{L}_{\text{Yukawa}} - V(\phi_i, \phi_j^\star), \tag{1.2.13}$$

with

$$\mathcal{L}_{\text{kin}} = \frac{i}{2}\left[\xi_i \sigma^\mu (\partial_\mu \bar{\xi}_i) - (\partial_\mu \xi_i)\sigma^\mu \bar{\xi}_i\right] + \partial_\mu \phi_i \partial^\mu \phi_i^\star, \tag{1.2.14}$$

$$\mathcal{L}_{\text{Yukawa}} = -\frac{1}{2}\left[\xi_i \xi_j \frac{\partial^2 \mathcal{W}}{\partial \Phi_i \Phi_j} + h.c.\right] = -\frac{1}{2}\left[\xi_i \xi_j (m_{ij} + f_{ijk}\phi_k) + h.c.\right], \tag{1.2.15}$$

$$V(\phi_i, \phi_j^\star) = \frac{\partial \mathcal{W}^\dagger}{\partial \Phi_i^\dagger}\frac{\partial \mathcal{W}}{\partial \Phi_i} = F_i^\star F_i. \tag{1.2.16}$$

Abelian $U(1)$ gauge interactions: To couple these chiral superfields Φ to an abelian gauge vector superfield V, we extend the first term in Eq. (1.2.10) to $\left[\Phi_i^\dagger e^{2g t_i V}\Phi_i + \eta V\right]_D$, where g is the gauge coupling and t_i is a real number, namely the $U(1)$ charge of Φ_i. Note that the D-component of the vector superfield V is gauge invariant as well, so we can add it, multiplied by a real constant η. In terms of component fields this part of the Lagrangian can be expressed as

$$\mathcal{L}_{\text{kin,chiral}} = i\xi_i \sigma^\mu \Delta_{i\mu}^\dagger \bar{\xi}_i + |\Delta_{i\mu}\phi_i|^2 - \sqrt{2} g t_i (\bar{\lambda}\xi_i \phi_i + h.c.), \tag{1.2.17}$$

where $\Delta_{i\mu} = \partial_\mu + i g t_i A_\mu$ is the gauge covariant derivative. The first two terms in Eq. (1.2.17) are ordinary kinetic terms for scalars and fermions in the chiral supermultiplet involving gauge interactions. The last term is a Yukawa interaction of a fermion, a sfermion and a gaugino. It is required by the supersymmetrization of the gauge coupling. Moreover we have a kinetic Lagrangian for the gauge vector superfield, which can be expressed in terms of component fields as

$$\mathcal{L}_{\text{kin,gauge,abelian}} = \frac{1}{2}D^2 - \frac{1}{4}F_{\mu\nu}F^{\mu\nu} + \frac{i}{2}\left[\lambda\sigma^\mu(\partial_\mu\bar{\lambda}) - (\partial_\mu\lambda)\sigma^\mu\bar{\lambda}\right], \tag{1.2.18}$$

where $F_{\mu\nu} \equiv \partial_\nu A_\mu - \partial_\mu A_\nu$ is the usual field strength tensor. The auxiliary field D can be eliminated using its equations of motion $D = -g\phi_i^\star t_i \phi_i - \eta$. This means that the first term in Eq. (1.2.18) generates quartic scalar interactions proportional to the gauge coupling. Note that in QED we need two left chiral superfields with opposite charge to describe a Dirac fermion.

Non-abelian gauge interactions: We will only sketch how we can extend the above Lagrangian to non-abelian gauge groups, because explicit formulae contain an inflation of indices. The representation matrices of the gauge group in the fundamental representation T^a_{ij} enter in the first term in Eq. (1.2.10) changing it compared to the abelian case to $\left[\Phi_i^\dagger e^{V^a T^a_{ij}} \Phi_j\right]_D$, where we sum over the indices i, j. Moreover the non-abelian structure introduces self-interactions among the components of the vector superfield. This means that the gaugino field λ is also coupled to the gauge field A^μ via a Yukawa-term in the Lagrangian $i\lambda^a \sigma^\mu \Delta_\mu \bar{\lambda}^a$. The self-interactions among the gauge fields A^μ can be obtained by substituting the partial derivatives in the field strength tensor with covariant derivatives. This changes the kinetic term in the gauge Lagrangian, Eq. (1.2.18) to

$$\mathcal{L}_{\text{kin,gauge,non}-\text{abelin}} = \frac{1}{2}D^2 - \frac{1}{4}F_{\mu\nu,a}F^{\mu\nu,a} + \frac{i}{2}\left[\lambda^a \sigma^\mu \Delta_\mu \bar{\lambda^a} - (\Delta_\mu \lambda^a)\sigma^\mu \bar{\lambda^a}\right]. \tag{1.2.19}$$

1.3 The Minimal Supersymmetric Extension of the SM

To construct the MSSM [14] we incorporate the SM particles in the $N = 1$ supermultiplets. The chiral SM fermions have to be Weyl fermions in the chiral supermultiplet. Putting them into the vector multiplet would introduce vector boson partners for all SM fermions and therefore new gauge interactions. Every SM fermion gets a scalar partner. The superpartners of the SM fermions are named like the SM particles, with an "s" (for scalar) in front and they are denoted by a tilde (˜), e.g. for an electron e_R, e_L there is a *selectron*[7] $\tilde{e}_R, \tilde{e}_L$. SUSY demands that the scalar superpartners have exactly the same gauge quantum numbers as the SM fermions, i.e. they reside in the same representation of the gauge group.
The Higgs fields are scalars and they therefore have to be in a chiral supermultiplet. Their supersymmetric partners are spin-$\frac{1}{2}$ Weyl fermions called *Higgsinos*, denoted by $\tilde{H}$. All fermionic superpartners will be named by an appended *-ino*. In contrast to the SM we need two Higgs doublets for several reasons. First we want a theory free of anomalies [15]. A necessary condition for a theory to be free of anomalies is that the trace of the cubed hypercharge $Tr[Y^3]$ over all left-handed Weyl fermions in the theory has to vanish. Since the Higgs field in the SM has hypercharge $Y = \pm 1$ the superpartners of the Higgs doublet would introduce an anomaly. We therefore introduce two Higgs doublets, with $Y = +1$ and $Y = -1$. Moreover two Higgs doublets are needed to define an analytical superpotential in which up- and down-quarks acquire their masses from different Higgs doublets. The MSSM consists of the chiral superfields $\Phi = \{L_i, E_i^c, Q_i^c, U_i^c, D_i, \hat{H}_1, \hat{H}_2\}$, where $i = 1, 2, 3$ is the family index. Table 1.1 shows all chiral superfields in the MSSM, specifying their particle content and their representation in the gauge group. The family index $i = 1, 2, 3$ comprises the fields $u_{iL} = (u_L, c_L, t_L)$, $d_{iL} = (d_L, s_L, b_L)$, $u_{iL} = (e_L, \mu_L, \tau_L)$ and equivalently for the sfermions and $L \to R$.
The SM gauge bosons have to be put in a vector multiplet. This implies three kinds of vector superfields $V = \{V_B, \vec{V}_W, V_g^a\}$, where $a = 1, \cdots, 8$. In the SM we have one B-boson, three W-bosons and 8 gluons. Their fermionic partners are called gauginos, denoted by a tilde (˜), in particular one bino $\tilde{B}$, three winos $\vec{\tilde{W}}$ and eight gluinos $\tilde{g}^a$. The content of the vector multiplet is shown in Table 1.2. The SM Lagrangian conserves both baryon number and lepton number. This is not imposed but emerges as an accidental symmetry. To conserve lepton and baryon number also in the MSSM, we impose *R-parity* symmetry. R-parity is a multiplicative quantum number, being $+1$ for all SM particles and -1 for all supersymmetric partners. This additional symmetry forbids terms that violate lepton and baryon number in the superpotential. It has important phenomenological consequences:

- The lightest particle with R-parity -1, called the *Lightest Supersymmetric Particle (LSP)* is absolutely stable. If it is electrically and color neutral, it interacts only weakly with ordinary matter and is thus a dark matter candidate.

[7] Note that the L and R index for the scalars are a little misleading because scalar particles do not carry helicity. They denote that the scalar fields have the same hypercharge as their superpartners.

Superfield	$SU(3)_C$	$SU(2)_L$	$U(1)_Y$	Particle content
Q_i^c	3	2	$\frac{1}{3}$	$(u_{iL}, d_{iL}), \tilde{Q}_i \equiv (\tilde{u}_{iL}, \tilde{d}_{iL})$
U_i	$\bar{3}$	1	$-\frac{4}{3}$	$\bar{u}_{iR}, \tilde{u}_{iR}^\star$
D_i^c	$\bar{3}$	1	$\frac{2}{3}$	$\bar{d}_{iR}, \tilde{d}_{iR}^\star$
L_i	1	2	-1	$(e_{iL}, \nu_{iL}), \tilde{L}_i \equiv (\tilde{e}_{iL}, \tilde{\nu}_{iL})$
E_i^c	1	1	2	$\bar{e}_{iR}, \tilde{e}_{iR}^\star$
$\hat{H}_1$	1	2	-1	$(\tilde{H}_1^0, \tilde{H}_1^-), H_1 \equiv (H_1^0, H_1^-)$
$\hat{H}_2$	1	2	1	$(\tilde{H}_2^+, \tilde{H}_2^0), H_2 \equiv (H_2^+, H_2^0)$

Table 1.1: The representation of the chiral superfields in the gauge groups and their particle content. Parentheses contain an $SU(2)$ doublet. The superscript c denotes charge conjugation.

Superfield	$SU(3)_C$	$SU(2)_L$	$U(1)_Y$	Particle content
V_B	1	1	0	$B, \tilde{B}$
$\vec{V}_W$	1	3	0	$\vec{W}, \tilde{\vec{W}}$
V_g^a	8	1	0	$g^a, \tilde{g}^a$

Table 1.2: The representation of the vector superfields in the gauge groups and their particle content. The gluon index is $a = 1, \cdots, 8$.

- Each particle with R-parity -1, other than the LSP, must eventually decay into a state that contains an odd number of LSPs.
- In collider experiments, particles with R-parity -1 can only be produced in even numbers.

To arrive at the Lagrangian for the MSSM we need to derive a supersymmetric Lagrangian with a non-abelian $U(1)_Y \times SU(2)_L \times SU(3)_C$ gauge group and R-parity symmetry. The MSSM Lagrangian consists of a kinetic Lagrangian analogous to Eq. (1.2.17) for all fermionic and scalar component fields contained in the MSSM chiral supermultiplets $\Phi = \{L_i, E_i^c, Q_i, U_i^c, D_i^c, \tilde{H}_1, \tilde{H}_2\}$, a kinetic Lagrangian analogous to Eq. (1.2.19) for all gaugino and vector component fields contained in the MSSM vector supermultiplets $V = \{V_B, \vec{V}_W, V_g^a\}$ and a superpotential Lagrangian consisting of a Yukawa term analogous to Eq. (1.2.15) and a potential term analogous to Eq. (1.2.16). The superpotential of the MSSM is the most general renormalizable, gauge, R-parity and SUSY invariant superpotential we can write down. It reads

$$\mathcal{W}_{\text{MSSM}} = \varepsilon_{mn}\mu\hat{H}_1^m\hat{H}_2^n + \varepsilon_{mn}\left[h_L\hat{H}_1^m L^n E + h_D\hat{H}_1^m Q^n D + h_U\hat{H}_2^m Q^n U\right], \tag{1.3.1}$$

where $m, n = 1, 2$ are $SU(2)_L$ indices, μ is called the Higgsino mass[8] and h_L, h_U, h_D are the Yukawa coupling matrices, which we assume to be diagonal for simplicity.
Since we have not detected superpartners to any of the SM particles yet, they cannot be of the same mass. This means that SUSY has to be broken. In order to maintain the nice UV behavior of SUSY, this breaking has to be *soft*, i.e. all field-dependent SUSY-breaking terms in the Lagrangian must have mass dimension ≤ 3. The fact that there are no terms in the Lagrangian with mass dimension four means that in the limit of high energies, $E \to \infty$, supersymmetry is restored. Moreover in order to solve the hierarchy problem the mass shift between the SM particles and their superpartner emerging from

[8]The Higgsino mass μ is the only dimensionful quantity in the MSSM that has its origin neither in the soft breaking Lagrangian nor from EWSB. This means that the size of this parameter is naturally at the UV-cutoff of the theory, usually referred to as the GUT or the Planck scale. In the MSSM, however, the size of this term is required to be around the soft breaking scale. The unnatural mismatch of these scales results in a little hierarchy problem usually called the *μ-problem*. In contrast to the hierarchy problem in the SM, the parameter μ is *technically natural*, which means that it is not quadratically divergent and only slightly modified by radiative corrections.

the soft-breaking Lagrangian must not be too large, see Eq. (1.1.2). It is usually assumed that SUSY breaking occurs at high energies, for example at the Planck mass or the GUT scale. Since we cannot probe such energy scales experimentally, it is very difficult to get any information about how SUSY is broken. For practical reasons, SUSY breaking is described by an effective Lagrangian parameterizing our ignorance about the SUSY breaking mechanism and containing only soft terms that explicitly break SUSY. The MSSM contains the most general gauge invariant and R-parity conserving soft Lagrangian

$$\begin{aligned}\mathcal{L}_{\text{soft}} = &-\frac{1}{2}\left(M_3\bar{\tilde{g}}^a\tilde{g}^a + M_2\bar{\vec{\tilde{W}}}\vec{\tilde{W}} + M_1\bar{\tilde{B}}\tilde{B} + h.c.\right)\\ &-\left(\tilde{u}^\star_{iR}h^U_{ij}A^U\tilde{Q}_j\cdot H_2 - \tilde{d}^\star_{iR}h^D_{ij}A^D\tilde{Q}_j\cdot H_1 - \tilde{e}^\star_{iR}h^L_{ij}A^L\tilde{L}_j\cdot H_2 + h.c.\right)\\ &-\tilde{Q}^\star_i(m^2_Q)_{ij}\tilde{Q}_j - \tilde{L}^\star_i(m^2_L)_{ij}\tilde{L}_j - \tilde{u}^\star_{iR}(m^2_U)_{ij}\tilde{u} - \tilde{d}^\star_{iR}(m^2_D)_{ij}\tilde{d}_{jR} - \tilde{E}(m^2_E)_{ij}\tilde{E}^\dagger\\ &-(m^H_1)^2H^\star_1H_1 - (m^H_2)^2H^\star_2H_2 - B\mu\varepsilon_{mn}(H^m_1H^n_2 + h.c.),\end{aligned} \tag{1.3.2}$$

where h_{ij} and m^2_{ij} are both 3 by 3 matrices in family space. Generally they are arbitrary, but in the following we assume the SUSY breaking mass matrices m^2_{ij} to be proportional to 1 and the trilinear couplings in the soft SUSY breaking Lagrangian are proportional to the diagonal Yukawa matrices. In this way CP-violating effects and additional Flavor Changing Neutral Currents (FCNC) are suppressed[9]. Note also that we suppressed $SU(2)_L$ indices. The $\cdot$ between the $SU(2)_L$ doublet fields in the second line of Eq. (1.3.2) corresponds to a contraction of the $SU(2)_L$ indices m, n with the totally antisymmetric tensor ε_{mn}, where $\varepsilon_{12} = +1$. In the third line of Eq. (1.3.2) the $SU(2)_L$ indices m, n of the first two terms are contracted in a symmetric way δ_{mn}.

1.3.1 Squark Sector in the MSSM

The mass degeneracy between the SM fermions and their superpartners is destroyed by the terms in the soft SUSY breaking Lagrangian, see Eq. (1.3.2). Moreover after EWSB there are chirality changing Yukawa interactions, see Eqs. (1.3.1, 1.3.2) that produce off-diagonal entries in the squark mass matrices in the chiral (or current eigenstate) basis. Last but not least there are D-term contributions that cause diagonal squark mass-terms proportional to the weak gauge couplings g and g'. Collecting all bilinear terms in the squark fields $\tilde{f}_L$ and $\tilde{f}_R$ yields the following squark mass matrix

$$\begin{aligned}M_{\tilde{q}_{L,R}} &= \begin{pmatrix} m^2_Q + m^2_q + (I^3_q - e_q\sin^2\theta_W)M^2_Z\cos 2\beta & m_q(A_q + \mu r_q)\\ m_q(A_q + \mu r_q) & m^2_{U,D} + m^2_q + e_q\sin^2\theta_W M^2_Z\cos 2\beta\end{pmatrix}\\ &\equiv \begin{pmatrix} M^2_{LL} & M^2_{LR}\\ M^2_{LR} & M^2_{RR}\end{pmatrix},\end{aligned} \tag{1.3.3}$$

where e_q is the electric charge, $I^3_{u,d} = \pm\frac{1}{2}$ is the third component of the weak isospin, θ_W is the Weinberg angle and

$$r_q = \begin{cases}\cot\beta & q = u\\ \tan\beta & q = d\end{cases}. \tag{1.3.4}$$

There are off-diagonal terms in the squark matrices, proportional to the quark masses. The chiral eigenstate squarks are therefore not the mass eigenstates. To express the mass matrix in terms of mass eigenstate squarks, denoted by $\tilde{q}_{1,2}$, we need to diagonalize the 2 by 2 matrix, Eq. (1.3.3)

$$R(\theta_{\tilde{q}})M_{\tilde{q}_{L,R}}R(\theta_{\tilde{q}})^\dagger = \begin{pmatrix} m_{\tilde{q}_1} & 0\\ 0 & m_{\tilde{q}_2}\end{pmatrix},\qquad \begin{pmatrix}\tilde{q}_1\\ \tilde{q}_2\end{pmatrix} = R(\theta_{\tilde{q}})\begin{pmatrix}\tilde{q}_L\\ \tilde{q}_R\end{pmatrix},\qquad R(\theta_{\tilde{q}}) = \begin{pmatrix}\cos\theta_{\tilde{q}} & \sin\theta_{\tilde{q}}\\ -\sin\theta_{\tilde{q}} & \cos\theta_{\tilde{q}}\end{pmatrix}, \tag{1.3.5}$$

[9]Scaling the trilinear couplings with the Yukawa matrices ensures that the parameters A^U, A^D, A^L do not have to be hierarchical.

where the masses of the physical squarks satisfy $m_{\tilde{q}_1} \geq m_{\tilde{q}_2}$ by convention and are given by

$$m_{\tilde{q}_{1,2}} = \frac{1}{2}\left(M_{LL}^2 + M_{RR}^2 \pm \sqrt{(M_{LL}^2 - M_{RR}^2)^2 + 4M_{LR}^4}\right). \tag{1.3.6}$$

The squark mixing angle $\theta_{\tilde{q}}$ is determined by either of the two following expressions

$$\sin 2\theta_{\tilde{q}} = \frac{2M_{LR}^2}{m_{\tilde{q}_1}^2 - m_{\tilde{q}_2}^2} = \frac{2m_q X_q}{m_{\tilde{q}_1}^2 - m_{\tilde{q}_2}^2}, \qquad \cos 2\theta_{\tilde{q}} = \frac{m_Q^2 - m_{U,D}^2}{m_{\tilde{q}_1}^2 - m_{\tilde{q}_2}^2}, \qquad X_q = A_q + \mu r_q \tag{1.3.7}$$

and X_q is called the squark mixing parameter.

1.4 MSSM Higgs Masses and Self-Couplings at Tree-Level

1.4.1 The Tree-Level Higgs Potential

The tree-level Higgs potential in the MSSM can be obtained by extracting all terms containing only scalar Higgs fields from the MSSM Lagrangian

$$\begin{aligned} V^0 =&((m_1^H)^2 + \mu^2)|H_1|^2 + ((m_2^H)^2 + \mu^2)|H_2|^2 - B\mu\epsilon_{ij}(H_1^i H_2^j + h.c.) + \\ &+ \frac{g^2 + g'^2}{8}(|H_1|^2 - |H_2|^2)^2 + \frac{g^2}{2}|H_1^\dagger H_2|^2, \end{aligned} \tag{1.4.1}$$

where H_1 and H_2 are complex $SU(2)_L$ Higgs doublet. The mass-terms for H_1 and H_2 arise on the one hand from the SUSY breaking Lagrangian Eq. (1.3.2) (m_1^H and m_2^H). The μ^2 in the first two terms originates from the F-terms, see Eq. (1.2.16). The third term contains the totally antisymmetric tensor ε_{ij} and emerges from soft SUSY breaking, see Eq. (1.3.2). The last two terms contain the electroweak coupling constants g and g', their origin is the D-term, see Eq. (1.2.19). Note that in supersymmetric theories all quartic self-couplings of the Higgs fields are related to the gauge couplings of the electroweak theory. This is a remarkable difference to the SM, where the quartic term is not related to any quantities outside the Higgs sector.
We will parameterize the two Higgs doublets in the following way

$$H_1 = \begin{pmatrix} H_1^1 \\ H_1^2 \end{pmatrix} \equiv \begin{pmatrix} H_1^0 \\ H_1^- \end{pmatrix}, \quad H_2 = \begin{pmatrix} H_2^1 \\ H_2^2 \end{pmatrix} \equiv \begin{pmatrix} H_2^+ \\ H_2^0 \end{pmatrix}. \tag{1.4.2}$$

The $+$, $-$ and 0 superscripts indicate the electric charge of the Higgs fields. In terms of the complex field components, the potential is given by

$$\begin{aligned} V^0 =&(m_1^2)(|H_1^0|^2 + |H_1^-|^2) + (m_2^2)(|H_2^+|^2 + |H_2^0|^2) - \\ &- B\mu(H_1^0 H_2^0 - H_1^- H_2^+ + h.c.) + \\ &+ \frac{g^2 + g'^2}{8}(|H_1^0|^2 + |H_1^-|^2 - |H_2^0|^2 - |H_2^+|^2)^2 + \frac{g^2}{2}|(H_1^0)^\star H_2^+ + H_1^+ H_2^0|^2, \end{aligned} \tag{1.4.3}$$

where we introduced the parameters $m_1^2 \equiv (m_1^H)^2 + \mu^2$ and $m_2^2 \equiv (m_2^H)^2 + \mu^2$.

1.4.2 Electroweak Symmetry Breaking

The Higgs field induces SSB if the minimum of the potential, i.e. the vacuum or ground state of the theory is attained at a nonzero value for the Higgs fields. For the breaking of the electroweak symmetry

we thus need a nonzero VEV for the Higgs fields, which is not invariant under $SU(2)_L \times U(1)_Y$ but only under $U(1)_{em}$. Since we do not want to break $U(1)_{em}$-invariance, we apply $SU(2)_L$ rotations on the complex Higgs doublets, such that the charged components H_1^- and H_2^+ do not get a VEV. Moreover we use the $SU(2)_L \times U(1)_Y$ invariance to make the VEVs of the neutral components real and positive and to write $m_3^2 = B\mu$, where m_3^2 is real and positive. We can write the neutral complex Higgs fields as a real and a complex part with a normalization factor $\sqrt{1/2}$

$$H_i^0 = \frac{1}{\sqrt{2}}(a_i + iP_i), \qquad a_i, P_i \in \mathcal{R}. \tag{1.4.4}$$

Minimizing the effective potential: Due to the residual $U(1)_{em}$ invariance we can rotate the neutral part of the Higgs doublets in such a way that only the real parts a_i acquire a VEV[10]. We call the minima of the tree-level potential v_i

$$\left.\frac{\partial V^0(a_k, P_k)}{\partial a_i}\right|_{a_k = v_k^{\min}, P_k = 0} = 0, \qquad i = 1, 2. \tag{1.4.5}$$

The above minimization conditions give the following two equations

$$m_1^2 - m_3^2 \tan(\beta) + \frac{g^2 + g'^2}{8}\left[v_1^2 - v_2^2\right] = 0 \tag{1.4.6}$$

$$m_2^2 - m_3^2 \cot(\beta) - \frac{g^2 + g'^2}{8}\left[v_1^2 - v_2^2\right] = 0, \tag{1.4.7}$$

where we introduced the angle β as $\tan\beta \equiv \frac{v_2}{v_1}$. These equations allow us to eliminate m_1^2 and m_2^2. The neutral parts of the Higgs doublets are expanded around these minima

$$H_i^0 = \frac{1}{\sqrt{2}}(v_i + S_i + iP_i). \tag{1.4.8}$$

The fluctuations around the VEVs S_i correspond to the physical CP-even Higgs current eigenstates with zero VEVs $\langle S_i \rangle = 0$. The minimization condition means that there are no tadpole terms, i.e. linear terms in the fields S_i and P_i. Eq. (1.4.8) is inserted in the complete Lagrangian, such that the whole theory is expanded around the minimum of the potential. In this way the VEVs of the Higgs fields give mass to the W- and Z-boson as well as to the SM fermions

$$m_Z^2 = \frac{g^2 + g'^2}{4}[v_1^2 + v_2^2], \qquad m_W^2 = \frac{g^2}{4}[v_1^2 + v_2^2], \qquad m_{u,l}^2 = \frac{h_{u,l}^2}{2}v_2^2, \qquad m_d^2 = \frac{h_d^2}{2}v_1^2. \tag{1.4.9}$$

We can therefore relate the VEV of the SM v, measured in the muon decay [16], with the VEVs of the MSSM

$$G_F = \frac{1}{\sqrt{2}[v_1^2 + v_2^2]} = 1.1663788(7) \cdot 10^{-5}\ \text{GeV}^{-2}, \quad \Rightarrow \quad v = \sqrt{v_1^2 + v_2^2} \simeq 246.22\ \text{GeV}. \tag{1.4.10}$$

Moreover the MSSM VEVs enter in the sfermion masses and in various trilinear couplings.
Note that the Higgs potential has to be bounded from below. Looking at the potential of the neutral Higgs fields only, one sees that for $|H_1^0|^2 = |H_2^0|^2$ we obtain the condition

$$m_1^2 + m_2^2 > 2m_3^2, \tag{1.4.11}$$

which has to be fulfilled also when radiative corrections are taken into account. Moreover for non-zero VEVs to develop, at least one of the eigenvalues of the mass squared matrix of the Higgs fields has to be negative. This requires

$$m_3^4 > m_1^2 m_2^2, \tag{1.4.12}$$

i.e. a necessary condition for EWSB to occur is that SUSY is broken.

[10] A VEV for the imaginary parts P_i would result in unwanted CP violation.

1.4.3 The Masses of the Physical Higgs Bosons

To define the masses of the physical Higgs bosons, the mass matrix, defined as the bilinear term in the fields, has to be considered. To get the tree-level masses, we therefore have to take two derivatives of the Higgs potential with respect to two fields ϕ_i and ϕ_j and evalute it at the minimum of the potential, i.e. all fields are substituted by their VEV

$$M^{ij} \equiv \left.\frac{\partial^2 V^0}{\partial\phi_i \partial\phi_j}\right|_{\min}. \tag{1.4.13}$$

Since the $U(1)_{em}$ symmetry is unbroken, there are no mass-terms that mix the charged and the uncharged Higgs bosons. This means both sectors can be treated separately. Moreover there is no CP violation and therefore no mixing between the CP-odd and the CP-even scalar fields $P_{1,2}$ and $S_{1,2}$. The 8 by 8 matrix of the Higgs sector therefore splits up into four 2 by 2 matrices.

The masses of the pseudoscalar Higgs bosons: The mass matrix for the CP-odd scalars is

$$(\mathcal{M}_P^2)_{ij} = \left.\frac{\partial^2 V^0}{\partial P_i \partial P_j}\right|_{\min} = m_3^2 \begin{pmatrix} \tan(\beta) & 1 \\ 1 & \cot(\beta) \end{pmatrix}, \qquad i,j = \{1,2\}, \tag{1.4.14}$$

where we used the minimization conditions Eqs. (1.4.6, 1.4.7) to eliminate m_1^2 and m_2^2. The fields $P_{1,2}$ are no mass eigenstates, because the mass matrix is not diagonal. To get the masses of the physical Higgs bosons, we can calculate the eigenvalues of the matrix $(\mathcal{M}_P^2)_{ij}$, which is easy for a 2 by 2 matrix, see appendix A.1. We label the CP-odd eigenstates by A and G. Their masses can be determined using Eq. (A.1.3)

$$m_{G,A}^2 = \frac{1}{2} m_3^2 \left(\frac{s_\beta}{c_\beta} + \frac{c_\beta}{s_\beta} \pm \sqrt{\left(\frac{s_\beta}{c_\beta} - \frac{c_\beta}{s_\beta}\right)^2 + 4} \right) \quad \Rightarrow \quad m_G^2 = 0, \qquad m_A^2 = \frac{2m_3^2}{\sin(2\beta)}, \tag{1.4.15}$$

where we use the obvious abbreviations for the trigonometric functions: $s_\beta \equiv \sin(\beta)$, $c_\beta \equiv \cos(\beta)$ and $t_\beta \equiv \tan(\beta)$. This means that G is a massless would-be Goldstone boson. From EWSB we expect to get three would-be Goldstone bosons which are "eaten up" in order to give the three massive gauge bosons ($W^\pm$ and Z) a longitudinal polarization direction. The mass of the state A is determined by the angle β and the parameter m_3^2. In the future we will take m_A^2 and β as input parameters, using $m_3^2 = m_A^2 s_\beta c_\beta$ to eliminate m_3^2. The tree-level Higgs sector can be therefore described by only two parameters.

The masses of the scalar CP-even Higgs bosons: We will proceed exactly in the same way as in the CP-odd case. The mass matrix for the CP-even scalars is

$$(\mathcal{M}_S^2)_{ij} = \left.\frac{\partial^2 V^0}{\partial S_i \partial S_j}\right|_{\min} = \begin{pmatrix} m_A^2 s_\beta^2 + m_Z^2 c_\beta^2 & -c_\beta s_\beta (m_A^2 + m_Z^2) \\ -c_\beta s_\beta (m_A^2 + m_Z^2) & m_A^2 c_\beta^2 + m_Z^2 s_\beta^2 \end{pmatrix}. \tag{1.4.16}$$

Using Appendix A.1 we find the masses of the two neutral CP-even Higgs bosons

$$m_{H,h}^2 = \frac{1}{2}\left[m_A^2 + m_Z^2 \pm \sqrt{(m_A^2 + m_Z^2)^2 - 4 m_A^2 m_Z^2 \cos^2(2\beta)} \right]. \tag{1.4.17}$$

We denote the light scalar mass eigenstate by h and the heavy eigenstate by H. Eq. (1.4.17) leads to an upper bound for the mass of the light scalar Higgs boson

$$m_h^2 \leq m_Z^2, m_A^2. \tag{1.4.18}$$

The plot in Figure 1.3 shows the tree-level Higgs masses for the light and the heavy scalar as a function of the pseudoscalar Higgs mass for different values of $\tan\beta$. The value of $\tan\beta$ determines the steepness of the slope of m_h for $m_A \lesssim m_Z$ and the steepness of the slope of m_H for $m_A \gtrsim m_Z$. Moreover it determines the upper bound for the light scalar Higgs mass[11] $m_h \leq m_Z |\cos 2\beta|$. For $m_A \gg m_Z$ the heavy Higgs states decouple $m_H \simeq m_A$ and m_h is at its maximum value, see also section 1.4.7. The region of $m_A \simeq m_Z$, where the curves of m_h and m_H are closest to each other is called the *transition region*.

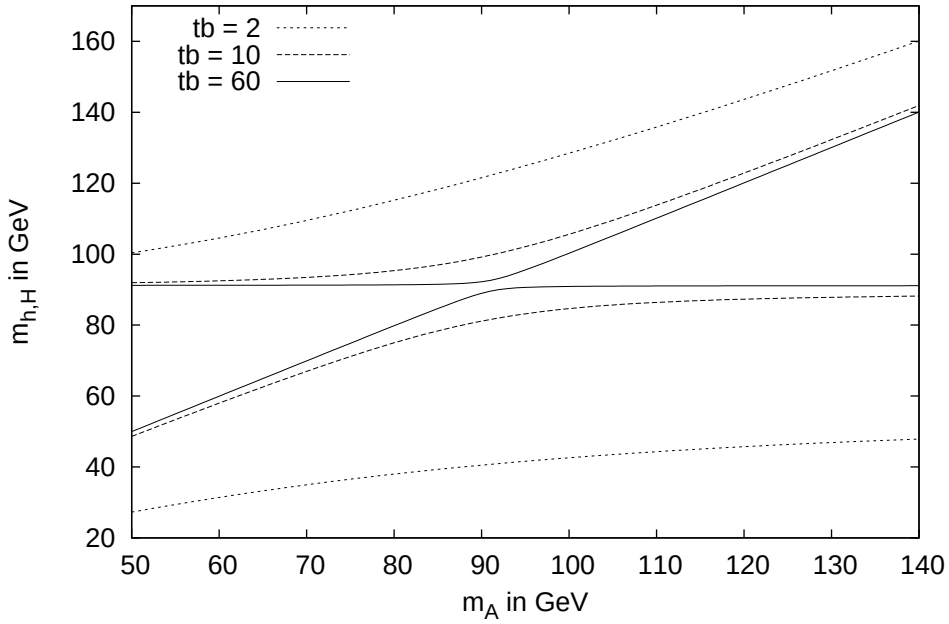

Figure 1.3: The CP-even scalar MSSM Higgs masses as functions of m_A for $\tan\beta = 2, 10, 60$ at leading order (LO). The three upper curves belong to the heavy scalar, whereas the three lower curves belong to the light scalar.

The MSSM at tree-level has already been ruled out by the LEP experiment, which could have produced a light scalar Higgs boson directly in the whole m_A-$\tan\beta$ parameter space. The MSSM Higgs sector, however, receives large radiative corrections, such that the light scalar Higgs mass is enhanced, such that the LEP exclusion bounds apply only to restricted regions of parameter space. Figure 1.4 shows regions in the m_A-$\tan\beta$-plane in the $m_h^{\max}$ scenario excluded by CMS (blue) and by the LEP experiment (green). For low values of $\tan\beta$ and m_A, the light scalar Higgs boson could be produced directly via Higgsstrahlung in the LEP experiment. Therefore values for $\tan\beta \lesssim 2.5$ and $m_A < 93$ GeV have been excluded at 95% CL already by LEP. Due to the enhanced coupling of the heavy scalar to leptons for large $\tan\beta$ the LHC can access regions of high $\tan\beta$ by analyzing $\tau\tau$ final states. With growing pseudoscalar Higgs masses m_A, however, the production rate for the heavy scalar Higgs boson H shrinks. For this reason regions of low pseudoscalar masses and high $\tan\beta$ can be excluded first by the LHC.

[11] This bound can be obtained by expanding Eq. (1.4.17) for $m_A \gg m_Z$.

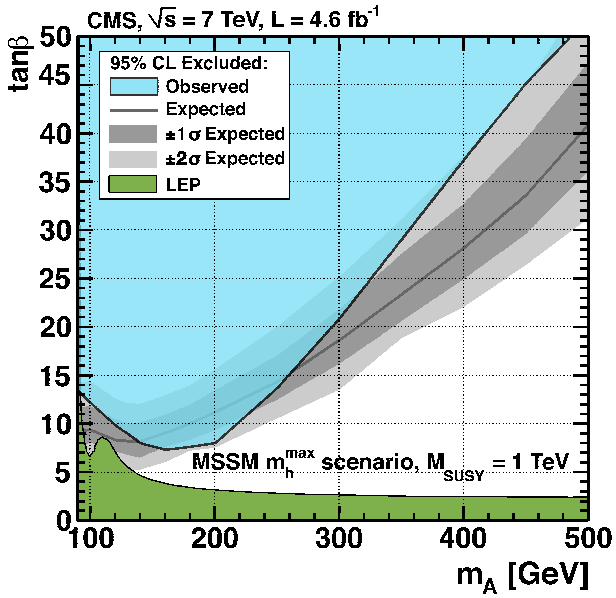

Figure 1.4: Regions in the m_A-tan β-plane in the $m_h^{\max}$ scenario excluded by CMS (blue) and by the LEP experiment (green) at 95% CL [17]. CMS uses $\tau\tau$ final states analysis from the full 2011 data set with an integrated luminosity of $4.6 fb^{-1}$ at a center of mass energy of $\sqrt{s} = 7$ TeV. The combined LEP result was obtained by analyzing $b\bar{b}$ and $\tau\tau$ final states from decaying Higgs bosons, produced via Higgsstrahlung and pair production [18].

The masses of the charged Higgs bosons: The terms of the potential that are bilinear in $H_{1,2}^+$ and $H_{1,2}^-$ are

$$\begin{aligned} V_\pm =&(m_1^2)(H_1^+H_1^-) + (m_2^2)(H_2^+H_2^-)+ \\ &+m_3^2(H_2^+H_1^- + H_1^+H_2^-) + \frac{m_Z^2}{2}\cos(2\beta)[H_1^+H_1^- + H_2^+H_2^-]+ \\ &+m_W^2[c_\beta^2 H_2^+H_2^- + s_\beta^2 H_1^+H_1^- s_\beta c_\beta (H_1^+H_2^- + H_2^+H_1^-)]. \end{aligned} \tag{1.4.19}$$

The mass matrix for the charged Higgs bosons is proportional to the CP-odd mass matrix

$$M_\pm^{ij} \equiv \left.\frac{\partial^2 V^0}{\partial H_i^+ \partial H_j^-}\right|_{\min} = \frac{\partial^2 V^\pm}{\partial H_i^+ \partial H_j^-} = s_\beta c_\beta (m_A^2 + m_W^2) \begin{pmatrix} t_\beta & 1 \\ 1 & t_\beta^{-1} \end{pmatrix}. \tag{1.4.20}$$

Calculating the eigenvalues, we obtain two charged massless would-be Goldstone boson and two charged Higgs bosons, with the following mass relations

$$m_{G^\pm} = 0, \qquad m_{H^\pm}^2 = m_A^2 + m_W^2. \tag{1.4.21}$$

The MSSM Higgs sector therefore consists of three would-be Goldstone bosons, i.e. longitudinal polarizations for the massive gauge bosons and five massive Higgs bosons. Note that for large m_A^2 the mass of the heavy scalar and the mass of the charged Higgs bosons also become large. For this reason it is usually said that there are four heavy and one light Higgs boson in the MSSM.

1.4.4 Mixing Angles

Finding the mixing matrices for the mass diagonalization is essential in order to determine the Higgs self-couplings of the mass eigenstates. In the MSSM this task is simplified, because we have only 2 by 2 matrices and we can therefore parameterize all three mixing matrices by only one angle Θ, see appendix A.2.

Mixing angle for the charged and the pseudoscalar Higgs bosons: For the charged and the CP-odd Higgs bosons we obtained the same mass matrix up to a constant factor

$$M \equiv \begin{pmatrix} t_\beta & 1 \\ 1 & t_\beta^{-1} \end{pmatrix}. \tag{1.4.22}$$

This means that the mixing angles must also be identical. From appendix A.2 it follows that $\Theta = \beta$ and therefore

$$D = R_\beta M R_\beta = (t_\beta + t_\beta^{-1}) \begin{pmatrix} 1 & 0 \\ 0 & 0 \end{pmatrix}, \qquad R_\beta \equiv \begin{pmatrix} s_\beta & c_\beta \\ c_\beta & -s_\beta \end{pmatrix}. \tag{1.4.23}$$

The matrix D is diagonal and the entries are exactly the masses we obtained in Eqs. (1.4.15, 1.4.21). We found that at tree-level the rotation angle for the CP-odd and the charged Higgs bosons is the same as the arctangent of the VEV ratios of the two Higgs doublets

$$\Theta = \beta = \arctan\left(\frac{v_2}{v_1}\right). \tag{1.4.24}$$

Mixing angle for the neutral CP-even Higgs bosons: The mass matrix for the neutral CP-even Higgs bosons $(\mathcal{M}_S^2)_{ij}$ is given in Eq. (1.4.16). We call the CP-even mixing angle $\alpha = -\Theta$ and use the results of appendix A.2. Using Eq. (A.2.4) yields the mixing angle

$$\alpha = \frac{1}{2} \arcsin \frac{-2 c_\beta s_\beta (m_A^2 + m_Z^2)}{m_H^2 - m_h^2}. \tag{1.4.25}$$

This implies that $\alpha \in [-\frac{\pi}{2}, 0]$. Note that the domain of α can change when radiative corrections are taken into account.

1.4.5 Higgs Couplings to Fermions and Gauge Bosons

In the SM the Higgs-quark couplings are generated by the Yukawa term in the Lagrangian

$$\mathcal{L}_{\mathrm{Y,SM}} = \sum_q y_q q \bar{q} \frac{1}{\sqrt{2}} (v + \eta), \tag{1.4.26}$$

where $y_q = \sqrt{2} m_q / v$ is the SM Yukawa coupling, $q = u, d, s, c, t, b$ is a SM quark and η is the CP-even, neutral SM scalar Higgs field fluctuating around the SM VEV v. In the MSSM the Higgs-quark couplings are very similar, except that up and down type quarks couple to different Higgs fields. The MSSM Yukawa part of the Lagrangian comes from the superpotential Eq. (1.3.1) and is given by

$$\mathcal{L}_{\mathrm{Y,MSSM}} = \sum_u h_u u \bar{u} \frac{1}{\sqrt{2}} H_2^0 + \sum_d h_d d \bar{d} \frac{1}{\sqrt{2}} H_1^0, \tag{1.4.27}$$

where $h_{u,d}$ denotes the up, respectively the down type Yukawa coupling in the MSSM. Note that the coupling of the leptons to the Higgs sector is down type. We want to express H_1^0 and H_2^0 in terms of the

	ϕ	g_u^ϕ	g_d^ϕ	g_V^ϕ
SM	H	1	1	1
MSSM	h	c_α/s_β	$-s_\alpha/c_\beta$	$\sin(\beta-\alpha)$
	H	s_α/s_β	c_α/c_β	$\cos(\beta-\alpha)$
	A	t_β^{-1}	t_β	0

Table 1.3: Couplings of the neutral MSSM Higgs bosons to fermions and gauge bosons.

physical fields h, H and A. To do so we use Eq. (1.4.8) and the results of the rotations in section 1.4.4, i.e.

$$\begin{pmatrix} P_1 \\ P_2 \end{pmatrix} = \begin{pmatrix} s_\beta & c_\beta \\ c_\beta & -s_\beta \end{pmatrix} \begin{pmatrix} A \\ G \end{pmatrix}, \qquad \begin{pmatrix} S_1 \\ S_2 \end{pmatrix} = \begin{pmatrix} -s_\alpha & c_\alpha \\ c_\alpha & s_\alpha \end{pmatrix} \begin{pmatrix} h \\ H \end{pmatrix} \tag{1.4.28}$$

To get the correct masses of the up respectively the down quarks $m_{d,u}$, we need the following MSSM Yukawa couplings: $h_d = m_d/v_1$ and $h_u = m_u/v_2$.
The Higgs boson can also couple to gauge bosons via the kinetic part of the Lagrangian of the Higgs field. In the MSSM we have

$$\mathcal{L}_{\text{kin}} = (D_\mu H_1)(D^\mu H_1)^\dagger + (D_\mu H_2)(D^\mu H_2)^\dagger, \tag{1.4.29}$$

where H_1 and H_2 are the doublet fields. In the SM this term is similar, but there is only one doublet field. Using Eqs. (1.4.2, 1.4.8, 1.4.28), we can derive the Higgs-gauge boson couplings.
Putting everything together it is easy to compare the Higgs-quark and Higgs-gauge boson couplings in the SM to the couplings in the MSSM. In Table 1.3 the couplings are listed. All values are normalized to the SM couplings.

1.4.6 Trilinear and Quartic Self-Couplings of the Scalar MSSM Higgs Bosons

The trilinear and quartic tree-level self-couplings of the scalar MSSM Higgs bosons h and H are defined by the trilinear respectively the quartic terms in the Higgs fields of the tree-level Higgs potential. They are obtained by taking three respectively four derivatives of V^0, with respect to the corresponding fields. The trilinear self-couplings can be expressed in the following simple form

$$\begin{aligned}
\lambda_{hhh} &\equiv \left.\frac{\partial^3 V^0}{\partial h^3}\right|_{\min} = \frac{3m_Z^2}{v}\cos(2\alpha)\sin(\alpha+\beta), \quad \lambda_{HHH} \equiv \left.\frac{\partial^3 V^0}{\partial H^3}\right|_{\min} = \frac{3m_Z^2}{v}\cos(2\alpha)\cos(\alpha+\beta), \\
\lambda_{hhH} &\equiv \left.\frac{\partial^3 V^0}{\partial h^2 \partial H}\right|_{\min} = \frac{m_Z^2}{v}(2\sin(2\alpha)\sin(\alpha+\beta) - \cos(2\alpha)\cos(\alpha+\beta)), \\
\lambda_{hHH} &\equiv \left.\frac{\partial^3 V^0}{\partial h \partial H^2}\right|_{\min} = -\frac{m_Z^2}{v}(2\sin(2\alpha)\cos(\alpha+\beta) + \cos(2\alpha)\sin(\alpha+\beta)), \\
\lambda_{hAA} &\equiv \left.\frac{\partial^3 V^0}{\partial h \partial A^2}\right|_{\min} = \frac{m_Z^2}{v}\cos(2\beta)\sin(\alpha+\beta), \quad \lambda_{HAA} \equiv \left.\frac{\partial^3 V^0}{\partial H \partial A^2}\right|_{\min} = -\frac{m_Z^2}{v}\cos(2\beta)\cos(\alpha+\beta), \\
\lambda_{hAG} &\equiv \left.\frac{\partial^3 V^0}{\partial h \partial A \partial G}\right|_{\min} = -\frac{m_Z^2}{v}\sin(2\beta)\sin(\alpha+\beta), \quad \lambda_{HAG} \equiv \left.\frac{\partial^3 V^0}{\partial H \partial A \partial G}\right|_{\min} = \frac{m_Z^2}{v}\sin(2\beta)\cos(\alpha+\beta), \\
\lambda_{hGG} &\equiv \left.\frac{\partial^3 V^0}{\partial h \partial G^2}\right|_{\min} = -\frac{m_Z^2}{v}\cos(2\beta)\sin(\alpha+\beta), \quad \lambda_{HGG} \equiv \left.\frac{\partial^3 V^0}{\partial H \partial G^2}\right|_{\min} = \frac{m_Z^2}{v}\cos(2\beta)\cos(\alpha+\beta).
\end{aligned} \tag{1.4.30}$$

Figure 1.5 shows all trilinear couplings λ_{hhh}, λ_{HHH}, λ_{hhH}, λ_{hHH}, λ_{hAA},λ_{HAA} as a function of the pseudoscalar Higgs mass m_A for two values of $\tan\beta = 2$ (dashed lines) and $\tan\beta = 30$ (solid lines). The

slope of the couplings is steepest in the transition region $m_A \simeq m_Z$ and the steepness grows with $\tan\beta$. In the decoupling limit $m_A \to \infty$ the couplings saturate to their asymptotic values.

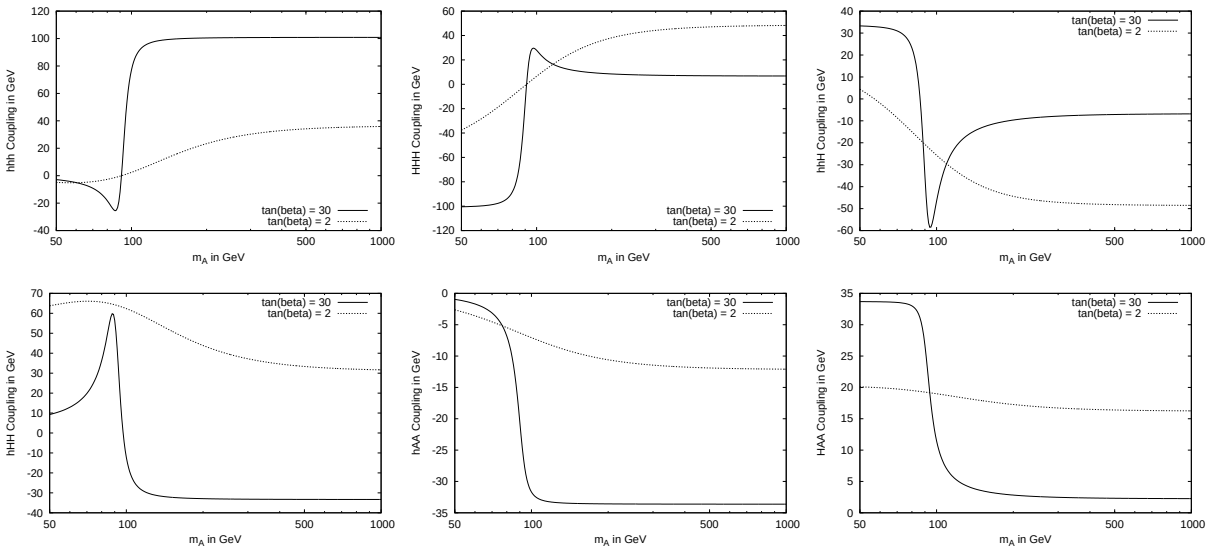

Figure 1.5: The trilinear couplings $\lambda_{hhh}, \lambda_{HHH}, \lambda_{hhH}$ (first line) and $\lambda_{hHH}, \lambda_{hAA}, \lambda_{HAA}$ (second line) as a function of the pseudoscalar Higgs mass m_A for two values of $\tan\beta$.

The quartic self-couplings are

$$
\begin{aligned}
\lambda_{hhhh} &\equiv \left.\frac{\partial^4 V^0}{\partial h^4}\right|_{\min} = \frac{3m_Z^2}{v^2}\cos(2\alpha)^2, \quad \lambda_{HHHH} \equiv \left.\frac{\partial^4 V^0}{\partial H^4}\right|_{\min} = \frac{3m_Z^2}{v^2}\cos(2\alpha)^2, \\
\lambda_{hhhH} &\equiv \left.\frac{\partial^4 V^0}{\partial h^3 \partial H}\right|_{\min} = \frac{3m_Z^2}{v^2}\sin(2\alpha)\cos(2\alpha), \quad \lambda_{hhHH} \equiv \left.\frac{\partial^4 V^0}{\partial h^2 \partial H^2}\right|_{\min} = \frac{m_Z^2}{v^2}(2\sin(2\alpha)^2 - \cos(2\alpha)^2), \\
\lambda_{hHHH} &\equiv \left.\frac{\partial^4 V^0}{\partial h \partial H^3}\right|_{\min} = -\frac{3m_Z^2}{v^2}\sin(2\alpha)\cos(2\alpha), \quad \lambda_{hhAA} \equiv \left.\frac{\partial^4 V^0}{\partial h^2 \partial A^2}\right|_{\min} = \frac{m_Z^2}{v^2}\cos(2\alpha)\cos(2\beta), \\
\lambda_{hHAA} &\equiv \left.\frac{\partial^4 V^0}{\partial h \partial H \partial A^2}\right|_{\min} = \frac{m_Z^2}{v^2}\cos(2\beta)\sin(2\alpha), \quad \lambda_{HHAA} \equiv \left.\frac{\partial^4 V^0}{\partial H^2 \partial A^2}\right|_{\min} = -\frac{m_Z^2}{v^2}\cos(2\alpha)\cos(2\beta), \\
\lambda_{hhAG} &\equiv \left.\frac{\partial^4 V^0}{\partial h^2 \partial A \partial G}\right|_{\min} = -\frac{m_Z^2}{v^2}\cos(2\alpha)\sin(2\beta), \quad \lambda_{hHAG} \equiv \left.\frac{\partial^4 V^0}{\partial h \partial H \partial A \partial G}\right|_{\min} = -\frac{m_Z^2}{v^2}\sin(2\alpha)\sin(2\beta), \\
\lambda_{HHAG} &\equiv \left.\frac{\partial^4 V^0}{\partial H^2 \partial A \partial G}\right|_{\min} = \frac{m_Z^2}{v^2}\cos(2\alpha)\sin(2\beta), \quad \lambda_{hhGG} \equiv \left.\frac{\partial^4 V^0}{\partial h^2 \partial G^2}\right|_{\min} = -\frac{m_Z^2}{v^2}\cos(2\alpha)\cos(2\beta), \\
\lambda_{hHGG} &\equiv \left.\frac{\partial^4 V^0}{\partial h \partial H \partial G^2}\right|_{\min} = -\frac{m_Z^2}{v^2}\sin(2\alpha)\cos(2\beta), \quad \lambda_{HHGG} \equiv \left.\frac{\partial^4 V^0}{\partial H^2 \partial G^2}\right|_{\min} = \frac{m_Z^2}{v^2}\cos(2\alpha)\cos(2\beta), \\
\lambda_{AAAA} &\equiv \left.\frac{\partial^4 V^0}{\partial A^4}\right|_{\min} = \frac{3m_Z^2}{v^2}\cos(2\beta)^2, \quad \lambda_{AAAG} \equiv \left.\frac{\partial^4 V^0}{\partial A^3 \partial G}\right|_{\min} = -\frac{3m_Z^2}{v^2}\cos(2\beta)\sin(2\beta), \\
\lambda_{AAGG} &\equiv \left.\frac{\partial^4 V^0}{\partial A^2 \partial G^2}\right|_{\min} = \frac{m_Z^2}{v^2}(2\sin(2\beta)^2 - \cos(2\beta)^2), \quad \lambda_{AGGG} \equiv \left.\frac{\partial^4 V^0}{\partial A \partial G^3}\right|_{\min} = \frac{3m_Z^2}{v^2}\sin(2\beta)\cos(2\beta), \\
\lambda_{GGGG} &\equiv \left.\frac{\partial^4 V^0}{\partial G^4}\right|_{\min} = \frac{3m_Z^2}{v^2}\cos(2\beta)^2. \qquad (1.4.31)
\end{aligned}
$$

Figure 1.6 shows all quartic couplings λ_{hhhh}, λ_{HHHH}, λ_{hhhH}, λ_{hhHH}, λ_{hHHH}, λ_{hhAA}, λ_{hHAA}, λ_{HHAA}, λ_{AAAA} as a function of the pseudoscalar Higgs mass m_A for two values of $\tan\beta = 2$ (dashed lines) and $\tan\beta = 30$ (solid lines). As for the trilinear couplings it is a universal feature also for the quartic couplings that the slope of the curves is steepest in the transition region $m_A \simeq m_Z$ and that the steepness grows with $\tan\beta$. In the decoupling limit $m_A \to \infty$ the couplings approach their asymptotic value.

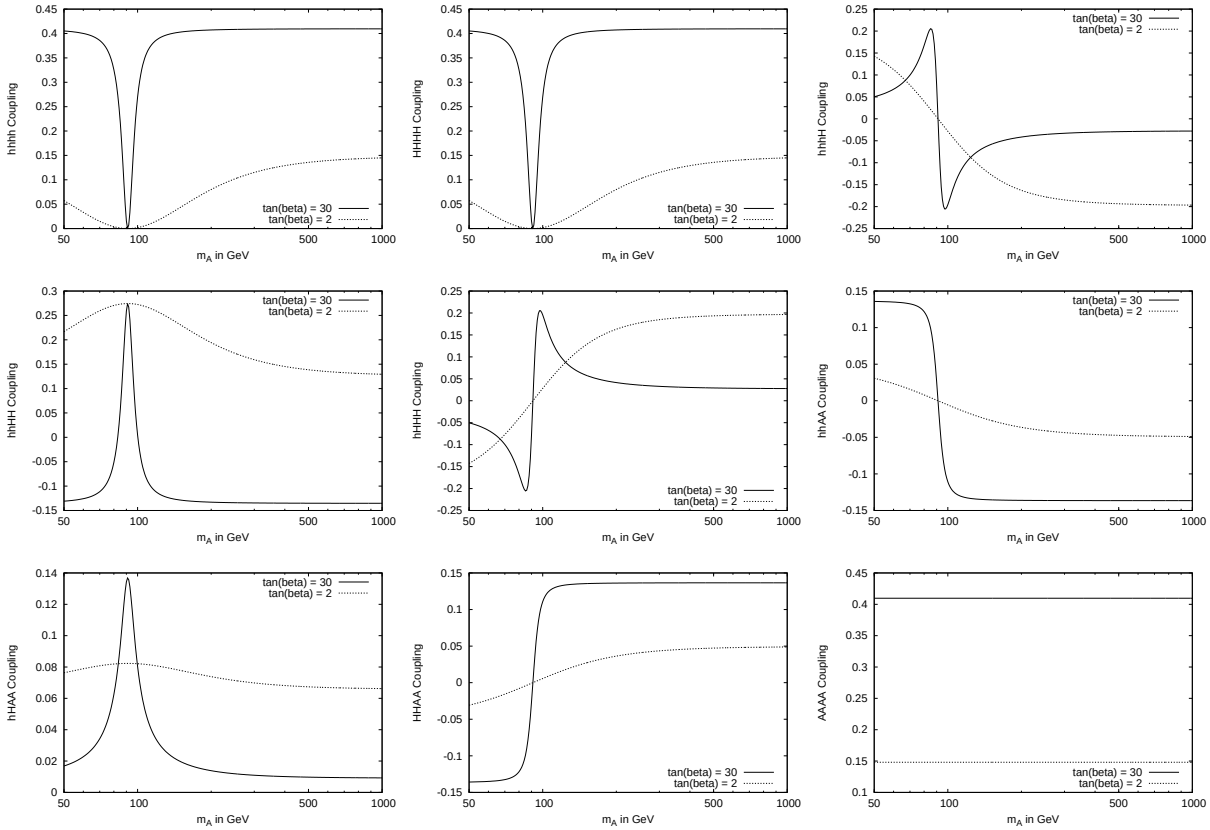

Figure 1.6: The quartic couplings $\lambda_{hhhh}, \lambda_{HHHH}, \lambda_{hhhH}$ (first line), $\lambda_{hhHH}, \lambda_{hHHH}, \lambda_{hhAA}$ (second line) and $\lambda_{hHAA}, \lambda_{HHAA}, \lambda_{AAAA}$ (third line) as a function of the pseudoscalar Higgs mass m_A for two values of $\tan\beta$.

1.4.7 Decoupling Limit

The decoupling limit corresponds to the limit where the masses of all supersymmetric particles[12] are large. Intuitively it is clear that all these particles decouple from the SM and therefore we expect that in this limit the MSSM looks just like the SM.
In the tree-level Higgs sector we go to this limit by setting $m_A^2 \to \infty$. Looking at Eqs. (1.4.21, 1.4.17) we see immediately that for very large m_A^2, the masses $m_{H^\pm}^2$ and m_H^2 also become very large. So there is only one light scalar Higgs boson h. Expanding m_h^2, see Eq. (1.4.17) in terms of $m_Z^2/m_A^2 \ll 1$ yields

$$(m_h^{\text{dec}})^2 = m_Z^2 \cos^2(2\beta), \tag{1.4.32}$$

[12]Supersymmetric particles means all non-SM particles in the MSSM, i.e. squarks, sleptons, gauginos, higgsinos and also additional Higgs bosons $H^\pm, A, H$.

which is the light scalar Higgs tree-level mass in the decoupling limit. We see that in the decoupling limit the light scalar Higgs mass is pushed to its upper bound. This effect is not only true at tree-level but it also holds when considering loop-corrections.

The mixing angles in the decoupling limit: Here we want to study the behavior of the Higgs-quark and Higgs-gauge boson couplings in the decoupling limit. First we need to see how the angle α behaves in the decoupling limit. Taking the limit $m_A \to \infty$ of Eq. (1.4.25), yields $\tan(\alpha) = -\cot(\beta)$. Since $\alpha \in [-\pi/2, 0]$ and $\beta \in [0, \pi/2]$ it follows that in decoupling limit

$$\alpha \to \beta - \frac{\pi}{2}. \tag{1.4.33}$$

Applying this result to Table 1.3, we see that in the decoupling limit the light scalar couples exactly as in the SM. The other Higgs bosons become very heavy and therefore decouple from the other particles. Another interesting limit is small m_A. This implies that $\alpha \to -\beta$ and then the couplings of H to quarks become SM-like for $t_\beta \gg 1$, up to sign differences.

Light scalar Higgs self-couplings in the decoupling limit: As before we want to investigate how the self-couplings for the light scalar Higgs boson h behave in the decoupling limit. Inserting $\alpha \to \beta - \frac{\pi}{2}$ into the first identity of Eq. (1.4.30) and Eq. (1.4.31) yields

$$\lambda_{hhh}^{\text{dec}} = \frac{3m_Z^2}{v}\cos^2(2\beta), \qquad \lambda_{hhhh}^{\text{dec}} = \frac{3m_Z^2}{v^2}\cos^2(2\beta). \tag{1.4.34}$$

Substituting the decoupling limit expression for m_h^2, Eq. (1.4.32) leads exactly to the SM expression for the trilinear and quartic Higgs self-couplings (see appendix E)

$$\lambda_{hhh}^{\text{dec}} = 3\frac{m_{h,0}^2}{v} = \lambda_{hhh}^{\text{SM}}, \qquad \lambda_{hhhh}^{\text{dec}} = 3\frac{m_{h,0}^2}{v^2} = \lambda_{hhhh}^{\text{SM}}. \tag{1.4.35}$$

This means that for pseudoscalar Higgs masses well above the electroweak scale the light scalar tree-level Higgs boson in the MSSM couples exactly as the SM Higgs boson. Furthermore it behaves completely SM-like in the decoupling limit even when loop-corrections are taken into account. This effect can be interpreted as an application of the *Appelquist-Carazzone theorem* [19]. The plot on the left hand side in Figure 1.7 shows the trilinear coupling of three Higgs bosons as a function of the pseudoscalar Higgs mass m_A for two values of $\tan\beta$. The black curves show the coupling of three light scalar MSSM Higgs bosons. The red curves show the trilinear coupling of the SM Higgs boson with a mass equal to the light scalar MSSM Higgs boson mass m_h for the corresponding values of m_A and $\tan\beta$. For high values of $\tan\beta \gtrsim 10$ the Higgs self-couplings in the SM and the MSSM are equal at the per mille level for $m_A \gtrsim 200$ GeV, whereas for lower values of $\tan\beta$ the trilinear couplings coincide at higher m_A. The same is valid also for the quartic couplings shown in the right plot of Figure 1.7.
The heavy scalar H can also become SM like. For this possibility, we consider the case of very small pseudo scalar Higgs masses m_A. Even though these scenarios are irrelevant from a phenomenological point of view[13], it is a nice property of the MSSM, that both scalar MSSM Higgs bosons can take on the role of the SM Higgs.
Taking the limit $m_A \to 0$ of Eq. (1.4.17), we obtain

$$m_H^2 \to m_Z^2, \qquad m_h^2 \to 0. \tag{1.4.36}$$

Moreover Eq. (1.4.25) leads to $\alpha \to -\beta$. We can thus calculate the heavy scalar Higgs self-couplings

$$\lambda_{HHH} \to \frac{3m_Z^2}{v}\cos(2\beta), \qquad \lambda_{HHHH} \to \frac{3m_Z^2}{v^2}\cos^2(2\beta). \tag{1.4.37}$$

[13] Values for $m_A < m_Z$ have been ruled out already by the LEP experiment, see Figure 1.4.

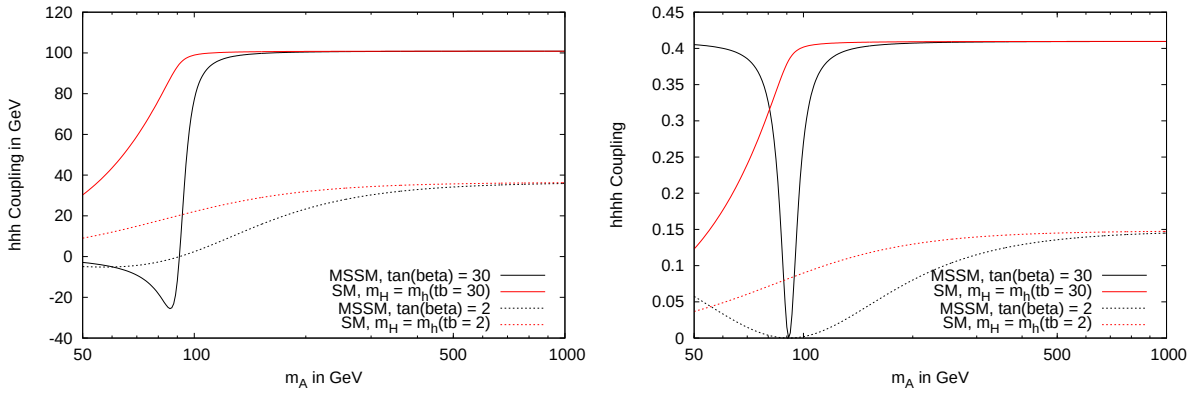

Figure 1.7: The trilinear (left) and quartic (right) Higgs self-couplings as a function of m_A for $\tan\beta = 2$ (dashed) and $\tan\beta = 30$ (solid). Black curves show the couplings of the light Higgs boson, whereas red curves show the couplings of the SM Higgs boson with mass equal to the mass of the light scalar Higgs boson m_h.

Setting $\tan\beta \gg 1$ and substituting $m_Z^2 \to m_H^2$, one obtains

$$\lambda_{HHH} \to -\frac{3m_h^2}{v} = -\lambda_{hhh}^{\rm SM}, \qquad \lambda_{HHHH} \to \frac{3m_h^2}{v^2} = \lambda_{hhhh}^{\rm SM}. \tag{1.4.38}$$

We conclude that in the limit for small m_A and reasonably large t_β the trilinear and quartic couplings of the heavy scalar Higgs boson are identical to the SM Higgs self-couplings, up to a different sign for the trilinear Higgs coupling.

1.5 Radiative Corrections to Higgs Masses and Self-Couplings

In the beginning of the 1990's, it was realized that the tree-level bound for the mass of the light scalar Higgs boson $m_h < m_Z$ is altered by sizable radiative corrections due to the large top-Yukawa coupling h_t. The first calculations of the corrections to the Higgs masses [20] were performed under various simplifying assumptions. The complete $\mathcal{O}(m_t^2\alpha_t)$ calculation[14] [21] used the *Effective Potential Approach (EPA)* and showed that the Higgs mass could be as large as 140 GeV. The dominant $\mathcal{O}(m_t^2\alpha_t)$ corrections to the Higgs masses can be written in the following form

$$m_h^2 \leq m_Z^2 + \frac{3G_F}{\sqrt{2}\pi^2}\frac{m_t^4}{\sin^2(\beta)}\left[\log\frac{m_{\tilde{t}_1}m_{\tilde{t}_2}}{m_t^2} + \frac{X_t^2}{M_{\rm SUSY}^2}\left(1 - \frac{X_t^2}{12M_{\rm SUSY}^2}\right)\right], \tag{1.5.1}$$

where we assumed a common SUSY breaking scale, i.e. $M_{\rm SUSY} = m_U, m_D$. The angle β is related to the ratio of the VEVs $\tan\beta = v_2/v_1$ and G_F is the Fermi constant. These corrections are proportional to the fourth power of the top mass. Moreover the logarithm involving the stop squarks can be sizable for SUSY-breaking scales much larger than the top mass $M_{\rm SUSY} \gg m_t$. Last but not least there can be relevant contributions from stop mixing $X_t = A_t + \mu\cot\beta$.
Soon after complete one-loop diagrammatic results were presented [22,23] taking into account electroweak

[14] Throughout this work, we use the notation $\alpha_t = \frac{h_t^2}{4\pi}$, where h_t is the top-Yukawa coupling. Moreover we use the same notation for the bottom ($t \to b$) and tau ($t \to \tau$) Yukawa couplings as well as for the strong gauge coupling $\alpha_s = \frac{g_s^2}{4\pi}$.

corrections and effects due to non-vanishing external momenta, i.e. $\mathcal{O}(gm_t)$ and $\mathcal{O}(gm_Z)$. Moreover one-loop corrections to Higgs self-couplings were calculated at $\mathcal{O}(m_t^2\alpha_t)$ showing also substantial radiative corrections [24].
These one-loop results exhibit sizable theoretical uncertainties. One way to include two-loop effects is to resum large logs using *Renormalization Group Equations (RGEs)* [25,26]. Using one-loop RGEs, one can resum leading logarithmic (LL) corrections at all loops, whereas two-loop RGEs include next-to-leading logarithmic (NLL) corrections. However, these RGE methods are very complicated for arbitrary MSSM parameters. Moreover they neglect finite (non-logarithmic) contributions.
For these reasons two-loop corrections to the masses were also computed using the EPA and by performing diagrammatic calculations in the limit of vanishing external momenta. The first two-loop calculation took into account $\mathcal{O}(\alpha_t\alpha_s)$ and $\mathcal{O}(\alpha_t^2)$ contributions under simplifying assumptions [27]. From the mid 1990's to the early 2000's $\mathcal{O}(\alpha_t\alpha_s)$ and $\mathcal{O}(\alpha_t^2)$ corrections were improved using the EPA [28–33] and by performing diagrammatic calculations [34]. Later $\mathcal{O}(\alpha_b\alpha_s)$ and $\mathcal{O}(\alpha_b^2)$ corrections due to the bottom-Yukawa coupling α_b were included [35]. To complete the corrections due to third-family-Yukawa couplings $\mathcal{O}(\alpha_b\alpha_\tau)$ and $\mathcal{O}(\alpha_\tau^2)$ corrections were calculated [36], where α_τ is proportional to the τ-Yukawa coupling squared.
Other improvements have been made by calculating the full two-loop effective potential in the MSSM [37]. Even three-loop effects have been studied recently, using RGE techniques [38] and by a diagrammatic calculation up to $\mathcal{O}(\alpha_t\alpha_s^2)$ in the limit of vanishing external momenta [39].
Efforts have been made to complete the one-loop corrections to the Higgs self-couplings [40]. Moreover implications on the self-couplings in the decoupling regime have been studied [41]. There have also been approximations for Higgs boson self-couplings in a general *Two Higgs Doublet Model (THDM)* presented [42]. However, at this point no complete investigation of the two-loop corrections to the Higgs boson self-couplings has been presented.

1.5.1 Motivation

In order to elucidate the origin of the mass of the gauge bosons and the fermions, we have to explore the mechanism of EWSB. In the MSSM EWSB is induced by the fact that the minimum of the Higgs potential resides at non-zero energy density. In order to probe the mechanism of EWSB in the MSSM we therefore have to reconstruct its full Higgs potential. The parameters in the Higgs potential determine the tree-level relations among the Higgs masses and self-couplings. Measuring the relations between the Higgs self-couplings and the masses is therefore crucial for our understanding of the origin of mass.
The Higgs sector in the MSSM, however, receives large radiative corrections such that the tree-level relations between the masses and couplings are substantially modified. In order to compare the theory predictions with the experiment, precise predictions of the observables are essential. The inclusion of two-loop $\mathcal{O}(\alpha_t\alpha_s + \alpha_t)$ effects in the calculation of the Higgs mass reduced the theoretical uncertainties from about 30% at the one-loop order to 5%.
The uncertainties in the existing one-loop $\mathcal{O}(\alpha_t)$ calculation for the trilinear Higgs self-couplings [24] can be as large as 30% and the corrections, compared to the tree-level, can be $\mathcal{O}(100\%)$. In this work we will calculate the two-loop $\mathcal{O}(\alpha_t\alpha_s + \alpha_t)$ radiative corrections to the trilinear and the quartic Higgs self-couplings. Since we work in the framework of an effective theory we obtain *effective couplings*, neglecting effects due to external momenta. These effective couplings should be useful to calculate processes that can be measured in collider experiments.
Higgs boson self-couplings can be probed by studying multiple Higgs production at collider experiments. A preliminary analysis showed that in the case of the LHC, studies of multiple Higgs production require a huge amount of luminosity [43]. Further analyses will demonstrate whether the LHC will be able to deliver results about Higgs self-couplings. A e^+e^- linear collider provides a much cleaner background for such analyses. Depending on the masses of the Higgs bosons, and the center of mass energy of the collider, the trilinear Higgs self-couplings should be measurable at an accuracy of about 20% [44, 45].

Chapter 2

Calculation of Two-Loop Corrections to Higgs Masses and Self-Couplings

2.1 Effective Potential Method

In this chapter we describe in detail how we perform higher order precision calculations in the MSSM Higgs sector. We choose to do this calculation using the *Effective Potential Approach (EPA)*, see [46, 47] for the following reasons. First, to compute the effective potential to some perturbative order we only need to evaluate all *vacuum diagrams*[1] to that order. This simplifies our calculation a lot since the amount and the difficulty of diagrams that have to be computed at the two-loop order is substantially reduced compared to the full diagrammatic approach. Nevertheless we obtain pure analytic results.
Second the EPA is defined in the limit of vanishing external momenta. This may seem like a drawback, but for the effective couplings this is quite convenient. All external momenta effects are highly process dependent. Thus to calculate a process at a collider these effective couplings can be used universally and process dependent corrections can be added afterwards. Moreover corrections due to finite external momenta are typically small because the virtual particles (e.g. tops, stops, gluinos and Higgs bosons) are quite heavy compared to the external momenta.
For some general remarks about the effective potential we will follow [48]. Expanding the effective action $\Gamma(\phi_c)$ in powers of external momenta, we define the *effective potential* $V(\phi_c)$ as the non-derivative part of the effective action

$$\Gamma(\phi_c) = \int dx^4 \left[-V(\phi_c) + \frac{1}{2}(\partial_\mu \phi_c)^2 Z(\phi_c) + \cdots \right]. \tag{2.1.1}$$

After some algebraic manipulation the effective potential can be cast into the following form

$$V(\phi_c) = -\sum_{n=1}^{\infty} \frac{1}{n!} \Gamma^{(n)}(0, ..., 0)[\phi_c]^n. \tag{2.1.2}$$

Here ϕ_c is a constant field (external momenta $p = 0 \Rightarrow \partial_\mu \phi = 0$) including its VEV. Moreover $\Gamma^{(n)}(p_1, ..., p_n)$ is the sum of all one particle irreducible (1PI) Feynman diagrams with n external lines with momenta p_1 to p_n. The effective potential is an effective operator depending on the Higgs fields, where all heavy DOF have been integrated out. The n-th derivative of the effective potential with respect to the fields ϕ_c is just the sum over all 1PI diagrams with n external lines and all external momenta set

[1] Vacuum diagrams, sometimes also called bubble diagrams, are diagrams without any external legs, this means that the number of possible topologies is very limited, see [47].

to zero

$$\Gamma^{(n)}(0,...,0) = -\left.\frac{d^n V(\phi_c)}{d\phi_c^n}\right|_{\phi_c=0}. \tag{2.1.3}$$

So far we have dealt with the *full* effective potential. To compute V in practice we have to approximate by making a loop expansion [47]. The zero-loop contribution corresponds simply to the tree-level potential of the classical Lagrangian. The one-loop approximation is the logarithm of the determinant of the inverse propagator. The higher loop contributions are the sum of all 1PI diagrams with $n > 1$ loops and with zero external momenta (vacuum diagrams), see [49].

2.2 Calculating the Effective Potential in Perturbation Theory

The effective potential can be calculated perturbatively. The relative size of the different orders in perturbation theory is known for the MSSM Higgs masses, see [20–23, 25–39]. For the MSSM Higgs self-couplings we expect the hierarchy between different orders in perturbation theory to be similar to the Higgs masses.

The dominant one-loop corrections emerge from the large *top-Yukawa coupling* h_t, introduced in the superpotential Eq. (1.3.1) [20–23]. Throughout the whole calculation we work in the limit $h_t \gg h_{q\neq t}$ and thus set to zero all Yukawa couplings other than the top-Yukawa coupling. Moreover we treat $h_t \gg g, g'$ (this is referred to as the *gaugeless limit* by [33] and as the *leading approximation* by [30]). The only contributing gauge coupling beyond tree-level is thus the strong gauge coupling g_s. The corresponding Lagrangians can be derived from Eqs. (1.2.15, 1.2.16, 1.2.17, 1.2.19) and are given in the appendix C.3.1 and C.4.1. At the one-loop level corrections to the Higgs effective potential can therefore only occur via the top-Yukawa coupling since the Higgs sector is color neutral. The one-loop diagrams are shown in Figure 2.1. They all go with the top-Yukawa coupling squared and are therefore called $\mathcal{O}(\alpha_t)$, where $\alpha_t = \frac{h_t^2}{4\pi}$.

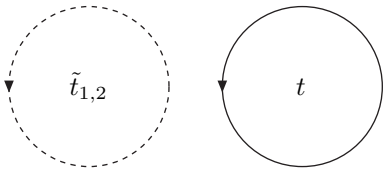

Figure 2.1: Vacuum diagrams that contribute to the one-loop $\mathcal{O}(\alpha_t)$ corrections to the effective potential.

The one-loop diagrams involve colored particles. It is therefore obvious that at the two-loop level we have corrections that go with the strong coupling α_s, which we call Supersymmetric Quantum ChromoDynamical (SQCD) corrections, i.e. $\mathcal{O}(\alpha_t\alpha_s)$. The corresponding diagrams that contribute to the effective potential involve gluon exchange in the top and stop loop of Figure 2.1. Moreover due to the supersymmetrization of the t-$\bar{t}$-gluon gauge coupling we also have a top-stop-gluino-diagram and also the four-stop-vertex depends on the gauge coupling due to the D-terms, see Eq. (1.2.19). In Figure 2.2 all two-loop SQCD diagrams are shown. It is known [26–28, 30, 33–37] that in most of the MSSM parameter space $\mathcal{O}(\alpha_t\alpha_s)$ constitutes the dominant two-loop corrections.

In the limit we are working in there is only one further two-loop correction, namely $\mathcal{O}(\alpha_t^2)$. The work of [33] showed that in regions of the MSSM parameter space, with large stop mixing X_t the $\mathcal{O}(\alpha_t^2)$ can be comparable in size to the $\mathcal{O}(\alpha_t\alpha_s)$. Looking at the corresponding Lagrangian Eq. (C.4.5) we see that there are a lot more particles involved, namely Higgs and would-be Goldstone bosons $\mathcal{H}_i = (H, h, G, A)$,

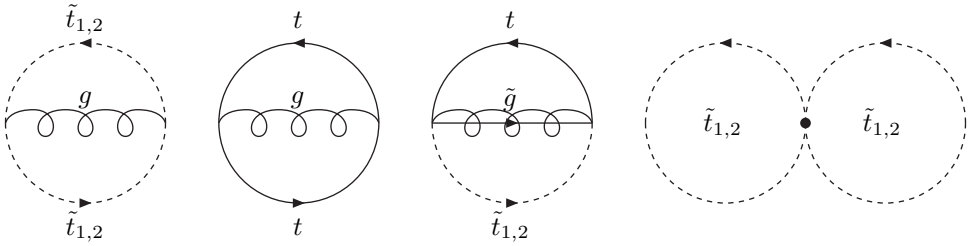

Figure 2.2: Vacuum diagrams that contribute to the two-loop $\mathcal{O}(\alpha_t\alpha_s)$ corrections to the effective potential.

$\mathcal{H}^{\pm}_{1,2} = (H^{\pm}, G^{\pm})$, Higgsinos $(\tilde{H}^0_{1,2}, \tilde{H}^{\pm})$, quarks (t, b) and squarks $(\tilde{t}_1, \tilde{t}_2, \tilde{b}_L)$. Figure 2.3 shows all diagrams that contribute to the effective potential at $\mathcal{O}(\alpha_t^2)$.

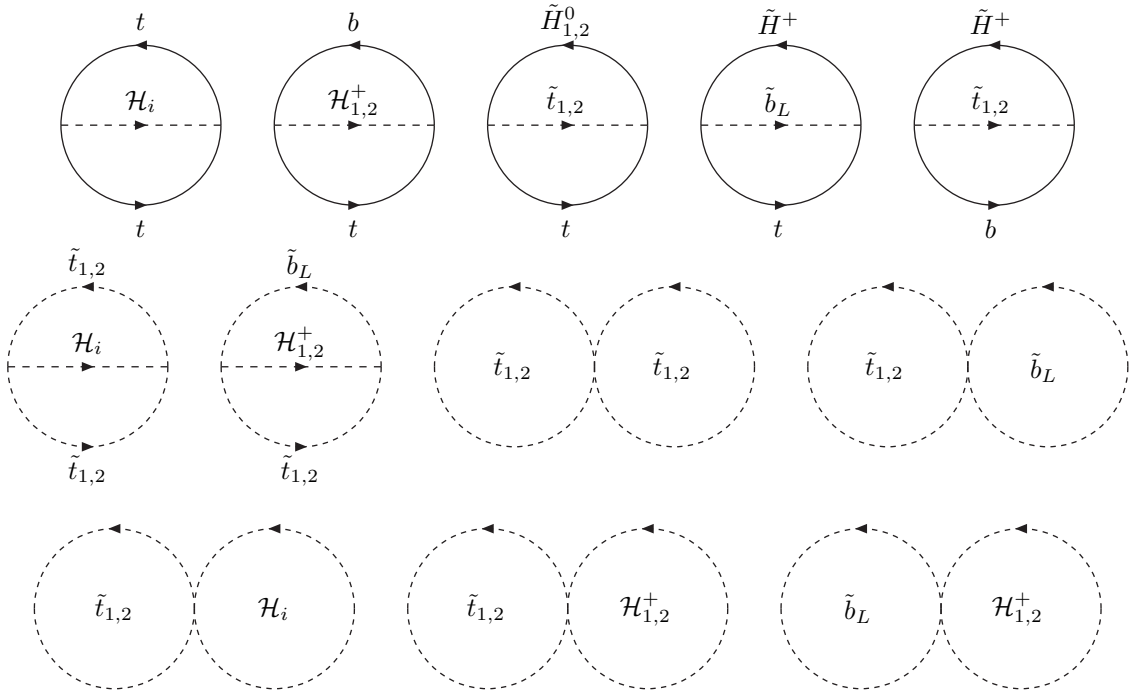

Figure 2.3: Vacuum diagrams that contribute to the two-loop $\mathcal{O}(\alpha_t^2)$ corrections to the effective potential.

2.2.1 Perturbative Expansion of the Effective Potential

At this point it is necessary to make some comments about the approximations in our perturbative expansion of the effective potential. First, since we work in the limit where the top-quark Yukawa coupling is much larger than all other Yukawa couplings, we treat all other SM fermions as massless. The

only non-top-quark[2] that shows up in the effective potential is the bottom quark with mass $m_b = 0$. This simplifies also the sbottom mass matrix, see Eq. (1.3.3), which becomes diagonal with entries (m_Q^2, m_D^2). In the absence of sbottom mixing, only the left sbottom contributes to the $\mathcal{O}(\alpha_t^2)$ potential with mass $m_{\tilde{b}_L} = m_Q$.
Second, the consequence of treating the electroweak gauge couplings to be much smaller than the top-Yukawa coupling is that also the weak gauge bosons are massless $m_W = m_Z = 0$ beyond the tree-level[3]. This also affects virtual Higgs particles that occur at $\mathcal{O}(\alpha_t^2)$ of the potential. We work with $m_h = 0$ and $m_H = m_{H^\pm} = m_A$ and therefore $\alpha = \beta - \pi/2$ at $\mathcal{O}(\alpha_t^2)$.
Third, at $\mathcal{O}(\alpha_t^2)$ Higgsinos do not mix with the gauginos since these mixing terms are proportional to g and g'. All Higgsinos have degenerate mass μ. The gluino mass is taken as an input parameter $m_{\tilde{g}} = M_3$, which corresponds to the SUSY-breaking gaugino mass M_3. We do not need to consider radiative corrections to Higgsino or gaugino masses, because they enter only at the two-loop level, i.e. corrections to these masses are three-loop effects.
Last but not least in the one-loop masses, terms of $\mathcal{O}(m_A^2\alpha_t)$ and $\mathcal{O}(m_Z^2\alpha_t)$ are not taken into account, because they partly emerge from non-vanishing momenta of external Higgs fields. The correct notation for the effective potential at one-loop order is actually $\mathcal{O}(m_t^2\alpha_t)$, similarly the two-loop corrections[4] are of $\mathcal{O}(m_t^2\alpha_t\alpha_s)$ and $\mathcal{O}(m_t^2\alpha_t^2)$. Although it is not obvious at first glance why these terms should be smaller than the one-loop $\mathcal{O}(m_t^2\alpha_t)$ from the effective potential, it is perfectly consistent in terms of our perturbative expansion to omit them. In fact $\mathcal{O}(m_A^2\alpha_t)$ and $mathcalO(m_Z^2\alpha_t)$-terms have a much smaller radius of convergence than the $\mathcal{O}(m_t^2\alpha_t)$-terms. Moreover effects due to non-vanishing external momenta are highly non-universal and for the one-loop light scalar Higgs mass these effects have been calculated to be at most $3-5\%$ [23].

2.2.2 Some Technical Details on Calculating the Effective Potential

After making up our minds about which orders we want to take into account, we have to evaluate the effective potential $V^{\mathcal{O}(0+\alpha_t+\alpha_t\alpha_s+\alpha_t^2)} \equiv V^0 + \delta V^{\alpha_t} + \delta V^{\alpha_t\alpha_s} + \delta V^{\alpha_t^2}$. These parts of the effective potential have already been calculated in [28, 30–33]. In principle we simply have to compute vacuum diagrams up to the desired order in perturbation theory and make the potential a Higgs field-dependent quantity. Naively this is done by re-expressing the Higgs VEVs with the corresponding fields, i.e. $v_1 \to \sqrt{2}H_1^0$ and $v_2 \to \sqrt{2}H_2^0$. There is a subtlety involved. The neutral Higgs fields are complex quantities, whereas the VEVs (as well as the top and stop masses, which depend on the VEVs) are real. To consistently implement the Higgs field-dependence we closely follow [32], see appendix C.1. The diagrams we have to evaluate consist of simply a loop without external lines for the $\mathcal{O}(\alpha_t)$ (Figure 2.1) and for the $\mathcal{O}(\alpha_t\alpha_s)$ and $\mathcal{O}(\alpha_t^2)$ two-loop cases we have the "sunset" and "eight" topologies (Figure 2.2 and 2.3). All two-loop integrations can be reduced by algebraic manipulation to the two following scalar master integrals

$$\frac{\mu_0^{2(4-d)}}{(2\pi)^{2d}} \int\int \frac{d^dp d^dq}{[p^2-m_1^2][q^2-m_2^2]} \equiv \frac{-1}{(16\pi^2)^2} J(m_1^2, m_2^2), \tag{2.2.1}$$

$$\frac{\mu_0^{2(4-d)}}{(2\pi)^{2d}} \int\int \frac{d^dp d^dq}{[p^2-m_1^2][q^2-m_2^2][(p-q)^2-m_3^2]} \equiv \frac{1}{(16\pi^2)^2} I(m_1^2, m_2^2, m_3^2). \tag{2.2.2}$$

The techniques to evaluate the integrals have been developed in the beginning of the 1990's. The first method was based on the Mellin-Barnes representation of massive denominators [50]. Another

[2] Remember that we assumed the soft SUSY breaking Lagrangian, see Eq. (1.3.2), to be flavor diagonal. If we took into account the possibility of flavor mixing other quarks would show up in the loops, too.

[3] In the tree-level calculation, however, we keep the $\mathcal{O}(m_Z)$-terms, which is consistent, since at the tree-level there are no h_t or α_s terms and thus the hierarchy $h_t, \alpha_s \gg g, g'$ does not apply.

[4] Effects of $\mathcal{O}(M_{\text{SUSY}}^2\alpha_t)$ are not present in the effective potential. However, we include them in the transversal self-energy of the W-bosons, see Eq. (D.3.5). Numerically they are not important since they are proportional to small logarithms.

powerful method uses differential equations [51]. Explicit expressions for the functions $J(m_1^2, m_2^2)$ and $I(m_1^2, m_2^2, m_3^2)$ are shown in appendix B. For a detailed derivation of the effective potential see section C in the Appendix.

Regularization of divergences: Naively evaluating these loop diagrams for the effective potential yields infinities. The reason for that is that in a quantum field theory we need to take into account all possible virtual particles that can occur in a loop. This means we also have to sum over all helicity states, colors and any other quantum number when evaluating a loop diagram and we also have to take into account all possible momenta k. We therefore have to integrate over the four-dimensional loop-momentum. Transforming to spherical coordinates yields integrals of the form

$$\int d^4k|k|^n \sim \int_0^\infty d|k||k|^{n+3}. \tag{2.2.3}$$

There are two kinds of divergences: *Ultra-Violet (UV)* divergences occur at infinite momentum. This means that any integrand $|k|^n$ with $n > -4$ will yield a power-like UV-divergence, whereas the case $n = -4$ leads to a logarithmic UV-divergence of the integral. The second type are *infra-red (IR)* divergences which occur when there is a massless particle in a loop

$$\int_0^\infty \frac{d|k|}{|k|^2 - m^2} \xrightarrow[m \to 0]{} \int_0^\infty \frac{d|k|}{|k|^2}. \tag{2.2.4}$$

This develops a pole for $k \to 0$, i.e. at low momentum. It has been shown that IR-divergences cancel against real corrections due to low energy emission of these massless particles. This is known as the Bloch-Nordsieck Theorem [52]. An extension of this is the Kinoshita-Lee-Nauenberg (KLN) theorem [53], which states that in all final states the IR singularities cancel in the SM[5].
The UV-divergences originate from the fact that we treat our theory as if it was valid up to arbitrary high energies. Experimentally we can only test a theory in a certain energy range and therefore it is completely fine to assume that any quantum field theory is only valid up to some cutoff energy. Although it has been proven in the beginning of the 1970's that the SM is renormalizable [54], (all UV poles in perturbatively calculated, renormalized observables cancel) the SM cannot be a UV complete theory. First the $U(1)_Y$ gauge coupling g', and the quartic Higgs coupling λ run into a Landau pole or $-\infty$ at very high energies. Second we know that at least at the Planck scale the SM has to be extended to include gravity, which becomes strong at this energy.
With this in the back of our mind it seems quite natural to cure these UV-divergent integrals by introducing some finite cutoff in energy Λ_{UV} and to only perform loop integrations up to that energy scale. The cutoff scale serves as a regulator in our theory and all loop integrals will depend on this regulator Λ_{UV}. This is one example of a regularization method, known as *momentum cutoff regularization*[6]. We introduce a new parameter (regulator) to give the divergent integrals a mathematically well-defined meaning. In the SM *dimensional regularization (DREG)* [56] is the most convenient method since it preserves all gauge symmetries[7] of the Lagrangian. In DREG we use the fact that our integrals diverge in four space-time dimensions but are finite in fewer dimensions. By performing the integration in $d = 4-2\epsilon$ space-time dimensions we obtain well-defined results which are analytical functions[8] in ϵ.

[5] Real emission of massless gauge bosons can also cause divergences in collinear regions of phase space. Divergences originating from initial state radiation have to be absorbed in parton distribution functions in QCD and electron density functions in QED.

[6] Naive application of a momentum cutoff regularization violates both Lorentz and gauge invariance. One of the first attempts to regularize UV divergent integrals with a momentum cutoff was conducted by Pauli and Villars [55].

[7] When using DREG in chiral gauge theories, γ_5-matrices cause problems. Defining γ_5-matrices in an arbitrary number of dimensions violated Ward [57] and Slavnov-Taylor [58] identities. These identities have to be fixed by hand, for example by introducing non-trivial counter terms [54].

[8] In general they can be distributions. In this calculation, however, we obtain functions in ϵ.

It is well known, however, that even DREG violates supersymmetry. This is easy to see, in DREG both momenta and vectors (e.g. the Lorentz index in the γ-matrices) are continued to d dimensions. This introduces a mismatch in the degrees of freedom between gauge bosons and their fermionic superpartners the gauginos. In our calculation we use the *dimensional reduction method (DRED)*, see [59] to avoid this problem. In DRED, the momenta are still continued to d dimensions but vectors are fixed to four dimensions. This comes at the price of extra 2ϵ components of the gauge fields, that transform as scalars in the adjoint representation of the gauge group and are known as *epsilon-scalars*. The renormalization scheme using modified minimal subtraction ($\overline{\text{MS}}$) associated with DRED is called $\overline{\text{DR}}$. It was shown [60], however, that by using a special version of the $\overline{\text{DR}}$ scheme these epsilon- scalars fully decouple from the calculation of the effective potential so we can ignore them in this calculation. We will turn to the issue of renormalization again in section 2.5 where we show how we get rid of the regulator ϵ and thus obtain finite quantities. First, however, we will use the regularized, but unrenormalized effective potential to calculate masses and couplings, which depend on the regulator ϵ.

Gauge invariance: One of the most fundamental principles in modern quantum field theory is that all observables, i.e. physical predictions of the theory, have to be gauge invariant. This means that we can perform calculations in any desired gauge. In our case we choose to do the calculation of the $\mathcal{O}(\alpha_t\alpha_s)$ potential in t'Hooft-Feynman gauge, because gauge boson propagators are easier to handle in that gauge. The $\mathcal{O}(\alpha_t)$ and $\mathcal{O}(\alpha_t^2)$ potentials will be calculated in Landau gauge. This is convenient because in this gauge would-be Goldstone bosons are massless. Note that the effective potential is not an observable and may in principle be a gauge dependent quantity. The masses and couplings that are generated by taking derivatives of the effective potential are physical, they must be gauge independent. Gauge dependent terms in the effective potential must therefore be field-independent.

2.2.3 Notation and Field-Dependence of the Effective Potential

In the previous section we have described how we calculate the effective potential. The result is given in the appendix Eqs. (C.2.54, C.3.9), C.4.19). Before we can use this potential to calculate masses and couplings, we have to make it a Higgs field-dependent quantity.
The tree-level Higgs potential was presented in Eq. (1.4.3). The loop-corrections to the effective potential are functions of field-dependent quantities, see appendix C.1, i.e.

$$\delta V^{\alpha_t}(\bar{m}_t^2, \bar{m}_{\tilde{t}_1}^2, \bar{m}_{\tilde{t}_2}^2), \qquad \delta V^{\alpha_t\alpha_s}(\bar{m}_t^2, \bar{m}_{\tilde{t}_1}^2, \bar{m}_{\tilde{t}_2}^2, s_{2\bar{\theta}}^2, \bar{\xi}), \qquad \delta V^{\alpha_t^2}(\bar{m}_t^2, \bar{m}_{\tilde{t}_1}^2, \bar{m}_{\tilde{t}_2}^2, s_{2\bar{\theta}}^2, \bar{\xi}). \tag{2.2.5}$$

Two remarks on the notation are necessary:
(i) A small letter δ in front of a quantity indicates that the quantity has a pole in the regulator ϵ, whereas a capital Δ means that the quantity is finite. The higher order corrections to the effective potential contain poles in ϵ.
(ii) The field-dependent arguments of the effective potential are denoted by a 'bar'

$$\bar{x}_i = (\bar{m}_t^2, \bar{m}_{\tilde{t}_1}^2, \bar{m}_{\tilde{t}_2}^2, s_{2\bar{\theta}}^2, \bar{\xi}), \qquad i = 1, \cdots, 5, \tag{2.2.6}$$

where $\bar{x}_i \equiv \bar{x}_i(H_j^0)$. When evaluating all fields at the minimum of the potential, denoted by $|_{\min}$ (i.e. substituting them by their VEVs: $H_1^0 \to \frac{v_1}{\sqrt{2}}$ and $H_2^0 \to \frac{v_2}{\sqrt{2}}$) we obtain the corresponding field-independent quantities $\bar{x}_i|_{\min} = x_i = (m_t^2, m_{\tilde{t}_1}^2, m_{\tilde{t}_2}^2, s_{2\theta}^2, m_t s_{2\theta})$, which were introduced in section 1.3.1 when we discussed sfermion masses.

The field-dependence of the arguments of the potentials $\bar{x}_i$ is given by

$$\bar{m}_t^2 = h_t^2 |H_2^0|^2, \tag{2.2.7}$$

$$\bar{m}_{\tilde{t}_1}^2 = \frac{1}{2}\left(m_U^2 + m_Q^2 + 2\bar{m}_t^2 + \sqrt{(m_Q^2 - m_U^2)^2 + 4|\tilde{X}|^2} \right), \tag{2.2.8}$$

$$\bar{m}_{\tilde{t}_2}^2 = \frac{1}{2}\left(m_U^2 + m_Q^2 + 2\bar{m}_t^2 - \sqrt{(m_Q^2 - m_U^2)^2 + 4|\tilde{X}|^2} \right), \tag{2.2.9}$$

$$s_{2\bar{\theta}}^2 = \frac{4|\tilde{X}|^2}{(\bar{m}_{\tilde{t}_1}^2 - \bar{m}_{\tilde{t}_2}^2)^2}, \tag{2.2.10}$$

$$\bar{\xi} = 2\frac{\Re(X)\Re(\tilde{X}) + \Im(X)\Im(\tilde{X})}{\bar{m}_{\tilde{t}_1}^2 - \bar{m}_{\tilde{t}_2}^2}, \tag{2.2.11}$$

where the following quantities are obviously field-dependent, but we omit the 'bar' notation

$$X = h_t H_2^0, \tag{2.2.12}$$

$$\tilde{X} = h_t (A_t H_2^0 + \mu (H_1^0)^\star). \tag{2.2.13}$$

quantities that have to be renormalized. The parameters that enter in the two-loop potentials $\delta V^{\alpha_t \alpha_s}$ and $\delta V^{\alpha_t^2}$ are $g_s, m_{\tilde{g}}, \beta, m_A, m_{\tilde{b}_L}$ and do not have to be renormalized, because any correction to them is a higher order effect. This was also the reason that made it possible for us to use the simplifications described in section 2.2.1 (e.g. $\alpha = \beta - \pi/2$, $m_H^2 = m_{H^\pm}^2 = m_A^2$, $m_h^2 = 0$ and $m_{\tilde{H}}^2 = \mu^2$).

2.3 Unrenormalized Masses and Couplings

In this section we describe how we take derivatives of the unrenormalized effective potential to obtain neutral Higgs masses and self-couplings. In section 2.5 we will explain how these masses and couplings are renormalized to obtain finite physical quantities.

2.3.1 Neutral Higgs Masses

In section 1.4 we discussed the MSSM Higgs sector and EWSB at tree-level. To calculate loop-corrected Higgs masses, we proceed in a similar way. We write the neutral complex Higgs fields as a real and an imaginary part with a normalization factor $\sqrt{1/2}$

$$H_i^0 = \frac{1}{\sqrt{2}}(a_i + iP_i), \qquad a_i, P_i \quad real \tag{2.3.1}$$

The VEV induced by the Higgs field, i.e. the ground state of the theory, induces SSB. It is determined by the minimum of the effective potential and is therefore affected by radiative corrections[9].

Minimizing the effective potential: Analogous to the tree-level discussion, only the real part a_i of the neutral Higgs fields acquires a VEV. We call the minimum of the complete loop-corrected potential $v_i^{\min}$

$$\left.\frac{\partial V^{\mathcal{O}(x)}(a_k, P_k)}{\partial a_i}\right|_{a_k = v_k^{\min}, P_k = 0} = 0, \qquad i,k = 1,2. \tag{2.3.2}$$

[9] S. Coleman and E. Weinberg suggested in [46] that radiative corrections could be the origin of EWSB. In the SM we also need spontaneous symmetry breaking in order to produce fermion and gauge boson masses. However, the effect of dynamical symmetry breaking is still relevant.

We split the effective potential into a tree-level and a higher order part $V^{\mathcal{O}(x)} = V^0 + \delta V^{\mathcal{O}(x)}$. Evaluating the tree-level part we can write the two minimization equations as

$$\begin{aligned}
(m_1^0)^2 + (m_3^0)^2 \frac{v_2^{\min}}{v_1^{\min}} + \frac{g^2+g'^2}{8}\left[(v_1^{\min})^2 - (v_2^{\min})^2\right] + \frac{1}{v_1^{\min}} \left.\frac{\partial \delta V^{\mathcal{O}(x)}(a_k, P_k)}{\partial a_1}\right|_{a_k = v_k^{\min}, P_k = 0} &= 0 \\
(m_2^0)^2 + (m_3^0)^2 \frac{v_1^{\min}}{v_2^{\min}} - \frac{g^2+g'^2}{8}\left[(v_1^{\min})^2 - (v_2^{\min})^2\right] + \frac{1}{v_2^{\min}} \left.\frac{\partial \delta V^{\mathcal{O}(x)}(a_k, P_k)}{\partial a_2}\right|_{a_k = v_k^{\min}, P_k = 0} &= 0. \quad (2.3.3)
\end{aligned}$$

The neutral parts of the Higgs doublets are expanded around these minima

$$H_i^0 = \frac{1}{\sqrt{2}}(v_i^{\min} + S_i + iP_i). \quad (2.3.4)$$

The fluctuations S_i around the VEVs correspond to the physical CP-even Higgs current eigenstates with zero VEVs $\langle S_i \rangle = 0$. The minimization condition means that there are no tadpole terms, i.e. linear terms in the fields S_i and P_i in the effective potential. Eq. (2.3.4) is inserted into the complete Lagrangian, such that the whole theory is expanded around the true, loop-corrected minima and we obtain the relations between the tree-level parameters and the VEV, similar to Eqs. (1.4.9, 1.4.10)

$$\begin{aligned}
G_F^0 = \frac{1}{\sqrt{2}[(v_1^{\min})^2 + (v_2^{\min})^2]}, \quad (m_Z^0)^2 = \frac{(g^0)^2 + (g'^0)^2}{4}[(v_1^{\min})^2 + (v_2^{\min})^2], \\
(m_W^0)^2 = \frac{(g^0)^2}{4}[(v_1^{\min})^2 + (v_2^{\min})^2], \quad (m_t^0)^2 = \frac{(h_t^0)^2}{2}(v_2^{\min})^2, \quad \cdots \quad (2.3.5)
\end{aligned}$$

The ellipses represent stop masses, other quark masses and the stop mixing angle, which do all depend on these minima $v_i^{\min}$. Note that here we explicitly indicated with a '0'-superscript that all parameters are the tree-level (bare) parameters. Even though the minima are computed using the loop-corrected potential, they receive radiative corrections, when they are matched to the loop-corrected Fermi constant. We will turn back to this issue in section 2.5.6, where we discuss renormalization schemes.

Masses: Bilinear terms in the fields S_i and P_i correspond to mass-terms. We expand the effective potential around the minimum, i.e. we use Eq. (2.3.4) to write the effective potential as a function of S_i and P_i. We define the CP-even and CP-odd mass matrices by taking two derivatives with respect to (w.r.t.) the corresponding fields and evaluate everything at the minimum of the potential, denoted by $|_{\min}$ which corresponds to substituting all fields by their VEVs, i.e. $S_k = 0, P_k = 0$

$$(\mathcal{M}_P^2)_{ij}^{\mathcal{O}(x)} \equiv \left.\frac{\partial^2 V^{\mathcal{O}(x)}(S_k, P_k)}{\partial P_i \partial P_j}\right|_{\min}, \qquad (\mathcal{M}_S^2)_{ij}^{\mathcal{O}(x)} \equiv \left.\frac{\partial^2 V^{\mathcal{O}(x)}(S_k, P_k)}{\partial S_i \partial S_j}\right|_{\min}. \quad (2.3.6)$$

Using the explicit tree-level part of the effective potential V^0, the minimization equations Eq. (2.3.3) can be used to eliminate the dependence on $(m_1^0)^2$ and $(m_2^0)^2$ in the mass matrices

$$\begin{aligned}
(\mathcal{M}_P^2)_{ij}^{\mathcal{O}(x)} &= -(m_3^0)^2 \frac{v_1^{\min} v_2^{\min}}{v_i^{\min} v_j^{\min}} - \frac{\delta_{ij}}{v_i^{\min}} \left.\frac{\partial \delta V^{\mathcal{O}(x)}(S_k, P_k)}{\partial S_i}\right|_{\min} + \left.\frac{\partial^2 \delta V^{\mathcal{O}(x)}(S_k, P_k)}{\partial P_i \partial P_j}\right|_{\min} \quad (2.3.7) \\
(\mathcal{M}_S^2)_{ij}^{\mathcal{O}(x)} &= (-1)^{i+j}\left[-(m_3^0)^2 \frac{v_1^{\min} v_2^{\min}}{v_i^{\min} v_j^{\min}} + \frac{g^2+g'^2}{4} v_i^{\min} v_j^{\min}\right] - \frac{\delta_{ij}}{v_i^{\min}} \left.\frac{\partial \delta V^{\mathcal{O}(x)}(S_k, P_k)}{\partial S_i}\right|_{\min} \\
&\quad + \left.\frac{\partial^2 \delta V^{\mathcal{O}(x)}(S_k, P_k)}{\partial S_i \partial S_j}\right|_{\min}. \quad (2.3.8)
\end{aligned}$$

This is convenient, because we have reduced the number of parameters and we do not have to worry about the renormalization of $(m_1^0)^2$ and $(m_2^0)^2$ but only about the renormalization of the minima $v_i^{\min}$. Combining the expression for the CP-odd and CP-even mass matrix Eqs. (2.3.7, 2.3.8) we use the former to express the latter

$$(\mathcal{M}_S^2)_{ij}^{\mathcal{O}(x)} = (\mathcal{M}_S^2)_{ij}^0 + (\delta\mathcal{M}_S^2)_{ij}^{\mathcal{O}(x)}, \tag{2.3.9}$$

where we split the CP-even mass matrix into a "tree-level-like" part $(\mathcal{M}_S^2)^0$ and a "higher order" part[10] $(\delta\mathcal{M}_S^2)^{\mathcal{O}(x)}$

$$(\mathcal{M}_S^2)_{ij}^0 \equiv (-1)^{i+j}\left[(\mathcal{M}_P^2)_{ij}^{\mathcal{O}(x)} + \frac{g^2+g'^2}{4} v_i^{\min} v_j^{\min}\right], \tag{2.3.10}$$

$$(\delta\mathcal{M}_S^2)_{ij}^{\mathcal{O}(x)} \equiv -(-1)^{i+j}\left.\frac{\partial^2 \delta V^{\mathcal{O}(x)}(S_k,P_k)}{\partial P_i \partial P_j}\right|_{\min} + \left.\frac{\partial^2 \delta V^{\mathcal{O}(x)}(S_k,P_k)}{\partial S_i \partial S_j}\right|_{\min}. \tag{2.3.11}$$

In the following paragraph we will express the CP-odd mass matrix in a nice form and in section 2.5.5 and 2.5.6 we will describe how the mass matrices are renormalized, such that it becomes apparent why we calculate $(\mathcal{M}_S^2)^{\mathcal{O}(x)}$ using Eqs. (2.3.10, 2.3.11).
To evaluate the derivatives of the effective potential we express $\delta V^{\mathcal{O}(x)}$ as a function of field-dependent quantities $\bar{x}_k(S_m,P_m) = (\bar{m}_t^2, \bar{m}_{\tilde{t}_1}^2, \bar{m}_{\tilde{t}_2}^2, s_{2\bar{\theta}}^2, \bar{\xi})$ and use the *chain rule*

$$\left.\frac{\partial \delta V^{\mathcal{O}(x)}(\bar{x}_k(S_m,P_m))}{\partial S_i}\right|_{\min} = \sum_{\hat{i}} \frac{\partial \delta V^{\mathcal{O}(x)}(\bar{x}_k)}{\partial \bar{x}_{\hat{i}}} \left.\frac{\partial \bar{x}_{\hat{i}}}{\partial S_i}\right|_{\min}, \tag{2.3.12}$$

$$\left.\frac{\partial^2 \delta V^{\mathcal{O}(x)}(\bar{x}_k(S_m,P_m))}{\partial S_i \partial S_j}\right|_{\min} = \sum_{\hat{i},\hat{j}} \frac{\partial^2 \delta V^{\mathcal{O}(x)}(\bar{x}_k)}{\partial \bar{x}_{\hat{i}} \partial \bar{x}_{\hat{j}}} \left.\frac{\partial \bar{x}_{\hat{i}}}{\partial S_j}\right|_{\min} \left.\frac{\partial \bar{x}_{\hat{j}}}{\partial S_i}\right|_{\min} + \sum_{\hat{i}} \frac{\partial \delta V^{\mathcal{O}(x)}(\bar{x}_k)}{\partial \bar{x}_{\hat{i}}} \left.\frac{\partial^2 \bar{x}_{\hat{i}}}{\partial S_i \partial S_j}\right|_{\min}. \tag{2.3.13}$$

Note that we use a 'hat' on an index to denote that it is a dummy index which we will sum over. For derivatives w.r.t. the CP-odd fields P_i we get formally the same by replacing $S_i \to P_i$. The result for the complete CP-odd mass matrix can be written in the following way

$$(\mathcal{M}_P^2)^{\mathcal{O}(x)} = \begin{pmatrix} \frac{v_2^{\min}}{v_1^{\min}} & 1 \\ 1 & \frac{v_1^{\min}}{v_2^{\min}} \end{pmatrix} \Bigg\{ -(m_3^0)^2 + \left(\frac{h_t^2 \mu A_t}{m_{\tilde{t}_1}^2 - m_{\tilde{t}_2}^2}\right)\Bigg[\frac{\partial \delta V^{\mathcal{O}(x)}}{\partial \bar{m}_{\tilde{t}_2}^2} - \frac{\partial \delta V^{\mathcal{O}(x)}}{\partial \bar{m}_{\tilde{t}_1}^2} - \frac{4c_{2\theta}^2}{m_{\tilde{t}_1}^2 - m_{\tilde{t}_2}^2}\frac{\partial \delta V^{\mathcal{O}(x)}}{\partial s_{2\bar{\theta}}^2} + \left(\frac{s_{2\theta}^2}{X_t} - \frac{1}{A_t}\right)\frac{\partial \delta V^{\mathcal{O}(x)}}{\partial \bar{\xi}}\Bigg]\Bigg\}. \tag{2.3.14}$$

This result has a very simple structure. The reason is that any single derivative of $\bar{m}_t^2, \bar{m}_{\tilde{t}_1}^2, \bar{m}_{\tilde{t}_2}^2, s_{2\bar{\theta}}^2, \bar{\xi}$ w.r.t. only one CP-odd field P_i vanishes at the minimum $S_k = 0, P_k = 0$. Only terms with two derivatives of the P_i contribute to the above expression.
The result for the loop-corrections to the CP-even mass matrix $(\delta\mathcal{M}_S^2)_{ij}^{\mathcal{O}(x)}$ is more complicated. In [32], it is expressed in terms of

$$(\delta\mathcal{M}_S^2)_{11}^{\mathcal{O}(x)} = \frac{1}{2} h_t^2 \mu^2 s_{2\theta}^2 F_3^{\mathcal{O}(x)}, \tag{2.3.15}$$

$$(\delta\mathcal{M}_S^2)_{12}^{\mathcal{O}(x)} = h_t^2 \mu m_t s_{2\theta} F_2^{\mathcal{O}(x)} + \frac{1}{2} h_t^2 A_t \mu s_{2\theta}^2 F_3^{\mathcal{O}(x)}, \tag{2.3.16}$$

$$(\delta\mathcal{M}_S^2)_{22}^{\mathcal{O}(x)} = 2h_t^2 m_t^2 F_1^{\mathcal{O}(x)} + 2h_t^2 A_t m_t s_{2\theta} F_2^{\mathcal{O}(x)} + \frac{1}{2} h_t^2 A_t^2 s_{2\theta}^2 F_3^{\mathcal{O}(x)}. \tag{2.3.17}$$

[10] This notation and the labeling "tree-level-like" and "higher order" are misleading. The "tree-level-like" part $(\mathcal{M}_S^2)^0$ contains already higher order contributions through $(\mathcal{M}_P^2)^{\mathcal{O}(x)}$.

The functions $F_i^{\mathcal{O}(x)}$, for $i = 1, 2, 3$ can be expressed as[11]

$$\begin{aligned}
F_1^{\mathcal{O}(x)} =& \frac{\partial^2\delta V^{\mathcal{O}(x)}}{\partial(\bar{m}_t^2)^2} + \frac{\partial^2\delta V^{\mathcal{O}(x)}}{\partial(\bar{m}_{\tilde{t}_1}^2)^2} + \frac{\partial^2\delta V^{\mathcal{O}(x)}}{\partial(\bar{m}_{\tilde{t}_2}^2)^2} + 2\frac{\partial^2\delta V^{\mathcal{O}(x)}}{\partial\bar{m}_t^2\partial\bar{m}_{\tilde{t}_1}^2} + 2\frac{\partial^2\delta V^{\mathcal{O}(x)}}{\partial\bar{m}_t^2\partial\bar{m}_{\tilde{t}_2}^2} \\
&+ \frac{s_{2\theta}}{m_t}\left(\frac{\partial^2\delta V^{\mathcal{O}(x)}}{\partial\bar{m}_t^2\partial\bar{\xi}} + \frac{\partial^2\delta V^{\mathcal{O}(x)}}{\partial\bar{m}_{\tilde{t}_1}^2\partial\bar{\xi}} + \frac{\partial^2\delta V^{\mathcal{O}(x)}}{\partial\bar{m}_{\tilde{t}_2}^2\partial\bar{\xi}}\right) + 2\frac{\partial^2\delta V^{\mathcal{O}(x)}}{\partial\bar{m}_{\tilde{t}_1}^2\partial\bar{m}_{\tilde{t}_2}^2} + \frac{s_{2\theta}^2}{4m_t^2}\frac{\partial^2\delta V^{\mathcal{O}(x)}}{\partial\bar{\xi}^2}, \qquad (2.3.18)\\
F_2^{\mathcal{O}(x)} =& -\frac{s_{2\theta}}{m_t(m_{\tilde{t}_1}^2 - m_{\tilde{t}_2}^2)}\frac{\partial\delta V^{\mathcal{O}(x)}}{\partial\bar{\xi}} + \frac{\partial^2\delta V^{\mathcal{O}(x)}}{\partial\bar{m}_t^2\partial\bar{m}_{\tilde{t}_1}^2} - \frac{\partial^2\delta V^{\mathcal{O}(x)}}{\partial\bar{m}_t^2\partial\bar{m}_{\tilde{t}_2}^2} + \frac{\partial^2\delta V^{\mathcal{O}(x)}}{\partial(\bar{m}_{\tilde{t}_1}^2)^2} - \frac{\partial^2\delta V^{\mathcal{O}(x)}}{\partial(\bar{m}_{\tilde{t}_2}^2)^2} \\
&+ \frac{4c_{2\theta}}{m_{\tilde{t}_1}^2 - m_{\tilde{t}_2}^2}\left(\frac{\partial^2\delta V^{\mathcal{O}(x)}}{\partial\bar{m}_t^2\partial s_{2\bar{\theta}}^2} + \frac{\partial^2\delta V^{\mathcal{O}(x)}}{\partial\bar{m}_{\tilde{t}_1}^2\partial s_{2\bar{\theta}}^2} + \frac{\partial^2\delta V^{\mathcal{O}(x)}}{\partial\bar{m}_{\tilde{t}_2}^2\partial s_{2\bar{\theta}}^2}\right) + \frac{2m_t c_{2\theta}^2}{s_{2\theta}(m_{\tilde{t}_1}^2 - m_{\tilde{t}_2}^2)}\frac{\partial^2\delta V^{\mathcal{O}(x)}}{\partial\bar{m}_t^2\partial\bar{\xi}} \\
&+ \left(\frac{2m_t c_{2\theta}^2}{s_{2\theta}(m_{\tilde{t}_1}^2 - m_{\tilde{t}_2}^2)} + \frac{s_{2\theta}}{2m_t}\right)\frac{\partial^2\delta V^{\mathcal{O}(x)}}{\partial\bar{m}_{\tilde{t}_1}^2\partial\bar{\xi}} + \left(\frac{2m_t c_{2\theta}^2}{s_{2\theta}(m_{\tilde{t}_1}^2 - m_{\tilde{t}_2}^2)} - \frac{s_{2\theta}}{2m_t}\right)\frac{\partial^2\delta V^{\mathcal{O}(x)}}{\partial\bar{m}_{\tilde{t}_2}^2\partial\bar{\xi}} \\
&+ \frac{2s_{2\theta}c_{2\theta}^2}{m_t(m_{\tilde{t}_1}^2 - m_{\tilde{t}_2}^2)}\frac{\partial^2\delta V^{\mathcal{O}(x)}}{\partial s_{2\bar{\theta}}^2\partial\bar{\xi}} + \frac{c_{2\theta}^2}{m_{\tilde{t}_1}^2 - m_{\tilde{t}_2}^2}\frac{\partial^2\delta V^{\mathcal{O}(x)}}{\partial\bar{\xi}^2}, \qquad (2.3.19)\\
F_3^{\mathcal{O}(x)} =& \frac{2}{m_{\tilde{t}_1}^2 - m_{\tilde{t}_2}^2}\left(\frac{\partial\delta V^{\mathcal{O}(x)}}{\partial\bar{m}_{\tilde{t}_1}^2} + \frac{\partial\delta V^{\mathcal{O}(x)}}{\partial\bar{m}_{\tilde{t}_2}^2}\right) + \frac{\partial^2\delta V^{\mathcal{O}(x)}}{\partial(\bar{m}_{\tilde{t}_1}^2)^2} + \frac{\partial^2\delta V^{\mathcal{O}(x)}}{\partial(\bar{m}_{\tilde{t}_2}^2)^2} - 2\frac{\partial^2\delta V^{\mathcal{O}(x)}}{\partial\bar{m}_{\tilde{t}_1}^2\partial\bar{m}_{\tilde{t}_2}^2} \\
&- \frac{32c_{2\theta}^2}{(m_{\tilde{t}_1}^2 - m_{\tilde{t}_2}^2)^2}\frac{\partial\delta V^{\mathcal{O}(x)}}{\partial s_{2\bar{\theta}}^2} + \frac{16m_t(3s_{2\theta} - 2)}{s_{2\theta}(m_{\tilde{t}_1}^2 - m_{\tilde{t}_2}^2)^2}\frac{\partial\delta V^{\mathcal{O}(x)}}{\partial\bar{\xi}} + \frac{8c_{2\theta}^2}{m_{\tilde{t}_1}^2 - m_{\tilde{t}_2}^2}\left(\frac{\partial^2\delta V^{\mathcal{O}(x)}}{\partial\bar{m}_{\tilde{t}_1}^2\partial s_{2\bar{\theta}}^2} - \frac{\partial^2\delta V^{\mathcal{O}(x)}}{\partial\bar{m}_{\tilde{t}_2}^2\partial s_{2\bar{\theta}}^2}\right) \\
&+ \frac{4m_t c_{2\theta}^2}{s_{2\theta}(m_{\tilde{t}_1}^2 - m_{\tilde{t}_2}^2)}\left(\frac{\partial^2\delta V^{\mathcal{O}(x)}}{\partial\bar{m}_{\tilde{t}_1}^2\partial\bar{\xi}} - \frac{\partial^2\delta V^{\mathcal{O}(x)}}{\partial\bar{m}_{\tilde{t}_2}^2\partial\bar{\xi}}\right) + \frac{16c_{2\theta}^4}{(m_{\tilde{t}_1}^2 - m_{\tilde{t}_2}^2)^2}\frac{\partial^2\delta V^{\mathcal{O}(x)}}{\partial(s_{2\bar{\theta}}^2)^2} \\
&+ \frac{16m_t c_{2\theta}^4}{s_{2\theta}(m_{\tilde{t}_1}^2 - m_{\tilde{t}_2}^2)^2}\frac{\partial^2\delta V^{\mathcal{O}(x)}}{\partial s_{2\bar{\theta}}\partial\bar{\xi}} + \frac{4m_t^2 c_{2\theta}^4}{s_{2\theta}^2(m_{\tilde{t}_1}^2 - m_{\tilde{t}_2}^2)^2}\frac{\partial^2\delta V^{\mathcal{O}(x)}}{\partial\bar{\xi}^2}. \qquad (2.3.20)
\end{aligned}$$

2.3.2 Neutral Higgs Self-Couplings

In the previous section we explained how we can calculate the CP-odd and CP-even mass matrices perturbatively up to $\mathcal{O}(x)$. We will apply the following rotations on the CP-odd and on the CP-even fields

$$S_i = R_{ij}(-\alpha^{\mathcal{O}(x)})H_j, \qquad H_j \equiv (h, H) \qquad (2.3.21)$$

$$P_i = R_{ij}(\beta^{\mathcal{O}(x)})A_j, \qquad A_j \equiv (A, G), \qquad (2.3.22)$$

for $i, j = 1, 2$ where

$$R_{ij}(\theta) \equiv \begin{pmatrix} \sin\theta & \cos\theta \\ \cos\theta & -\sin\theta \end{pmatrix}. \qquad (2.3.23)$$

The mixing angle is called $\alpha^{\mathcal{O}(x)}$ in the CP-even case and $\beta^{\mathcal{O}(x)}$ in the CP-odd case[12]. They are determined by diagonalizing the mass matrices $(\mathcal{M}_S^2)_{ij}^{\mathcal{O}(x)}$ and $(\mathcal{M}_P^2)_{ij}^{\mathcal{O}(x)}$, see section A.2 in the appendix. The fields h, H, A are the three neutral, physical Higgs bosons, the state G is a neutral, massless would-be

[11] Our result looks a little bit different from the result given in [32] because we used different dependences of the effective potential (we used $s_{2\theta}$ and ξ instead of $c_{2\theta}$ and $c_{\varphi\bar{\varphi}}$).

[12] At this point it is not yet clear whether the tangent of the CP-odd mixing angle $\beta^{\mathcal{O}(x)}$ coincides with the loop-corrected ratio of the VEVs. This is a question of the renormalization scheme, which we will address in section 2.5.5.

Goldstone boson, which corresponds to the longitudinal polarization of the Z-Boson. There are three and four particle vertices in these Higgs fields, whose strengths are determined by the trilinear and quartic couplings. Here we will discuss the calculation of the trilinear couplings in detail. The quartic couplings can be obtained analogously. We define the vector $\mathcal{H}_i = (H_j, A_j) = (h, H, A, G)$ for $i = 1, ..., 4$ and $j = 1, 2$.

Trilinear couplings: The self-couplings of three neutral Higgs bosons are determined by the terms in the effective potential which are trilinear in the Higgs fields. We can therefore define the trilinear couplings analogously to the mass matrix. We express the effective potential as the tree-level potential $V^0(\mathcal{H}_k)$, where we use the rotations[13] of Eqs. (2.3.21, 2.3.22) to express it in terms of the physical fields h, H, A, G, supplemented by the loop-corrected potential $\delta V^{\mathcal{O}(x)}(\bar{x}_k(\mathcal{H}_k))$, with the dependence of the quantities $\bar{x}_k$ changed to the physical fields h, H, A, G by using the same rotations Eqs. (2.3.21, 2.3.22). Taking three derivatives w.r.t. neutral Higgs fields $\mathcal{H}_i = (h, H, A, G)$ and evaluating everything at the minimum $(h, H, A, G) = 0$ yields the desired trilinear terms in the Higgs fields

$$\lambda^{\mathcal{O}(x)}_{\mathcal{H}_i\mathcal{H}_j\mathcal{H}_k} \equiv \lambda^0_{\mathcal{H}_i\mathcal{H}_j\mathcal{H}_k} + \delta\lambda^{\mathcal{O}(x)}_{\mathcal{H}_i\mathcal{H}_j\mathcal{H}_k}, \tag{2.3.24}$$

where

$$\lambda^0_{\mathcal{H}_i\mathcal{H}_j\mathcal{H}_k} = \frac{\partial^3 V^0(\mathcal{H}_l)}{\partial\mathcal{H}_i\partial\mathcal{H}_j\partial\mathcal{H}_k}\bigg|_{\min}, \qquad \delta\lambda^{\mathcal{O}(x)}_{\mathcal{H}_i\mathcal{H}_j\mathcal{H}_k} = \frac{\partial^3 \delta V^{\mathcal{O}(x)}(\bar{x}_l(\mathcal{H}_m))}{\partial\mathcal{H}_i\partial\mathcal{H}_j\partial\mathcal{H}_k}\bigg|_{\min}. \tag{2.3.25}$$

Here $|_{\min}$ means evaluating at the minimum of the effective potential, all fields are substituted by their VEV, i.e. $(h, H, A, G) = 0$.

Chain rule: To calculate the above derivatives of the effective potential, again, we use the *chain rule*

$$\begin{aligned}\delta\lambda^{\mathcal{O}(x)}_{\mathcal{H}_i\mathcal{H}_j\mathcal{H}_k} = \frac{\partial^3 \delta V^{\mathcal{O}(x)}(\bar{x}_l(\mathcal{H}_m))}{\partial\mathcal{H}_i\partial\mathcal{H}_j\partial\mathcal{H}_k}\bigg|_{\min} &= \sum_{\hat{i}\hat{j}\hat{k}} \frac{\partial^3 \delta V^{\mathcal{O}(x)}}{\partial\bar{x}_{\hat{i}}\partial\bar{x}_{\hat{j}}\partial\bar{x}_{\hat{k}}} \cdot \frac{\partial\bar{x}_{\hat{i}}}{\partial\mathcal{H}_i}\bigg|_{\min} \cdot \frac{\partial\bar{x}_{\hat{j}}}{\partial\mathcal{H}_j}\bigg|_{\min} \cdot \frac{\partial\bar{x}_{\hat{k}}}{\partial\mathcal{H}_k}\bigg|_{\min} \\ &+ 3\sum_{\hat{j}\hat{k}} \frac{\partial^2 \delta V^{\mathcal{O}(x)}}{\partial\bar{x}_{\hat{j}}\partial\bar{x}_{\hat{k}}} \cdot \frac{\partial^2\bar{x}_{\hat{k}}}{\partial\mathcal{H}_j\partial\mathcal{H}_k}\bigg|_{\min} \cdot \frac{\partial\bar{x}_{\hat{i}}}{\partial\mathcal{H}_i}\bigg|_{\min} + \sum_{\hat{k}} \frac{\partial\delta V^{\mathcal{O}(x)}}{\partial\bar{x}_{\hat{k}}} \cdot \frac{\partial^3\bar{x}_{\hat{k}}}{\partial\mathcal{H}_i\partial\mathcal{H}_j\partial\mathcal{H}_k}\bigg|_{\min}. \end{aligned} \tag{2.3.26}$$

As for the calculation of the mass matrix, a 'hat' on an index denotes that it is a dummy index which we will sum over. The quartic couplings are obtained analogously, they just involve one more partial derivative. The essence is that we can construct the unrenormalized couplings at every order in perturbation theory by putting together the following two building blocks.
(i) Partial derivatives of the effective potential with respect to field-dependent quantities $\bar{x}_{\hat{k}}$

$$\frac{\partial^n \delta V^{\mathcal{O}(x)}}{\partial\bar{x}_{\hat{k_1}} \cdots \partial\bar{x}_{\hat{k_n}}}. \tag{2.3.27}$$

(ii) Partial derivatives of field-dependent quantities $\bar{x}_{\hat{k}}$ with respect to Higgs fields $\mathcal{H}_i$ evaluated at the minimum of the potential, i.e. $(h, H, A, G) = 0$

$$\frac{\partial^n\bar{x}_{\hat{k}}}{\partial\mathcal{H}_{i_1} \cdots \partial\mathcal{H}_{i_n}}\bigg|_{\min}, \tag{2.3.28}$$

where $n = 1, 2, 3$ for the trilinear and $n = 1, 2, 3, 4$ for the quartic couplings. Of course this is a trivial statement from the mathematical point of view, but for the generation of an efficient code it is useful to implement these building blocks and recycle them whenever possible.

[13] The mixing angles for these rotations have to be the ones determined by the diagonalization of the mass matrices at $\mathcal{O}(x)$. $\lambda^0_{\mathcal{H}_i\mathcal{H}_j\mathcal{H}_k}$ as well as $\delta\lambda^{\mathcal{O}(x)}_{\mathcal{H}_i\mathcal{H}_j\mathcal{H}_k}$ depend on $\beta^{\mathcal{O}(x)}$ and $\alpha^{\mathcal{O}(x)}$.

2.4 Explicit One-Loop $\mathcal{O}(\alpha_t)$ Results

2.4.1 One-Loop $\mathcal{O}(\alpha_t)$ CP-Even Higgs Masses

The calculation for the complete $\mathcal{O}(\alpha_t)$ corrections for the CP-even Higgs masses was first performed in [21]. To reproduce these we use the general expression Eqs. (2.3.15 - 2.3.20) and evaluate it inserting the one-loop $\mathcal{O}(\alpha_t)$ potential $V^{\mathcal{O}(x)} \to V^{\mathcal{O}(\alpha_t)}$. The $\mathcal{O}(\alpha_t)$ expression for the functions F_1, F_2 and F_3 including $\mathcal{O}(\epsilon)$-terms are

$$F_1^{\alpha_t} = \frac{N_C}{16\pi^2}\left[\log\frac{m_{\tilde{t}_1}^2 m_{\tilde{t}_2}^2}{m_t^4} - \frac{\epsilon}{2}\left(\log^2\frac{m_{\tilde{t}_1}^2}{Q^2} + \log^2\frac{m_{\tilde{t}_2}^2}{Q^2} - 2\log^2\frac{m_t^2}{Q^2}\right)\right], \tag{2.4.1}$$

$$F_2^{\alpha_t} = \frac{N_C}{16\pi^2}\left[\log\frac{m_{\tilde{t}_1}^2}{m_{\tilde{t}_2}^2} - \frac{\epsilon}{2}\left(\log^2\frac{m_{\tilde{t}_1}^2}{Q^2} - \log^2\frac{m_{\tilde{t}_2}^2}{Q^2}\right)\right], \tag{2.4.2}$$

$$F_3^{\alpha_t} = \frac{N_C}{16\pi^2}\left[1 - \frac{\epsilon}{2}\left(\log\frac{m_{\tilde{t}_1}^2}{Q^2} + \log\frac{m_{\tilde{t}_2}^2}{Q^2} - 2\right)\right]\left(2 - \frac{m_{\tilde{t}_1}^2 + m_{\tilde{t}_2}^2}{m_{\tilde{t}_1}^2 - m_{\tilde{t}_2}^2}\log\frac{m_{\tilde{t}_1}^2}{m_{\tilde{t}_2}^2}\right), \tag{2.4.3}$$

where $Q^2 \equiv 4\pi\mu_0^2 e^{-\gamma_E}$ is introduced in the Appendix after Eq. (C.2.50). Looking at the $\mathcal{O}(\alpha_t)$ effective potential Eq. (C.2.54), we observe that there are ϵ-poles. In the $\mathcal{O}(\alpha_t)$ corrections to the CP-even Higgs mass matrix $(\Delta M_S^2)^{\mathcal{O}(\alpha_t)}$ these divergences cancel. They are physical quantities[14]. This cancellation had to take place because there is no contribution from counter term insertion at tree-level. The $\mathcal{O}(\epsilon)$-terms in the above expressions will result in finite contributions at $\mathcal{O}(\alpha_s\alpha_t)$ and $\mathcal{O}(\alpha_t^2)$. This will be explained in section 2.5.6.
From this result for the CP-even Higgs mass matrix one can derive an upper bound for the one-loop $\mathcal{O}(\alpha_t)$ corrected light scalar Higgs mass, see Eq. (1.5.1).

2.4.2 One-Loop $\mathcal{O}(\alpha_t)$ Trilinear Higgs Self-Couplings

The one-loop $\mathcal{O}(\alpha_t)$ corrections to the trilinear couplings for the neutral Higgs bosons have been calculated more than 20 years ago [24]. In the previous section, we have build up all the relevant tools to reproduce these results. Using Eq. (2.3.26) with $\delta V^{\mathcal{O}(x)} = \delta V^{\alpha_t}$ we obtain the $\mathcal{O}(\alpha_t)$ corrections to the couplings $\Delta\lambda_{\mathcal{H}_i\mathcal{H}_j\mathcal{H}_k}^{\mathcal{O}(\alpha_t)}$.
We will need the results for the $\mathcal{O}(\alpha_t)$ couplings also for the two-loop calculation and for this reason we need to modify the result of [24] a little bit. First let us introduce some notational simplifications

$$X_t = A_t + \mu\cot\beta, \qquad Y_t = A_t - \mu\tan\beta, \qquad Z_t = A_t + \mu\cot\alpha, \qquad W_t = A_t - \mu\tan\alpha. \tag{2.4.4}$$

The mixing angles α and β are defined by the diagonalization of the CP-even and CP-odd mass matrix respectively, see Eqs. (2.3.21, 2.3.22). In view of the two-loop calculation it is important to distinguish between the mixing angle β and the ratio of the VEVs $\frac{v_1^{\min}}{v_2^{\min}}$ in the one-loop result, since they might receive different radiative corrections[15] at $\mathcal{O}(\alpha_t)$. Moreover thinking of the two-loop renormalization, we have to take $\mathcal{O}(\epsilon)$-terms into account, because they yield finite contributions when multiplied by a divergent counter term. They are presented in appendix F.1. We also include the couplings of the would-be Goldstone bosons G, because they are relevant to construct WFR counter terms, see section 2.5.7.

[14] For the mass matrix as well as for the couplings we use a capital Δ to denote that the derivatives of $\delta V^{\mathcal{O}(x)}$ are finite.
[15] In section 2.5.5 we will introduce a renormalization scheme, where the relation $\tan\beta = v_2/v_1$ is fulfilled up to all orders in perturbation theory. However, we first want to cast the result into a form in which we can apply any renormalization scheme.

The results can be displayed in the following form

$$\Delta\lambda_{hhh}^{\mathcal{O}(\alpha_t)} = \frac{3m_t^4 c_a^3}{4\pi^2 v_2^3}\left\{3\log\left(\frac{m_{\tilde{t}_1}^2 m_{\tilde{t}_2}^2}{m_t^4}\right) + 3W_t\frac{s_{2\theta}}{2m_t}\log\left(\frac{m_{\tilde{t}_1}^2}{m_{\tilde{t}_2}^2}\right) + \frac{(2m_t + s_{2\theta}W_t)^3}{4m_t m_{\tilde{t}_1}^2} + \frac{(2m_t - s_{2\theta}W_t)^3}{4m_t m_{\tilde{t}_2}^2} + c_{2\theta}^2\left[\frac{3W_t^2}{m_{\tilde{t}_1}^2 - m_{\tilde{t}_2}^2}\log\left(\frac{m_{\tilde{t}_1}^2}{m_{\tilde{t}_2}^2}\right) + \frac{3s_{2\theta}W_t^3}{2m_t(m_{\tilde{t}_1}^2 - m_{\tilde{t}_2}^2)}\left(2 - \frac{m_{\tilde{t}_1}^2 + m_{\tilde{t}_2}^2}{m_{\tilde{t}_1}^2 - m_{\tilde{t}_2}^2}\log\left(\frac{m_{\tilde{t}_1}^2}{m_{\tilde{t}_2}^2}\right)\right)\right] - 4\right\}, \tag{2.4.5}$$

$$\Delta\lambda_{HHH}^{\mathcal{O}(\alpha_t)} = \frac{3m_t^4 s_a^3}{4\pi^2 v_2^3}\left\{3\log\left(\frac{m_{\tilde{t}_1}^2 m_{\tilde{t}_2}^2}{m_t^4}\right) + 3Z_t\frac{s_{2\theta}}{2m_t}\log\left(\frac{m_{\tilde{t}_1}^2}{m_{\tilde{t}_2}^2}\right) + \frac{(2m_t + s_{2\theta}Z_t)^3}{4m_{\tilde{t}_1}^2 m_t} + \frac{(2m_t - s_{2\theta}Z_t)^3}{4m_{\tilde{t}_2}^2 m_t} + c_{2\theta}^2\left[\frac{3Z_t^2}{m_{\tilde{t}_1}^2 - m_{\tilde{t}_2}^2}\log\left(\frac{m_{\tilde{t}_1}^2}{m_{\tilde{t}_2}^2}\right) + \frac{3s_{2\theta}Z_t^3}{2m_t(m_{\tilde{t}_1}^2 - m_{\tilde{t}_2}^2)}\left(2 - \frac{m_{\tilde{t}_1}^2 + m_{\tilde{t}_2}^2}{m_{\tilde{t}_1}^2 - m_{\tilde{t}_2}^2}\log\left(\frac{m_{\tilde{t}_1}^2}{m_{\tilde{t}_2}^2}\right)\right)\right] - 4\right\}, \tag{2.4.6}$$

$$\Delta\lambda_{hhH}^{\mathcal{O}(\alpha_t)} = \frac{3m_t^4 c_a^2 s_a}{4\pi^2 v_2^3}\left\{3\log\left(\frac{m_{\tilde{t}_1}^2 m_{\tilde{t}_2}^2}{m_t^4}\right) + \frac{s_{2\theta}}{2m_t}(Z_t + 2W_t)\log\left(\frac{m_{\tilde{t}_1}^2}{m_{\tilde{t}_2}^2}\right) + c_{2\theta}^2\left[\frac{W_t(2Z_t + W_t)}{m_{\tilde{t}_1}^2 - m_{\tilde{t}_2}^2}\log\left(\frac{m_{\tilde{t}_1}^2}{m_{\tilde{t}_2}^2}\right) + \frac{3Z_t W_t^2 s_{2\theta}}{2m_t(m_{\tilde{t}_1}^2 - m_{\tilde{t}_2}^2)}\left(2 - \frac{m_{\tilde{t}_1}^2 + m_{\tilde{t}_2}^2}{m_{\tilde{t}_1}^2 - m_{\tilde{t}_2}^2}\log\left(\frac{m_{\tilde{t}_1}^2}{m_{\tilde{t}_2}^2}\right)\right)\right] + \frac{(2m_t + s_{2\theta}Z_t)(2m_t + s_{2\theta}W_t)^2}{4m_t m_{\tilde{t}_1}^2} + \frac{(2m_t - s_{2\theta}Z_t)(2m_t - s_{2\theta}W_t)^2}{4m_t m_{\tilde{t}_2}^2} - 4\right\}, \tag{2.4.7}$$

$$\Delta\lambda_{hHH}^{\mathcal{O}(\alpha_t)} = \frac{3m_t^4 c_a s_a^2}{4\pi^2 v_2^3}\left\{3\log\left(\frac{m_{\tilde{t}_1}^2 m_{\tilde{t}_2}^2}{m_t^4}\right) + \frac{s_{2\theta}}{2m_t}(2Z_t + W_t)\log\left(\frac{m_{\tilde{t}_1}^2}{m_{\tilde{t}_2}^2}\right) + c_{2\theta}^2\left[\frac{Z_t(Z_t + 2W_t)}{m_{\tilde{t}_1}^2 - m_{\tilde{t}_2}^2}\log\left(\frac{m_{\tilde{t}_1}^2}{m_{\tilde{t}_2}^2}\right) + \frac{3Z_t^2 W_t s_{2\theta}}{2m_t(m_{\tilde{t}_1}^2 - m_{\tilde{t}_2}^2)}\left(2 - \frac{m_{\tilde{t}_1}^2 + m_{\tilde{t}_2}^2}{m_{\tilde{t}_1}^2 - m_{\tilde{t}_2}^2}\log\left(\frac{m_{\tilde{t}_1}^2}{m_{\tilde{t}_2}^2}\right)\right)\right] + \frac{(2m_t + s_{2\theta}Z_t)^2(2m_t + s_{2\theta}W_t)}{4m_t m_{\tilde{t}_1}^2} + \frac{(2m_t - s_{2\theta}Z_t)^2(2m_t - s_{2\theta}W_t)}{4m_t m_{\tilde{t}_2}^2} - 4\right\}, \tag{2.4.8}$$

$$\Delta\lambda_{hAA}^{\mathcal{O}(\alpha_t)} = \frac{3m_t^4 c_a c_\beta^2}{4\pi^2 v_2^3}\left\{\log\left(\frac{m_{\tilde{t}_1}^2 m_{\tilde{t}_2}^2}{m_t^4}\right) + \left[\frac{Y_t^2}{m_{\tilde{t}_1}^2 - m_{\tilde{t}_2}^2} + W_t\frac{s_{2\theta}}{2m_t}\left(1 - Y_t^2\frac{m_{\tilde{t}_1}^2 + m_{\tilde{t}_2}^2}{(m_{\tilde{t}_1}^2 - m_{\tilde{t}_2}^2)^2}\right)\right]\log\left(\frac{m_{\tilde{t}_1}^2}{m_{\tilde{t}_2}^2}\right) + \frac{s_{2\theta}}{m_t}\frac{W_t Y_t^2}{(m_{\tilde{t}_1}^2 - m_{\tilde{t}_2}^2)}\right\}, \tag{2.4.9}$$

$$\Delta\lambda_{HAA}^{\mathcal{O}(\alpha_t)} = \frac{3m_t^4 s_a c_\beta^2}{4\pi^2 v_2^3}\left\{\log\left(\frac{m_{\tilde{t}_1}^2 m_{\tilde{t}_2}^2}{m_t^4}\right) + \left[\frac{Y_t^2}{m_{\tilde{t}_1}^2 - m_{\tilde{t}_2}^2} + Z_t\frac{s_{2\theta}}{2m_t}\left(1 - Y_t^2\frac{m_{\tilde{t}_1}^2 + m_{\tilde{t}_2}^2}{(m_{\tilde{t}_1}^2 - m_{\tilde{t}_2}^2)^2}\right)\right]\log\left(\frac{m_{\tilde{t}_1}^2}{m_{\tilde{t}_2}^2}\right) + \frac{s_{2\theta}}{m_t}\frac{Z_t Y_t^2}{(m_{\tilde{t}_1}^2 - m_{\tilde{t}_2}^2)}\right\}, \tag{2.4.10}$$

$$\Delta\lambda_{hGG}^{\mathcal{O}(\alpha_t)} = \frac{3c_\alpha s_\beta^2}{8\pi^2 v_2^3}m_t^3\left\{2s_{2\theta}\frac{W_t X_t^2}{m_{\tilde{t}_1}^2 - m_{\tilde{t}_2}^2} + 2m_t\log\frac{m_{\tilde{t}_1}^2 m_{\tilde{t}_2}^2}{m_t^4} + \left(W_t s_{2\theta} - s_{2\theta}W_t X_t^2\frac{m_{\tilde{t}_1}^2 + m_{\tilde{t}_2}^2}{(m_{\tilde{t}_1}^2 - m_{\tilde{t}_2}^2)^2} + \frac{2m_t X_t^2}{m_{\tilde{t}_1}^2 - m_{\tilde{t}_2}^2}\right)\log\frac{m_{\tilde{t}_1}^2}{m_{\tilde{t}_2}^2}\right\}, \tag{2.4.11}$$

$$\Delta\lambda_{HGG}^{\mathcal{O}(\alpha_t)} = \frac{3 s_\alpha s_\beta^2}{8 v_2^3 \pi^2} m_t^3 \Bigg\{ 2 s_{2\theta} \frac{Z_t X_t^2}{m_{\tilde{t}_1}^2 - m_{\tilde{t}_2}^2} + 2 m_t \log \frac{m_{\tilde{t}_1}^2 m_{\tilde{t}_2}^2}{m_t^4} + \left(Z_t s_{2\theta} - s_{2\theta} X_t^2 Z_t \frac{m_{\tilde{t}_1}^2 + m_{\tilde{t}_2}^2}{(m_{\tilde{t}_1}^2 - m_{\tilde{t}_2}^2)^2} + \frac{2 m_t X_t^2}{m_{\tilde{t}_1}^2 - m_{\tilde{t}_2}^2} \right) \log \frac{m_{\tilde{t}_1}^2}{m_{\tilde{t}_2}^2} \Bigg\}, \tag{2.4.12}$$

$$\Delta\lambda_{hAG}^{\mathcal{O}(\alpha_t)} = \frac{3 s_\beta c_\beta c_\alpha}{8 v_2^3 \pi^2} m_t^3 \Bigg\{ - 2 s_{2\theta} \frac{W_t Y_t X_t}{m_{\tilde{t}_1}^2 - m_{\tilde{t}_2}^2} - 2 m_t \log \frac{m_{\tilde{t}_1}^2 m_{\tilde{t}_2}^2}{m_t^4} + \left(- W_t s_{2\theta} + Y_t W_t s_{2\theta} X_t \frac{m_{\tilde{t}_1}^2 + m_{\tilde{t}_2}^2}{(m_{\tilde{t}_1}^2 - m_{\tilde{t}_2}^2)^2} - \frac{2 m_t Y_t X_t}{m_{\tilde{t}_1}^2 - m_{\tilde{t}_2}^2} \right) \log \frac{m_{\tilde{t}_1}^2}{m_{\tilde{t}_2}^2} \Bigg\}, \tag{2.4.13}$$

$$\Delta\lambda_{HAG}^{\mathcal{O}(\alpha_t)} = \frac{3 s_\alpha s_\beta c_\beta}{8 v_2^3 \pi^2} m_t^3 \Bigg\{ - 2 s_{2\theta} \frac{Y_t X_t Z_t}{m_{\tilde{t}_1}^2 - m_{\tilde{t}_2}^2} - 2 m_t \log \frac{m_{\tilde{t}_1}^2 m_{\tilde{t}_2}^2}{m_t^4} + \left(- Z_t s_{2\theta} + Y_t Z_t s_{2\theta} X_t \frac{m_{\tilde{t}_1}^2 + m_{\tilde{t}_2}^2}{(m_{\tilde{t}_1}^2 - m_{\tilde{t}_2}^2)^2} - \frac{2 m_t Y_t X_t}{m_{\tilde{t}_1}^2 - m_{\tilde{t}_2}^2} \right) \log \frac{m_{\tilde{t}_1}^2}{m_{\tilde{t}_2}^2} \Bigg\}. \tag{2.4.14}$$

Analogous to the mass matrix all divergences from δV^{α_t} cancel in the one-loop couplings. They correspond to the physical quantities. Note that these results are not explicitly dependent on A_t and μ anymore. Together with α and β they have been absorbed into Y_t, W_t, Z_t and X_t up to some universal prefactors. The dependence on $v_1^{\min}$ and $v_2^{\min}$ has been absorbed into the parameters $s_{2\theta}$ and $c_{2\theta}$.
We see that all one-loop $\mathcal{O}(\alpha_t)$ corrections to the Higgs masses and self-couplings are proportional to m_t^4, i.e. they are potentially large. Especially the corrections to the light scalar Higgs mass are comparable in size to the tree-level value, for large $\tan\beta$, see Eq. (1.5.1). The Higgs self-couplings are proportional to trigonometric functions of the CP-even and CP-odd mixing angles α and β. In parameter spaces, where these are not much smaller than 1, the corrections to the Higgs self-couplings can be also comparable to the tree-level values.

2.5 Renormalization

2.5.1 General Remarks about Two-loop $\mathcal{O}(\alpha_s\alpha_t)$ and $\mathcal{O}(\alpha_t^2)$ Calculations

In this section we will comment about the two-loop $\mathcal{O}(\alpha_s\alpha_t)$ and $\mathcal{O}(\alpha_t^2)$ calculation for the Higgs masses and self-couplings. They are calculated using the regularized but unrenormalized effective potential, i.e. we use Eqs. (2.3.15 - 2.3.20, 2.3.26) with $\delta V^{\mathcal{O}(x)} = \delta V^{\alpha_t\alpha_s} + \delta V^{\alpha_t^2}$. We will not put any analytical results here because the expressions are too long to be displayed here.
Looking at the two-loop effective potentials Eqs. (C.3.9, C.4.19), we see that there are ϵ^2-divergences. These quadratic divergences cancel in $(\delta\mathcal{M}_S^2)^{\mathcal{O}(\alpha_t\alpha_s)}$ and $(\delta\mathcal{M}_S^2)^{\mathcal{O}(\alpha_t^2)}$ individually. Analogously they cancel in the couplings $\delta\lambda_{\mathcal{H}_i\mathcal{H}_j\mathcal{H}_k}^{\mathcal{O}(\alpha_t\alpha_s)}$ and $\delta\lambda_{\mathcal{H}_i\mathcal{H}_j\mathcal{H}_k}^{\mathcal{O}(\alpha_t^2)}$. This has to be the case because there are no counter term contributions at one-loop (or at tree-level) that yield ϵ^2-divergences. However, there are ϵ^{-1}-divergences in the masses and couplings at $\mathcal{O}(\alpha_t\alpha_s)$ and $\mathcal{O}(\alpha_t^2)$ which do not cancel among the two-loop contribution. To get rid of these divergences we need to *renormalize*.

2.5.2 General Remarks about Renormalization

The collection of techniques to get rid of the UV-infinities (which we transformed into poles in the regulator) in a quantum field theory is called *renormalization*. The crucial point here is to realize that

the quantities that appear in the initial bare Lagrangian (as well as in the effective potential) do not correspond to the quantities that are actually measured in the laboratory. These bare physical constants that appear in the Lagrangian (e.g. masses m^0 , couplings g^0) receive loop-corrections themselves, such that they become just as divergent as the amplitudes, masses and couplings that we want to calculate. In order to make contact to reality these bare quantities have to be rewritten in terms of physical, i.e. renormalized quantities. This means we substitute the divergent bare quantities by their physical value plus[16] a divergent *counter term* $x^0 \to x^R + \delta x$. Pictorially this corresponds to the insertion of counter term diagrams. In any renormalizable field theory such as the SM or the MSSM, we can introduce a finite number of counter terms such that all poles in the regulator ϵ cancel in a physical prediction and we therefore obtain finite results also in the limit $\epsilon \to 0$. In fact divergences cancel at every order in perturbation theory[17]. When we calculate a renormalized coupling, we obtain a dependence on an unphysical renormalization scale μ_R. This means that coupling constants, (e.g. the elementary electrical charge) are not constants anymore but they depend on the energy scale where they are measured. In QED this effect is known as *screening*, in QCD this leads to *asymptotic freedom* [61]. Observables, such as hadronic cross sections or pole masses have to be independent of the renormalization scale μ_R. For any perturbatively calculated observable, the remaining dependence on the renormalization scale μ_R corresponds to higher orders in perturbation theory that have not been taken into account. This dependence is therefore unphysical and should become smaller with every higher order included, such that in the limit of an exact result this dependence vanishes. The variation of μ_R can then be used to estimate theoretical errors due to neglected higher orders.

2.5.3 Scale Dependence of Quark Masses in the SM

To describe the above *scale dependence* of masses and couplings a little bit better, I will present a small detour about two different renormalization schemes for the masses.
In the SM the on-shell self-energy for $\not{p} = m$ of a quark at one-loop order α_s in DRED is[18]

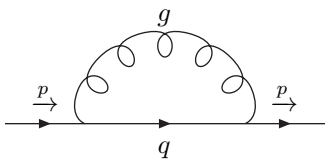

$$\Rightarrow \quad \Sigma(m) = mC_F \frac{\alpha_s}{\pi} \Gamma(1+\epsilon) \left(\frac{4\pi\mu_0^2}{m^2}\right)^{\epsilon} \left(\frac{3}{4\epsilon} + \frac{5}{4}\right), \tag{2.5.1}$$

where μ_0 is the unphysical t'Hooft or regularization scale. The renormalization scheme fixes the relation between the physical and the bare quantities m^0. Due to renormalizability the divergence has to be the same in all schemes, but we are free to shift any finite terms between the renormalized mass and the counter term. The pole mass corresponds to an on-shell evaluation of the self-energy, the corresponding scheme is called the *on-shell* OS scheme and the renormalized mass as well as the counter term is independent of any renormalization scale[19] μ_R

$$m^{\text{OS}} = m^0 + \Sigma(m) \equiv m^0 - \delta^{\text{OS}} m. \tag{2.5.2}$$

[16]The sign here is a matter of convention. In the way we do it here, the mass counter term is the negative of the self-energy, see section 2.5.3.

[17]This is an important statement. It means that in all our calculations, we first properly expand our results perturbatively, with ϵ fixed. Then in the very end we may take the limit $\epsilon \to 0$.

[18]In general a fermionic self-energy consists of a scalar (S), a vectorial (V) and an axial (A) part $\Sigma(\not{p}) = m\Sigma_S(p^2) + \not{p}\Sigma_V(p^2) + \not{p}\gamma_5\Sigma_A(p^2)$. An on-shell evaluation of the self-energy at $\not{p} = m$ results in $\Sigma(m) = m(\Sigma_S(m^2) + \Sigma_V(m^2))$.

[19]This scale independence doesn't make the on-shell scheme superior to the $\overline{\text{DR}}$ scheme. It is just that we evaluated the counter term at a special scale, namely the pole mass.

The modified minimal subtraction scheme together with DRED ($\overline{\text{DR}}$ scheme) is defined by taking only the divergent part of the self-energy plus some universal constants. This introduces the renormalization scale μ_R as the scale where the counter term and the renormalized parameter are separated[20].

$$m^{\overline{\text{DR}}}(\mu_R^2) = m^0 - \delta m^{\overline{\text{DR}}}(\mu_R^2), \quad \delta^{\overline{\text{DR}}} m(\mu_R^2) = -mC_F \frac{\alpha_s}{\pi} \Gamma(1+\epsilon) \left(\frac{4\pi\mu_0^2}{\mu_R^2}\right)^{\epsilon} \frac{3}{4\epsilon}. \tag{2.5.3}$$

We can then relate the running $\overline{DR}$ mass to the pole mass

$$m^{\overline{\text{DR}}}(\mu_R^2) = m^0 - \delta^{\overline{\text{DR}}} m(\mu_R^2) = m^{\text{OS}} - \left[\delta^{\overline{\text{DR}}} m(\mu_R^2) - \delta^{\text{OS}} m\right]. \tag{2.5.4}$$

We see that the ϵ-poles of the counter terms cancel. Eq. (2.5.4) gives us an analytical formula to calculate running $\overline{\text{DR}}$ parameters from renormalized on-shell parameters. Note that Eq. (2.5.4) is only a naive estimate of the running. Usually the running of a quantity depends on other running quantities. To get a more reliable result one has to solve coupled differential renormalization group equations.

2.5.4 Renormalizing a Cross Section in a Toy Model

Let's take a look at renormalization from a perturbative perspective. We work in a toy model, where we computed some LO cross section $\sigma(m_0)$ and its $\mathcal{O}(\alpha)$ correction $\delta\sigma(m_0)$ (any δ corresponds to an $\mathcal{O}(\alpha)$). These unrenormalized cross sections depend only on bare parameters. In our toy model we restrict ourselves to simply one parameter m_0. The one-loop-corrected $\mathcal{O}(\alpha)$ cross section expressed in terms of bare parameters is

$$\sigma_1 = \sigma_0(m_0) + \delta\sigma(m_0) + \mathcal{O}(\alpha^2). \tag{2.5.5}$$

This unrenormalized cross section generally develops poles in ϵ in the correction $\delta\sigma$, i.e. it is divergent. We choose a renormalization scheme and insert for the bare quantities the renormalized mass plus the corresponding counter term and expand in α. In the $\overline{\text{DR}}$ scheme we use Eq. (2.5.3) to get

$$\begin{aligned} \sigma_1^{\overline{\text{DR}}} &= \sigma_0(\overline{m} + \delta\overline{m}) + \delta\sigma(\overline{m} + \delta\overline{m}) + \mathcal{O}(\alpha^2) \\ &= \sigma_0(\overline{m}) + \left.\frac{\partial\sigma_0}{\partial m_0}\right|_{m_0=\overline{m}} \delta\overline{m} + \delta\sigma(\overline{m}) + \mathcal{O}(\alpha^2). \end{aligned} \tag{2.5.6}$$

For any renormalizable theory the divergences in the counter term and those in the corrections to the cross section have to cancel. Note that in the last equation above the $\overline{\text{DR}}$-masses and counter terms are scale dependent. In the on-shell scheme we use Eq. (2.5.2) and obtain a scale independent equation

$$\sigma_1^{\text{OS}} = \sigma_0(m + \delta m) + \delta\sigma(m + \delta m) + \mathcal{O}(\alpha^2) \tag{2.5.7}$$

$$= \sigma_0(m) + \left.\frac{\partial\sigma_0}{\partial m_0}\right|_{m_0=m} \delta m + \delta\sigma(m) + \mathcal{O}(\alpha^2). \tag{2.5.8}$$

By inserting the "definition" of the running $\overline{\text{DR}}$-mass Eq. (2.5.4) into the loop-corrected $\sigma_1^{\overline{\text{DR}}}$ we obtain exactly the on-shell result σ_1^{OS} up to $\mathcal{O}(\alpha^2)$. This demonstrates that the remaining scale dependence of a loop-corrected $\overline{\text{DR}}$ quantity is a higher order (sub-leading) effect. In practice we can use the scale variation as well as the scheme variation as a measure for the theoretical uncertainty due to neglected higher order effects.

[20] Sometimes the regularization and renormalization scale is identified $\mu_0 = \mu_R$, such that the counter term is independent of either scale. Still we will keep both scales in our calculation and explain their role later in section 2.5.6.

2.5.5 Renormalization of the Two-Loop CP-Odd Mass Matrix

To discuss the renormalization of the CP-odd mass matrix we start with Eq. (2.3.14). We define a new parameter[21] $\mathrm{tb}^0 \equiv \frac{v_2^{\min}}{v_1^{\min}}$ to write

$$(\mathcal{M}_P^2)^{\mathcal{O}(x)} = \begin{pmatrix} \mathrm{tb}^0 & 1 \\ 1 & \mathrm{tb}^0 \end{pmatrix} \left\{ -(m_3^0)^2 + G^{\mathcal{O}(x)}(y_i^0) \right\}, \tag{2.5.9}$$

where we defined

$$G^{\mathcal{O}(x)} \equiv \left(\frac{h_t^2 \mu A_t}{m_{\tilde{t}_1}^2 - m_{\tilde{t}_2}^2} \right) \left[\frac{\partial \delta V^{\mathcal{O}(x)}}{\partial m_{\tilde{t}_2}^2} - \frac{\partial \delta V^{\mathcal{O}(x)}}{\partial m_{\tilde{t}_1}^2} - \frac{4 c_{2\theta}^2}{m_{\tilde{t}_1}^2 - m_{\tilde{t}_2}^2} \frac{\partial \delta V^{\mathcal{O}(x)}}{\partial s_{2\theta}^2} + \left(\frac{s_{2\theta}^2}{X_t} - \frac{1}{A_t} \right) \frac{\partial \delta V^{\mathcal{O}(x)}}{\partial \xi} \right] \tag{2.5.10}$$

and the arguments of the function $G^{\mathcal{O}(x)}(y_i^0)$ are bare parameters.

Renormalizing the external fields: Besides the bare parameters in Eq. (2.5.9), we also have to renormalize the external fields of the amputated Greens functions that we obtained with the EPA. For a bare scalar field F_i^0 this is usually referred to as *wave function renormalization (WFR)*

$$F_i^0 = \sqrt{Z_{ij}^F} F_j^R = \sqrt{\delta_{ij} + \delta Z_{ij}^F} F_j^R = \left(\delta_{ij} + \frac{1}{2} \delta Z_{ij}^F \right) F_j^R + \mathcal{O}\left((\delta Z_{ij}^F)^2 \right), \qquad (F_i^0 = P_i^0, S_i^0) \tag{2.5.11}$$

where in the last step we made a first order perturbative expansion[22] in δZ_{ij}^F. In order to transform the Greens functions into matrix elements, we have to apply external self-energies, which means that the WFR counter terms δZ_{ij}^F are the derivatives of the self-energies w.r.t. the external momentum squared, evaluated at zero external momentum consistent with the EPA.

$$\delta Z_{ij}^F = - \frac{\partial}{\partial p^2} \Sigma_{ij}^F(p^2) \Big|_{p^2=0}. \tag{2.5.12}$$

Note that the self-energies in the equation above also contain divergences in ϵ. The renormalization of the external fields is therefore essential to get finite masses and couplings[23]. In the present work we will always use the WFR counter term defined in Eq. (2.5.12) and refer to it as the on-shell renormalization of the external fields.

The Goldstone theorem: For the CP-odd and CP-even fields the external WFR constants are diagonal, i.e. $\delta Z_{ij}^P = \delta_{ij} \delta Z_i^P$ and $\delta Z_{ij}^S = \delta_{ij} \delta Z_i^S$. The calculation and explicit formulae can be found in appendix D.4. To renormalize the CP-odd Higgs mass matrix we have to multiply every element of the mass matrix by the WFR constant of the corresponding fields. Moreover we renormalize all bare parameters by substituting them by the renormalized parameters plus a counter term $y_i^0 \to y_i^R + \delta y_i$

$$(\mathcal{M}_P^2)^{\mathcal{O}(x),R} = \begin{pmatrix} (\mathrm{tb}^R + \delta \mathrm{tb}) Z_1^P & \sqrt{Z_1^P Z_2^P} \\ \sqrt{Z_1^P Z_2^P} & (\mathrm{tb}^R + \delta \mathrm{tb})^{-1} Z_2^P \end{pmatrix} \left\{ -(m_3^R)^2 - \delta m_3 + G^{\mathcal{O}(x)}(y_i^R + \delta y_i) \right\}, \tag{2.5.13}$$

[21] The careful reader notices the similarity to $\tan\beta$, however, at this point β is still the mixing angle of the CP-odd mass matrix.

[22] We will see later on that for our purpose only the $\mathcal{O}(\alpha_t)$-term of the WFR is needed, so that a first order perturbative expansion in δZ_{ij}^F is sufficient.

[23] In [31] only the divergences of the external self-energies have been used, such that the final result also in the on-shell scheme had a dependence on the renormalization scale Q. To treat the renormalization of the external fields in a consistent way, we have to use the WFR counter term defined in Eq. (2.5.12).

From this equation we already see that the Goldstone theorem holds at every order in perturbation theory. This matrix has determinant 0, which means that at least one eigenvalue has to be zero (corresponding to a massless pseudoscalar would-be Goldstone boson G)[24]. Moreover the other eigenvalue is nonzero and corresponds to the mass of the physical pseudoscalar Higgs boson A. This mass is equal to the trace of $(\mathcal{M}_P^2)^{\mathcal{O}(x)}$

$$m_A^2 = \left[(\mathrm{tb}^R + \delta\mathrm{tb})Z_1^P + (\mathrm{tb}^R + \delta\mathrm{tb})^{-1} Z_2^P\right] \left\{-(m_3^R)^2 - \delta m_3 + G^{\mathcal{O}(x)}(y_i^R + \delta y_i)\right\}. \tag{2.5.14}$$

Moreover Eq. (2.5.13) tells us that the CP-odd mixing angle β is a combination of tb^0 and Z_i^P. (The relation $\tan\beta = \mathrm{tb}^R$ is not fulfilled in general.)

Renormalizing $(\mathcal{M}_P^2)$ at $\mathcal{O}(\alpha_t + \alpha_t\alpha_s + \alpha_t^2)$: In this paragraph we will investigate how we renormalize the pseudoscalar Higgs mass matrix up to $\mathcal{O}(\alpha_t + \alpha_t\alpha_s + \alpha_t^2)$. We take Eq. (2.5.13) and expand it up to the desired order in perturbation theory. This generates the complete formula for the renormalized CP-odd mass matrix

$$\begin{aligned}(\mathcal{M}_P^2)^{\alpha_t+\alpha_t\alpha_s+\alpha_t^2,R} = &\begin{pmatrix} \mathrm{tb}^R & 1 \\ 1 & (\mathrm{tb}^R)^{-1} \end{pmatrix} \Bigg\{ -(m_3^R)^2 - \delta^{\alpha_t} m_3^2 - \delta^{\alpha_t\alpha_s} m_3^2 - \delta^{\alpha_t^2} m_3^2 + G^{\alpha_t}(y_i^R) \\ &\qquad + \left.\frac{\partial G^{\alpha_t}(y_i^0)}{\partial y_i^0}\right|_{y_i^0 = y_i^R} (\delta^{\alpha_t} y_i + \delta^{\alpha_s} y_i) + G^{\mathcal{O}(\alpha_t\alpha_s)}(y_i^R) + G^{\mathcal{O}(\alpha_t^2)}(y_i^R) \Bigg\} \\ &+ \begin{pmatrix} \delta^{\alpha_t}\mathrm{tb} + \mathrm{tb}^R \delta^{\alpha_t} Z_1^P & \frac{1}{2}(\delta^{\alpha_t} Z_1^P + \delta^{\alpha_t} Z_2^P) \\ \frac{1}{2}(\delta^{\alpha_t} Z_1^P + \delta^{\alpha_t} Z_2^P) & \delta^{\alpha_t}\mathrm{tb}^{-1} + (\mathrm{tb}^R)^{-1}\delta^{\alpha_t} Z_2^P \end{pmatrix} \Bigg\{ -\delta^{\alpha_t} m_3^2 + G^{\mathcal{O}\alpha_t}(y_i^R) \Bigg\}.\end{aligned} \tag{2.5.15}$$

This expression has to be discussed in detail. First, in terms that are already of $\mathcal{O}(\alpha_t\alpha_s)$ or $\mathcal{O}(\alpha_t^2)$ we can simply substitute the bare with the renormalized parameters, since any counter term contribution is of higher order in perturbation theory. Second we need to expand $G^{\mathcal{O}(\alpha_t)}(y_i^R + \delta^{\alpha_t} y_i + \delta^{\alpha_s} y_i)$ at the first order in α_t and α_s and we therefore have to take the first derivative of $G^{\mathcal{O}(\alpha_t)}$. This corresponds to the insertion of counter term diagrams in the one-loop contribution. Moreover we do not consider $\mathcal{O}((m_3^R)^2\alpha_t)$-terms, since these are of the same order as terms with non-vanishing external momentum[25]. The counter term $\delta^{\alpha_t} m_3^2$, however, is not proportional to m_3^2 but to $A_t\mu$. It therefore contributes also when multiplied by another $\mathcal{O}(\alpha_t)$. Now it becomes clear that the counter term for tb and the WFR counter term are only needed at $\mathcal{O}(\alpha_t)$ and $\mathcal{O}(\alpha_s)$, since they are multiplied by $(m_3^R)^2$ and $\mathcal{O}(\alpha_t)$-terms only. Note that the Higgs sector is color neutral and therefore neither $\delta Z_{ij}^{P,S}$ nor tb receive $\mathcal{O}(\alpha_s)$ corrections. All divergences of the counter terms and the G-functions cancel. The result is finite but it still depends on the renormalization scheme.

Renormalization scheme: We want to find a renormalization scheme, such that at $\mathcal{O}(\alpha_t + \alpha_t\alpha_s + \alpha_t^2)$ the relation $\tan\beta^R = \mathrm{tb}^R$ is fulfilled[26]. Keeping in mind that the renormalization scheme shifts finite terms between the renormalized input parameters and the counter term, we can choose $\delta^{\alpha_t} m_3^2$ in such a way that the last line in Eq. (2.5.15) vanishes

$$\delta^{\alpha_t} m_3^2 \equiv G^{\mathcal{O}(\alpha_t)}(y_i^R). \tag{2.5.16}$$

[24] From Eq. (2.5.13) one can also see that the Goldstone theorem requires δZ_{ij}^P to be diagonal. Otherwise the determinant of $(\mathcal{M}_P^2)^{\mathcal{O}(x)}$ would be nonzero.

[25] Nonzero momenta of external fields P_i or S_i result in terms proportional to m_3^2 and m_Z^2 when evaluated on-shell. Since we neglect these terms in the EPA, it would be inconsistent to include their counter term contribution, see section 2.2.1.

[26] β^R is the CP-odd mixing angle at $\mathcal{O}(\alpha_t + \alpha_t\alpha_s + \alpha_t^2)$. For brevity we write $\beta^R = \beta^{\mathcal{O}(\alpha_t+\alpha_t\alpha_s+\alpha_t^2)}$, remembering that β^R is the renormalized mixing angle in scheme R.

The remaining matrix $(\mathcal{M}_P^2)^{\mathcal{O}(\alpha_t+\alpha_t\alpha_s+\alpha_t^2),R}$ is diagonalized with the mixing angle β, determined by $\tan\beta = \mathrm{tb}^R$. Note that the scheme for the renormalization of β or tb respectively is not fixed yet. We will fix this scheme later in section 2.5.6. Moreover we can also fix

$$\delta^{\alpha_t\alpha_s} m_3^2 \equiv G^{\mathcal{O}(\alpha_t\alpha_s)}(y_i^R) + \left.\frac{\partial G^{\mathcal{O}(\alpha_t)}(y_i^0)}{\partial y_i^0}\right|_{y_i^0=y_i^R} \delta^{\alpha_s} y_i, \qquad \delta^{\alpha_t^2} m_3^2 \equiv G^{\mathcal{O}(\alpha_t^2)}(y_i^R) + \left.\frac{\partial G^{\mathcal{O}(\alpha_t)}(y_i^0)}{\partial y_i^0}\right|_{y_i^0=y_i^R} \delta^{\alpha_t} y_i, \tag{2.5.17}$$

such that we restore exactly the tree-level relation

$$(\mathcal{M}_P^2)^{\mathcal{O}(\alpha_t+\alpha_t\alpha_s+\alpha_t^2),R_1} = \begin{pmatrix} \mathrm{tb}^R & 1 \\ 1 & (\mathrm{tb}^R)^{-1} \end{pmatrix} \Big\{ -(m_3^{R_1})^2 \Big\}. \tag{2.5.18}$$

We will use the above scheme for the renormalization of m_3^2 during this work and refer to it as R_1, meaning that the input parameter $(m_3^{R_1})^2$ is defined in that particular scheme.
Nevertheless there is another way to restore the relation $\tan\beta = \mathrm{tb}^R$ by fixing the counter term of tb, without choosing a scheme for m_3^2

$$\delta^{\alpha_t}\mathrm{tb} = \frac{\mathrm{tb}}{2}(\delta^{\alpha_t} Z_2^P - \delta^{\alpha_t} Z_1^P). \tag{2.5.19}$$

The CP-odd mass matrix in this scheme R_2 is

$$\begin{aligned}(\mathcal{M}_P^2)^{\mathcal{O}(\alpha_t+\alpha_t\alpha_s+\alpha_t^2),R_2} = \begin{pmatrix} \mathrm{tb}^{R_2} & 1 \\ 1 & (\mathrm{tb}^{R_2})^{-1} \end{pmatrix} \Big\{ & -(m_3^R)^2 - \delta^{\alpha_t} m_3^2 - \delta^{\alpha_t\alpha_s} m_3^2 - \delta^{\alpha_t^2} m_3^2 \\ & + G^{\mathcal{O}(\alpha_t)}(y_i^R) + \left.\frac{\partial G^{\mathcal{O}(\alpha_t)}(y_i^0)}{\partial y_i^0}\right|_{y_i^0=y_i^R} (\delta^{\alpha_t} y_i + \delta^{\alpha_s} y_i) + G^{\mathcal{O}(\alpha_t\alpha_s)}(y_i^R) + G^{\mathcal{O}(\alpha_t^2)}(y_i^R) \Big\}. \end{aligned} \tag{2.5.20}$$

Note that by taking only the divergent $\overline{\mathrm{DR}}$-part of δZ_i^P and $\delta\mathrm{tb}$ the condition Eq. (2.5.19) is automatically fulfilled. This is what was done in [31], but here we want to calculate matrix elements and therefore it is essential to take into account also the finite part of the WFR counter term δZ_i^P.

2.5.6 Renormalization of the Two-Loop CP-Even Mass Matrix

Renormalizing the "tree-level-like" part: To discuss the renormalization of the CP-even mass matrix, we start with the first term of Eq. (2.3.9), $(\mathcal{M}_S^2)_{ij}^0$, because this can be done almost analogously to the renormalization of the CP-odd mass matrix. We renormalize by applying WFR counter terms to this mass matrix while keeping the bare parameters y_k^0 for the moment

$$(\mathcal{M}_S^2)_{ij}^{0,R} = (-1)^{i+j}\left[\frac{g^2+g'^2}{4} v_i^{\min} v_j^{\min}\right] + \begin{pmatrix} Z_1^S (\mathcal{M}_P^2)_{11}^{\mathcal{O}(x)}(y_k^0) & -\sqrt{Z_1^S Z_2^S}(\mathcal{M}_P^2)_{12}^{\mathcal{O}(x)}(y_k^0) \\ -\sqrt{Z_1^S Z_2^S}(\mathcal{M}_P^2)_{12}^{\mathcal{O}(x)}(y_k^0) & Z_2^S (\mathcal{M}_P^2)_{22}^{\mathcal{O}(x)}(y_k^0) \end{pmatrix}. \tag{2.5.21}$$

Due to the hierarchy $h_t \gg g, g'$, we do not take into account $\mathcal{O}(\alpha_t(g^2+g'^2))$-terms. Besides they are of the same order as terms with non-vanishing external momentum[27]. Moreover higher order corrections to g^2 and g'^2 are proportional to themselves, i.e. $\delta g^2 \sim g^2$ and $\delta g'^2 \sim g'^2$. The first term in Eq. (2.5.21) is proportional to $(g^2+g'^2)$ and will therefore not be renormalized. We can express it by the mass of the Z-boson[28]. The second term is the same as Eq. (2.5.13) with $Z_i^P \to Z_i^S$ and a minus sign for the off-diagonal matrix elements. Using the renormalization scheme R_1 for $(m_3^0)^2$ we arrive at an expression analogous to

[27] The argument is the same as for $\mathcal{O}((m_3^R)^2\alpha_t)$-terms, see section 2.5.5.

[28] We are free to choose the scheme for m_Z, because in the absence of any radiative corrections, we can identify the tree-level mass with the renormalized mass.

Eq. (refm3RismAR), which is completely independent of Z_i^P or Z_i^S. This part can therefore be expressed by the renormalized mass ($m_A^{R_1}$) and the renormalized mixing angle β^R. The "tree-level-like" part of the CP-even mass matrix can then be written in the following form

$$(\mathcal{M}_S^2)^{0,R} = \begin{pmatrix} m_Z^2 c_{\beta^R}^2 + (m_A^{R_1})^2 s_{\beta^R}^2 & -(m_Z^2 + (m_A^{R_1})^2) c_{\beta^R} s_{\beta^R} \\ -(m_Z^2 + (m_A^{R_1})^2) c_{\beta^R} s_{\beta^R} & m_Z^2 s_{\beta^R}^2 + (m_A^{R_1})^2 c_{\beta^R}^2 \end{pmatrix}. \tag{2.5.22}$$

The parameters $m_A^{R_1}$ and β^R will serve as input parameters for the CP-even masses and also for the couplings. In this way the CP-even masses and couplings can be calculated without using the explicit formulae for the CP-odd masses derived in section 2.5.5. The calculation of the CP-odd mass only defines a relation between the parameter m_3^R and m_A^R in different renormalization schemes.

Renormalizing the "higher order" part: To study the renormalization of $(\delta\mathcal{M}_S^2)_{ij}^{\mathcal{O}(x)}$ we explicitly look at $\mathcal{O}(x) = \mathcal{O}(\alpha_t + \alpha_t\alpha_s + \alpha_t^2)$. Adding external WFR counter terms, replacing bare parameters and expanding perturbatively yields

$$\begin{aligned}(\Delta\mathcal{M}_S^2)_{ij}^{\mathcal{O}(\alpha_t+\alpha_t\alpha_s+\alpha_t^2),R} = &\begin{pmatrix} \delta Z_1^S (\Delta\mathcal{M}_S^2)_{11}^{\mathcal{O}(\alpha_t)}(y_k^R) & -\frac{1}{2}(\delta Z_1^S + \delta Z_2^S)(\Delta\mathcal{M}_S^2)_{12}^{\mathcal{O}(\alpha_t)}(y_k^R) \\ -\frac{1}{2}(\delta Z_1^S + \delta Z_2^S)(\Delta\mathcal{M}_S^2)_{12}^{\mathcal{O}(\alpha_t)}(y_k^R) & \delta Z_2^S (\Delta\mathcal{M}_S^2)_{22}^{\mathcal{O}(\alpha_t)}(y_k^R) \end{pmatrix} \\ &+ (\delta\mathcal{M}_S^2)_{ij}^{\mathcal{O}(\alpha_t+\alpha_t\alpha_s+\alpha_t^2)}(y_k^R) + \sum_k \left.\frac{\partial(\Delta\mathcal{M}_S^2)_{ij}^{\mathcal{O}(\alpha_t)}(y_k^0)}{\partial y_k^0}\right|_{y_k^0=y_k^R} (\delta^{\alpha_s} y_k + \delta^{\alpha_t} y_k)\,.\end{aligned} \tag{2.5.23}$$

The RHS of the first line corresponds to applying external WFR counter terms to the one-loop part. The first term on the second line is simply the higher order piece, expressed by renormalized parameters. The last term is the counter term contribution, which corresponds to a first order expansion of the one-loop part. The divergent parts of the counter terms δy_k and $\delta Z_i^{P,S}$ contain poles in ϵ when they are multiplied by the finite parts of $(\Delta\mathcal{M}_S^2)^{\mathcal{O}(\alpha_t)}$. These poles cancel against the ones coming from the pure two-loop piece $(\delta\mathcal{M}_S^2)^{\mathcal{O}(\alpha_t\alpha_s+\alpha_t^2)}$ such that the renormalized mass matrix$(\Delta\mathcal{M}_S^2)^{\mathcal{O}(\alpha_t+\alpha_t\alpha_s+\alpha_t^2),R}$ is finite. Moreover the divergences in δy_k and $\delta Z_i^{P,S}$ yield finite contributions when multiplied by $\mathcal{O}(\epsilon)$-terms in $(\Delta\mathcal{M}_S^2)^{\mathcal{O}(\alpha_t)}$. This is an important feature of DREG and DRED: We first expand perturbatively while keeping ϵ fixed and only in the very end we send ϵ to zero. To evaluate the first and the last term of Eq. (2.5.23) we use the explicit form for the matrix $(\Delta\mathcal{M}_S^2)^{\mathcal{O}(\alpha_t)}$, presented in section 2.4.1.

Counter terms and renormalization scheme: In this section we will discuss in detail the counter term contribution to the $\mathcal{O}(\alpha_t + \alpha_t\alpha_s + \alpha_t^2)$ masses

$$\sum_k \left.\frac{\partial(\Delta\mathcal{M}_S^2)_{ij}^{\mathcal{O}(\alpha_t)}(y_k^0)}{\partial y_k^0}\right|_{y_k^0=y_k^R} (\delta^{\alpha_s} y_k + \delta^{\alpha_t} y_k)\,. \tag{2.5.24}$$

We have to renormalize all bare parameters that occur in the one-loop correction to the mass matrix $(\Delta\mathcal{M}_S^2)^{\mathcal{O}(\alpha_t)}$, namely

$$y_k^0 = m_t, m_{\tilde{t}_1}^2, m_{\tilde{t}_2}^2, h_t^2, \mu, A_t, s_{2\theta}. \tag{2.5.25}$$

For this we have to derive all counter terms up to $\mathcal{O}(\alpha_t + \alpha_s)$ for all bare quantities in the one-loop masses Eq. (2.5.25). Remember that a counter term consists of a uniquely determined divergent piece plus a scheme-dependent finite part. The scheme-dependence is absorbed in the input parameters. We will describe in the following how we choose the schemes for the different counter terms (most of this is analogous to [32,33]). Note that the renormalization scheme introduced in the following will also be used

for the couplings. We choose to define the counter terms for the masses in the on-shell scheme, which means that the counter term is simply the negative real part of the self-energy evaluated at the pole mass itself. The top mass counter term is given by

$$\delta m_t^2 = -2m_t \Re\Sigma_t(m_t), \tag{2.5.26}$$

where Σ_t is the self-energy of the top quark. The renormalization of the stop sector is described in appendix D.1. The counter terms for the squared stop masses are the real parts of the diagonal entries of the stop self-energy-matrix $\Pi_{ij}^{\tilde{t}}$ in the mass eigenstate basis

$$\delta m_{\tilde{t}_1}^2 = -\Re\Pi_{11}^{\tilde{t}}(m_{\tilde{t}_1}^2), \qquad \delta m_{\tilde{t}_2}^2 = -\Re\Pi_{22}^{\tilde{t}}(m_{\tilde{t}_2}^2). \tag{2.5.27}$$

The counter term for the stop mixing angle is obtained from the off-diagonal entries of the stop self-energy matrix in the mass eigenstate basis evaluated in an anti-symmetric way, see Eq. (D.1.8)

$$\delta\theta = -\frac{1}{2}\frac{\Pi_{12}(m_{\tilde{t}_1}^2) + \Pi_{12}(m_{\tilde{t}_2}^2)}{m_{\tilde{t}_1}^2 - m_{\tilde{t}_2}^2}. \tag{2.5.28}$$

Trigonometric functions of the mixing angle can be renormalized by using the chain rule, e.g. $\delta s_{2\theta} = 2c_{2\theta}\delta\theta$.
We want a renormalization scheme for $v_1^{\min}$ and $v_2^{\min}$, such that the relation $G_F = [\sqrt{2}(v_1^2 + v_2^2)]^{-1}$, see Eq. (2.3.5) is fulfilled also when taking into account higher orders. We introduce the parameter $(v^0)^2 = (v_1^{\min})^2 + (v_2^{\min})^2$. The renormalized muon decay constant is

$$G_F^R = \frac{1+\delta r}{\sqrt{2}v_0^2} = \frac{1+\delta r}{\sqrt{2}[(v^R)^2 + 2v^R\delta v]}, \tag{2.5.29}$$

where the only contribution to δr at $\mathcal{O}(\alpha_t)$ comes from the transversal self-energy of the W-boson. $\delta r = \frac{-\Pi_{WW}^T(0)}{m_W^2}$. Solving this for δv we find

$$\delta v = -\frac{v^R}{2}\frac{\Pi_{WW}^T(0)}{m_W^2}. \tag{2.5.30}$$

Moreover we can express the renormalized MSSM VEVs by $v_1^R = v^R\cos\beta^R$ and $v_2^R = v^R\sin\beta^R$. As shown earlier in this section, β^R is the renormalized CP-odd mixing angle coinciding with the renormalized ratio of the VEVs. In this way the renormalized VEVs v_1^R, v_2^R and v^R are fixed by two input parameters: the measured muon decay constant G_F^R and $\tan\beta^R$.
Since there is no obvious OS definition for the CP-odd mixing angle, we are free to define $\tan\beta^R$ in any scheme we like. We will simply choose the $\overline{\text{DR}}$ scheme, where the counter term is evaluated at the scale $\mu_R^{\alpha_t} = m_t$. The $\overline{\text{DR}}$-counter term for β can be obtained from the divergent part of the external self-energies of the neutral Higgs fields δZ_i^S, see appendix D.4.

$$\delta^{\overline{\text{DR}}}\beta = -s_\beta c_\beta \delta Z_2^S|_{\epsilon^{-1}}\left(1 + \epsilon\log\frac{m_t^2}{Q^2}\right) \tag{2.5.31}$$

The counter term for μ is also chosen to be in the $\overline{\text{DR}}$ scheme, evaluated at the scale $\mu_R^{\alpha_t} = m_t$. The $\overline{\text{DR}}$ counter term can be obtained from the fact that $\delta(\mu v_2) = \delta(\mu v s_\beta) = 0$, which follows from a SUSY-non-renormalization theorem[29] [13]. Applying the chain rule yields

$$\delta^{\overline{\text{DR}}}\mu = -\mu\left[\frac{\delta v|_{\epsilon^{-1}}}{v}\left(1 + \epsilon\log\frac{m_t^2}{Q^2}\right) + \frac{c_\beta}{s_\beta}\delta^{\overline{\text{DR}}}\beta\right]. \tag{2.5.32}$$

[29] Alternatively one could calculate the counter term for μ via the Higgsino self-energy.

The counter term for A_t is fixed such that the tree-level relation Eq. (1.3.7) remains also valid for the renormalized parameters. Applying the chain rule yields

$$\delta A_t = \left(\frac{\delta m^2_{\tilde{t}_1} - \delta m^2_{\tilde{t}_2}}{m^2_{\tilde{t}_1} - m^2_{\tilde{t}_2}} + \frac{\delta s^2_{2\theta}}{2 s^2_{2\theta}} - \frac{\delta m^2_t}{2 m^2_t} \right) \left(A_t + \mu \frac{c_\beta}{s_\beta} \right) - \frac{c_\beta}{s_\beta} \delta\mu + \mu \frac{\delta\beta}{s^2_\beta}. \tag{2.5.33}$$

The counter term δh_t is also defined via the tree-level expression $m_t^2 = \frac{1}{2} h_t^2 v_2^2$ by using the chain rule

$$\delta h_t^2 = \frac{2\delta m_t^2}{v_2^2} - 2 h_t^2 \left(\frac{\delta v}{v} + \frac{c_\beta}{s_\beta} \delta\beta \right). \tag{2.5.34}$$

We will refer to the above collection of counter terms and the corresponding input parameters as the *on-shell (OS)* scheme. The calculations and the results for the self-energies are presented in appendix D. Note that the Higgs sector as well as the W's are color neutral. The self-energy $\Pi^T_{WW}(0)$ and the $\delta Z_i^{P,S}$ do not acquire any α_s contribution and therefore $\delta^{\alpha_s}\beta = \delta^{\alpha_s}\mu = \delta^{\alpha_s} v = 0$. As a consequence the counter terms $\delta^{\alpha_s} A_t$ and $\delta^{\alpha_s} h_t$ have a simpler structure and also the RHS of the first line of Eq. (2.5.23) has no $\mathcal{O}(\alpha_s)$ contribution.
As already explained in section 2.5.3 the masses in the OS scheme are manifestly invariant under a change in the renormalization scale. However, the OS counter terms and the effective potential explicitly depend on the regularization scale $Q^2 \equiv 4\pi\mu_0^2 e^{-\gamma_E}$ via a logarithm. Each of these logarithms in Q is connected to a pole in the regulator and therefore the cancellation of the poles in the regulator also implies a calculation of the logarithms involving the regularization scale. It serves as a nontrivial consistency check in our calculation to check that the renormalized masses and couplings are independent of the regularization scale.

Evaluating the CP-even mass in $\overline{\text{DR}}$ scheme: Having specified all the counter terms in a certain scheme, we can easily shift the masses also to the $\overline{\text{DR}}$ scheme. For this we use the $\overline{\text{DR}}$ counter term, which is simply the divergent part of the OS counter term multiplied by $(1 + \epsilon \log Q^2/{\mu_R}^2)$, see appendix D.5 and D.6. The corresponding input parameters are then the running $\overline{\text{DR}}$ parameters.
Note that also in the $\overline{\text{DR}}$ renormalized CP-even mass matrix the dependence on the regularization scale Q has to cancel between the counter terms and the derivatives of the effective potential. However, there is still a dependence on the renormalization scale μ_R from the input parameters and the counter terms. The sensitivity of the mass $(\Delta\mathcal{M}_S^2)^{\mathcal{O}(\alpha_t + \alpha_t\alpha_s + \alpha_t^2), \overline{\text{DR}}}$ to a variation of μ_R serves as a measure of how well the perturbative calculation approximates the full result[30].
As we explained in section 2.5.5 we cannot consistently define a $\overline{\text{DR}}$ scheme for the external WFR counter terms. We therefore use the "on-shell" definition for the WFR counter terms regardless of what scheme was used for the other counter terms.

Shifting the CP-even mass to any other scheme: The $\overline{\text{DR}}$ renormalized mass can be shifted to any other renormalization scheme R by adding a finite counter term and evaluating the mass using the input parameters in scheme R

$$\begin{aligned}(\Delta\mathcal{M}_S^2)^{\mathcal{O}(\alpha_t + \alpha_t\alpha_s + \alpha_t^2), R} = {} & (\Delta\mathcal{M}_S^2)^{\mathcal{O}(\alpha_t + \alpha_t\alpha_s + \alpha_t^2), \overline{\text{DR}}} \Big|_{y_k^{\overline{\text{DR}}} = y_k^R} \\ & + \sum_k \frac{\partial (\Delta\mathcal{M}_S^2)^{\mathcal{O}(\alpha_t)}(y_k^0)}{\partial y_k^0} \Big|_{y_k^0 = y_k^R} \left(\Delta^{\alpha_s, R} y_k + \Delta^{\alpha_t, R} y_k \right). \end{aligned} \tag{2.5.35}$$

[30] Note that the Higgs masses we calculate correspond to the pole masses in the limit of vanishing external momentum independent of the renormalization scheme that we use. The Higgs mass renormalized in the $\overline{\text{DR}}$ scheme is not the same as the running $\overline{\text{DR}}$ Higgs mass.

Note that our $\overline{\text{DR}}$ counter terms also contain logarithms of the regularization scale Q, which have to be absorbed in the finite counter terms $\Delta^R y_k$.

Renormalized masses of physical CP-even Higgs bosons: The eigenvalues of the renormalized loop-corrected CP-even mass matrix in scheme R are the squared masses of the loop-corrected, physical CP-even Higgs bosons. They can be easily calculated using Eq. (A.1.3). The renormalized loop-corrected masses of the light and heavy scalar Higgs bosons h and H in scheme R are thus given by

$$\left(m_{H,h}^{\mathcal{O}(x),R}\right)^2 = \frac{1}{2}\left[(\mathcal{M}_S^2)_{11}^{\mathcal{O}(x),R} + (\mathcal{M}_S^2)_{22}^{\mathcal{O}(x),R} \pm \sqrt{\left((\mathcal{M}_S^2)_{11}^{\mathcal{O}(x),R} - (\mathcal{M}_S^2)_{22}^{\mathcal{O}(x),R}\right)^2 + 4\left((\mathcal{M}_S^2)_{12}^{\mathcal{O}(x),R}\right)^2}\right]. \tag{2.5.36}$$

2.5.7 Renormalization of the Two-Loop Couplings

The bare trilinear couplings are calculated using Eq. (2.3.24). The tree-level parts λ^0 were explicitly given in Eq. (1.4.30). They are of $\mathcal{O}(g^2 + g'^2)$ and are therefore not renormalized. To renormalize the higher order contribution $\delta\lambda^{\mathcal{O}(x)}$ up to $\mathcal{O}(x) = \mathcal{O}(\alpha_t + \alpha_t\alpha_s + \alpha_t^2)$, we proceed as usual. We add external self-energies, substitute bare parameters and expand perturbatively

$$\begin{aligned}\Delta\lambda_{\mathcal{H}_i\mathcal{H}_j\mathcal{H}_k}^{\mathcal{O}(\alpha_t+\alpha_t\alpha_s+\alpha_t^2),R} =& \delta\lambda_{\mathcal{H}_i\mathcal{H}_j\mathcal{H}_k}^{\mathcal{O}(\alpha_t+\alpha_t\alpha_s+\alpha_t^2)}(y_m^R) + \sum_l \left.\frac{\partial\Delta\lambda_{\mathcal{H}_i\mathcal{H}_j\mathcal{H}_k}^{\mathcal{O}(\alpha_t)}(y_m^0)}{\partial y_l^0}\right|_{y_m^0=y_m^R} (\delta^{\alpha_s} y_l + \delta^{\alpha_t} y_l) \\ &+ \Pi_{\mathcal{H}_i\mathcal{H}_j\mathcal{H}_k}^{\mathcal{O}(\alpha_t^2)},\end{aligned} \tag{2.5.37}$$

where $\Pi_{\mathcal{H}_i\mathcal{H}_j\mathcal{H}_k}^{\mathcal{O}(\alpha_t^2)}$ are the external self-energies of the external fields $\mathcal{H}_i, \mathcal{H}_j, \mathcal{H}_k$. The one-loop $\mathcal{O}(\alpha_t)$ couplings $\Delta\lambda^{\mathcal{O}(\alpha_t)}$ are given in terms of the following bare parameters

$$y_i^0 = h_t^2, v_2^{\min}, s_{2\theta}, c_{2\theta}^2, Y_t, W_t, Z_t, m_t, m_{\tilde{t}_1}^2, m_{\tilde{t}_2}^2. \tag{2.5.38}$$

Moreover all λ's depend on the two-loop mixing angles $\alpha^{\mathcal{O}(\alpha_t+\alpha_t\alpha_s+\alpha_t^2)}$ and $\beta^{\mathcal{O}(\alpha_t+\alpha_t\alpha_s+\alpha_t^2)}$. The former is determined by diagonalizing the renormalized CP-even mass matrix $(\Delta\mathcal{M}_S^2)^{\mathcal{O}(\alpha_t+\alpha_t\alpha_s+\alpha_t^2),R}$, whereas the latter corresponds to the renormalized input parameter β^R.

Counter terms and renormalization scheme: For the two-loop couplings we use the OS and $\overline{\text{DR}}$ scheme defined in the previous section. The counter terms for the quantities $c_{2\theta}^2, Y_t, W_t, Z_t$ can be derived using the chain rule

$$\delta c_{2\theta}^2 = -2 s_{2\theta}\delta s_{2\theta}, \tag{2.5.39}$$
$$\delta Y_t = \delta A_t - \delta\mu\tan\beta, \tag{2.5.40}$$
$$\delta Z_t = \delta A_t + \delta\mu\cot\alpha, \tag{2.5.41}$$
$$\delta W_t = \delta A_t - \delta\mu\tan\alpha, \tag{2.5.42}$$

where at $\mathcal{O}(\alpha_s)$ these counter terms simplify to

$$\delta^{\alpha_s} c_{2\theta}^2 = -2 s_{2\theta}\delta^{\alpha_s} s_{2\theta}, \qquad \delta^{\alpha_s} Y_t = \delta^{\alpha_s} Z_t = \delta^{\alpha_s} W_t = \delta^{\alpha_s} A_t. \tag{2.5.43}$$

External WFR counter terms for the couplings: We need to calculate external WFR counter terms for the couplings in the physical fields multiplied with the corresponding one-loop couplings, denoted by $\Pi^{\mathcal{O}(\alpha_t^2)}_{\mathcal{H}_i\mathcal{H}_j\mathcal{H}_k}$. These self-energies involve the mixing of the CP-odd and CP-even eigenstates and therefore several one-loop couplings contribute to a particular two-loop coupling. This correlation between different one-loop couplings makes the renormalization of the external fields for the couplings more involved than for the mass matrix. We will present an algorithm that explains how the renormalization of the external fields for the couplings can be derived from the one-loop couplings and the WFR counter terms of the current eigenstates. We start by writing the Lagrangian with trilinear one-loop couplings as

$$\mathcal{L}^{\mathcal{O}(\alpha_t)}_{\text{tril}}(h^0,H^0,A^0,G^0) = \sum_{i,j,k} \Delta\lambda^{\mathcal{O}(\alpha_t)}_{\mathcal{H}_i\mathcal{H}_j\mathcal{H}_k} \mathcal{H}^0_i\mathcal{H}^0_j\mathcal{H}^0_k. \tag{2.5.44}$$

Using the chain rule we renormalize the fields of this Lagrangian $P^0_i = \left(1+\frac{1}{2}\delta^{\alpha_t}Z^P_i\right)P^R_i$ and $S^0_i = \left(1+\frac{1}{2}\delta^{\alpha_t}Z^S_i\right)S^R_i$

$$\delta\mathcal{L}^{\mathcal{O}(\alpha_t^2)}_{\text{tril}} = \frac{1}{2}\sum_i \left\{ \frac{\partial\mathcal{L}^{\mathcal{O}(\alpha_t)}_{\text{tril}}}{\partial P_i}\delta^{\alpha_t}Z^P_i + \frac{\partial\mathcal{L}^{\mathcal{O}(\alpha_t)}_{\text{tril}}}{\partial S_i}\delta^{\alpha_t}Z^S_i \right\} \tag{2.5.45}$$

$$= \frac{1}{2}\sum_{i,k} \left\{ \frac{\partial\mathcal{L}^{\mathcal{O}(\alpha_t)}_{\text{tril}}}{\partial\mathcal{H}_k}\frac{\partial\mathcal{H}_k}{\partial P_i}\delta^{\alpha_t}Z^P_i + \frac{\partial\mathcal{L}^{\mathcal{O}(\alpha_t)}_{\text{tril}}}{\partial\mathcal{H}_k}\frac{\partial\mathcal{H}_k}{\partial S_i}\delta^{\alpha_t}Z^S_i \right\}. \tag{2.5.46}$$

To evaluate the derivatives $\frac{\partial\mathcal{H}_k}{\partial P_i}$ and $\frac{\partial\mathcal{H}_k}{\partial S_i}$ we use the inverse of Eqs. (2.3.21, 2.3.22)

$$h = c_\alpha S_1 - s_\alpha S_2, \quad H = s_\alpha S_1 + c_\alpha S_2, \quad A = s_\alpha P_1 + c_\alpha P_2, \quad G = c_\alpha P_1 - s_\alpha P_2. \tag{2.5.47}$$

The remaining fields S^R_i and P^R_i of the counter terms are written in terms of the fields h^R, H^R, A^R, G^R using the original rotations Eqs. (2.3.21, 2.3.22), such that we obtain a "counter term-Lagrangian" as a function of these fields $\delta\mathcal{L}^{\mathcal{O}(\alpha_t^2)}_{\text{tril}}(h,H,A,G)$. By taking derivatives w.r.t. these fields we can then generate the external WFR counter terms for the couplings

$$\Pi^{\mathcal{O}(\alpha_t^2)}_{\mathcal{H}_i\mathcal{H}_j\mathcal{H}_k} = \frac{\partial\delta\mathcal{L}^{\mathcal{O}(\alpha_t^2)}_{\text{tril}}(h^R,H^R,A^R,G^R)}{\partial\mathcal{H}^R_i\partial\mathcal{H}^R_j\partial\mathcal{H}^R_k}. \tag{2.5.48}$$

The explicit expressions are

$$\Pi^{\mathcal{O}(\alpha_t^2)}_{hhh} = \frac{3}{2}\left\{\Delta\lambda^{\mathcal{O}(\alpha_t)}_{hhH}c_\alpha s_\alpha\left(\delta Z^S_2 - \delta Z^S_1\right) + \Delta\lambda^{\mathcal{O}(\alpha_t)}_{hhh}(c^2_\alpha\delta Z^S_2 + s^2_\alpha\delta Z^S_1)\right\}, \tag{2.5.49}$$

$$\Pi^{\mathcal{O}(\alpha_t^2)}_{HHH} = \frac{3}{2}\left\{\Delta\lambda^{\mathcal{O}(\alpha_t)}_{hHH}c_\alpha s_\alpha\left(\delta Z^S_2 - \delta Z^S_1\right) + \Delta\lambda^{\mathcal{O}(\alpha_t)}_{HHH}\left(c^2_\alpha\delta Z^S_1 + s^2_\alpha\delta Z^S_2\right)\right\}, \tag{2.5.50}$$

$$\Pi^{\mathcal{O}(\alpha_t^2)}_{hhH} = \frac{1}{2}\left\{\Delta\lambda^{\mathcal{O}(\alpha_t)}_{hhH}\left[\delta Z^S_1(1+s^2_\alpha) + \delta Z^S_2(1+c^2_\alpha)\right] + \left(\delta Z^S_2 - \delta Z^S_1\right)c_\alpha s_\alpha\left(\Delta\lambda^{\mathcal{O}(\alpha_t)}_{hhh} + 2\Delta\lambda^{\mathcal{O}(\alpha_t)}_{hHH}\right)\right\}, \tag{2.5.51}$$

$$\Pi^{\mathcal{O}(\alpha_t^2)}_{hHH} = \frac{1}{2}\left\{\Delta\lambda^{\mathcal{O}(\alpha_t)}_{hHH}\left[\delta Z^S_1(1+c^2_\alpha) + \delta Z^S_2(1+s^2_\alpha)\right] + c_\alpha s_\alpha(\delta Z^S_2 - \delta Z^S_1)(\Delta\lambda^{\mathcal{O}(\alpha_t)}_{HHH} + 2\Delta\lambda^{\mathcal{O}(\alpha_t)}_{hhH})\right\}, \tag{2.5.52}$$

$$\Pi^{\mathcal{O}(\alpha_t^2)}_{hAA} = \frac{1}{2}\left\{\Delta\lambda^{\mathcal{O}(\alpha_t)}_{hAA}\left[+2\delta Z^P_1 s^2_\beta + 2\delta Z^P_2 c^2_\beta + \delta Z^S_1 s^2_\alpha + \delta Z^S_2 c^2_\alpha\right] + \Delta\lambda^{\mathcal{O}(\alpha_t)}_{HAA}c_\alpha s_\alpha(\delta Z^S_2 - \delta Z^S_1)\right.$$
$$\left. + \Delta\lambda^{\mathcal{O}(\alpha_t)}_{hAG}2c_\beta s_\beta(\delta Z^P_1 - \delta Z^P_2)\right\}, \tag{2.5.53}$$

$$\Pi^{\mathcal{O}(\alpha_t^2)}_{HAA} = \frac{1}{2}\Big\{\Delta\lambda^{\mathcal{O}(\alpha_t)}_{HAA}\left[\delta Z_1^S c_\alpha^2 + \delta Z_2^S s_\alpha^2 + 2\delta Z_1^P s_\beta^2 + 2\delta Z_2^P c_\beta^2\right] + \Delta\lambda^{\mathcal{O}(\alpha_t)}_{hAA} c_\alpha s_\alpha(\delta Z_2^S - \delta Z_1^S)$$
$$+ \Delta\lambda^{\mathcal{O}(\alpha_t)}_{HAG} 2c_\beta s_\beta(\delta Z_1^P - \delta Z_2^P)\Big\}, \tag{2.5.54}$$

$$\Pi^{\mathcal{O}(\alpha_t^2)}_{hGG} = \frac{1}{2}\Big\{\Delta\lambda^{\mathcal{O}(\alpha_t)}_{hGG}\left[\delta Z_1^S s_\alpha^2 + \delta Z_2^S c_\alpha^2 + 2\delta Z_1^P c_\beta^2 + 2\delta Z_2^P s_\beta^2\right] + \Delta\lambda^{\mathcal{O}(\alpha_t)}_{HGG} c_\alpha s_\alpha(\delta Z_2^S - \delta Z_1^S)$$
$$+ 2s_\beta c_\beta \Delta\lambda^{\mathcal{O}(\alpha_t)}_{hAG}(\delta Z_1^P - \delta Z_2^P)\Big\}, \tag{2.5.55}$$

$$\Pi^{\mathcal{O}(\alpha_t^2)}_{HGG} = \frac{1}{2}\Big\{\Delta\lambda^{\mathcal{O}(\alpha_t)}_{HGG}\left[\delta Z_1^S c_\alpha^2 + \delta Z_2^S s_\alpha^2 + 2\delta Z_2^P s_\beta^2 + 2\delta Z_1^P c_\beta^2\right] + \Delta\lambda^{\mathcal{O}(\alpha_t)}_{hGG} c_\alpha s_\alpha\left(\delta Z_2^S - \delta Z_1^S\right)$$
$$+ 2s_\beta c_\beta \Delta\lambda^{\mathcal{O}(\alpha_t)}_{HAG} c_\beta s_\beta(\delta Z_1^P - \delta Z_2^P)\Big\}, \tag{2.5.56}$$

$$\Pi^{\mathcal{O}(\alpha_t^2)}_{hAG} = \frac{1}{2}\Big\{\Delta\lambda^{\mathcal{O}(\alpha_t)}_{hAG}\left[\delta Z_1^S s_\alpha^2 + \delta Z_2^S c_\alpha^2 + \delta Z_1^P + \delta Z_2^P\right] + \Delta\lambda^{\mathcal{O}(\alpha_t)}_{HAG} c_\alpha s_\alpha(\delta Z_2^S - \delta Z_1^S))$$
$$+ c_\beta s_\beta(\delta Z_1^P - \delta Z_2^P)\left(\Delta\lambda^{\mathcal{O}(\alpha_t)}_{hAA} + \Delta\lambda^{\mathcal{O}(\alpha_t)}_{hGG}\right)\Big\}, \tag{2.5.57}$$

$$\Pi^{\mathcal{O}(\alpha_t^2)}_{HAG} = \frac{1}{2}\Big\{\Delta\lambda^{\mathcal{O}(\alpha_t)}_{HAG}\left[\delta Z_1^S c_\alpha^2 + \delta Z_2^S s_\alpha^2 + \delta Z_1^P + \delta Z_2^P\right] + \Delta\lambda^{\mathcal{O}(\alpha_t)}_{hAG} c_\alpha s_\alpha(\delta Z_2^S - \delta Z_1^S)$$
$$+ c_\beta s_\beta(\delta Z_1^P - \delta Z_2^P)\left(\Delta\lambda^{\mathcal{O}(\alpha_t)}_{HAA} + \Delta\lambda^{\mathcal{O}(\alpha_t)}_{HGG}\right)\Big\}. \tag{2.5.58}$$

Chapter 3

Numerical Analysis of Higgs Masses and Self-Couplings

In the previous chapter, we explained how $\mathcal{O}(\alpha_s\alpha_t+\alpha_t^2)$ corrections to the Higgs masses and self-couplings can be calculated using the EPA. In section 2.5.6 and 2.5.7 we introduced two renormalization schemes, the on-shell and the $\overline{\text{DR}}$ scheme. In this section we will numerically evaluate the Higgs masses and self-couplings and discuss the implications of the higher order corrections.

3.1 Higgs Masses

Our analytical results for the $\mathcal{O}(\alpha_t + \alpha_s\alpha_t + \alpha_t^2)$ corrections to the Higgs masses in $\overline{\text{DR}}$ scheme have been checked to agree with [32, 33] except for terms due to the difference in the WFR counter term, see Eq. (2.5.12). In contrast to [32,33] we will only take into account results from the EPA at $\mathcal{O}(\alpha_t+\alpha_s\alpha_t+\alpha_t^2)$ for the numerical analysis, without including the full one-loop calculation [22].
In the following we discuss how we fix the numerical values of the parameters entering the expression for the renormalized CP-even Higgs mass matrix, given in Eqs. (2.5.22, 2.5.23). To evaluate the "tree-level-like" part, Eq. (2.5.22) we need the mass of the Z-boson m_Z in no specified scheme (see footnote 28), the renormalized CP-odd mixing angle β^R and the CP-odd Higgs mass $m_A^{R_1}$, in renormalization scheme R_1. This renormalization scheme corresponds to an on-shell mass, determined with the EPA, i.e. external momenta are set to zero. For m_Z we will simply choose the pole mass of the Z-boson, which is determined experimentally up to high precision [62]

$$m_Z = 91.1876 \pm 0.0021 \text{ GeV}. \tag{3.1.1}$$

The quantities β^R and $m_A^{R_1}$ affect m_h in the same way as the input parameters for the tree-level Higgs sector used in Figure 1.3. They will be varied, keeping in mind the latest exclusion limits from LEP and the LHC, see Figure 1.4.
The expression for the "higher order" part, Eq. (2.5.23) can either be evaluated in the OS or $\overline{\text{DR}}$ scheme. We only have to fix the input parameters in the OS scheme, because the latter are calculated using the first by means of Eq. (2.5.4).

3.1.1 On-Shell Scheme

The top pole mass has been measured by the experiments at the LHC and the Tevatron. We will use the top pole mass, $m_t = 172.9$ GeV [63] as the input value for the OS top mass in all our analyses. The

SM VEV v can be extracted from the most recently measured values for the Fermi constant [64] using $G_F = [\sqrt{2}v^2]^{-1} = 1.16637 \cdot 10^{-5}$ GeV^{-2}. Moreover we use $\alpha_s(m_Z^2) = 0.118$. Since α_s enters only at the two-loop level, any scale variation accounts for three-loop effects and is therefore irrelevant for our purpose[1]. The top-Yukawa coupling is determined by the tree-level relation $h_t = \sqrt{2}\frac{m_t}{v s_\beta}$. Moreover we need to fix the MSSM parameters of the stop sector $m_Q^{\rm OS}$, $m_U^{\rm OS}$, $X_t^{\rm OS}$ and the Higgsino and gluino mass mu and $m_{\tilde{g}}$. Since these parameters have not yet been measured, we use two benchmark scenarios, the $m_h^{\rm max}$ and the *no-mixing* scenario [65] to determine the values for these parameters[2]. The $m_h^{\rm max}$ scenario uses a common SUSY scale $m_Q^{\rm OS} = m_U^{\rm OS} = M_{\rm SUSY} = 1$ TeV and is tuned to obtain the largest possible Higgs mass, by fixing the stop mixing parameter to $X_t^{\rm OS} = 2M_{\rm SUSY} = 2$ TeV and the Higgsino and gluino mass to $\mu = 200$ GeV and $m_{\tilde{g}} = 800$ GeV respectively. The no-mixing scenario uses the same input, except for $X_t^{\rm OS} = 0$ TeV. Note that the OS-label for m_Q, m_U and X_t only means that these parameters are fixed in a scheme such that the tree-level relations to the stop pole masses Eq. (1.3.6) and the stop mixing angle Eq. (1.3.7) are restored [33, 66]. For the following discussion, we will omit these OS labels. The gluino mass enters only at the two-loop level and we can therefore identify it with the gluino pole mass. Moreover the left sbottom mass enters only at two-loop level. We set $m_{\tilde{b}_L}^2 = m_{\tilde{Q}}^2$, such that the tree-level relation in the limit $g = g' = h_b = 0$ is restored. This fixes all OS parameters in two different scenarios, such that we can numerically evaluate the CP-even Higgs mass matrix in the OS scheme.

3.1.2 $\overline{\rm DR}$-Scheme

To evaluate the CP-even Higgs masses also in the $\overline{\rm DR}$-scheme, we need to calculate running $\overline{\rm DR}$ input parameters[3] using Eq. (2.5.4). The Higgs masses in the $\overline{\rm DR}$ scheme will then depend on the renormalization scale μ_R. To derive a result that is perturbatively stable, this scale should be fixed in a way such that the logarithms of this scale remain small. These logarithms involve the mass of the virtual particles running in the loops $\log(\mu_R^2/m_{\rm virtual}^2)$. In our calculation the dominant logarithmic contributions involve stop and top masses, so the renormalization scale should be fixed somewhere between m_t and $m_{\tilde{t}_{1,2}}$. In this work we fix the central renormalization scale to be $\mu_R^{\rm central} = \frac{M_{\rm SUSY}}{2}$. At the central scale the loop-corrections are expected to be small. To estimate the theoretical uncertainties, the renormalization scale is varied by a factor of two around the central value, i.e. $[\frac{1}{2}\mu_R^{\rm central}, 2\mu_R^{\rm central}] = [\frac{1}{4}M_{\rm SUSY}, M_{\rm SUSY}]$.
Since we take into account two different perturbative orders at the two-loop level $\mathcal{O}(\alpha_s)$ and $\mathcal{O}(\alpha_t)$, the renormalization scale variation becomes a little bit more complicated. To understand this properly, let us first discuss the one-loop $\mathcal{O}(\alpha_t)$ corrections to the light scalar Higgs mass. As explained in section 2.4.1 we did not have to renormalize the one-loop correction, i.e. there are no counter term contributions involved. This means we can evaluate the one-loop masses with input parameters in any renormalization scheme. The main correction to the light scalar Higgs mass is proportional to the fourth power of the top mass. The $\overline{\rm DR}$ top mass, varied w.r.t. $\mathcal{O}(\alpha_s)$, is determined by using Eq. (2.5.4) with only $\mathcal{O}(\alpha_s)$-counter terms, see Eqs. (D.5.1, D.5.5)

$$m_t^{\overline{\rm DR},\alpha_s}(\mu_R) = m_t^{\rm OS} - \left[\delta^{\overline{\rm DR},\alpha_s} m_t(\mu_R) - \delta^{OS,\alpha_s} m_t\right]. \tag{3.1.2}$$

We can also vary the $\overline{\rm DR}$ top mass w.r.t. $\mathcal{O}(\alpha_t)$ and the full $\mathcal{O}(\alpha_s + \alpha_t)$, by substituting $\alpha_s \to \alpha_t$ or $\alpha_s \to \alpha_s + \alpha_t$ respectively in Eq. (3.1.2). The resulting numerical values for the top mass in the $m_h^{\rm max}$ scenario with $\tan\beta = 20$ evaluated at $\frac{1}{4}M_{\rm SUSY} = 250$ GeV and $M_{\rm SUSY} = 1000$ GeV are shown in Table 3.1.

[1] One could use the variation of the Higgs masses under evaluation of α_s at different scales as a simple estimate for the size of three loop effects.

[2] We use a slightly different version of the no-mixing benchmark scenario, fixing the SUSY scale to $M_{\rm SUSY} = 1$ TeV instead of $M_{\rm SUSY} = 2$ TeV.

[3] Note that this determination of the running $\overline{\rm DR}$ input parameters is rather simplistic. For a decent analysis of the scale invariance of the Higgs masses, one should solve the coupled RGEs for the input parameters at two-loop level to get a NLL determination.

$m_t^{\overline{\rm DR}}(\mu_R)$	$\mu_R = 250$ GeV	$\mu_R = 1$ TeV
α_s	154.67 GeV	140.61 GeV
α_t	173.80 GeV	178.22 GeV
$\alpha_s + \alpha_t$	155.67 GeV	147.10 GeV

Table 3.1: The $\overline{\rm DR}$ running top mass in the $m_h^{\rm max}$ scenario with $\tan\beta = 20$ evaluated at $\mu_R = 250$ GeV and $\mu_R = 1$ TeV at different perturbative orders.

For the $\overline{\rm DR}$ top mass running at $\mathcal{O}(\alpha_s + \alpha_t)$ with one common renormalization scale we see that the individual contributions from $\mathcal{O}(\alpha_s)$ and $\mathcal{O}(\alpha_t)$ almost cancel the running. This is of course not a reliable estimate for the $\overline{\rm DR}$ top mass, because the scale dependence of any $\overline{\rm DR}$ parameter should increase with every additional perturbative order considered. A better estimate of the running of the top mass can be obtained by varying the renormalization scale at $\mathcal{O}(\alpha_s)$ independently of $\mathcal{O}(\alpha_t)$. This means we have to distinguish between the renormalization scale in the counter terms at $\mathcal{O}(\alpha_s)$, i.e. $\mu_R^{\alpha_s}$ and the renormalization scale in the counter terms at $\mathcal{O}(\alpha_t)$, i.e. $\mu_R^{\alpha_t}$. The $\overline{\rm DR}$ top mass then depends on both renormalization scales

$$m_t^{\overline{\rm DR},\alpha_s+\alpha_t}(\mu_R^{\alpha_s},\mu_R^{\alpha_t}) = m_t^{\rm OS} - \left[\delta^{\overline{\rm DR},\alpha_s} m_t(\mu_R^{\alpha_s}) + \delta^{\overline{\rm DR},\alpha_t} m_t(\mu_R^{\alpha_t}) - \delta^{OS,\alpha_s} m_t - \delta^{OS,\alpha_t} m_t\right]. \qquad (3.1.3)$$

For all further analyses of the $\overline{\rm DR}$ masses and couplings, we will use Eq. (3.1.3) to determine the running $\overline{\rm DR}$ input parameters. To estimate the scale variation of the Higgs masses and self-couplings we evaluate both scales, $\mu_R^{\alpha_s}$ and $\mu_R^{\alpha_t}$, at three values $[\frac{1}{4}M_{\rm SUSY}, \frac{1}{2}M_{\rm SUSY}, M_{\rm SUSY}]$. Table 3.2 shows the top mass in the $m_h^{\rm max}$ scenario with $\tan\beta = 20$ evaluated at nine different values for the renormalization scales. One can see that the running of the $\overline{\rm DR}$ top mass is increased, which also increases the scale variation of the $\overline{\rm DR}$ Higgs mass.

$m_t^{\overline{\rm DR}}(\mu_R^{\alpha_s},\mu_R^{\alpha_t})$	$\mu_R^{\alpha_s} = 250$ GeV	$\mu_R^{\alpha_s} = 500$ GeV	$\mu_R^{\alpha_s} = 1$ TeV
$\mu_R^{\alpha_t} = 250$ GeV	155.67 GeV	148.86 GeV	141.71 GeV
$\mu_R^{\alpha_t} = 500$ GeV	158.15 GeV	151.45 GeV	144.43 GeV
$\mu_R^{\alpha_t} = 1$ TeV	160.59 GeV	154.00 GeV	147.10 GeV

Table 3.2: The $\overline{\rm DR}$ running top mass in the $m_h^{\rm max}$ scenario with $\tan\beta = 20$ as a function of two distinct renormalization scales $\mu_R^{\alpha_s}$ and $\mu_R^{\alpha_t}$, both evaluated at $\mu_R = 250$ GeV, $\mu_R = 500$ GeV and $\mu_R = 1$ TeV.

In the following plots the filled bands show the scale variation, as described above, for the one-loop $\mathcal{O}(\alpha_t)$ (green), the two-loop $\mathcal{O}(\alpha_t + \alpha_s\alpha_t)$ (red) and the two-loop $\mathcal{O}(\alpha_t + \alpha_s\alpha_t + \alpha_t^2)$ (blue) Higgs masses and self-couplings. Moreover the solid lines show the OS Higgs masses and self-coupling at one-loop $\mathcal{O}(\alpha_t)$ (green), the two-loop $\mathcal{O}(\alpha_t + \alpha_s\alpha_t)$ (red) and the two-loop $\mathcal{O}(\alpha_t + \alpha_s\alpha_t + \alpha_t^2)$ (blue).

3.1.3 Numerical Analysis of the Light Scalar Higgs Mass

The plots in Figure 3.1 show the light scalar Higgs mass m_h at different orders in perturbation theory in the OS and $\overline{\rm DR}$ scheme as a function of the pseudoscalar Higgs mass m_A. The plots on the left are in the no-mixing scenario, whereas the plots on the right hand side are in the $m_h^{\rm max}$ scenario. The upper plots use $\tan\beta = 2$, whereas the lower plots use $\tan\beta = 30$. The first outcome is that the shape of the slope is still mainly determined by β and m_A in the same way as they determined the slope at the tree-level, see Figure 1.3. The slope of the curve is determined by $\tan\beta$ but the transition region is moved to the loop-corrected light scalar Higgs mass $m_A = m_h^{\mathcal{O}(x)}$. This shift of the transition region is a universal

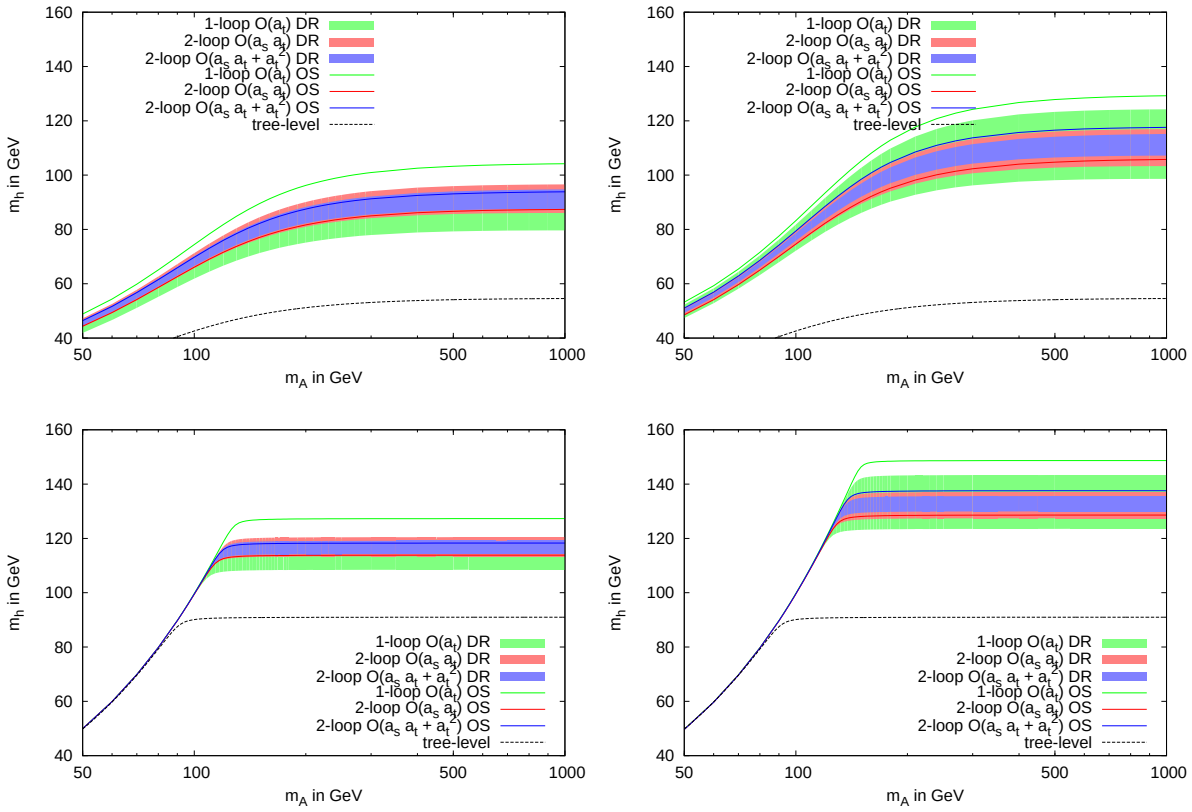

Figure 3.1: The light scalar Higgs mass m_h as a function of the pseudoscalar Higgs mass m_A. The plots on the left are in the no-mixing scenario, whereas the right plots are in the m_h^{max} scenario. The upper plots use $\tan\beta = 2$, whereas the lower plots use $\tan\beta = 30$.

feature for the m_A-dependence of loop-corrected Higgs masses and self-couplings.
To discuss the size of the corrections, we can compare the numerical result in the OS-scheme to [33]. Correcting for the non-zero external momentum lowers the Higgs mass by up to ~ 3 GeV in the no-mixing scenario and by up to ~ 6 GeV in the m_h^{max} scenario. There is only one further difference between our analysis and [33], which is the different WFR counter term. Our choice of this term increases the Higgs mass by up to 3 GeV compared to [33]. Concerning the uncertainty due to the renormalization scale and scheme, we see that the one-loop $\mathcal{O}(\alpha_t)$, the two-loop $\mathcal{O}(\alpha_t + \alpha_s\alpha_t)$ and the two-loop $\mathcal{O}(\alpha_t + \alpha_s\alpha_t + \alpha_t^2)$ bands all overlap, which means that the radiative corrections to m_h are small at the central scale $\mu_R^{\alpha_s} = \mu_R^{\alpha_t} = \frac{1}{2}M_{\text{SUSY}}$. Moreover the bands become smaller with every additional order in perturbation theory included. However, the scale uncertainty[4] of the two-loop $\mathcal{O}(\alpha_t+\alpha_s\alpha_t+\alpha_t^2)$ light scalar Higgs mass is still about ± 3 GeV in the decoupling limit of the m_h^{max} scenario. In the OS scheme the size of the correction is much bigger. The QCD corrections to the one-loop $\mathcal{O}(\alpha_t)$ reduce the Higgs mass in the decoupling limit of the m_h^{max} scenario with $\tan\beta = 30$ by about 20 GeV, whereas the complete two-loop $\mathcal{O}(\alpha_t+\alpha_s\alpha_t+\alpha_t^2)$ corrections raise the Higgs mass by about 9 GeV compared to the two-loop $\mathcal{O}(\alpha_t + \alpha_t\alpha_s)$. Taking into account also the scheme dependence, the theoretical uncertainty of the Higgs masses in the decoupling

[4] Note again that this estimate of the scale uncertainty is not very involved. For a more reliable scale variation one should use $\overline{\text{DR}}$ input parameters determined from solving the RGEs.

limit of the m_h^{max} scenario with $\tan\beta = 30$ is almost ± 4 GeV, whereas in the no-mixing scenario it is ± 2 GeV. In the following analysis we will vary a single MSSM parameter, while keeping all the other parameters fixed as in the m_h^{max} scenario. In this way we can get a feeling of how the light scalar Higgs mass depends on the various parameters, without having to analyze the complete parameter space. We work in the decoupling limit, setting $m_A = M_{\text{SUSY}}$ for the following plots.
Figure 3.2 shows the dependence of m_h on the stop mixing parameter X_t, for $M_{\text{SUSY}} = 0.5$ TeV on the left hand side and $M_{\text{SUSY}} = 1$ TeV on the right hand side. Moreover we set $\tan\beta = 10$. One can see that the Higgs mass is maximized[5] for $X_t \simeq 2M_{\text{SUSY}}$. Moreover, for $M_{\text{SUSY}} \simeq 0.5$ TeV the scale dependence grows very large for $X_t \simeq 2M_{\text{SUSY}}$, such that for such large mixing the results are not perturbatively stable anymore[6]. The plot on the left hand side in Figure 3.3 shows the dependence of m_h on the gluino

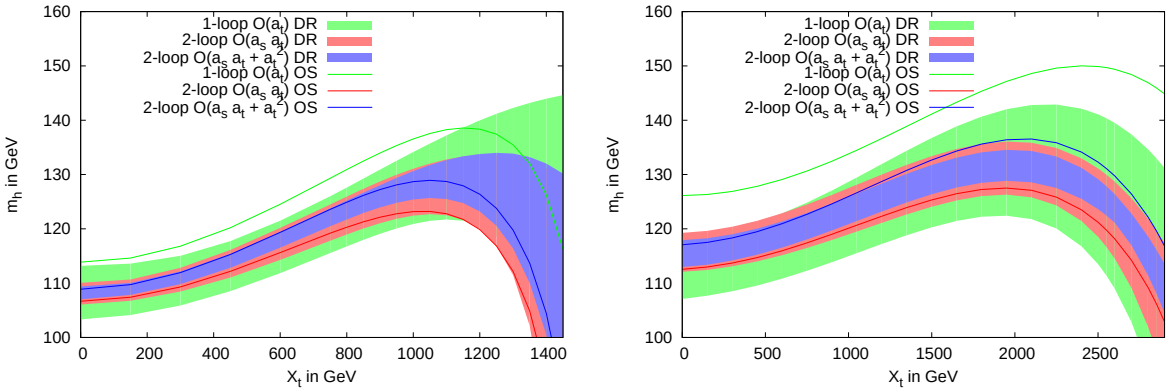

Figure 3.2: The light scalar Higgs mass m_h as a function of the stop mixing parameter X_t. All other parameters are fixed as in the no-mixing and m_h^{max} scenarios. The left plot uses $M_{\text{SUSY}} = 0.5$ TeV, whereas the right plot uses $M_{\text{SUSY}} = 1$ TeV. Both plots are for $\tan\beta = 10$.

mass $m_{\tilde{g}}$ for $\tan\beta = 20$. In the OS scheme the Higgs mass is maximized for about $m_{\tilde{g}} = 800$ GeV, whereas in the $\overline{\text{DR}}$ scheme the peak of m_h is shifted to about $m_{\tilde{g}} = 2$ TeV. The gluino mass dependence can alter the Higgs mass by up to 5 GeV.
The plot on the right hand side in Figure 3.3 shows m_h as a function of the Higgsino mass μ with $\tan\beta = 20$ and all other parameters fixed as in the m_h^{max} scenario. One can observe that the Higgs mass is almost independent of μ. This shows that the two-loop diagrams due to virtual Higgsinos are almost irrelevant.

[5]Note that the value for the stop mixing parameter X_t that maximizes the Higgs mass differs between the OS and $\overline{\text{DR}}$ renormalization scheme [67]. This effect can account for a few GeV in the Higgs mass.

[6]For very high values of X_t the stop mass eigenvalues squared can become negative. These results in a breaking of the charge $U(1)_{em}$ and the color $SU(3)_C$ gauge symmetries. It follows that for $X_t \gtrsim 3M_{\text{SUSY}}$ the MSSM is not phenomenologically viable anymore [68].

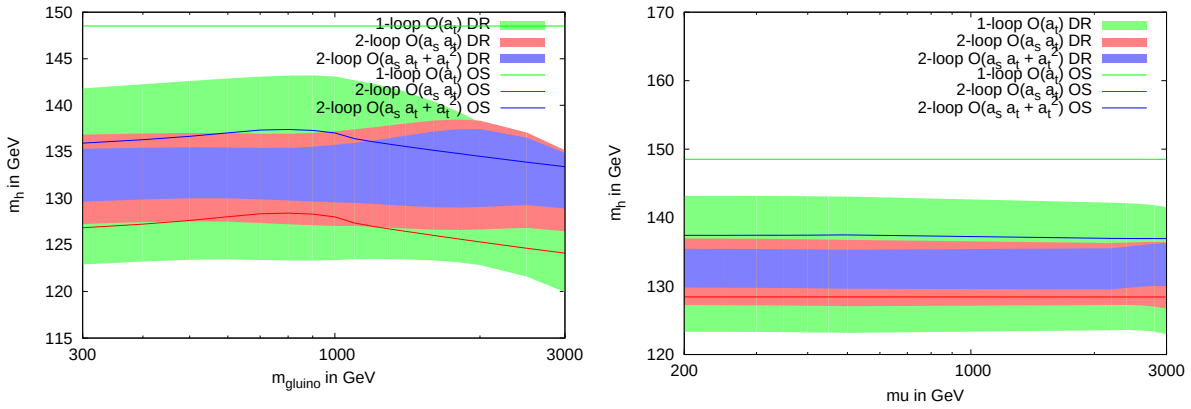

Figure 3.3: The plot on the left hand side shows m_h as a function of $m_{\tilde{g}}$ with $m_A = M_{\text{SUSY}} = 1$ TeV, $\mu = 200$ GeV and $X_t = 2M_{\text{SUSY}} = 2$ TeV as in the m_h^{max} scenario and $\tan\beta = 20$. The plot right shows m_h as a function of μ with $\tan\beta = 20$ and all other parameters fixed as in the m_h^{max} scenario.

Figure 3.4 shows on the left hand side the dependence of m_h on the tangent of the CP-odd mixing angle in terms of $\tan\beta$. For low values of $\tan\beta \lesssim 5$ the light scalar Higgs mass grows rapidly, whereas for $\tan\beta \gtrsim 10$ the curve of m_h is almost flat. The scale uncertainty becomes smaller at every order of perturbation theory, and the bands overlap. For very small values of $\tan\beta \lesssim 1.5$ the scale dependence of the Higgs mass increases.
Last but not least let us look at the plot on the right hand side of Figure 3.4, where the SUSY mass M_{SUSY} is varied, setting $X_t = 2M_{\text{SUSY}}$ and $m_A = m_U = m_Q = m_{\tilde{g}} = M_{\text{SUSY}}$. First one notices that the OS Higgs mass at $\mathcal{O}(\alpha_t)$ grows steadily with M_{SUSY}. The scale uncertainty grows with M_{SUSY}, such that for high SUSY masses of $M_{\text{SUSY}} \gtrsim 3$ TeV the perturbative stability of the light scalar Higgs becomes less reliable. The $\overline{\text{DR}}$ mass at $\mathcal{O}(\alpha_t)$ peaks at $M_{\text{SUSY}} = 1$ TeV, whereas the two-loop corrected $\overline{\text{DR}}$ masses grow slowly up to $M_{\text{SUSY}} = 3$ TeV.

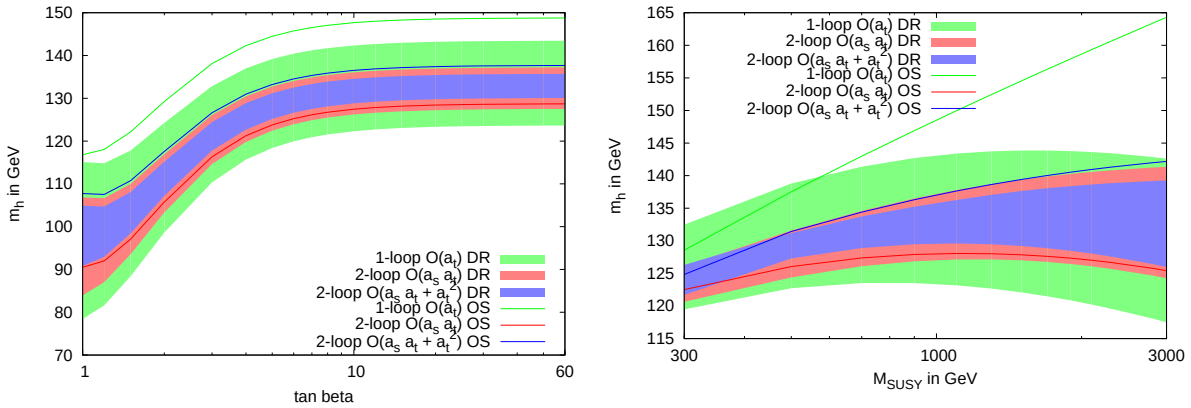

Figure 3.4: The plot on the left shows m_h as a function of $\tan\beta$ in the m_h^{max} scenario with $m_A = M_{\text{SUSY}} = 1$ TeV. The plot on the right shows m_h as a function of M_{SUSY}. Here we set $m_A = m_{\tilde{g}} = M_{\text{SUSY}}$, $\mu = 200$ GeV and $\tan\beta = 20$ with maximal mixing $X_t = 2M_{\text{SUSY}}$.

3.2 Higgs Self-Couplings

In section 2.5.7 we described how we obtain analytical results for the renormalized trilinear Higgs self-couplings in the OS and the $\overline{\text{DR}}$ renormalization scheme. Analogously to the masses, the self-couplings can be evaluated numerically in the OS scheme by using the same set of OS input parameters introduced in section 3.1.1 and in the $\overline{\text{DR}}$ scheme by using the set of running $\overline{\text{DR}}$ input parameters introduced in section 3.1.2. The only input parameter that we need for the evaluation of the self-couplings that was not used for the masses is the CP-even mixing angle α. The renormalized mixing angle $\alpha^{\mathcal{O}(x),R}$ at $\mathcal{O}(x)$ in scheme R can be obtained from the renormalized CP-even mass matrix at $\mathcal{O}(x)$ in scheme R, $(\mathcal{M}_S^2)^{\mathcal{O}(x),R}$ by the following equation

$$\alpha^{\mathcal{O}(x),R} = \frac{1}{2}\arcsin\left(\frac{(\mathcal{M}_S^2)_{12}^{\mathcal{O}(x),R}}{\left(m_H^{\mathcal{O}(x),R}\right)^2 - \left(m_h^{\mathcal{O}(x),R}\right)^2}\right), \tag{3.2.1}$$

where $m_{H,h}^{\mathcal{O}(x),R}$ are the squared masses of the CP-even scalar Higgs bosons at $\mathcal{O}(x)$ and in scheme R, obtained by Eq. (2.5.36). Note that the domain of the arcsin function is $\left[-\frac{\pi}{2},\frac{\pi}{2}\right]$. At tree level, the off-diagonal CP-even matrix element is $(\mathcal{M}_S^2)_{12}^{\text{tree}} \leq 0$, see Eq. (1.4.16), such that the tree-level CP-even mixing angle is negative $\alpha^{\text{tree}} \in \left[-\frac{\pi}{2},0\right]$. Radiative corrections, however, can alter the off-diagonal CP-even matrix element, such that it becomes positive. If $(\mathcal{M}_S^2)_{12}^{\mathcal{O}(x),R} \geq 0$ the mixing angle will be in $\left[0,\frac{\pi}{2}\right]$.

3.2.1 Numerical Analysis of the Neutral Trilinear Higgs Self-Couplings

We will plot the same perturbative orders in two different renormalization scheme with the same colors as we did for the masses. The solid lines show the OS self-coupling at one-loop $\mathcal{O}(\alpha_t)$ (green), two-loop $\mathcal{O}(\alpha_t + \alpha_s\alpha_t)$ (red) and two-loop $\mathcal{O}(\alpha_t + \alpha_s\alpha_t + \alpha_t^2)$ (blue). To estimate the scale variation of the self-couplings we use the $\overline{\text{DR}}$ scheme, evaluating the two renormalization scales, $\mu_R^{\alpha_s}$ and $\mu_R^{\alpha_t}$, at three different values $[\frac{1}{4}M_{\text{SUSY}}, \frac{1}{2}M_{\text{SUSY}}, M_{\text{SUSY}}]$. The filled bands show the scale variation, as described above, for the one-loop $\mathcal{O}(\alpha_t)$ (green), the two-loop $\mathcal{O}(\alpha_t+\alpha_s\alpha_t)$ (red) and the two-loop $\mathcal{O}(\alpha_t+\alpha_s\alpha_t+\alpha_t^2)$ (blue) Higgs self-couplings.

***hhh*-coupling:** We will first discuss the coupling of three light scalar Higgs bosons. Figure 3.5 shows λ_{hhh} as a function of the pseudoscalar Higgs mass m_A. The plots on the left are in the no-mixing scenario, whereas the right plots are in the m_h^{max} scenario. The upper plots use $\tan\beta = 2$, whereas the lower plots use $\tan\beta = 10$. The slope of the curve in the transition region $m_A \simeq m_h^{\mathcal{O}(x),R}$ increases with the tangent of the CP-odd mixing angle. For $\tan\beta = 10$ the uncertainty bands do not overlap in the transition region, because this region is shifted to the corrected light scalar Higgs mass. In the decoupling limit, λ_{hhh} approaches its asymptotic value and the corrections to the tree level are fairly large $\gtrsim 100\%$. In this region the bands all overlap, which means that the size of the two-loop corrections is small at the central scale $\mu_R^{\alpha_s} = \mu_R^{\alpha_t} = \frac{1}{2}M_{\text{SUSY}}$. In the OS scheme the two-loop corrections are larger, the QCD corrections to the one-loop result reduce the coupling by about 75 GeV in the m_h^{max} scenario for $\tan\beta = 10$, corresponding to $\simeq 30\%$. The two-loop $\mathcal{O}(\alpha_t^2)$ corrections, however, increase the coupling again by about 30 GeV. In the no-mixing scenario the corrections as well as the scale uncertainties are smaller.

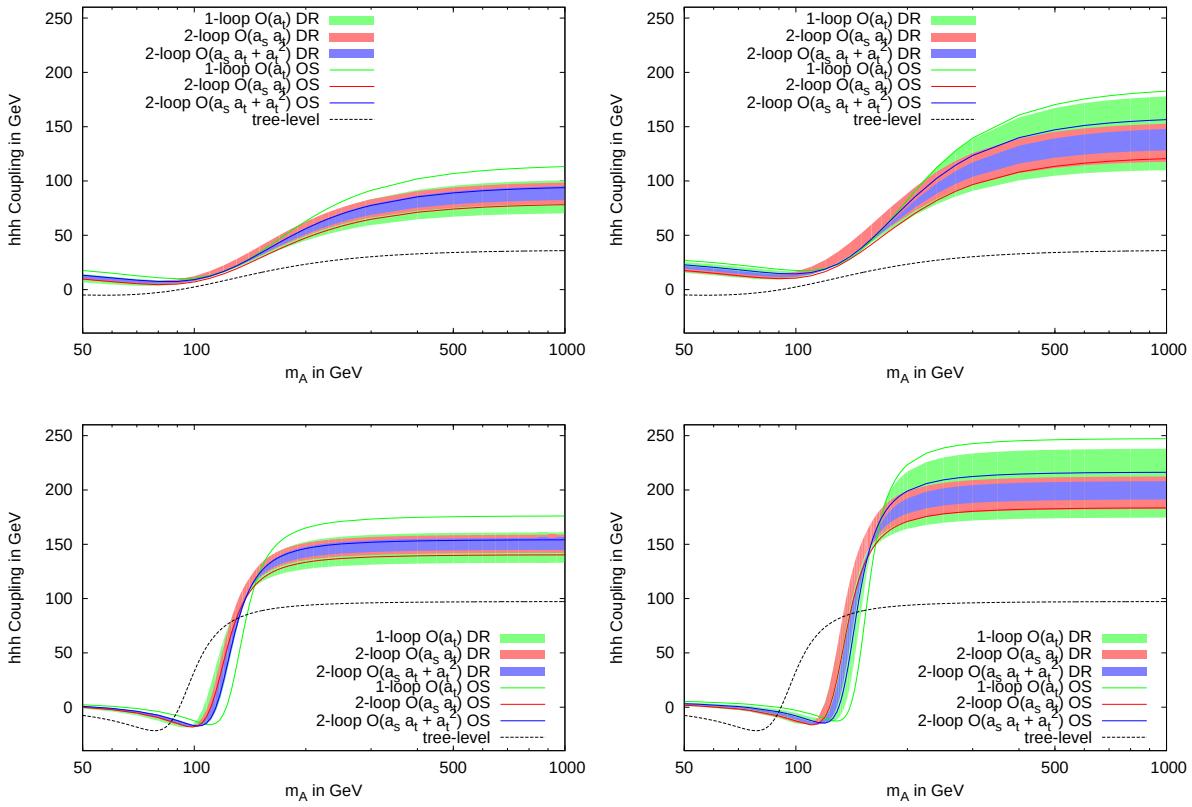

Figure 3.5: The coupling of three light scalar Higgs bosons λ_{hhh} as a function of the pseudoscalar Higgs mass m_A. The plots on the left are in the no-mixing scenario, whereas the right plots are in the m_h^{max} scenario. The upper plots use $\tan\beta = 2$, whereas the lower plots use $\tan\beta = 10$.

In the following we will apply the same analysis of the MSSM parameter space that we did in section 3.1.3 for the masses also for the self-couplings. We will vary a single MSSM parameter, while keeping all the other parameters fixed as in the m_h^{max} scenario. In this way we can get a feeling of how the coupling of three light scalar Higgs bosons depends on the various parameters, without having to analyze the complete parameter space. We work in the decoupling limit, setting $m_A = M_{\text{SUSY}}$ for the following plots.

The two plots in Figure 3.6 show the coupling of three light scalar Higgs bosons λ_{hhh} as a function of the stop mixing parameter X_t with $\tan\beta = 10$. All other parameters are fixed as in the no-mixing and the m_h^{max} scenarios. The left plot uses $M_{\text{SUSY}} = 0.5$ TeV, whereas the right plot uses $M_{\text{SUSY}} = 1$ TeV. The coupling λ_{hhh} is maximized for $X_t \simeq 2M_{\text{SUSY}}$. For $M_{\text{SUSY}} = 0.5$ TeV the uncertainties grow very large for $X_t \gtrsim 2M_{\text{SUSY}}$, such that for such high mixing also the couplings are not perturbatively stable anymore.

The plot on the left hand side of Figure 3.7 shows the coupling of three light scalar Higgs bosons λ_{hhh} as a function of $m_{\tilde{g}}$ with $m_A = M_{\text{SUSY}} = 1$ TeV, $\mu = 200$ GeV and $X_t = 2M_{\text{SUSY}} = 2$ TeV as in the m_h^{max} scenario and $\tan\beta = 10$. In the OS scheme the coupling is maximized for $m_{\tilde{g}} \simeq 800$ GeV, whereas in the $\overline{\text{DR}}$ scheme the coupling peaks around $m_{\tilde{g}} \simeq 2$ TeV. The dependence on the gluino mass can alter the trilinear Higgs self-couplings by about 10 GeV, corresponding to a $\mathcal{O}(5\%)$ effect.

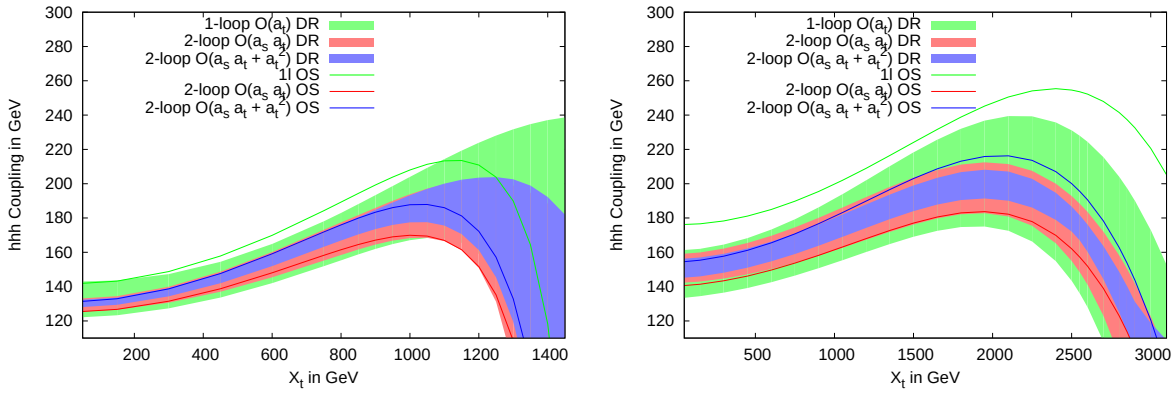

Figure 3.6: The coupling of three light scalar Higgs bosons λ_{hhh} as a function of the stop mixing parameter X_t with $\tan\beta = 10$. The left plot uses $M_{\rm SUSY} = 0.5$ TeV, whereas the right plot uses $M_{\rm SUSY} = 1$ TeV. All other parameters are fixed as in the no-mixing and $m_h^{\rm max}$ scenarios.

The plot on the right hand side of Figure 3.7 shows λ_{hhh} as a function of μ with $\tan\beta = 10$ and all other parameters fixed as in the $m_h^{\rm max}$ scenario. One can observe that in both renormalization schemes and at all perturbative orders, the coupling is almost independent of μ. The reason for this is that through the fixing of X_t, the main effect of the variation of μ is canceled by the parameter A_t. The Higgsino mass μ also shows up in two-loop diagrams at $\mathcal{O}(\alpha_t^2)$. The parameter μ in these diagrams seems to have almost no effect on the Higgs self-couplings.

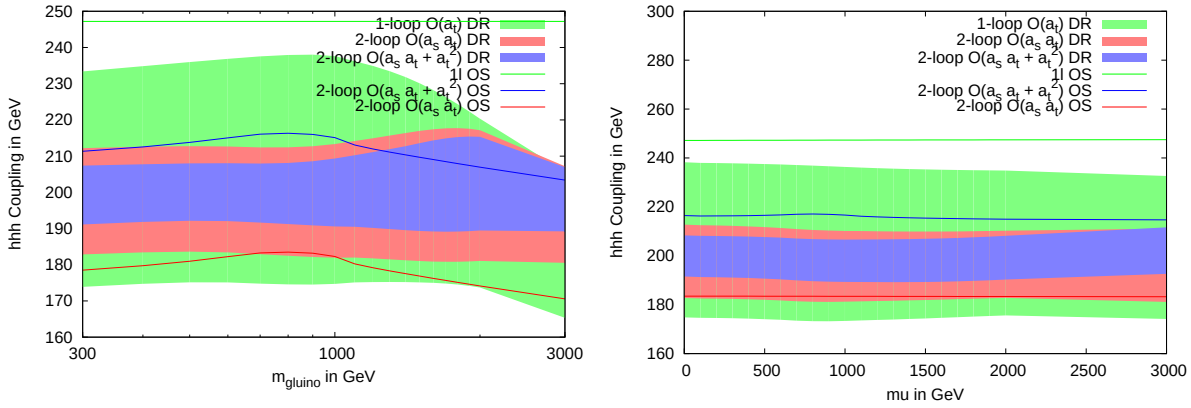

Figure 3.7: The plot on the left hand side shows the coupling of three light scalar Higgs bosons λ_{hhh} as a function of $m_{\tilde{g}}$ with $m_A = M_{\rm SUSY} = 1$ TeV, $\mu = 200$ GeV and $X_t = 2M_{\rm SUSY} = 2$ TeV as in the $m_h^{\rm max}$ scenario and $\tan\beta = 10$. The right plot shows λ_{hhh} as a function of μ with $\tan\beta = 10$ and all other parameters fixed as in the $m_h^{\rm max}$ scenario.

The plot on the left hand side of Figure 3.8 shows the dependence of the coupling of three light scalar Higgs bosons λ_{hhh} on the CP-odd mixing angle in terms of $\tan\beta$ in the $m_h^{\rm max}$ scenario with $m_A = M_{\rm SUSY} = 1$ TeV. The coupling grows rapidly for $\tan\beta \lesssim 5$ and it is almost flat for $\tan\beta \gtrsim 10$ at all perturbative orders. The scale uncertainty is almost constant for $\tan\beta > 1.5$ and it becomes larger for very low values

of $\tan\beta$.
The plot on the right in Figure 3.8 shows λ_{hhh} as a function of M_{SUSY}. Here we set $m_A = m_{\tilde{g}} = M_{\text{SUSY}}$, $\mu = 200$ GeV and $\tan\beta = 10$ with maximal mixing $X_t = 2M_{\text{SUSY}}$. The $\mathcal{O}(\alpha_t)$ coupling in the OS scheme grows steadily with the SUSY scale, whereas the coupling at the other perturbative orders grows only very slowly for large M_{SUSY}. This fact shows nicely that the one-loop $\mathcal{O}(\alpha_t)$ result in the OS scheme is not a reliable estimate of the coupling λ_{hhh} in the whole MSSM parameter space. Moreover one can observe that the scale uncertainty grows bigger with M_{SUSY}.

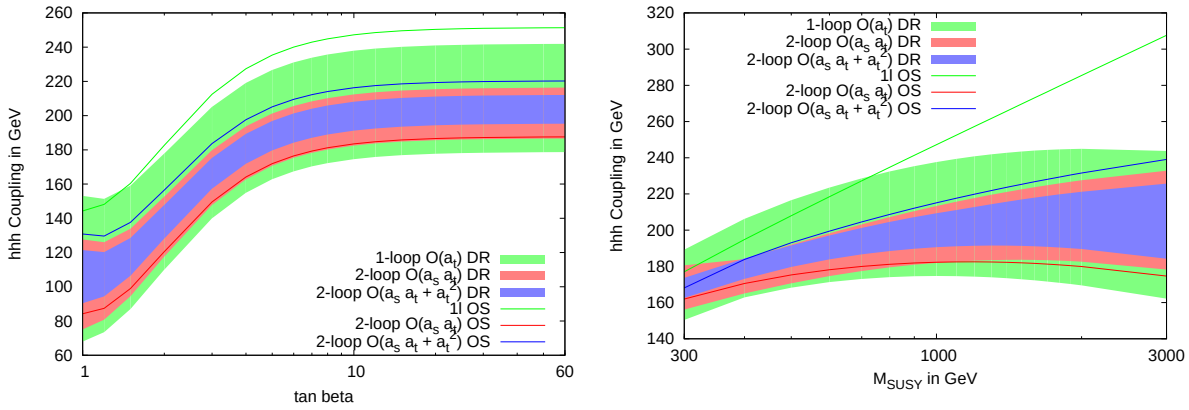

Figure 3.8: The plot on the left shows λ_{hhh} as a function of $\tan\beta$ in the m_h^{max} scenario with $m_A = M_{\text{SUSY}} = 1$ TeV. The plot on the right shows λ_{hhh} as a function of M_{SUSY}. Here we set $m_A = m_{\tilde{g}} = M_{\text{SUSY}}$, $\mu = 200$ GeV and $\tan\beta = 10$ with maximal mixing $X_t = 2M_{\text{SUSY}}$.

In general the corrections to the trilinear light scalar Higgs coupling in decoupling limit are expected to have the same structure as the corrections to the light scalar Higgs mass. Most of the corrections to λ_{hhh} can be absorbed into the corrected Higgs mass squared by

$$\lambda_{hhh}^{\mathcal{O}(x),R} \simeq \frac{3}{v}\left(m_h^{\mathcal{O}(x),R}\right)^2, \tag{3.2.2}$$

similarly to Eq. (1.4.35). Since the light scalar Higgs mass has to behave absolutely SM-like in the decoupling limit, we can calculate corrections to the relation of the SM Higgs mass to the SM Higgs self-couplings perturbatively and check how well they approximate the relation between the light scalar Higgs mass and its self-couplings in the MSSM. At the one-loop $\mathcal{O}(\alpha_t)$ this analysis has been done [41]. For the $\mathcal{O}(\alpha_t\alpha_s + \alpha_t^2)$ corrections this can be done in an analogous way.

***HHH*-coupling:** Figure 3.9 shows the coupling of three heavy scalar Higgs bosons λ_{HHH} as a function of the pseudoscalar Higgs mass m_A. The plots on the left hand side are in the no-mixing scenario, whereas the plots on the right are in the $m_h^{\max}$ scenario. The upper plots use $\tan\beta = 2$, whereas the lower plots use $\tan\beta = 10$. It is a general property of all Higgs self-couplings that the slope of the curve is highest in the transition region $m_A \simeq m_h^{\mathcal{O}(x),R}$ and that the slope increases with $\tan\beta$. In the decoupling region the size as well as the perturbative corrections of the coupling become small. For small values of m_A, however, the corrections to and the size of the coupling become very large and they show similar properties as λ_{hhh} in the decoupling region. For $m_A = 50$ GeV the scale uncertainty is largest for small $\tan\beta$ and large stop mixing. The uncertainty bands do all overlap indicating small corrections at the central renormalization scale.

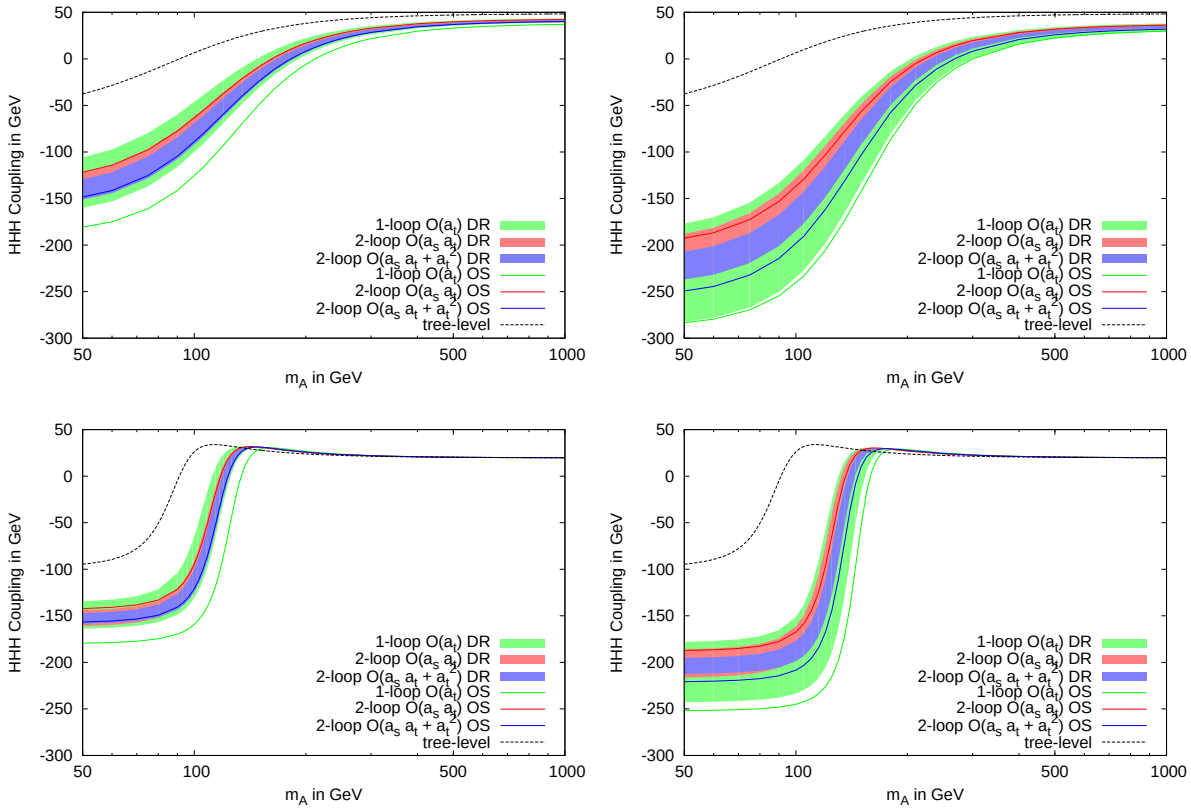

Figure 3.9: The coupling of three heavy scalar Higgs bosons λ_{HHH} as a function of the pseudoscalar Higgs mass m_A. The plots on the left are in the no-mixing scenario, whereas the right plots are in the $m_h^{\max}$ scenario. The upper plots use $\tan\beta = 2$, whereas the lower plots use $\tan\beta = 10$.

***hhH*-coupling:** Figure 3.10 shows the coupling of two light and one heavy scalar Higgs boson λ_{hhH} as a function of the pseudoscalar Higgs mass m_A. The plots on the left hand side are in the no-mixing scenario, whereas the right plots are in the m_h^{max} scenario. The upper plots use $\tan\beta = 2$, whereas the lower plots use $\tan\beta = 10$. For $\tan\beta = 2$ the corrections to the coupling are quite sizable, especially in the m_h^{max} scenario and the uncertainties are moderate. For $\tan\beta = 10$ the absolute value of the coupling peaks in the transition region and the bands do not overlap, especially for large mixing. In the decoupling limit the corrections and the uncertainties of the coupling become smaller.
Note that this coupling can be phenomenologically relevant to study the decay of a heavy scalar into two light scalar Higgs bosons.

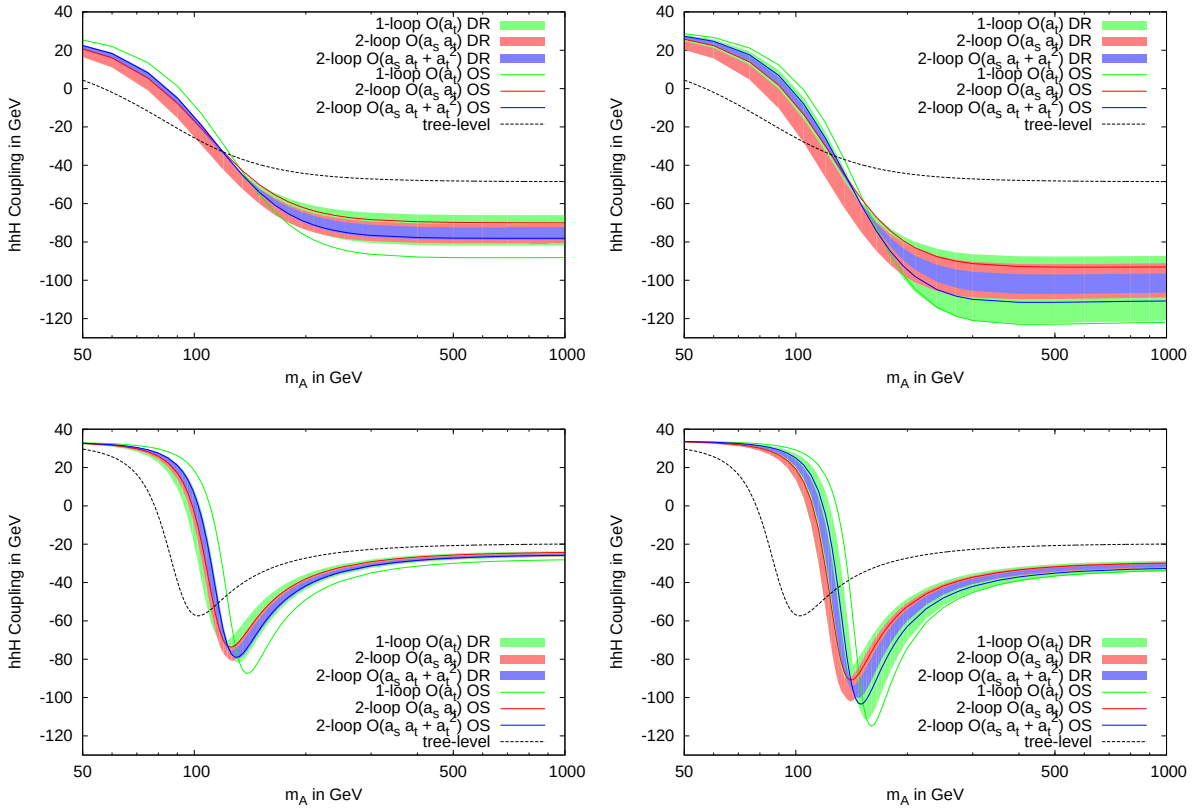

Figure 3.10: The coupling of two light scalar and one heavy scalar Higgs boson λ_{hhH} as a function of the pseudoscalar Higgs mass m_A. The plots on the left are in the no-mixing scenario, whereas the right plots are in the m_h^{max} scenario. The upper plots use $\tan\beta = 2$, whereas the lower plots use $\tan\beta = 10$.

***hHH*-coupling:** Figure 3.11 shows the coupling of one light scalar and two heavy scalar Higgs bosons λ_{hHH} as a function of the pseudoscalar Higgs mass m_A. The plots on the left hand side are in the no-mixing scenario, whereas the plots on the right are in the m_h^{max} scenario. The upper plots use $\tan\beta = 2$, whereas the lower plots use $\tan\beta = 10$. This coupling peaks in the transition region, i.e. around $m_A \simeq m_h^{\mathcal{O}(x)}$. The width of the peak is large for small values of $\tan\beta$ and its height grows with the stop mixing parameter. For $\tan\beta = 2$ the one-loop $\mathcal{O}(\alpha_t)$ corrections to the coupling are sizable and they grow with the stop mixing parameter X_t. The bands of the scale uncertainties all overlap for $\tan\beta = 2$ and the total uncertainty is rather small in the no-mixing scenario, whereas it is bigger in the m_h^{max} scenario. For $\tan\beta = 10$ the scale uncertainty bands do not overlap in the transition region, so it is questionable whether the perturbative result is valid in this region. In decoupling limit the coupling attains an asymptotic value of around -20 GeV and the corrections as well as the scale uncertainty are very small.

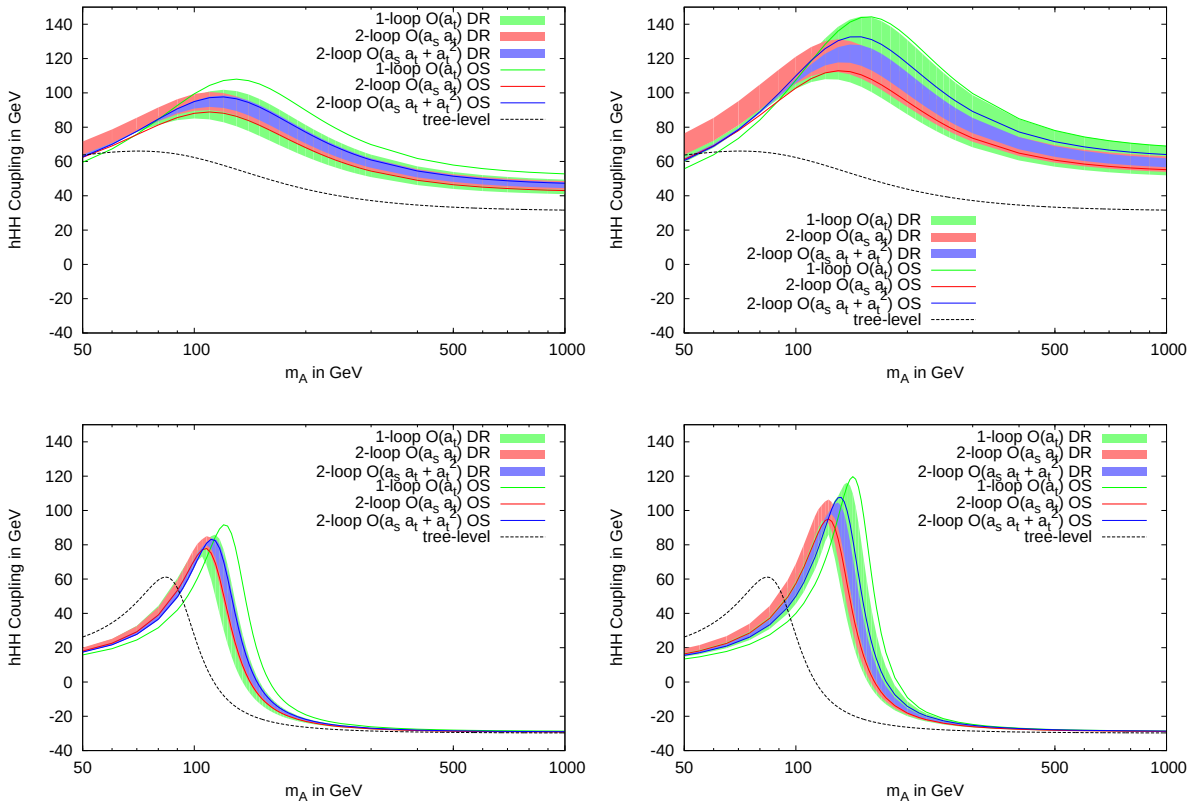

Figure 3.11: The coupling of one light scalar and two heavy scalar Higgs bosons λ_{hHH} as a function of the pseudoscalar Higgs mass m_A. The plots on the left are in the no-mixing scenario, whereas the right plots are in the m_h^{max} scenario. The upper plots use $\tan\beta = 2$, whereas the lower plots use $\tan\beta = 10$.

***hAA*-coupling:** Figure 3.12 shows the coupling of one light scalar and two pseudoscalar Higgs bosons λ_{hAA} as a function of the pseudoscalar Higgs mass m_A. The plots on the left hand side are in the no-mixing scenario, whereas the plots on the right are in the $m_h^{\max}$ scenario. The upper plots use $\tan\beta = 2$, whereas the lower plots use $\tan\beta = 10$. The coupling is much weaker than λ_{hhh} at large and λ_{HHH} at small values of m_A. For low $\tan\beta$ the coupling is very weak and the curve is rather flat with scale uncertainties of about ± 2 GeV corresponding to more than $\pm 50\%$. For large values of $\tan\beta$ the radiative corrections and the uncertainties are very small apart from the transition region.

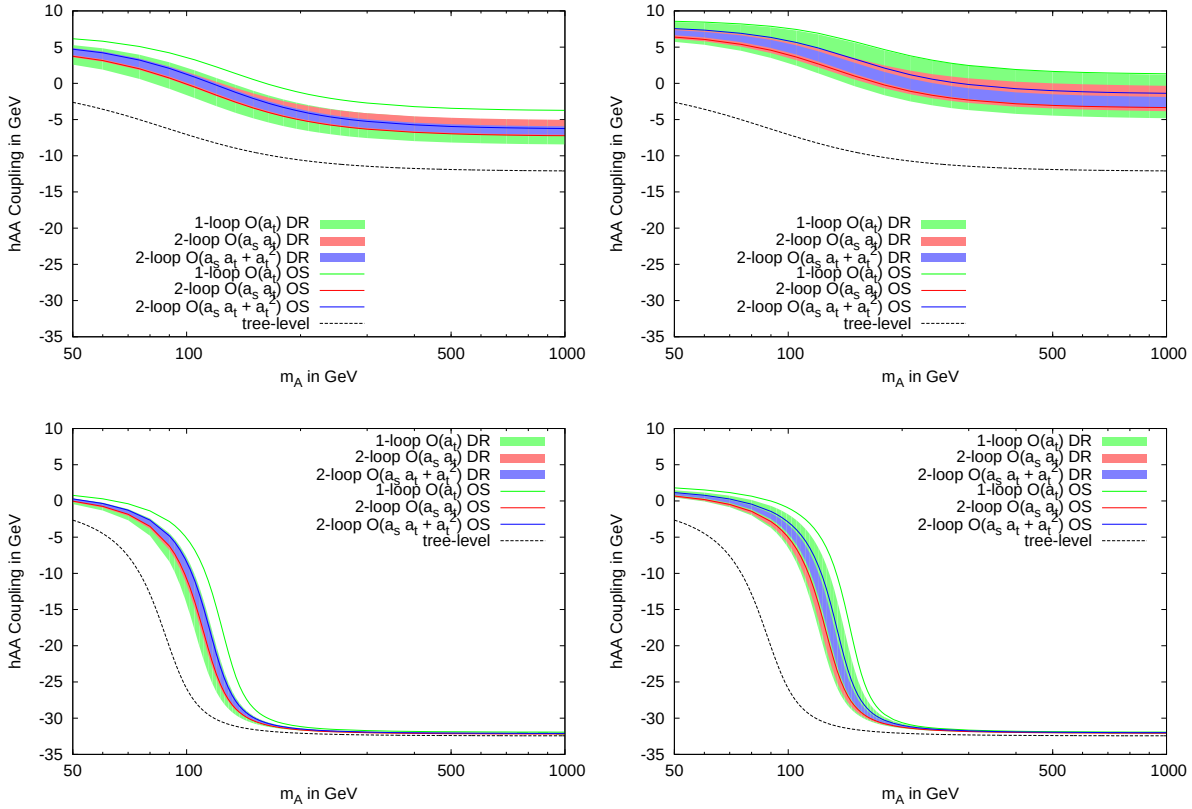

Figure 3.12: The coupling of one light scalar and two pseudoscalar Higgs bosons λ_{hAA} as a function of the pseudoscalar Higgs mass m_A. The plots on the left are in the no-mixing scenario, whereas the right plots are in the $m_h^{\max}$ scenario. The upper plots use $\tan\beta = 2$, whereas the lower plots use $\tan\beta = 10$.

***HAA*-coupling:** Figure 3.13 shows the coupling of one heavy scalar and two pseudoscalar Higgs bosons λ_{HAA} as a function of the pseudoscalar Higgs mass m_A. The plots on the left are in the no-mixing scenario, whereas the right plots are in the $m_h^{\max}$ scenario. The upper plots use $\tan\beta = 2$, whereas the lower plots use $\tan\beta = 10$. The strength of the coupling is similar to the strength of λ_{hAA}. For low $\tan\beta$ the coupling is weak and the curve is rather flat with scale uncertainties of about ± 4 GeV corresponding to about $\pm 50\%$. For large values of $\tan\beta$ the coupling shrinks rapidly from about 35 GeV at low m_A to about 7 GeV in the decoupling region. Similarly to λ_{hAA} the corrections and the uncertainties are very small apart from the transition region.

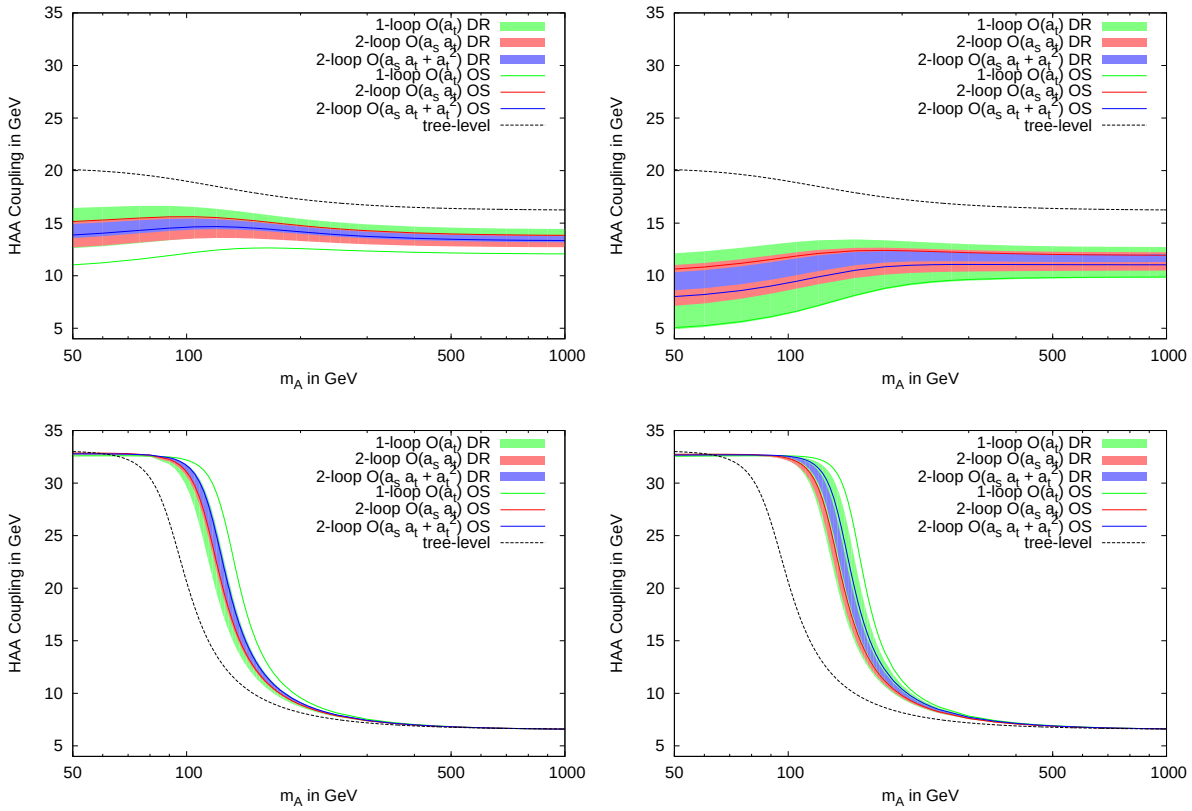

Figure 3.13: The coupling of one heavy scalar and two pseudoscalar Higgs bosons λ_{HAA} as a function of the pseudoscalar Higgs mass m_A. The plots on the left are in the no-mixing scenario, whereas the right plots are in the $m_h^{\max}$ scenario. The upper plots use $\tan\beta = 2$, whereas the lower plots use $\tan\beta = 10$.

3.2.2 Numerical Analysis of the Neutral Quartic Higgs Self-Couplings

The $\mathcal{O}(\alpha_t + \alpha_s\alpha_t + \alpha_t^2)$ corrections to the quartic Higgs self-couplings have been obtained in an analogous way to the trilinear Higgs self-couplings. For the numerical evaluation of the quartic couplings we use exactly the same input parameters in the OS and the $\overline{\text{DR}}$ scheme as for the trilinear couplings. The plots of the quartic self-couplings are arranged in the same way as for the trilinear self-couplings. However, we will restrict our analysis to only two of the nine quartic self-couplings, namely the coupling of four light scalar Higgs bosons and the coupling of three light scalar and one heavy scalar Higgs boson. The former is interesting, because we want to check whether its corrections can be absorbed by the loop-corrected mass and the latter might be phenomenologically relevant to study the decays of a heavy scalar. In general cross sections involving quartic vertices of heavy particles are quite small, so the other quartic couplings are phenomenologically not too interesting in the context of the present (and near future) colliders.

***hhhh*-coupling:** Figure 3.14 shows the coupling of four light scalar Higgs boson λ_{hhhh} as a function of the pseudoscalar Higgs mass m_A. The plots on the left are in the no-mixing scenario, whereas the right plots are in the m_h^{max} scenario. The upper plots use $\tan\beta = 2$, whereas the lower plots use $\tan\beta = 10$. It is a general property not only for the trilinear couplings, but also for all quartic couplings that the m_A-region of the highest slope is shifted to the loop-corrected light scalar Higgs mass. Moreover the steepness of the slope grows with $\tan\beta$. We observe that the corrections to and the uncertainties λ_{hhhh} are small in the no-mixing scenario. In the m_h^{max} scenario the corrections are fairly large $\sim 80\%$ and the uncertainties are sizable as well.

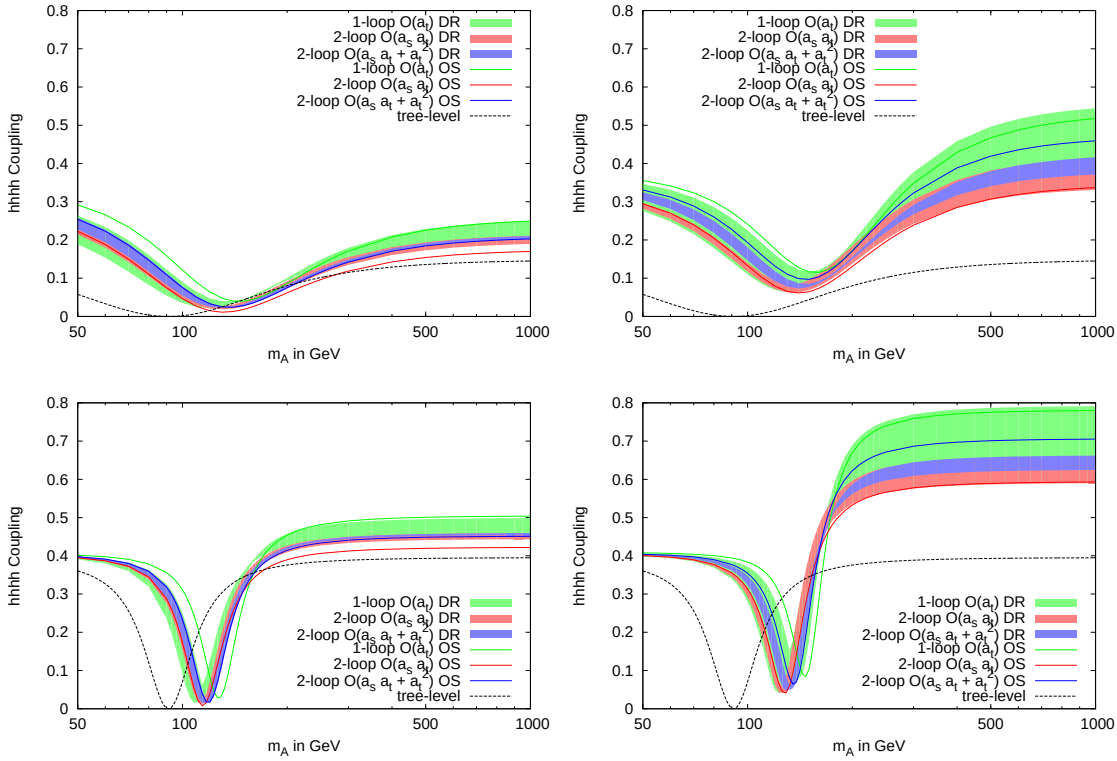

Figure 3.14: The coupling of four light scalar Higgs boson λ_{hhhh} as a function of the pseudoscalar Higgs mass m_A. The plots on the left are in the no-mixing scenario, whereas the right plots are in the m_h^{max} scenario. The upper plots use $\tan\beta = 2$, whereas the lower plots use $\tan\beta = 10$.

***hhhH*-coupling:** Figure 3.15 shows the coupling of three light scalar and one heavy scalar Higgs boson λ_{hhhH} as a function of the pseudoscalar Higgs mass m_A. The plots on the left are in the no-mixing scenario, whereas the right plots are in the $m_h^{\max}$ scenario. The upper plots use $\tan\beta = 2$, whereas the lower plots use $\tan\beta = 10$. In the no-mixing scenario the corrections are quite small and also the uncertainties are almost negligible. In the $m_h^{\max}$ scenario for $\tan\beta = 10$ the corrections and the uncertainties are still quite small. The only sizable corrections show up in the $m_h^{\max}$ scenario for $\tan\beta = 2$. In the decoupling limit the corrections are $\sim 80\%$. Also for this coupling the uncertainty bands do not overlap in the transition region for $\tan\beta = 10$.

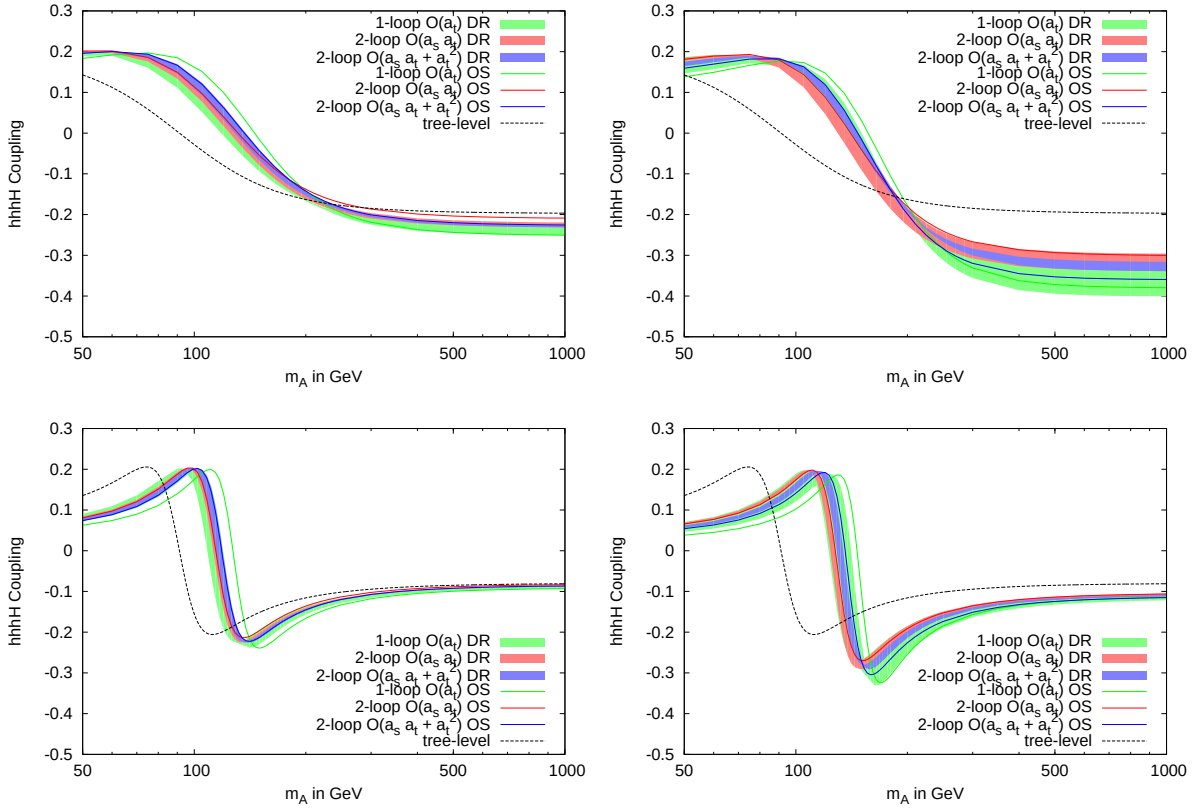

Figure 3.15: The coupling of three light scalar and one heavy scalar Higgs boson λ_{hhhH} as a function of the pseudoscalar Higgs mass m_A. The plots on the left are in the no-mixing scenario, whereas the right plots are in the $m_h^{\max}$ scenario. The upper plots use $\tan\beta = 2$, whereas the lower plots use $\tan\beta = 10$.

Chapter 4

Summary and Outlook

The aim of this work was to determine the two-loop $\mathcal{O}(\alpha_s\alpha_t + \alpha_t^2)$ corrections to the trilinear and quartic Higgs self-couplings in the real MSSM. Measuring these couplings is essential for the reconstruction of the Higgs potential that mediates EWSB. The one-loop corrections and their uncertainties are known to be large [24]. The two-loop corrections are expected to reduce these uncertainties substantially. This calculation was performed in the framework of the effective potential [46, 47, 49] which is equivalent to the full diagrammatic approach up to effects due to finite external momenta. This simplifies our calculation, since we only have to compute a small number of vacuum diagrams. Nevertheless we obtain fully analytical results.

By taking two, three and four derivatives of the unrenormalized, loop-corrected effective potential w.r.t. Higgs fields, we obtained bare masses, trilinear couplings and quartic couplings. These bare quantities have to be renormalized. This was done by substituting all bare parameters in the one-loop masses and couplings by their physical value plus a counter term. In this way all divergences in the calculation canceled and we were left with renormalized Higgs masses and self-couplings.

We explained how these results can be evaluated numerically in two different renormalization schemes, namely the $\overline{\text{DR}}$ and the OS scheme. The dependence of the result on the renormalization scheme and the renormalization scale allows us to estimate the remaining theoretical uncertainties of the self-couplings due to neglected higher orders in perturbation theory.

In most of the parameter space of the MSSM the result shows a good perturbative behavior. This means the theoretical uncertainties are small $\lesssim \mathcal{O}(5\%)$ and the uncertainty bands overlap, meaning that the corrections are small at the central scale $\mu^{\text{central}} = \frac{1}{2}M_{\text{SUSY}}$. In the transition region, where the pseudoscalar Higgs mass is equal to the loop-corrected light scalar Higgs mass at $\mathcal{O}(x)$ in renormalization scheme R, $m_A \simeq m_h^{\mathcal{O}(x),R}$, the slope is steep and the bands do not overlap anymore. This effect is pronounced for large values of $\tan\beta$. In these regions the perturbative reliability is questionable. Moreover regions with large SUSY masses $M_{\text{SUSY}} \gtrsim 3$ TeV or large mixing $X_t \gtrsim 2M_{\text{SUSY}}$ comprise large theoretical uncertainties.

These effective couplings can be useful to calculate processes of multiple Higgs production at a linear e^+e^- collider[1]. The idea is that a calculation for a process, including effects due to finite external momenta and due to higher orders, can be modified by means of these effective self-couplings. In this way the effective couplings can be used to match the measurements to the parameters in the theory.

In the decoupling limit the light scalar Higgs boson in the MSSM behaves completely SM-like. This

[1]The trilinear couplings can of course also be used to calculate processes at a hadron collider like the LHC. However, the cross sections of processes involving multiple Higgs production and Higgs to Higgs decays are very small. Thus huge luminosities are needed in order to distinguish these signals from the background [43]. For the quartic couplings the cross sections are even lower [44]. Depending on the design of the linear collider one has to reinvestigate whether measuring the quartic couplings is a realistic task.

means that also in this calculation the SM relation between the Higgs mass and the self-couplings at higher orders have to be satisfied. It will be the task of a further investigation of our results, to check numerically to what extend these SM relations are fulfilled, in the various regions of the parameter space. Moreover these relations can help to find approximate formulae for the self-couplings that are valid in certain limits of the parameter space.
Since the complete analytic results are much too long to be published in a printed form, we plan to publish them in a computer code. In this way the trilinear and quartic self-couplings can be used by the community for further calculations and analyses.

Appendix A

Mathematical Functions and Identities

A.1 Eigenvalues of a 2 by 2 Matrix

To find the eigenvalues of a square matrix A, one has to calculate the zeros of the characteristic polynomial of A. The characteristic polynomial of A is defined by $\det(A-\lambda\cdot 1)$, where 1 is the unit matrix with the same size as A. For a 2 by 2 matrix this is fairly simple. The characteristic polynomial is

$$\det(A-\lambda\cdot 1)\equiv\det\begin{pmatrix} a-\lambda & b \\ c & d-\lambda \end{pmatrix}=(a-\lambda)(d-\lambda)-bc \tag{A.1.1}$$

$$=\lambda^2-\lambda(a+d)+(ad-bc). \tag{A.1.2}$$

The zeros of this are then the eigenvalues

$$\lambda_{1,2}=\frac{1}{2}\left(a+d\pm\sqrt{(a+d)^2-4(ad-bc)}\right)=\frac{1}{2}\left(a+d\pm\sqrt{(a-d)^2+4bc}\right). \tag{A.1.3}$$

Mass matrices are always symmetric so we can set $b=c$.

A.2 Diagonalization of a Symmetric 2 by 2 Matrix

To diagonalize a symmetric 2 by 2 matrix A, we make the ansatz

$$D=R_\Theta A R_\Theta\equiv R_\Theta\begin{pmatrix} a & b \\ b & d \end{pmatrix}R_\Theta, \tag{A.2.1}$$

where $D=diag(\lambda_1,\lambda_2)$ the diagonalized matrix which has the eigenvalues on the diagonal and

$$R_\Theta\equiv\begin{pmatrix} s_\Theta & c_\Theta \\ c_\Theta & -s_\Theta \end{pmatrix} \tag{A.2.2}$$

is the rotation matrix, parameterized by the angle Θ. This parameterization is convenient because $R_\Theta R_\Theta=1$ and R_Θ is therefore equal to its inverse $R_\Theta=R_\Theta^{-1}$. The off-diagonal entries of D have to vanish, i.e.

$$(a-d)\sin(2\Theta)+2b\cos(2\Theta)=0\quad\Rightarrow\quad\tan(2\Theta)=\frac{2b}{d-a}. \tag{A.2.3}$$

Using Eq. (A.1.3) we can solve for Θ

$$\sin 2\Theta = \frac{2b}{\lambda_1 - \lambda_2} \quad \Rightarrow \quad \Theta = \frac{1}{2}\arcsin\left(\frac{2b}{\lambda_1 - \lambda_2}\right). \tag{A.2.4}$$

A.3 The Gamma Function

The gamma function is an extension of the factorial function and for positive integers n it is defined as

$$\Gamma(n) = (n-1)!. \tag{A.3.1}$$

For complex numbers z, with $Re(z) > 0$ the gamma function can be defined by an integral

$$\Gamma(z) \equiv \int_0^\infty dt t^{z-1} e^{-t}. \tag{A.3.2}$$

The gamma function satisfies the recurrence relation

$$\Gamma(z+1) = z\Gamma(z). \tag{A.3.3}$$

A.4 The Beta Function in Mathematics

The beta function can be defined by

$$\beta(x,y) = \int_0^1 dz z^{x-1}(1-z)^{y-1}, \tag{A.4.1}$$

for complex numbers x and y, with $Re(x) > 0$ and $Re(y) > 0$. The beta function is symmetric in x and y and can be expressed in terms of gamma functions,

$$\beta(x,y) = \frac{\Gamma(x)\Gamma(y)}{\Gamma(x+y)}. \tag{A.4.2}$$

A.5 The hypergeometric function

The hypergeometric function is defined by the integral

$$F(a,b,c;z) \equiv \frac{\Gamma(c)}{\Gamma(b)\Gamma(c-b)} \int_0^1 dt \frac{t^{b-1}(1-t)^{c-b-1}}{(1-tz)^a}, \tag{A.5.1}$$

and obeys numerous identities. One of these we will use to calculate the effective potential at $\mathcal{O}(\alpha_t)$, namely

$$F(a,b,c;z) = (1-z)^{c-a-b} F(c-a, c-b, c; z). \tag{A.5.2}$$

Appendix B

Loop Integrals

B.1 One-Loop Functions

The one-loop self-energies are calculated using dimensional regularization and can be expressed in terms of the two Passarino-Veltman functions A_0 and B_0

$$A_0(m^2) \equiv \frac{16\pi^2}{i}\frac{\mu_0^{4-d}}{(2\pi)^d}\int \frac{d^dq}{q^2-m^2+i\epsilon}, \tag{B.1.1}$$

$$B_0(p^2,m_1^2,m_2^2) \equiv \frac{16\pi^2}{i}\frac{\mu_0^{4-d}}{(2\pi)^d}\int \frac{d^dq}{[q^2-m_1^2+i\epsilon][(p-q)^2-m_2^2+i\epsilon]}. \tag{B.1.2}$$

To express the one-loop self-energies in a compact form, we also use the following combinations of A_0 and B_0

$$B_1(p^2,m_1^2,m_2^2) = \frac{1}{2p^2}\left(A_0(m_2^2)-A_0(m_1^2)+(p^2+m_1^2-m_2^2)B_0(p^2,m_1^2,m_2^2)\right), \tag{B.1.3}$$

$$G(p^2,m_1^2,m_2^2) = (p^2-m_1^2-m_2^2)B_0(p^2,m_1^2,m_2^2)-A_0(m_1^2)-A_0(m_2^2). \tag{B.1.4}$$

An analytic expression for the one-point function A_0 can be easily found using standard techniques

$$A_0(m^2) = m^2\left(\frac{1}{\epsilon}+1-\log\frac{m^2}{Q^2}\right)+\epsilon m^2\left(\frac{\pi^2}{12}+1-\log\frac{m^2}{Q^2}+\frac{1}{2}\log^2\frac{m^2}{Q^2}\right), \tag{B.1.5}$$

where $Q^2 \equiv 4\pi\mu_0^2 e^{-\gamma_E}$ is the usual rescaling of the regularization scale. The $\mathcal{O}(\epsilon)$ terms are not relevant for the self-energies, but they are useful to calculate the two-loop integral $J(x,y)$, defined in Eq. (2.2.1). The two-point function B_0 can be cast into the following form

$$B_0(p^2,m_1^2,m_2^2) = \frac{1}{\epsilon}-\int_0^1 dt\log\frac{(1-t)m_1^2+tm_2^2-t(1-t)p^2}{Q^2}. \tag{B.1.6}$$

An explicit analytical form can be found in [69]. The derivative of the B_0-function w.r.t. the first argument and evaluated at zero external momentum is

$$B_0'(0,m_1^2,m_2^2) \equiv \left.\frac{\partial}{\partial p^2}B_0(p^2,m_1^2,m_2^2)\right|_{p^2=0} = \int_0^1 dt\left[\frac{m_1^2}{t}+\frac{m_2^2}{1-t}\right]^{-1}. \tag{B.1.7}$$

We will need B_0' for the external self-energies of the P_i and S_i fields, see Eqs. (D.4.7 - D.4.10). These are defined in the limit $p^2 \to 0$, see Eq. (2.5.12). Explicit expressions for $B_0'(0,y,z)$ are

$$B_0'(0,m_1^2,m_2^2) = \frac{m_1^2 m_2^2}{(m_1^2-m_2^2)^3}\log\frac{m_2^2}{m_1^2} + \frac{m_2^1+m_2^2}{2(m_2^2-m_1^2)^2}, \tag{B.1.8}$$

$$B_0'(0,m^2,m^2) = \frac{1}{6m^2}. \tag{B.1.9}$$

B.2 Two-Loop Master Integrals

Analytical expressions for the two-loop master integrals defined in Eqs. (2.2.1, 2.2.2) are given by[1]

$$\begin{aligned} J(x,y) =& xy\left[\frac{1}{\epsilon^2}+\frac{1}{\epsilon}\left(2-\log\frac{x}{Q^2}-\log\frac{y}{Q^2}\right)-2\left(\log\frac{x}{Q^2}+\log\frac{y}{Q^2}\right)+\frac{1}{2}\left(\log\frac{x}{Q^2}+\log\frac{y}{Q^2}\right)^2\right. \\ &\left.+3+\frac{\pi^2}{6}\right], \end{aligned} \tag{B.2.1}$$

$$\begin{aligned} I(x,y,z) =& -\frac{1}{2\epsilon^2}(x+y+z)-\frac{1}{\epsilon}\left[x\left(\frac{3}{2}-\log\frac{x}{Q^2}\right)+y\left(\frac{3}{2}-\log\frac{y}{Q^2}\right)+z\left(\frac{3}{2}-\log\frac{z}{Q^2}\right)\right] \\ &+\frac{1}{2}\left(x\log\frac{y}{Q^2}\log\frac{z}{Q^2}+y\log\frac{z}{Q^2}\log\frac{x}{Q^2}+z\log\frac{x}{Q^2}\log\frac{y}{Q^2}\right)-\frac{1}{2}(x+y+z)\left(7+\frac{\pi^2}{6}\right) \\ &-\frac{1}{2}\left(x\log\frac{x}{Q^2}+y\log\frac{y}{Q^2}+z\log\frac{z}{Q^2}\right)\left(\log\frac{x}{Q^2}+\log\frac{y}{Q^2}+\log\frac{z}{Q^2}-6\right) \\ &-\frac{\Delta(x,y,z)}{2z}\Phi(x,y,z), \end{aligned} \tag{B.2.2}$$

where $\Delta(x,y,z) = x^2+y^2+z^2-2xy-2xz-2yz$ and the derivatives of Φ are given by

$$\frac{\partial\Phi(x,y,z)}{\partial x} = \frac{(y+z-x)\Phi(x,y,z)}{\Delta(x,y,z)} + \frac{1}{\Delta(x,y,z)}\frac{z}{x}\left[(y-z)\log\frac{z}{y}+x\left(\log\frac{x}{y}+\log\frac{x}{z}\right)\right]. \tag{B.2.3}$$

Thus we can calculate the second, third and fourth derivative of Φ by recursion and end up with all known objects, except for the function Φ itself (but not its derivatives). An analytic definition for Φ which applies in the case of $z>x$ and $z>y$ is

$$\Phi(x,y,z) = \frac{1}{\lambda}\left(2\log(x_+)\log(x_-)-\log\frac{x}{z}\log\frac{y}{z}-2\left[\mathrm{Li}_2(x_+)+\mathrm{Li}_2(x_-)\right]+\frac{\pi^2}{3}\right), \tag{B.2.4}$$

where

$$\lambda = \sqrt{\left(1-\frac{x}{z}-\frac{y}{z}\right)^2-4\frac{xy}{z^2}}, \qquad x_+ = \frac{1}{2}\left(1+\frac{x}{z}-\frac{y}{z}-\lambda\right), \qquad x_- = \frac{1}{2}\left(1-\frac{x}{z}+\frac{y}{z}-\lambda\right) \tag{B.2.5}$$

and $Li_2(z)$ denotes the dilogarithm, defined by the integral

$$Li_2(z) \equiv -\int_0^z \frac{\log(1+t)}{t}dt. \tag{B.2.6}$$

If the arguments are not ordered correctly we can use the following symmetry relations

$$\Phi(x,y,z) = \Phi(y,x,z), \qquad x\Phi(x,y,z) = z\Phi(z,y,x). \tag{B.2.7}$$

[1] It is easy to show that the integral $J(x,y)$ is equal to the a product of two one-point functions $J(x,y) = A_0(x)A_0(y)$.

The following simplified case of the two-loop master integrals Eqs. (B.2.2, B.2.1) show up in the effective potential

$$\begin{aligned} I(x,y,0) =& -\frac{x+y}{2\epsilon^2} + \frac{1}{\epsilon}\left[x\log\frac{x}{Q^2} + y\log\frac{y}{Q^2} - \frac{3}{2}(x+y)\right] - \frac{7}{2} + \frac{\pi^2}{12}(x+y) \\ &+ 3\left(x\log\frac{x}{Q^2} + y\log\frac{y}{Q^2}\right) + \omega(x,y,z), \end{aligned} \tag{B.2.8}$$

$$I(x,x,0) = -\frac{x}{\epsilon^2} - \frac{x}{\epsilon}\left(3 - 2\log\frac{x}{Q^2}\right) - x\left(2\log\frac{x}{Q^2}\log\frac{x}{Q^2} + 6\log\frac{x}{Q^2} - 7 - \frac{\pi^2}{6}\right), \tag{B.2.9}$$

$$I(x,0,0) = -\frac{x}{2\epsilon^2} + \frac{1}{\epsilon}\left(x\log\frac{x}{Q^2} - \frac{3}{2}x\right) + x\left(-\log^2\frac{x}{Q^2} + 3\log\frac{x}{Q^2} - \frac{\pi^2}{4} - \frac{7}{2}\right), \tag{B.2.10}$$

where

$$\omega(x,y,z) \equiv \log^2\frac{x}{Q^2}(y-x) - \frac{y}{2}\left(\log\frac{y}{Q^2} + \log\frac{x}{Q^2}\right)^2 - (x-y)\mathrm{Li}_2\left(1-\frac{y}{x}\right). \tag{B.2.11}$$

Moreover the following combination of the master integrals Eqs. (B.2.2, B.2.1) is convenient

$$L(x,y,z) = J(y,z) - J(x,y) - J(x,z) - (x-y-z)I(x,y,z). \tag{B.2.12}$$

Appendix C

Feynman Rules and the Effective Potential

The goal of this part of the appendix is to explain how to calculate the effective potential at $\mathcal{O}(\alpha_t+\alpha_t\alpha_s+\alpha_t^2)$. The effective potential is calculated using Feynman diagrams. We will start with the Lagrangian of the MSSM, manipulate it and collect all terms that are needed to calculate the effective potential. A naive application of the Feynman rules results in an expression depending on real quantities, e.g. $m_t, m_{\tilde{t}_{1,2}}, \theta_{\tilde{t}}$. These quantities depend on the Higgs VEVs. In the EPA the dependence is shifted from the VEVs, which are real, to the Higgs fields, which are complex objects. The Higgs field-dependence of the effective potential has to be implemented already on the Lagrangian level, such that the masses, couplings and mixing angles in the propagators and vertices are functions of the complex Higgs fields H_i^0. At the perturbative order that we are considering the Higgs dependence only shows up in the top/stop sector. We start with the bilinear top and stop Lagrangians and implement the Higgs field-dependence explicitly:

C.1 Higgs Field-Dependence in the Top and Stop Sector

Written in a Higgs field-dependent way the Lagrangian bilinear in the top fields reads

$$\mathcal{L}_{2t} = (\overline{t'_L}, \overline{t'_R}) \begin{pmatrix} i\partial\!\!\!/ & -X^\star \\ -X & i\partial\!\!\!/ \end{pmatrix} \begin{pmatrix} t'_L \\ t'_R \end{pmatrix}, \tag{C.1.1}$$

where t'_L and t'_R are four component fermion fields in the chiral basis and X is a Higgs field-dependent mixing term

$$X = h_t H_2^0 \equiv |X|\, e^{i\varphi}, \quad (0 \leq \varphi < 2\pi). \tag{C.1.2}$$

In our calculation we set $h_t > 0$. Note that evaluating X at the minimum of the potential, i.e. substituting all fields by their VEVs, gives the top mass $X|_{\min} = m_t$. This means that we obtain the usual Lagrangian in the field-independent case. The field-dependent top mass is defined by $\bar{m}_t \equiv |X|$.
Analogously, we also write the bilinear top squark terms, see Eq. (1.3.3), in an Higgs field-dependent way

$$\mathcal{L}_{2\tilde{t}} = -(\tilde{t}'^\star_L \tilde{t}'^\star_R) \begin{pmatrix} \Box + m_L^2 & \tilde{X}^\star \\ \tilde{X} & \Box + m_R^2 \end{pmatrix} \begin{pmatrix} \tilde{t}'_L \\ \tilde{t}'_R \end{pmatrix}, \tag{C.1.3}$$

where the field-dependent entries in the matrix are[1]

$$m_L^2 = m_Q^2 + h_t^2|H_2^0|^2, \quad m_R^2 = m_U^2 + h_t^2|H_2^0|^2, \tag{C.1.4}$$

$$\tilde{X} \equiv \left|\tilde{X}\right| e^{i\tilde{\varphi}} = h_t \left(AtH_2^0 + \mu H_1^{0\star}\right), \quad (0 \leq \tilde{\varphi} < 2\pi), \tag{C.1.5}$$

and m_Q^2, m_U^2 and A_t are soft supersymmetry breaking parameters of the stop sector, see Eq. (1.3.2). The phases φ and $\tilde{\varphi}$ are Higgs field-dependent quantities. Since the effective potential depends on these phases we must not neglect them when taking derivatives of the effective potential w.r.t. the Higgs fields. To simplify the calculations, we choose to redefine the fields in such a way that the top and stop mass matrices become real

$$t'_L = e^{-i\frac{\varphi}{2}} t_L, \quad t'_R = e^{i\frac{\varphi}{2}} t_R, \qquad \tilde{t}'_L = e^{-i\frac{\tilde{\varphi}}{2}} \tilde{t}_L, \quad \tilde{t}'_R = e^{i\frac{\tilde{\varphi}}{2}} \tilde{t}_R. \tag{C.1.6}$$

The goal here is to redefine the top and stop fields in such a way that we get a real, field-dependent mass $m_t \equiv h_t \left|H_2^0\right|$ such that the substitution of the VEV in m_t with the Higgs is uniquely determined and we thus get a consistent field-dependent effective potential. Similarly we want the stop mass matrix to be real and symmetric, such that it can be diagonalized by the usual orthogonal transformation Eq. (1.3.5) with field-dependent mixing angles

$$\begin{pmatrix} \tilde{t}_1 \\ \tilde{t}_2 \end{pmatrix} = \begin{pmatrix} \cos\bar{\theta}_{\tilde{t}} & \sin\bar{\theta}_{\tilde{t}} \\ -\sin\bar{\theta}_{\tilde{t}} & \cos\bar{\theta}_{\tilde{t}} \end{pmatrix} \begin{pmatrix} \tilde{t}_L \\ \tilde{t}_R \end{pmatrix}. \tag{C.1.7}$$

The diagonalized field-dependent stop masses are thus

$$\bar{m}^2_{\tilde{t}_{1,2}} = \frac{1}{2}\left[(m_L^2 + m_R^2) \pm \sqrt{(m_L^2 - m_R^2)^2 + 4\left|\tilde{X}\right|^2}\right]. \tag{C.1.8}$$

The mixing angle $\bar{\theta}_{\tilde{t}}$ is also a field-dependent quantity, defined by

$$s_{2\bar{\theta}} \equiv \sin 2\bar{\theta}_{\tilde{t}} = \frac{2\left|\tilde{X}\right|}{\bar{m}^2_{\tilde{t}_1} - \bar{m}^2_{\tilde{t}_2}}, \qquad c_{2\bar{\theta}} \equiv \cos 2\bar{\theta}_{\tilde{t}} = \frac{m_Q^2 - m_U^2}{\bar{m}^2_{\tilde{t}_1} - \bar{m}^2_{\tilde{t}_2}}, \tag{C.1.9}$$

where we use the obvious abbreviations for the trigonometric functions sin and cos and define $\bar{\theta} \equiv \bar{\theta}_{\tilde{t}}$. When we want to calculate Feynman diagrams we start with the usual Lagrangian, which is expressed in terms of the fields $t'_{L,R}$ and $\tilde{t}'_{L,R}$. We then rotate these fields according to Eq. (C.1.6) such that we can evaluate Feynman diagrams, using the unprimed fields $t_{R,L}$ and $\tilde{t}_{1,2}$ with real field-dependent masses in the propagators and real orthogonal field-dependent mixing angels.
It will turn out that the two-loop potentials depend only on the top and stop mixing phases φ and $\tilde{\varphi}$ through the combination $\bar{\xi} \equiv \bar{m}_t s_{2\bar{\theta}_{\tilde{t}}} \cos(\varphi - \tilde{\varphi})$, which has the following field-dependence

$$\bar{\xi} = 2\frac{\Re(X)\Re(\tilde{X}) + \Im(X)\Im(\tilde{X})}{\bar{m}^2_{\tilde{t}_1} - \bar{m}^2_{\tilde{t}_2}}. \tag{C.1.10}$$

Note that $\cos(\varphi - \tilde{\varphi})|_{\min} = 1$ and therefore $\bar{\xi}$ evaluated at the minimum is simply $\xi \equiv \bar{\xi}\big|_{\min} = m_t s_{2\theta}$.

[1] There are D-term contributions to the stop masses, which do also depend on the Higgs fields, see Eq. (1.3.3). However, we will not include them here, because they are of $\mathcal{O}(g^2 + g'^2)$ and would therefore contribute to the $\mathcal{O}(m_Z^2\alpha_t)$ potential. In the numerical evaluation for the stop masses on the other hand we will include D-terms. Including them here is still not relevant for any gain in perturbative precision, however, it helps us to numerically stabilize terms that diverge in the limit of vanishing stop mixing.

C.2 Derivation of the One-Loop Effective Potential at $\mathcal{O}(\alpha_t)$

In this section we will give a detailed description of how to calculate the one-loop effective potential due to stop and top loops. We start with Eq. (2.1.2) and first want to find the sum over all 1PI Feynman diagrams with n legs and zero external momentum at $\mathcal{O}(\alpha_t)$

$$\Gamma^{(n),\mathcal{O}(\alpha_t)}(0,...,0) \equiv \Gamma^{(n),\mathcal{O}(\alpha_t)}_{\text{top}}(0,...,0) + \Gamma^{(n),\mathcal{O}(\alpha_t)}_{\text{stop}}(0,...,0). \tag{C.2.1}$$

C.2.1 Top-Quark Loops

The Higgs field-dependent Lagrangian containing terms bilinear in the top fields was presented Eq. (C.1.1) and the Higgs top vertex is shown in Figure C.1. Note that the Higgs field changes the helicity of the top quark. This means that we cannot have an odd number of external Higgs fields coupling to the top loop.

In the SM as well as in the MSSM the quark masses are generated by the Yukawa couplings to the

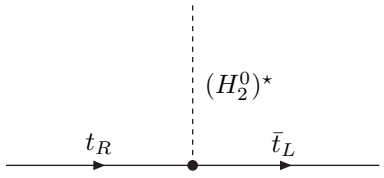

Figure C.1: Higgs-top vertex

Higgs. The idea is now that we treat the top-quark as massless and shift the mass into the top-Higgs coupling. This simplifies our calculation, because massless loops are much easier to handle than massive loops.

We therefore deduce that for the effective potential we have to consider the sum of all diagrams with an even number of external legs $\sum_n \Gamma^{(2n),\mathcal{O}(\alpha_t)}_{\text{top}}(0,...,0)$, see Figure C.2.

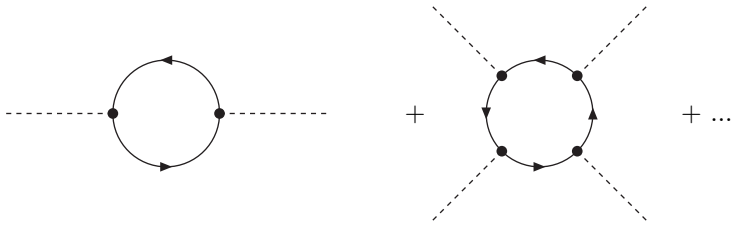

Figure C.2: Diagrams involving virtual top particles, contributing to the one-loop effective potential. The ellipses stand for diagrams with a higher, even number of external top legs.

The analytical expression for $\Gamma^{(2n),\mathcal{O}(\alpha_t)}_{\text{top}}(0,...,0)$ can be written down easily using Feynman rules

$$\Gamma^{(2n),\mathcal{O}(\alpha_t)}_{\text{top}}(0,...,0) = -iS_{2n}\int \frac{d^4k}{(2\pi)^4}(-ih_t)^{2n}(-1)tr\left[\frac{i(\not{k})}{k^2+i\epsilon}\right]^{2n}. \tag{C.2.2}$$

The Expression contains a symmetry factor $S_{2n} = \frac{(2n)!}{2n}$ corresponding to the fact that there are $(2n)!$ ways to distribute $2n$ particles to the external lines and that there are n rotations and 2 reflections that

do not lead to new contributions. The factor $-ih_t$ comes from the vertex and is the Higgs-top-Yukawa coupling, the (-1) corresponds to closed fermion lines. As mentioned above, the top-quark can be treated as massless, when interacting with the Higgs boson. Moreover we have to take the trace over the fermion loop, which gives simply a factor 4, because the massless fermion propagator squared is proportional to the four by four identity matrix.
To obtain an analytic expression for the effective potential we insert Eq. (C.2.2) into Eq. (2.1.2)

$$\delta V_{\text{top}}^{\alpha_t}(H_2^0) = -\sum_n \frac{1}{(2n)!}\Gamma_{\text{top}}^{(2n),\mathcal{O}(\alpha_t)}(0,...,0)[H_2^0]^n[(H_2^0)^\star]^n \tag{C.2.3}$$

$$= -2i\int \frac{d^4k}{(2\pi)^4}\sum_n \frac{1}{n}\left[\frac{h_t^2|H_2^0|^2}{k^2+i\epsilon}\right]^n. \tag{C.2.4}$$

We use the fact that the above sum corresponds exactly to the Taylor expansion of a logarithm

$$\log(1+x) = \sum_{n=1}^{\infty}\frac{(-1)^{n+1}}{n}x^n, \tag{C.2.5}$$

to write the effective potential as

$$\delta V_{\text{top}}^{\alpha_t}(H_2^0) = 2i\int \frac{d^4k}{(2\pi)^4}\log\left(1-\frac{h_t^2|H_2^0|^2}{k^2+i\epsilon}\right). \tag{C.2.6}$$

We redefine $\bar{m}_t^2 \equiv h_t^2|H_2^0|^2$, using the "bar" to denote that the top mass is a Higgs-field-dependent quantity. Note that the one-loop potential due to top loops does only depend on the top mass squared. This means that there is no dependence on the phase φ. This integral will be solved in section C.2.3 using dimensional regularization.

C.2.2 Stop Loops

Calculating the one-loop effective potential due to stop loops is a little more difficult. The bilinear, field-dependent stop quark Lagrangian was given in Eq. (C.1.3). The main difference to the top quarks is that there are also terms in the diagonal, which contain the Higgs field H_2^0. Moreover the off-diagonal terms contain two different Higgs fields, which make the computation of $\Gamma_{\text{stop}}^{(2n),\mathcal{O}(\alpha_t)}(0,...,0)$ a little more involved.
In [47] it was shown that the scalar one-loop potential is

$$\delta V_{\text{stop}}^{\alpha_t}(H_1^0,H_2^0) = -\frac{1}{2}i\int\frac{d^4k}{(2\pi)^4}\log\left[\det\left(iD^{-1}(k)\right)\right], \tag{C.2.7}$$

where $iD^{-1}(k)$ is the inverse propagator in momentum space and therefore the Fourier transform of the bilinear terms in $\tilde{t}_{L,R}$. Performing this Fourier transform yields

$$iD^{-1}(k) = -\begin{pmatrix} k^2-m_L^2 & -\tilde{X}^\star \\ -\tilde{X} & k^2-m_R^2 \end{pmatrix}. \tag{C.2.8}$$

The determinant of this 2 by 2 matrix is easy to calculate

$$\det iD^{-1}(k) = (k^2-m_L^2)(k^2-m_R^2)-|\tilde{X}|^2 \tag{C.2.9}$$

$$= k^4-k^2(m_L^2+m_R^2)+m_L^2m_R^2-|\tilde{X}|^2. \tag{C.2.10}$$

The $\tilde{t}_{L,R}$ are not mass eigenstates, and thus have to be rotated first. The mass eigenstates will be denoted $\tilde{t}_{1,2}$ with field-dependent masses $\bar{m}_{\tilde{t}_1}$ and $\bar{m}_{\tilde{t}_2}$, see Eqs. (2.2.8, 2.2.9). The mass matrix of the stop quarks before and after diagonalization is

$$M_{L,R} = \begin{pmatrix} m_L^2 & \tilde{X}^\star \\ \tilde{X} & m_R^2 \end{pmatrix}, \qquad M_{1,2} = \begin{pmatrix} \bar{m}_{\tilde{t}_1}^2 & 0 \\ 0 & \bar{m}_{\tilde{t}_2}^2 \end{pmatrix}. \tag{C.2.11}$$

The trace and the determinant of a matrix are invariant under diagonalization. We can therefore express the determinant of the inverse propagator by

$$\begin{aligned} \det iD^{-1}(k) &= k^4 - k^2\,\mathrm{Tr}(M_{L,R}) + \det(M_{L,R}) && \text{(C.2.12)} \\ &= k^4 - k^2\,\mathrm{tr}(M_{1,2}) + \det(M_{1,2}) && \text{(C.2.13)} \\ &= k^4 - k^2(\bar{m}_{\tilde{t}_1}^2 + \bar{m}_{\tilde{t}_2}^2) + \bar{m}_{\tilde{t}_1}^2\bar{m}_{\tilde{t}_2}^2 = (k^2 - \bar{m}_{\tilde{t}_1}^2)(k^2 - \bar{m}_{\tilde{t}_2}^2). && \text{(C.2.14)} \end{aligned}$$

Using an $i\epsilon$ prescription the effective potential due to stop loops leads to the integral

$$\delta V_{\mathrm{stop}}^{\alpha_t}(H_1^0, H_2^0) = -\frac{1}{2} i \int \frac{d^4k}{(2\pi)^4} \log\left((k^2 - \bar{m}_{\tilde{t}_1}^2 + i\epsilon)(k^2 - \bar{m}_{\tilde{t}_2}^2 + i\epsilon)\right), \tag{C.2.15}$$

which will be solved the following section.

C.2.3 Solving the Integrals

Stops: The integral for the stop loops is

$$\delta V_{\mathrm{stop}}^{\alpha_t}(H_1^0, H_2^0) = -\frac{1}{2} i \int \frac{d^4k}{(2\pi)^4} \log\left((k^2 - \bar{m}_{\tilde{t}_1}^2 + i\epsilon)(k^2 - \bar{m}_{\tilde{t}_2}^2 + i\epsilon)\right). \tag{C.2.16}$$

We perform a Wick rotation to transform the integration from Minkowski space into Euclidean space

$$\delta V_{\mathrm{stop}}^{\alpha_t}(H_1^0, H_2^0) = \frac{1}{2} \int \frac{d^4k}{(2\pi)^4} \log\left((-k^2 - \bar{m}_{\tilde{t}_1}^2 + i\epsilon)(-k^2 - \bar{m}_{\tilde{t}_2}^2 + i\epsilon)\right). \tag{C.2.17}$$

We define the logarithm of a complex quantity with a branch cut on the negative real axis, i.e. $\log(-|a| + i\epsilon) = \log(|a|) + i\pi$. The logarithm of a product can be written as

$$\log(ab) = \log(a) + \log(b) + 2\pi i \eta(a,b), \tag{C.2.18}$$

where $\eta(a,b)$ is a function giving either 0 or ± 1 and is defined as

$$\eta(a,b) = [\Theta(\Im(-a))\Theta(\Im(-b))\Theta(\Im(ab)) - \Theta(\Im(a))\Theta(\Im(b))\Theta(\Im(-ab))] \tag{C.2.19}$$

and $\Theta(x)$ is the Heaviside function. This means that every crossing of the branch cut yields an additional $\pm 2\pi i$-term. The logarithm in Eq. (C.2.17) is therefore

$$\begin{aligned} & \log((-k^2 - \bar{m}_{\tilde{t}_1}^2 + i\epsilon)(-k^2 - \bar{m}_{\tilde{t}_2}^2 + i\epsilon)) && \text{(C.2.20)} \\ = \; & \log(-k^2 - \bar{m}_{\tilde{t}_1}^2 + i\epsilon) + \log(-k^2 - \bar{m}_{\tilde{t}_2}^2 + i\epsilon) - 2\pi i && \text{(C.2.21)} \\ = \; & \log(k^2 + \bar{m}_{\tilde{t}_1}^2) + \log(k^2 + \bar{m}_{\tilde{t}_2}^2) && \text{(C.2.22)} \end{aligned}$$

Note that all $i\pi$-terms cancel. We write $V_{1,stop} = H(m_{\tilde{t}_1}) + H(m_{\tilde{t}_2})$, where

$$H(m) \equiv \frac{1}{2} \int \frac{d^4k}{(2\pi)^4} \log(k^2 + m^2). \tag{C.2.23}$$

We will solve this integral using DRED, see section 2.2.2. Changing the number of dimensions from 4 to d and expressing the integration measure in spherical coordinates yields

$$\int d^d k = \int d\Omega_d \int_0^{+\infty} d|k||k|^{d-1} \mu_0^{4-d}, \tag{C.2.24}$$

where μ_0 is the t'Hooft or regularization scale. This unphysical scale has mass dimension one and has to be introduced in DREG and DRED to restore the number of space-time dimensions of the integral to 4. Moreover

$$\int d\Omega_d = \frac{2\pi^{d/2}}{\Gamma(d/2)} \tag{C.2.25}$$

is the surface of the d-dimensional unit sphere. There is only a one-dimensional integration left

$$H(m) = \frac{\mu_0^{4-d}}{(4\pi)^{d/2}\Gamma(d/2)} \int_0^{+\infty} d|k||k|^{d-1} \log(|k|^2 + m^2). \tag{C.2.26}$$

Performing a substitution $x \equiv |k|^2$ to get rid of the quadratic integration variable and setting $d = 4 - 2\epsilon$, with $\epsilon > 0$ yields

$$H(m) = \frac{(m^2)^{2-\epsilon}\mu_0^{2\epsilon}}{2(4\pi)^{2-\epsilon}\Gamma(2-\epsilon)} \int_0^{+\infty} dx x^{1-\epsilon} \log(x + m^2). \tag{C.2.27}$$

To get a dimensionless integration variable we substitute $y \equiv x/m^2$, i.e.

$$H(m) = \frac{(m^2)^{2-\epsilon}\mu_0^{2\epsilon}}{2(4\pi)^{2-\epsilon}\Gamma(2-\epsilon)} \int_0^{+\infty} dy y^{1-\epsilon} \log(m^2(y+1)). \tag{C.2.28}$$

Our goal is to express this integral in terms of beta functions and hypergeometric functions. For this we change the integration range to $[0, 1]$. This is achieved by another change of variables $z = \frac{1}{1+y}$. We obtain

$$H(m) = \frac{(m^2)^2}{2(4\pi)^{2-\epsilon}\Gamma(2-\epsilon)} \left(\frac{\mu_0^2}{m^2}\right)^{\epsilon} \int_0^1 dz \frac{(1-z)^{1-\epsilon}}{z^{3-\epsilon}} \left\{\log(m^2) - \log(z)\right\}. \tag{C.2.29}$$

The integral with a $\log(m^2)$ prefactor is simply a beta function (see appendix A.4) and therefore easy to evaluate

$$\int_0^1 dz z^{-3+\epsilon}(1-z)^{1-\epsilon} = \beta(-2+\epsilon, 2-\epsilon) = \frac{\Gamma(-2+\epsilon)\Gamma(2-\epsilon)}{\Gamma(0)} = 0. \tag{C.2.30}$$

The remaining integral has an additional logarithm in the integrand and therefore needs a little more work

$$B \equiv \int_0^1 dz \cdot z^{-3+\epsilon}(1-z)^{1-\epsilon} \log(z). \tag{C.2.31}$$

The first step is to integrate by parts

$$f'(z) \equiv z^{-3+\epsilon}(1-z)^{1-\epsilon}, \qquad g(z) \equiv \log(z) \tag{C.2.32}$$

$$\Rightarrow \quad f(z) = \int_0^z d\bar{z} \cdot \bar{z}^{-3+\epsilon}(1-\bar{z})^{1-\epsilon}, \qquad g'(z) = \frac{1}{z}. \tag{C.2.33}$$

Looking at $f(z)$ we see that by changing the upper integration boundary to 1, we get a hypergeometric function (see appendix A.5). This is achieved by a substitution $t \equiv \frac{\bar{z}}{z}$ and yields

$$f(z)z^{2-\epsilon} = \int_0^1 dt (t)^{-3+\epsilon}(1-zt)^{1-\epsilon}, \tag{C.2.34}$$

which can be expressed using a hypergeometric function and several gamma functions

$$f(z) = z^{-2+\epsilon} F(\epsilon-1, \epsilon-2, \epsilon-1; z) \frac{\Gamma(\epsilon-2)\Gamma(1)}{\Gamma(\epsilon-1)}. \tag{C.2.35}$$

Next we use a property of the hypergeometric function Eq. (A.5.2) to reduce the above to a beta function, which can then be further reduced to gamma functions

$$\begin{aligned} F(\epsilon-1, \epsilon-2, \epsilon-1; z) &= (1-z)^{2-\epsilon} F(0, 1, \epsilon-1; z) && \text{(C.2.36)} \\ &= (1-z)^{2-\epsilon} \int_0^1 dt (1-t)^{\epsilon-3} \frac{\Gamma(\epsilon-1)}{\Gamma(1)\Gamma(\epsilon-2)} && \text{(C.2.37)} \\ &= (1-z)^{2-\epsilon} \beta(1, \epsilon-2) \frac{\Gamma(\epsilon-1)}{\Gamma(1)\Gamma(\epsilon-2)} && \text{(C.2.38)} \\ &= (1-z)^{2-\epsilon} \frac{\Gamma(\epsilon-1)\Gamma(2)\Gamma(\epsilon-2)}{\Gamma(1)\Gamma(\epsilon-2)\Gamma(\epsilon-1)} = (1-z)^{2-\epsilon}. && \text{(C.2.39)} \end{aligned}$$

The integral B is now be evaluated

$$\begin{aligned} B &= f(z)g(z)|_0^1 - \int_0^1 dz f(z) g'(z) && \text{(C.2.40)} \\ &= z^{\epsilon-2}(1-z)^{2-\epsilon} \frac{\Gamma(\epsilon-2)}{\Gamma(\epsilon-1)} \log(z) \Big|_0^1 - \int_0^1 dz \cdot z^{\epsilon-2}(1-z)^{2-\epsilon} \frac{\Gamma(\epsilon-2)}{\Gamma(\epsilon-1)} \frac{1}{z} && \text{(C.2.41)} \\ &= \frac{\Gamma(\epsilon-2)}{\Gamma(\epsilon-1)} \left\{ \left(\frac{1-z}{z} \right)^{2-\epsilon} \log(z) \Big|_0^1 - \beta(\epsilon-2, 3-\epsilon) \right\}. && \text{(C.2.42)} \end{aligned}$$

The first term of the above expression is not defined for all ϵ. However, in dimensional regularization, we can choose an ϵ interval in which the expression is well-defined and analytically continue, such that the integral takes on the same value for all $\epsilon > 0$. For the above quantities we get

$$\left(\frac{1-z}{z} \right)^{2-\epsilon} \log(z) \Big|_0 = 0, \qquad \epsilon > 2, \tag{C.2.43}$$

$$\left(\frac{1-z}{z} \right)^{2-\epsilon} \log(z) \Big|_1 = 0, \qquad 0 < \epsilon < 2. \tag{C.2.44}$$

We can now insert

$$B = -\frac{\Gamma(\epsilon-2)}{\Gamma(\epsilon-1)} \beta(\epsilon-2, 3-\epsilon) \tag{C.2.45}$$

into Eq. (C.2.29) and obtain

$$\begin{aligned} H(m) &= \frac{(m^2)^2}{2(4\pi)^{2-\epsilon}\Gamma(2-\epsilon)} \left(\frac{\mu_0^2}{m^2} \right)^{\epsilon} \left\{ A \log(m^2) - B \right\} && \text{(C.2.46)} \\ &= \frac{1}{2} \left(\frac{(m^2)}{(4\pi)} \right)^2 \left(\frac{4\pi\mu_0^2}{m^2} \right)^{\epsilon} \frac{\Gamma(\epsilon-2)\Gamma(\epsilon-2)\Gamma(3-\epsilon)}{\Gamma(\epsilon-1)\Gamma(2-\epsilon)\Gamma(1)}. && \text{(C.2.47)} \end{aligned}$$

The last step is to reduce the remaining gamma functions via Eq. (A.3.3) and then expand everything up to $\mathcal{O}(\epsilon)$, using the following Taylor expansions

$$a^{\epsilon} = \exp(\epsilon \cdot \log a) = 1 + \epsilon \cdot \log a + \epsilon^2 \cdot \frac{\log^2 a}{2} + \mathcal{O}(\epsilon^3), \tag{C.2.48}$$

$$\Gamma(\epsilon) = \frac{1}{\epsilon} - \gamma_E + \epsilon \cdot \left(\frac{\pi^2}{12} + \frac{\gamma_E^2}{2} \right) + \mathcal{O}(\epsilon^2), \tag{C.2.49}$$

where $\gamma_E \simeq 0.57721$ is the Euler-Mascheroni constant. The final result is

$$H(m) = -\frac{1}{64\pi^2}(m^2)^2 \left\{ \frac{1}{\epsilon} + \frac{3}{2} - \log\left(\frac{m^2}{Q^2}\right) + \epsilon \left(\frac{7}{4} - \frac{3}{2}\log\frac{m^2}{Q^2} + \frac{1}{2}\log^2\frac{m^2}{Q^2} + \frac{\pi^2}{12} \right) \right\} + \mathcal{O}(\epsilon^2), \quad \text{(C.2.50)}$$

where $Q^2 \equiv 4\pi\mu_0^2 e^{-\gamma_E}$ is a rescaling of the regularization scale, which absorbs some finite terms such that we obtain a logarithm of a dimensionless quantity. We will refer to Q as the regularization scale.

Tops: We first perform a Wick rotation to transform the integration measure from Minkowski into Euclidean space

$$\delta V_{\text{top}}^{\alpha_t}(H_2^0) = -2 \int \frac{d^4k}{(2\pi)^4} \log\left(1 + \frac{\bar{m}_t^2}{k^2 + i\epsilon}\right). \quad \text{(C.2.51)}$$

Using Eq. (C.2.18), we can manipulate the logarithm

$$\begin{aligned} \delta V_{\text{top}}^{\alpha_t}(H_2^0) &= -2 \int \frac{d^4k}{(2\pi)^4} \left\{ \log(k^2 + \bar{m}_t^2) - \log(k^2) \right\} & \text{(C.2.52)} \\ &= -4 \left\{ H(\bar{m}_t) - H(0) \right\}, & \text{(C.2.53)} \end{aligned}$$

where we have used the definition of Eq. (C.2.23).
We get exactly the same integral as in the stop case. The minus sign emerges from the fermionic nature of the tops. The factor of four comes from the Dirac trace, taking into account two different helicities and the antiparticle.

Final Result: We can now put everything together to get the one-loop effective potential in the MSSM at $\mathcal{O}(\alpha_t)$ in DRED

$$\begin{aligned} \delta V^{\alpha_t}(\bar{m}_t^2, \bar{m}_{\tilde{t}_1}^2, \bar{m}_{\tilde{t}_2}^2) = \frac{N_C}{16\pi^2} \Bigg\{ \bar{m}_t^4 \left[\frac{1}{\epsilon} + \frac{3}{2} - \log\frac{\bar{m}_t^2}{Q^2} + \epsilon \left(\frac{7}{4} - \frac{3}{2}\log\frac{\bar{m}_t^2}{Q^2} + \frac{1}{2}\log^2\frac{\bar{m}_t^2}{Q^2} + \frac{\pi^2}{12} \right) \right] \\ - \frac{1}{2} \left[(\bar{m}_t \leftrightarrow \bar{m}_{\tilde{t}_1}) + (\bar{m}_t \leftrightarrow \bar{m}_{\tilde{t}_2}) \right] \Bigg\}, \quad \text{(C.2.54)} \end{aligned}$$

where N_C is the number of colors and the factor of two takes into account stops and anti-stops. The $\mathcal{O}(\alpha_t)$ potential has a pole in ϵ, we will see that all poles cancel when we use this potential to calculate one-loop masses and couplings. Moreover every pole in ϵ is connected to a logarithm in the regularization scale Q. This is a universal feature of DREG and DRED where the integral results in terms proportional to

$$\sim \Gamma(1+\epsilon) \left(\frac{4\pi\mu_0^2}{m^2}\right)^{\epsilon} \epsilon^{-1} = (1 - \gamma_E\epsilon + \mathcal{O}(\epsilon^2)) \left(1 + \epsilon \log\left(\frac{4\pi\mu_0^2}{m^2}\right) + \mathcal{O}(\epsilon^2)\right) \frac{1}{\epsilon} = \frac{1}{\epsilon} + \log\frac{Q^2}{m^2} + \mathcal{O}(\epsilon). \quad \text{(C.2.55)}$$

It is therefore clear that a cancellation of the poles in ϵ also implies a cancellation of the logarithms in Q. Moreover the $\mathcal{O}(\epsilon)$-terms will give finite contributions at the two-loop level. This issue is discussed in section 2.5.6.
Note that in the literature the one-loop effective potential is usually given in the following, $\overline{\text{DR}}$ renormalized form

$$\Delta V^{\alpha_t} = \frac{1}{64\pi^2} \text{Str} \left\{ \mathcal{M}^4(Q) \left[\log\frac{\mathcal{M}^2(Q)}{Q^2} - \frac{3}{2} \right] \right\}, \quad \text{(C.2.56)}$$

where $\text{Str}\, f(\mathcal{M}^2) = \sum_i (-1)^{2J_i}(2J_i+1) f(m_i^2)$ denotes the *supertrace* and m_i^2 is the field-dependent mass eigenvalue of the i-th particle with spin J_i. Field dependent terms have been omitted. For our calculation we will not renormalize the effective potential, but we will use the unrenormalized effective potential to calculate masses and couplings and renormalize them afterwards.

C.3 Calculating the Effective Potential up to $\mathcal{O}(\alpha_t\alpha_s)$

The two-loop SQCD effective potential is defined as the sum over all vacuum diagrams at $\mathcal{O}(\alpha_t\alpha_s)$, see Figure 2.2. In this part of the appendix we will derive all relevant Feynman rules for the SQCD corrections to the effective potential.

C.3.1 Lagrangian and Feynman Rules

Top-stop-gluino Feynman rules: The top-stop-gluino Lagrangian emerges from a supersymmetrization of the $SU(3)$ gauge interactions, see Eq. (1.2.17)

$$\mathcal{L}_{g_s}^{t\tilde{t}\tilde{g}} = -\sqrt{2}g_s\left(\overline{t'}^i_L\tilde{g}^A T^A_{ij}\tilde{t'}^j_L - \overline{t'}^i_R\tilde{g}^A T^A_{ij}\tilde{t'}^j_R\right) + h.c.. \tag{C.3.1}$$

To extract the Feynman rules we first apply the rotations Eq. (C.1.6) to make the top and stop mass matrices real. Next we rotate the stop fields in the L, R basis using Eq. (1.3.5) in order to obtain physical mass eigenstate stop fields $\tilde{t}_{1,2}$. Moreover we write the chiral fermions in terms of spinors and projectors $t_{R,L} = P_{R,L}t$, where $P_L = \frac{1}{2}(1-\gamma_5)$ and $P_R = \frac{1}{2}(1+\gamma_5)$. The resulting Feynman rule for the Top-stop-gluino vertex is

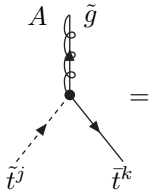

$$= -ig_s(P_R T^A_{kl} e^{\frac{i}{2}(\varphi-\tilde{\varphi})}c_\theta - P_L T^A_{kl} e^{-\frac{i}{2}(\varphi-\tilde{\varphi})}s_\theta). \tag{C.3.2}$$

Top-top-gluon Feynman rules: The top-top-gluon diagram can be calculated using ordinary QCD Feynman rules.

Four stop Feynman rules: The four stop vertex depending on the gauge coupling arises from the D-terms, see Eq. (1.2.19)

$$\mathcal{L}_{g_s}^{4\tilde{t}} = -\frac{g_s^2}{2}\left|(\tilde{t'}^i_L)^\star T^A_{ij}\tilde{t'}^j_L - (L\to R)\right|^2. \tag{C.3.3}$$

Note that the square sums over the gauge index A. The phase $\tilde{\varphi}$ drops out and we can rotate the stops in their mass eigenstate basis, using Eq. (1.3.5). Moreover we can evaluate the product of the two $SU(3)_C$ generators $T^A_{ij}T^A_{kl} = \frac{1}{2}(\delta_{il}\delta_{jk} - N_C^{-1}\delta_{ij}\delta_{kl})$. The Lagrangian can thus be written as

$$\mathcal{L}_{g_s}^{4\tilde{t}} = -\frac{g_s^2}{2}(\delta_{il}\delta_{jk} - N_C^{-1}\delta_{ij}\delta_{kl})P_{\alpha\beta}P_{\gamma\delta}(\tilde{t}^i_\alpha)^\star\tilde{t}^j_\beta(\tilde{t}^k_\gamma)^\star\tilde{t}^l_\delta, \tag{C.3.4}$$

where

$$P_{\alpha\beta} = \begin{pmatrix} c_{2\theta} & -s_{2\theta} \\ -s_{2\theta} & -c_{2\theta}\end{pmatrix}. \tag{C.3.5}$$

The four stop vertex depending on the strong gauge coupling is therefore

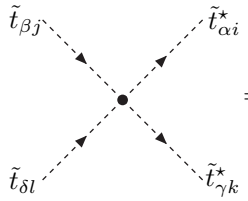

$$= -i\frac{g_s^2}{2}\left[(\delta_{il}\delta_{jk} - N_C^{-1}\delta_{ij}\delta_{kl})P_{\alpha\beta}P_{\gamma\delta} + (\delta_{ij}\delta_{kl} - N_C^{-1}\delta_{il}\delta_{jk})P_{\alpha\delta}P_{\gamma\beta}\right]. \tag{C.3.6}$$

Stop-stop-gluon Feynman rules: The strong gauge vertex for the stops comes from the kinetic Lagrangian for the stops with the covariant derivative inserted, see Eq. (1.2.17)

$$\mathcal{L}_{2\tilde{t}G} = g_s T^A_{ij} G^{A,\mu} R^T_{1,\beta} \tilde{t}^\star_{\beta i} k^{\beta j}_\mu R^T_{1\alpha} \tilde{t}_{\alpha j} + g_s k^{\mu\star}_{\beta j} T^A_{ij} G^A_\mu R^T_{1,\beta} \tilde{t}^\star_{\beta i} R^T_{1\alpha} \tilde{t}_{\alpha j} + (1 \leftrightarrow 2), \tag{C.3.7}$$

where Greek letters α, β, γ and δ denote mass eigenstates of the stops, i.e. $\alpha = 1, 2$. Capital roman letters are the gauge indices A. Small roman letters denote color and μ and ν are Lorentz indices. The two stop-gluon gauge vertex contributing to the $\mathcal{O}(\alpha_t \alpha_s)$ effective potential is

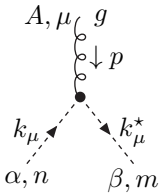

$$= -ig_s T^A_{mn} (k_\mu + k^\star_\mu)(R^T_{1\alpha} R^T_{1\beta} + R^T_{2\alpha} R^T_{2\alpha}). \tag{C.3.8}$$

C.3.2 Result for the $\mathcal{O}(\alpha_t \alpha_s)$ Effective Potential

Using the Feynman rules for the vertices given in the previous section, we can calculate the diagrams presented in Figure 2.2. We express the two-loop effective potential up to $\mathcal{O}(\alpha_t \alpha_s)$ as a function of five field-dependent quantities, see Eqs. (2.2.7 - 2.2.11):

$$\begin{aligned}\delta V^{\alpha_t \alpha_s}(\bar{m}_t^2, \bar{m}_{\tilde{t}_1}^2, \bar{m}_{\tilde{t}_2}^2, s_{2\bar{\theta}}^2, \bar{\xi}) = \frac{8 g_s^2}{(16\pi^2)^2} \Bigg[& J(\bar{m}_t^2, \bar{m}_t^2) - 2\bar{m}_t^2 I(\bar{m}_t^2, \bar{m}_t^2, 0) + \left\{ \frac{1}{4}\left(2 - s_{2\bar{\theta}}^2\right) J(\bar{m}_{\tilde{t}_1}^2, \bar{m}_{\tilde{t}_1}^2) \right. \\ & + \frac{s_{2\bar{\theta}}^2}{4} J(\bar{m}_{\tilde{t}_1}^2, \bar{m}_{\tilde{t}_2}^2) + \bar{m}_{\tilde{t}_1}^2 I(\bar{m}_{\tilde{t}_1}^2, \bar{m}_{\tilde{t}_1}^2, 0) + L(\bar{m}_{\tilde{t}_1}^2, m_{\tilde{g}}^2, \bar{m}_t^2) \\ & \left. - 2 m_{\tilde{g}} \bar{\xi} I(\bar{m}_{\tilde{t}_1}^2, \bar{m}_t^2, m_{\tilde{g}}^2) + \left[\bar{m}_{\tilde{t}_1}^2 \leftrightarrow \bar{m}_{\tilde{t}_2}^2, \bar{\xi} \to -\bar{\xi} \right] \right\} \Bigg]. \end{aligned} \tag{C.3.9}$$

C.4 Calculating the Effective Potential up to $\mathcal{O}(\alpha_t^2)$

C.4.1 Lagrangian and Feynman Rules

We will first derive the Feynman rules relevant for the calculation of the effective potential up to $\mathcal{O}(\alpha_t^2)$. The only part in the MSSM Lagrangian where Yukawa couplings show up is the superpotential, see Eq. (1.3.1). As we outlined in section 2.2.1 we work in the limit where all quarks except for the top are massless $h_{q \neq t} = 0$. The corresponding superpotential is

$$W_{h_t}^{\text{MSSM}} = \mu(H_1^0 H_2^0 - H_2^+ H_1^-) - h_t \left[H_2^+ \tilde{b}_L^i \tilde{t}_R^{\star j} \delta_{ij} - H_2^0 \tilde{t}_L^i \tilde{t}_R^{\star j} \delta_{ij} \right], \tag{C.4.1}$$

where $i, j = 1, 2, 3$ denote color indices. The Lagrangian can be derived from the superpotential in the following way

$$\mathcal{L}_W = -\sum_i \left| \frac{\partial W}{\partial \phi_i} \right|^2 - \frac{1}{2} \left[\sum_{ij} \overline{\Psi_{iL}^c} \frac{\partial^2 W}{\partial \phi_i \partial \phi_j} \Psi_{jL} + h.c. \right]. \tag{C.4.2}$$

The sum over ϕ_i, ϕ_j here means that we sum over all scalar fields. The fields Ψ are fermions in the chiral basis and c means charge conjugated. The last term in the square brackets $+h.c.$ means that we add the

hermitian conjugate. Note that the $i \leftrightarrow j$ symmetry cancels the $\frac{1}{2}$ factor. The Lagrangian resulting from the superpotential in Eq. (C.4.1) is

$$\begin{aligned}\mathcal{L}_{h_t}^W = &- \left|\mu H_1^0 + h_t \tilde{t'}_L^i \tilde{t'}_R^{\star j} \delta_{ij}\right|^2 - \left|\mu H_1^- - h_t \tilde{b}_L^i \tilde{t'}_R^{\star j} \delta_{ij}\right|^2 \\ &- \left|-h_t H_2^+ \tilde{t'}_R^{\star k}\right|^2 - \left|-h_t \left(H_2^+ \tilde{b}_L^k - H_2^0 \tilde{t'}_L^k\right)\right|^2 - \left|h_t \tilde{t'}_R^{\star k} H_2^0\right|^2 \\ &- h_t \left\{\overline{t_L^{c\prime}} \tilde{t'}_R^{\star} H_2^0 + \overline{t_R^{c\prime}} \tilde{t'}_L \tilde{H}_2^0 + \overline{t_R^{c\prime}} H_2^0 t'_L - \overline{b_L^c} \tilde{t'}_R^{\star} \tilde{H}_2^+ - \overline{t_R^{c\prime}} b_L H_2^+ - \overline{t_R^{c\prime}} \tilde{H}_2^+ \tilde{b}_L + h.c.\right\}, \end{aligned} \tag{C.4.3}$$

where we omitted the color indices in the fermionic part. Moreover there are terms proportional to the top-Yukawa coupling h_t in the soft SUSY breaking Lagrangian

$$\mathcal{L}_{h_t}^{\text{soft}} = -h_t A_t \tilde{t'}_R^{\star i} \delta_{ij} \left(\tilde{t'}_L^j H_2^0 - \tilde{b}_L^j H_2^+\right) + h.c. \tag{C.4.4}$$

The complete Lagrangian proportional to the top-Yukawa coupling is the sum of the contribution from the superpotential plus the contribution arising from soft SUSY breaking

$$\mathcal{L}_{h_t} = \mathcal{L}_{h_t}^{\text{soft}} + \mathcal{L}_{h_t}^W. \tag{C.4.5}$$

To calculate the Feynman diagrams for the $\mathcal{O}(\alpha_t^2)$ effective potential, we have to express the Lagrangian in terms of physical fields[2]. First we apply the rotations in Eq. (C.1.6) to make the top and stop mass matrices real. Next we rotate the stop fields in the L, R basis using Eq. (1.3.5) in order to obtain physical mass eigenstate stop fields $\tilde{t}_{1,2}$.
In the two-loop $\mathcal{O}(\alpha_t^2)$ Lagrangian, the VEV also shows up in the Higgs fields. In order to make the potential a field-dependent quantity the real VEV is substituted by complex Higgs fields. Expressing the Higgs fields in the Lagrangian as follows for the calculation of the potential implements the field-dependence in the correct way

$$H_2^0 = \frac{1}{\sqrt{2}} \left(\sqrt{2} \frac{m_t}{h_t} e^{i\varphi} + S_2 + i P_2\right), \tag{C.4.6}$$

$$H_1^0 = \frac{1}{\sqrt{2}} \left(\sqrt{2} \frac{m_t}{h_t} e^{i\varphi} \cot\beta + S_1 + i P_1\right). \tag{C.4.7}$$

As we argued in section 2.2.1, all fields and mixing angles entering at the two-loop $\mathcal{O}(\alpha_t^2)$ are understood as tree-level fields with $g = g' = 0$. This also implies that the light scalar Higgs boson is massless, see Eq. (1.4.17). Moreover the remaining Higgs states (H,A and $H^\pm$) have degenerate mass m_A, see Eqs. (1.4.15, 1.4.17, 1.4.21). The CP-even mixing angle is also modified $\alpha \to \beta - \frac{\pi}{2}$. To write the Lagrangian in terms of Higgs mass eigenstates, we apply the first rotation of Eq. (1.4.28) to the CP-odd Higgs bosons. For the charged and CP-even Higgs bosons we use

$$\begin{pmatrix} H_1^+ \\ H_2^+ \end{pmatrix} = \begin{pmatrix} s_\beta & c_\beta \\ c_\beta & -s_\beta \end{pmatrix} \begin{pmatrix} H^+ \\ G^+ \end{pmatrix}, \qquad \begin{pmatrix} S_1 \\ S_2 \end{pmatrix} = \begin{pmatrix} c_\beta & s_\beta \\ s_\beta & -c_\beta \end{pmatrix} \begin{pmatrix} h \\ H \end{pmatrix}. \tag{C.4.8}$$

Since we are working with massless bottom quarks, i.e. $h_b = 0$, the off-diagonal terms in the sbottom mass matrix are zero. Therefore the left sbottom state $\tilde{b}_L$ is already a mass eigenstate and its mass is equal to the soft SUSY breaking mass-term $m_{\tilde{b}_L}^2 = m_Q^2$. Also the masses of the Higgsinos simplify considerably in the limit $g = g' = 0$. Since the off-diagonal terms in the Higgsino mass matrices are proportional to m_Z all Higgsinos have degenerate mass $|\mu|$.

[2]Physical fields correspond to the mass eigenstates which are the poles of the propagators in the Feynman rules.

We start by writing down the Lagrangians for the different vertices. First the stop-stop-Higgs Lagrangian is

$$\begin{aligned}\mathcal{L}_{\tilde{t}\tilde{t}H} = \frac{h_t}{\sqrt{2}}\Big\{&\Big[s_\beta\left(2m_t c_\varphi + s_{2\theta}X_t c_{\tilde{\varphi}}\right)h\tilde{t}_1^\star\tilde{t}_1 - c_\beta\left(2m_t c_\varphi + s_{2\theta}Y_t c_{\tilde{\varphi}}\right)H\tilde{t}_1^\star\tilde{t}_1 \\ &+ s_\beta\left(2m_t s_\varphi + s_{2\theta}X_t s_{\tilde{\varphi}}\right)G\tilde{t}_1^\star\tilde{t}_1 + c_\beta\left(2m_t s_\varphi + s_{2\theta}Y_t s_{\tilde{\varphi}}\right)A\tilde{t}_1^\star\tilde{t}_1 + (\tilde{t}_1 \leftrightarrow \tilde{t}_2, \quad s_{2\theta} \leftrightarrow -s_{2\theta})\Big] \\ &+ \Big[s_\beta X_t(c_\theta^2 e^{-i\tilde{\varphi}} - s_\theta^2 e^{i\tilde{\varphi}})h\tilde{t}_1\tilde{t}_2^\star - c_\beta Y_t(c_\theta^2 e^{-i\tilde{\varphi}} - s_\theta^2 e^{i\tilde{\varphi}})H\tilde{t}_1\tilde{t}_2^\star \\ &+ is_\beta X_t(c_\theta^2 e^{-i\tilde{\varphi}} + s_\theta^2 e^{i\tilde{\varphi}})G\tilde{t}_1\tilde{t}_2^\star + ic_\beta Y_t(c_\theta^2 e^{-i\tilde{\varphi}} + s_\theta^2 e^{i\tilde{\varphi}})A\tilde{t}_1\tilde{t}_2^\star + h.c\Big]\Big\}. \end{aligned} \tag{C.4.9}$$

The sbottom-stop-charged Higgs Lagrangian is

$$\begin{aligned}\mathcal{L}_{\tilde{b}\tilde{t}H^\pm} = \frac{h_t}{\sqrt{2}}\Big\{&\sqrt{2}s_\beta e^{i\frac{\tilde{\varphi}}{2}}\left(m_t e^{i(\varphi-\tilde{\varphi})}c_\theta + X_t s_\theta\right)G^-\tilde{t}_1\tilde{b}_L^\star \\ &- \sqrt{2}c_\beta e^{i\frac{\tilde{\varphi}}{2}}\left(m_t e^{i(\varphi-\tilde{\varphi})}c_\theta + Y_t s_\theta\right)H^-\tilde{t}_1\tilde{b}_L^\star + h.c. + (\tilde{t}_1 \leftrightarrow \tilde{t}_2, \quad c_\theta \to -s_\theta, \quad s_\theta \to c_\theta)\Big\}. \end{aligned} \tag{C.4.10}$$

The two stop two neutral Higgs Lagrangian is

$$\mathcal{L}_{2\tilde{t}2H} = \frac{h_t^2}{2}\left(|\tilde{t}_1|^2 + |\tilde{t}_2|^2\right)\left[c_\beta^2 H^2 + s_\beta^2 h^2 + s_\beta^2 (G)^2 + c_\beta^2 A^2\right]. \tag{C.4.11}$$

The two sbottom two charged Higgs Lagrangian is

$$\mathcal{L}_{2\tilde{b}2H^\pm} = h_t^2\left|\tilde{b}_L\right|^2\left(s_\beta^2 G^+G^- + c_\beta^2 H^+H^- - s_\beta c_\beta(G^+H^- + h.c.)\right). \tag{C.4.12}$$

The two stop two charged Higgs Lagrangian is

$$\mathcal{L}_{2\tilde{t}2H^\pm} = h_t^2\left[s_\beta^2 G^+G^- + c_\beta^2 H^+H^- - s_\beta c_\beta(H^+G^- + h.c.)\right]\left[s_\theta^2|\tilde{t}_1|^2 + c_\theta^2|\tilde{t}_2|^2 + c_\theta s_\theta(\tilde{t}_1\tilde{t}_2^\star + h.c.)\right]. \tag{C.4.13}$$

In the above Lagrangians we suppressed the color structure. They are all color diagonal, which means that all diagrams involving these vertices have a factor δ_{ii}, summed over from 1 to 3. The following Lagrangians have a more complex color structure. The Lagrangian which is relevant for two-loop "eight" diagrams with only stops is

$$\begin{aligned}\mathcal{L}_{4\tilde{t}} = -h_t^2\Big\{&(\tilde{t}_1^i\tilde{t}_1^{\star j}\delta_{ij})^2 s_\theta^2 c_\theta^2 + (\tilde{t}_2^i\tilde{t}_2^{\star j}\delta_{ij})^2 s_\theta^2 c_\theta^2 \\ &- 2c_\theta^2 s_\theta^2(\tilde{t}_1^i\tilde{t}_1^{\star j})(\tilde{t}_2^k\tilde{t}_2^{\star l})\delta_{ij}\delta_{lk} + (c_\theta^4 + s_\theta^4)(\tilde{t}_1^i\tilde{t}_1^{\star l})(\tilde{t}_2^k\tilde{t}_2^{\star j})\delta_{ij}\delta_{lk}\Big\}. \end{aligned} \tag{C.4.14}$$

Another Lagrangian that involves four colored particles is

$$\mathcal{L}_{2\tilde{t}2\tilde{b}} = -h_t^2\left[\tilde{b}_L^i(s_\theta\tilde{t}_1^{\star j} + c_\theta\tilde{t}_2^{\star j})\delta_{ij}\right]\left[\tilde{b}_L^{\star l}(s_\theta\tilde{t}_1^k + c_\theta\tilde{t}_2^k)\delta_{lk}\right]. \tag{C.4.15}$$

Last but not least there are the Yukawa terms, where the charge conjugation matrix $\mathcal{C} = i\gamma^2\gamma^0$ shows up. The corresponding Feynman rules have been presented in [30] but without the phases φ, $\tilde{\varphi}$. Including these phases, the Feynman rules for the $\tilde{H}^0 t\tilde{t}_j$ couplings can be written as $-i(aP_L + bP_R)$ and those of $\tilde{H}^+ t\tilde{b}_L$ as $i\mathcal{C}^{-1}(aP_L + bP_R)$, with

$$-ia_{\tilde{H}_2^0 t\tilde{t}_1} = ib_{\tilde{H}_2^0 t\tilde{t}_2} = \frac{h_t}{\sqrt{2}}c_\theta e^{-\frac{i}{2}(\varphi+\tilde{\varphi})}, \qquad ia_{\tilde{H}_2^0 t\tilde{t}_2} = ib_{\tilde{H}_2^0 t\tilde{t}_1} = \frac{h_t}{\sqrt{2}}s_\theta e^{-\frac{i}{2}(\varphi+\tilde{\varphi})}, \tag{C.4.16}$$

$$a_{\tilde{H}^+ t\tilde{b}_L} = -h_t e^{-\frac{i}{2}\varphi}, \qquad a_{\tilde{H}^+ b\tilde{t}_1} = -h_t s_\theta e^{-\frac{i}{2}\tilde{\varphi}}, \qquad a_{\tilde{H}^+ b\tilde{t}_2} = -h_t c_\theta e^{-\frac{i}{2}\tilde{\varphi}}. \tag{C.4.17}$$

The rest of the Yukawa Lagrangian does not involve Higgsino fields and reads

$$\mathcal{L}_{\text{Yukawa}} = \overline{t_L} t_R (S_2 + iP_2)\frac{1}{\sqrt{2}} e^{i\varphi} - \overline{t_R} b_L (s_\beta G^+ + c_\beta H^+) e^{-i\frac{\varphi}{2}}. \tag{C.4.18}$$

C.4.2 Result for the $\mathcal{O}(\alpha_t^2)$ Effective Potential

Feynman rules for the vertices in h_t can be obtained by taking the functional derivative of the above Lagrangians w.r.t. the corresponding fields. These Feynman rules can be used to calculate the diagrams in Figure 2.3. We express the two-loop effective potential up to $\mathcal{O}(\alpha_t^2)$ in the following way

$$\begin{aligned}
\delta V^{\alpha_t^2} = \frac{h_t^2 N_C}{(16\pi^2)^2}\Bigg(& s_\beta^2 \left[J(\bar{m}_t^2, \bar{m}_t^2) + 2\bar{m}_t^2 I(\bar{m}_t^2, \bar{m}_t^2, 0) + \bar{m}_t^2 I(\bar{m}_t^2, 0, 0) \right] \\
& + c_\beta^2 \left[L(m_A^2, \bar{m}_t^2, \bar{m}_t^2) + L(m_A^2, \bar{m}_t^2, 0) \right] + L(m_{\tilde{b}_L}^2, \bar{m}_t^2, \mu^2) + c_\beta^2 J(m_A^2, m_{\tilde{b}_L}^2) \\
& + \Bigg\{ c_\beta^2 (1 + s_{\bar{\theta}}^2) J(m_A^2, \bar{m}_{\tilde{t}_1}^2) + s_{\bar{\theta}}^2 J(m_{\tilde{b}_L}^2, \bar{m}_{\tilde{t}_1}^2) + L(\bar{m}_{\tilde{t}_1}^2, \mu^2, \bar{m}_t^2) + s_{\bar{\theta}}^2 L(\bar{m}_{\tilde{t}_1}^2, \mu, 0) \\
& + \frac{N_C + 1}{4} s_{2\bar{\theta}}^2 J(\bar{m}_{\tilde{t}_1}^2, \bar{m}_{\tilde{t}_1}^2) + \frac{1}{4}\left(2c_{2\bar{\theta}}^2 - (N_C - 1) s_{2\bar{\theta}}^2 \right) J(\bar{m}_{\tilde{t}_1}^2, \bar{m}_{\tilde{t}_2}^2) \\
& - \frac{s_\beta^2}{4}\left(4\bar{m}_t^2 + s_{2\bar{\theta}}^2 X_t^2 + 4X_t \bar{\xi} \right) I(0, \bar{m}_{\tilde{t}_1}^2, \bar{m}_{\tilde{t}_1}^2) \\
& - \frac{c_\beta^2}{4}\left(4\bar{m}_t^2 + s_{2\bar{\theta}}^2 Y_t^2 + 4Y_t \bar{\xi} \right) I(m_A^2, \bar{m}_{\tilde{t}_1}^2, \bar{m}_{\tilde{t}_1}^2) \\
& - \frac{s_\beta^2}{4} X_t^2 (1 + c_{2\bar{\theta}}^2) I(0, \bar{m}_{\tilde{t}_1}^2, \bar{m}_{\tilde{t}_2}^2) - \frac{c_\beta^2}{4} Y_t^2 (1 + c_{2\bar{\theta}}^2) I(m_A^2, \bar{m}_{\tilde{t}_1}^2, \bar{m}_{\tilde{t}_2}^2) \\
& - s_\beta^2 (\bar{m}_t^2 c_{\bar{\theta}}^2 + X_t^2 s_{\bar{\theta}}^2 + X_t \bar{\xi}) I(0, m_{\tilde{b}_L}^2, \bar{m}_{\tilde{t}_1}^2) - c_\beta^2 (\bar{m}_t^2 c_{\bar{\theta}}^2 + Y_t^2 s_{\bar{\theta}}^2 + Y_t \bar{\xi}) I(m_A^2, m_{\tilde{b}_L}^2, \bar{m}_{\tilde{t}_1}^2) \\
& + \left[\bar{m}_{\tilde{t}_1}^2 \leftrightarrow \bar{m}_{\tilde{t}_2}^2, c_{\bar{\theta}} \to -s_{\bar{\theta}}, s_{\bar{\theta}} \to c_{\bar{\theta}} \right] \Bigg\} \Bigg).
\end{aligned} \tag{C.4.19}$$

Note that the substitution in the last line also implies $\bar{\xi} \to -\bar{\xi}$. Moreover $s_{\bar{\theta}}^2$ and $c_{\bar{\theta}}^2$ are field-dependent quantities, which can expressed as $s_{\bar{\theta}}^2 = \frac{1}{2}(1 - c_{2\bar{\theta}})$ and $c_{\bar{\theta}}^2 = \frac{1}{2}(1 + c_{2\bar{\theta}})$. Using Eq. (C.1.9) we can make the following substitutions in the effective potential

$$c_{\bar{\theta}}^2 \to \frac{1}{2}\left(1 + \frac{m_Q^2 - m_U^2}{\bar{m}_{\tilde{t}_1}^2 - \bar{m}_{\tilde{t}_2}^2} \right), \qquad s_{\bar{\theta}}^2 \to \frac{1}{2}\left(1 - \frac{m_Q^2 - m_U^2}{\bar{m}_{\tilde{t}_1}^2 - \bar{m}_{\tilde{t}_2}^2} \right). \tag{C.4.20}$$

In this way we obtain the effective potential up to $\mathcal{O}(\alpha_t^2)$ as a function of five field-dependent quantities $\bar{x}_i = (\bar{m}_t^2, \bar{m}_{\tilde{t}_1}^2, \bar{m}_{\tilde{t}_2}^2, s_{2\bar{\theta}}^2, \bar{\xi})$, $i = 1, \cdots, 5$.
Note that $m_Q^2 - m_U^2 = \cos 2\theta_{\tilde{t}} (m_{\tilde{t}_1}^2 - m_{\tilde{t}_2}^2)$ does not depend on the Higgs fields. We use this identity to get expressions that do not depend on the SUSY breaking parameters m_U^2 and m_Q^2, but only on the stop masses $m_{\tilde{t}_{1,2}}$ and the stop mixing angle $\theta_{\tilde{t}}$.

Appendix D

Renormalization and Counter Terms

D.1 Renormalization of the Stop Masses and Mixing Angle

The tree-level bilinear stop Lagrangian[1] $\mathcal{L}^0_{m_{\tilde{t}}}$ in the chiral basis is diagonalized by the tree-level mixing matrix, see section 1.3.1

$$R^0 \equiv R(\theta_0), \qquad R(\theta) = \begin{pmatrix} c_\theta & s_\theta \\ -s_\theta & c_\theta \end{pmatrix}. \tag{D.1.1}$$

We calculated the $\mathcal{O}(\alpha)$ self-energy matrix $\Pi^{\tilde{t}}_{ij}$ in the mass eigenstate basis

$$\mathcal{L}^{\mathcal{O}(\alpha)}_{m_{\tilde{t}}} = \left(\tilde{t}^0\right)^\star_i \Pi^{\tilde{t}}_{ij} \left(\tilde{t}^0\right)_j. \tag{D.1.2}$$

Note that this is calculated using the bare tree-level Lagrangian and is therefore given in terms of bare fields and bare mixing angles. The one-loop-corrected Lagrangian in the chiral basis is

$$\mathcal{L}^{\mathcal{O}(\alpha)}_{m_{\tilde{t}}} = \left(\tilde{t}^0_{LR}\right)^\star_k \left[(M_{\tilde{q}_{L,R}})_{kl} + R^0_{ki}\Pi^{\tilde{t}}_{ij}(R^0_{jl})^\dagger\right] \left(\tilde{t}^0_{LR}\right)_l \qquad \left(\tilde{t}^0_{LR}\right)_l \equiv \begin{pmatrix} \tilde{t}^0_L \\ \tilde{t}^0_R \end{pmatrix}, \tag{D.1.3}$$

To find the renormalized, loop-corrected masses and mixing angles, the terms in the square brackets have to be diagonalized by a loop-corrected matrix $R^{\mathcal{O}(\alpha)} \equiv R(\theta^{\mathcal{O}(\alpha)})$ with $\theta^{\mathcal{O}(\alpha)} = \theta_0 - \delta\theta$, where $\delta\theta$ is of order α. When we expand $R^{\mathcal{O}(\alpha)}$ around the tree-level mixing angle θ_0 in α we obtain

$$R^{\mathcal{O}(\alpha)} = R(\theta^{\mathcal{O}(\alpha)}) = R(\theta_0) - \left.\frac{\partial R(\theta)}{\partial\theta}\right|_{\theta=\theta_0} \delta\theta. \tag{D.1.4}$$

The diagonalization condition requires the off-diagonal elements of the following matrix to vanish, such that the diagonal entries are the renormalized stop masses

$$(R^{\mathcal{O}(\alpha)}_{mk})^\dagger \left[(M_{\tilde{q}_{L,R}})_{kl} + R^0_{ki}\Pi^{\tilde{t}}_{ij}(R^0_{jl})^\dagger\right] R^{\mathcal{O}(\alpha)}_{ln} \equiv \delta_{mn}\left(m^R_{\tilde{t}_n}\right)^2. \tag{D.1.5}$$

The loop-corrected stop field in the mass eigenstate basis is $R^{\mathcal{O}(\alpha)}_{ij}\left(\tilde{t}^0_{LR}\right)_j = \tilde{t}^{\mathcal{O}(\alpha)}_i$. Expanding this matrix in α yields

$$\delta_{mn}\left(m^R_{\tilde{t}_n}\right)^2 = \begin{pmatrix} (m^0_{\tilde{t}_1})^2 & 0 \\ 0 & (m^0_{\tilde{t}_2})^2 \end{pmatrix} - \left[\begin{pmatrix} 0 & m^2_{\tilde{t}_1} - m^2_{\tilde{t}_2} \\ m^2_{\tilde{t}_1} - m^2_{\tilde{t}_2} & 0 \end{pmatrix}\delta\theta - \begin{pmatrix} \Pi^{\tilde{t}}_{11}(p^2) & \Pi^{\tilde{t}}_{12}(p^2) \\ \Pi^{\tilde{t}}_{12}(p^2) & \Pi^{\tilde{t}}_{22}(p^2) \end{pmatrix}\right]. \tag{D.1.6}$$

[1] Note that the parameters φ and $\tilde{\varphi}$ arise only at the two-loop level. We can therefore omit them in the renormalization of the one-loop stop sector.

From this equation we find the counter terms for the stop masses and the counter term for the stop mixing angle in terms of the stop self-energies

$$\left(m^R_{\tilde{t}_i}\right)^2 = \left(m^0_{\tilde{t}_i}\right)^2 + \Pi^{\tilde{t}}_{ii}(p^2), \qquad \delta\theta = -\frac{\Pi^{\tilde{t}}_{12}(p^2)}{m^2_{\tilde{t}_1} - m^2_{\tilde{t}_2}}. \tag{D.1.7}$$

The on-shell version of the stop mass counter terms can be defined straightforward by evaluating the self-energies at the mass itself. The stop mixing angle counter term in the on-shell scheme we will use[2] is anti-symmetric in $m^2_{\tilde{t}_1}$ and $m^2_{\tilde{t}_2}$ and is defined by

$$\delta^{\text{OS}}\theta \equiv -\frac{1}{2}\frac{\Pi^{\tilde{t}}_{12}(m_{\tilde{t}_1}) + \Pi^{\tilde{t}}_{12}(m_{\tilde{t}_2})}{m^2_{\tilde{t}_1} - m^2_{\tilde{t}_2}} \tag{D.1.8}$$

D.2 Self-Energies at $\mathcal{O}(\alpha_s)$

The counter terms defined in Eqs. (2.5.26, 2.5.27, 2.5.28, 2.5.30) are defined in terms of the self-energies at $\mathcal{O}(\alpha_s + \alpha_t)$. The self-energies at $\mathcal{O}(\alpha_s)$ can be calculated using the SQCD Feynman rules presented in appendix C.3.1. The self-energies are not treated as Higgs field-dependent quantities. We can therefore set the phases $\varphi = \tilde{\varphi} = 0$. Note that the transversal self-energy of the W's $\Pi^T_{WW}(0)$ receives no α_s corrections, the other self-energies are

$$\begin{aligned}
\Sigma^{\alpha_s}_t(m_t) = -\frac{g_s^2}{16\pi^2}C_F m_t\Big\{ & 2B_1(m_t^2, m_t^2, 0) - 4B_0(m_t^2, m_t^2, 0) + B_1(m_t^2, m_{\tilde{g}}^2, m^2_{\tilde{t}_1}) + B_1(m_t^2, m_{\tilde{g}}^2, m^2_{\tilde{t}_2}) \\
& - s^2_{2\theta}\frac{m_{\tilde{g}}}{m_t}B_0(m_t^2, m_{\tilde{g}}^2, m^2_{\tilde{t}_1}) + s^2_{2\theta}\frac{m_{\tilde{g}}}{m_t}B_0(m_t^2, m_{\tilde{g}}^2, m^2_{\tilde{t}_2})\Big\},
\end{aligned} \tag{D.2.1}$$

$$\begin{aligned}
\Pi^{\tilde{t},\alpha_s}_{11}(m^2_{\tilde{t}_1}) = -\frac{g_s^2}{16\pi^2}C_F\Big\{ & -4m^2_{\tilde{t}_1}B_1(m^2_{\tilde{t}_1}, m^2_{\tilde{t}_1}, 0) - s^2_{2\theta}(A_0(m^2_{\tilde{t}_1}) - A_0(m^2_{\tilde{t}_2})) + 2G(m^2_{\tilde{t}_1}, m_t^2, m_{\tilde{g}}^2) \\
& + 4s^2_{2\theta}m_t m_{\tilde{g}}B_0(m^2_{\tilde{t}_1}, m_t^2, m_{\tilde{g}}^2)\Big\},
\end{aligned} \tag{D.2.2}$$

$$\begin{aligned}
\Pi^{\tilde{t},\alpha_s}_{22}(m^2_{\tilde{t}_2}) = -\frac{g_s^2}{16\pi^2}C_F\Big\{ & -4m^2_{\tilde{t}_2}B_1(m^2_{\tilde{t}_2}, m^2_{\tilde{t}_2}, 0) - s^2_{2\theta}(A_0(m^2_{\tilde{t}_2}) - A_0(m^2_{\tilde{t}_1})) + 2G(m^2_{\tilde{t}_2}, m_t^2, m_{\tilde{g}}^2) \\
& - 4s^2_{2\theta}m_t m_{\tilde{g}}B_0(m^2_{\tilde{t}_2}, m_t^2, m_{\tilde{g}}^2)\Big\},
\end{aligned} \tag{D.2.3}$$

$$\Pi^{\tilde{t},\alpha_s}_{12}(p^2) = -\frac{g_s^2}{16\pi^2}C_F\Big\{4m_t m_{\tilde{g}}c_{2\theta}B_0(p^2, m_t^2, m_{\tilde{g}}^2) - s^2_{2\theta}c_{2\theta}(A_0(m^2_{\tilde{t}_1}) - A_0(m^2_{\tilde{t}_2}))\Big\}. \tag{D.2.4}$$

[2] In our calculation only this version of the OS stop mixing counter term produces the right divergences [31]. A discussion about the definition of the stop mixing angle counter term can be found in [70].

D.3 Self-Energies at $\mathcal{O}(\alpha_t)$

The self-energies at $\mathcal{O}(\alpha_t)$ can be calculated using the Feynman rules presented in appendix C.4.1 with $\varphi = \tilde{\varphi} = 0$. They read

$$\begin{aligned}
\Sigma_t^{\alpha_t}(m_t) = -\frac{h_t^2}{32\pi^2} m_t \Big\{ & s_\beta^2 \left[2B_1(m_t^2, m_t^2, 0) + B_1(m_t^2, 0, 0)\right] + c_\beta^2 \left[2B_1(m_t^2, m_t^2, m_A^2) + B_1(m_t^2, 0, m_A^2)\right] \\
& + B_1(m_t^2, \mu^2, m_{\tilde{t}_1}^2) + B_1(m_t^2, \mu^2, m_{\tilde{t}_2}^2) + B_1(m_t^2, \mu^2, m_{\tilde{b}_L}^2) \Big\},
\end{aligned} \tag{D.3.1}$$

$$\begin{aligned}
\Pi_{11}^{\tilde{t},\alpha_t}(m_{\tilde{t}_1}^2) = -\frac{h_t^2}{16\pi^2} \Big\{ & G(m_{\tilde{t}_1}^2, m_t^2, \mu^2) + s_\theta^2 G(m_{\tilde{t}_1}^2, 0, \mu^2) + c_\beta^2(1+s_\theta^2) A_0(m_A^2) + s_\theta^2 A_0(m_{\tilde{b}_L}^2) \\
& + \left(c_{2\theta}^2 - \frac{N_C - 1}{2} s_{2\theta}^2\right) A_0(m_{\tilde{t}_2}^2) + \frac{N_C + 1}{2} s_{2\theta}^2 A_0(m_{\tilde{t}_1}^2) \\
& + \frac{1}{2}\Big[s_\beta^2 (2m_t + s_{2\theta} X_t)^2 B_0(m_{\tilde{t}_1}^2, m_{\tilde{t}_1}^2, 0) + c_\beta^2 (2m_t + s_{2\theta} Y_t)^2 B_0(m_{\tilde{t}_1}^2, m_{\tilde{t}_1}^2, m_A^2) \\
& \quad + s_\beta^2 (1 + c_{2\theta}^2) X_t^2 B_0(m_{\tilde{t}_1}^2, m_{\tilde{t}_2}^2, 0) + c_\beta^2 (1 + c_{2\theta}^2) Y_t^2 B_0(m_{\tilde{t}_1}^2, m_{\tilde{t}_2}^2, m_A^2) \Big] \\
& + s_\beta^2 (m_t c_\theta + X_t s_\theta)^2 B_0(m_{\tilde{t}_1}^2, m_{\tilde{b}_L}^2, 0) + c_\beta^2 (m_t c_\theta + Y_t s_\theta)^2 B_0(m_{\tilde{t}_1}^2, m_{\tilde{b}_L}^2, m_A^2) \Big\},
\end{aligned} \tag{D.3.2}$$

$$\begin{aligned}
\Pi_{22}^{\tilde{t},\alpha_t}(m_{\tilde{t}_2}^2) = -\frac{h_t^2}{16\pi^2} \Big\{ & G(m_{\tilde{t}_2}^2, m_t^2, \mu^2) + c_\theta^2 G(m_{\tilde{t}_2}^2, 0, \mu^2) + c_b^2 (1 + c_\theta^2) A_0(m_A^2) + c_\theta^2 A_0(m_{\tilde{b}_L}^2) \\
& + \left(c_{2\theta}^2 - \frac{N_C - 1}{2} s_{2\theta}^2\right) A_0(m_{\tilde{t}_1}^2) + \frac{N_C + 1}{2} s_{2\theta}^2 A_0(m_{\tilde{t}_2}^2) \\
& + \frac{1}{2}\Big[s_\beta^2 (2m_t - s_{2\theta} X_t)^2 B_0(m_{\tilde{t}_2}^2, m_{\tilde{t}_2}^2, 0) + c_\beta^2 (2m_t - s_{2\theta} Y_t)^2 B_0(m_{\tilde{t}_2}^2, m_{\tilde{t}_2}^2, m_A^2) \\
& \quad + s_\beta^2 (1 + c_{2\theta}^2) X_t^2 B_0(m_{\tilde{t}_2}^2, m_{\tilde{t}_1}^2, 0) + c_\beta^2 (1 + c_{2\theta}^2) Y_t^2 B_0(m_{\tilde{t}_2}^2, m_{\tilde{t}_1}^2, m_A^2) \Big] \\
& - s_\beta^2 (m_t s_\theta - X_t c_\theta)^2 B_0(m_{\tilde{t}_2}^2, m_{\tilde{b}_L}^2, 0) - c_\beta^2 (m_t s_\theta - Y_t c_\theta)^2 B_0(m_{\tilde{t}_2}^2, m_{\tilde{b}_L}^2, m_A^2) \Big\},
\end{aligned} \tag{D.3.3}$$

$$\begin{aligned}
\Pi_{12}^{\tilde{t},\alpha_t}(p^2) = -\frac{h_t^2}{32\pi^2} \Big\{ & s_{2\theta} G(p^2, 0, \mu^2) + s_{2\theta} c_\beta^2 A_0(m_A^2) + s_{2\theta} A_0(m_{\tilde{b}_L}^2) + 4 c_{2\theta} s_{2\theta} (A_0(m_{\tilde{t}_1}^2) - A_0(m_{\tilde{t}_2}^2)) \\
& + s_\beta^2 c_{2\theta} X_t (2m_t + s_{2\theta} X_t) B_0(p^2, m_{\tilde{t}_1}^2, 0) + c_\beta^2 c_{2\theta} Y_t (2m_t + s_{2\theta} Y_t) B_0(p^2, m_{\tilde{t}_1}^2, m_A^2) \\
& + s_\beta^2 c_{2\theta} X_t (2m_t - s_{2\theta} X_t) B_0(p^2, m_{\tilde{t}_2}^2, 0) + c_\beta^2 c_{2\theta} Y_t (2m_t - s_{2\theta} Y_t) B_0(p^2, m_{\tilde{t}_2}^2, m_A^2) \\
& - 2 s_\beta^2 (m_t c_\theta + X_t s_\theta)(m_t s_\theta - X_t c_\theta) B_0(p^2, m_{\tilde{b}_L}^2, 0) \\
& - 2 c_\beta^2 (m_t c_\theta + Y_t s_\theta)(m_t s_\theta - Y_t c_\theta) B_0(p^2, m_{\tilde{b}_L}^2, m_A^2) \Big\},
\end{aligned} \tag{D.3.4}$$

$$\begin{aligned}
\Pi_{WW}^{T,\alpha_t}(0) = -\frac{3 m_W^2}{8\pi^2 v^2} \Big\{ & m_t^2 \left(-\frac{1}{\epsilon} - \frac{1}{2} + \log\left(\frac{m_t^2}{Q^2}\right)\right) - c_\theta^2 \left(\frac{m_{\tilde{t}_1}^2 + m_{\tilde{b}_L}^2}{2} - \frac{m_{\tilde{t}_1}^2 m_{\tilde{b}_L}^2}{m_{\tilde{t}_1}^2 - m_{\tilde{b}_L}^2} \log\left(\frac{m_{\tilde{t}_1}^2}{m_{\tilde{b}_L}^2}\right)\right) \\
& - s_\theta^2 \left(\frac{m_{\tilde{t}_2}^2 + m_{\tilde{b}_L}^2}{2} - \frac{m_{\tilde{t}_2}^2 m_{\tilde{b}_L}^2}{m_{\tilde{t}_2}^2 - m_{\tilde{b}_L}^2} \log\left(\frac{m_{\tilde{t}_2}^2}{m_{\tilde{b}_L}^2}\right)\right) \Big\}.
\end{aligned} \tag{D.3.5}$$

D.4 Wave Function Renormalization Counter Terms

The WFR counter terms are defined by taking the derivative of the neutral Higgs self-energies w.r.t. the external momentum, evaluated at zero external momentum, see Eq. (2.5.12). The self-energies of the Higgs fields P_i and S_i receive no corrections at $\mathcal{O}(\alpha_s)$. The Lagrangian relevant for the external self-energies at $\mathcal{O}(\alpha_t)$ are the terms in Eq. (C.4.5) involving only the neutral Higgs fields P_i and S_i. They read

$$\mathcal{L}_{S_1 2\tilde{t}} = S_1 \left(\frac{-h_t\mu}{\sqrt{2}}\right)\left[s_{2\theta}(|\tilde{t}_1|^2 - |\tilde{t}_2|^2) + c_{2\theta}(\tilde{t}_1\tilde{t}_2^\star + h.c.)\right], \tag{D.4.1}$$

$$\mathcal{L}_{P_1 2\tilde{t}} = P_1 \left(\frac{h_t\mu}{\sqrt{2}}\right)\left[i\tilde{t}_1\tilde{t}_2^\star + h.c.\right], \tag{D.4.2}$$

$$\mathcal{L}_{S_2 2\tilde{t}} = S_1 \left\{\left(\frac{-h_t A_t}{\sqrt{2}}\right)\left[s_{2\theta}(|\tilde{t}_1|^2 - |\tilde{t}_2|^2) + c_{2\theta}(\tilde{t}_1\tilde{t}_2^\star + h.c.)\right] - \frac{h_t}{\sqrt{2}}\bar{t}t - h_t^2 v_2(|\tilde{t}_1|^2 + |\tilde{t}_2|^2)\right\}, \tag{D.4.3}$$

$$\mathcal{L}_{P_2 2\tilde{t}} = P_2 \left\{\left(\frac{-h_t A_t}{\sqrt{2}}\right)\left[i\tilde{t}_1\tilde{t}_2^\star + h.c.\right] + \frac{h_t}{\sqrt{2}} i\bar{t}\gamma_5 t\right\}, \tag{D.4.4}$$

$$\mathcal{L}_{2S_2 2\tilde{t}} = S_2^2 \left(\frac{-h_t^2}{2}\right)(|\tilde{t}_1|^2 + |\tilde{t}_2|^2), \tag{D.4.5}$$

$$\mathcal{L}_{2P_2 2\tilde{t}} = P_2^2 \left(\frac{-h_t^2}{2}\right)(|\tilde{t}_1|^2 + |\tilde{t}_2|^2), \tag{D.4.6}$$

where the color structure is trivial and was omitted. The Feynman rules extracted from the above Lagrangian are used to calculate the self-energies of the Higgs fields P_i and S_i, which can be expressed in terms of two-point functions B_0. The corresponding WFR counter terms are

$$\delta Z_1^P = \frac{N_C h_t^2}{16\pi^2}\mu^2 B_0'(0, m_{\tilde{t}_1}^2, m_{\tilde{t}_2}^2), \tag{D.4.7}$$

$$\delta Z_1^S = \frac{N_C h_t^2}{16\pi^2}\mu^2(-1)\left\{s_\theta^2 B_0'(0, m_{\tilde{t}_1}^2, m_{\tilde{t}_1}^2) + s_\theta^2 B_0'(0, m_{\tilde{t}_2}^2, m_{\tilde{t}_2}^2) + 2c_{2\theta}^2 B_0'(0, m_{\tilde{t}_1}^2, m_{\tilde{t}_2}^2)\right\}, \tag{D.4.8}$$

$$\delta Z_2^P = \frac{N_C h_t^2}{16\pi^2}(-1)\left\{A_t^2 B_0'(0, m_{\tilde{t}_1}^2, m_{\tilde{t}_2}^2) + B_0(0, m_t^2, m_t^2)\right\}, \tag{D.4.9}$$

$$\begin{aligned}\delta Z_2^S = \frac{N_C h_t^2}{16\pi^2}(-1)\Big\{ &\frac{A_t^2}{2} s_\theta^2 (B_0'(0, m_{\tilde{t}_1}^2, m_{\tilde{t}_1}^2) + B_0'(0, m_{\tilde{t}_2}^2, m_{\tilde{t}_2}^2)) + A_t^2 c_{2\theta}^2 B_0'(0, m_{\tilde{t}_1}^2, m_{\tilde{t}_2}^2) \\ &+ 2m_t^2\left(B_0'(0, m_{\tilde{t}_1}^2, m_{\tilde{t}_1}^2) + B_0'(0, m_{\tilde{t}_2}^2, m_{\tilde{t}_2}^2)\right) + B_0(0, m_{\tilde{t}_1}^2, m_{\tilde{t}_2}^2)\Big\}.\end{aligned} \tag{D.4.10}$$

D.5 $\overline{\text{DR}}$ Counter Terms at $\mathcal{O}(\alpha_s)$

The $\overline{\text{DR}}$ counter terms are simply the divergent parts of the OS counter terms defined in section 2.5.6 multiplied by $(1 + \epsilon \log Q^2/{\mu_R}^2)$. Note that in the $\overline{\text{DR}}$ counter terms we distinguish the renormalization

scale $\mu_R^{\alpha_s}$ at $\mathcal{O}(\alpha_s)$ from the renormalization scale $\mu_R^{\alpha_t}$ at $\mathcal{O}(\alpha_t)$

$$\delta^{\overline{\rm DR},\alpha_s} m_t^2 = -\frac{g_s^2}{4\pi^2} C_F m_t^2 \left[\frac{1}{\epsilon} + \log\left(\frac{Q^2}{{\mu_R^{\alpha_s}}^2}\right)\right], \tag{D.5.1}$$

$$\delta^{\overline{\rm DR},\alpha_s} m_{\tilde{t}_1}^2 = \frac{g_s^2}{16\pi^2} C_F \left[(m_{\tilde{t}_2}^2 - m_{\tilde{t}_1}^2)s_{2\theta}^2 - 4(m_{\tilde{g}}^2 + m_t^2 + m_{\tilde{g}} m_t \sin(2\theta))\right] \left[\frac{1}{\epsilon} + \log\left(\frac{Q^2}{{\mu_R^{\alpha_s}}^2}\right)\right], \tag{D.5.2}$$

$$\delta^{\overline{\rm DR},\alpha_s} m_{\tilde{t}_2}^2 = \frac{g_s^2}{16\pi^2} C_F \left[(m_{\tilde{t}_1}^2 - m_{\tilde{t}_2}^2)s_{2\theta}^2 - 4(m_{\tilde{g}}^2 + m_t^2 + m_{\tilde{g}} m_t \sin(2\theta))\right] \left[\frac{1}{\epsilon} + \log\left(\frac{Q^2}{{\mu_R^{\alpha_s}}^2}\right)\right], \tag{D.5.3}$$

$$\delta^{\overline{\rm DR},\alpha_s} s_{2\theta}^2 = \frac{g_s^2}{4\pi^2} C_F \cos^2(2\theta) \left[-s_{2\theta}^2 + \frac{4 m_{\tilde{g}} m_t \sin(2\theta)}{(m_{\tilde{t}_1}^2 - m_{\tilde{t}_2}^2)}\right] \left[\frac{1}{\epsilon} + \log\left(\frac{Q^2}{{\mu_R^{\alpha_s}}^2}\right)\right], \tag{D.5.4}$$

$$\delta^{\overline{\rm DR},\alpha_s} A_t = \frac{g_s^2}{4\pi^2} C_F m_{\tilde{g}} \left[\frac{1}{\epsilon} + \log\left(\frac{Q^2}{{\mu_R^{\alpha_s}}^2}\right)\right]. \tag{D.5.5}$$

D.6 $\overline{\rm DR}$ Counter Terms at $\mathcal{O}(\alpha_t)$

The $\overline{\rm DR}$ counter terms at $\mathcal{O}(\alpha_t)$ are simply the divergent parts of the OS counter terms at $\mathcal{O}(\alpha_t)$ defined in section 2.5.6 multiplied by $(1 + \epsilon \log Q^2/{\mu_R}^2)$

$$\delta^{\overline{\rm DR},\alpha_t} m_t^2 = \frac{3h_t^2}{16\pi^2} m_t^2 \left[\frac{1}{\epsilon} + \log\left(\frac{Q^2}{{\mu_R^{\alpha_t}}^2}\right)\right], \tag{D.6.1}$$

$$\begin{aligned}\delta^{\overline{\rm DR},\alpha_t} m_{\tilde{t}_1}^2 = \frac{h_t^2}{16\pi^2} \Bigg\{ &\left(1 + s_\theta^2 + \frac{N_C+1}{2} s_{2\theta}^2\right) m_{\tilde{t}_1}^2 + \left(c_{2\theta}^2 - \frac{N_C+1}{2} s_{2\theta}^2\right) m_{\tilde{t}_2}^2 - 2(1+s_\theta^2)\mu^2 + c_\theta^2 m_t^2 + s_\theta^2 m_{\tilde{b}_L}^2 \\ &+ c_\beta^2 (1+s_\theta^2) m_A^2 + 3 s_{2\theta} m_t A_t + (1+s_\theta^2)(s_\beta^2 X_t^2 + c_\beta^2 Y_t^2)\Bigg\} \left[\frac{1}{\epsilon} + \log\left(\frac{Q^2}{{\mu_R^{\alpha_t}}^2}\right)\right],\end{aligned} \tag{D.6.2}$$

$$\begin{aligned}\delta^{\overline{\rm DR},\alpha_t} m_{\tilde{t}_2}^2 = \frac{h_t^2}{16\pi^2} \Bigg\{ &\left(1 + c_\theta^2 + \frac{N_C+1}{2} s_{2\theta}^2\right) m_{\tilde{t}_2}^2 + \left(c_{2\theta}^2 - \frac{N_C-1}{2} s_{2\theta}^2\right) m_{\tilde{t}_1}^2 - 2(1+c_\theta^2)\mu^2 + s_\theta^2 m_t^2 + c_\theta^2 m_{\tilde{b}_L}^2 \\ &+ c_\beta^2 (1+c_\theta^2) m_A^2 - 3 s_{2\theta} m_t A_t + (1+c_\theta^2)(s_\beta^2 X_t^2 + c_\beta^2 Y_t^2)\Bigg\} \left[\frac{1}{\epsilon} + \log\left(\frac{Q^2}{{\mu_R^{\alpha_t}}^2}\right)\right],\end{aligned} \tag{D.6.3}$$

$$\begin{aligned}\delta^{\overline{\rm DR},\alpha_t} s_{2\theta}^2 = \frac{h_t^2}{8\pi^2} \frac{s_{2\theta}^2 c_{2\theta}}{m_{\tilde{t}_1}^2 - m_{\tilde{t}_2}^2} \Bigg\{ &\frac{m_{\tilde{t}_1}^2 + m_{\tilde{t}_2}^2}{2} - m_t^2 - 2\mu^2 + 4 c_{2\theta}(m_{\tilde{t}_1}^2 - m_{\tilde{t}_2}^2) + c_\beta^2 m_A^2 \\ &+ m_{\tilde{b}_L}^2 + s_\beta^2 X_t^2 + c_\beta^2 Y_t^2 + 6 \frac{c_{2\theta}}{s_{2\theta}} m_t A_t \Bigg\} \left[\frac{1}{\epsilon} + \log\left(\frac{Q^2}{{\mu_R^{\alpha_t}}^2}\right)\right],\end{aligned} \tag{D.6.4}$$

$$\delta^{\overline{\rm DR},\alpha_t} A_t = \frac{3h_t^2}{8\pi^2} A_t \left[\frac{1}{\epsilon} + \log\left(\frac{Q^2}{{\mu_R^{\alpha_t}}^2}\right)\right], \qquad \delta^{\overline{\rm DR},\alpha_t} v = -\frac{3h_t^2}{32\pi^2} s_\beta^2 v \left[\frac{1}{\epsilon} + \log\left(\frac{Q^2}{{\mu_R^{\alpha_t}}^2}\right)\right], \tag{D.6.5}$$

$$\delta^{\overline{\rm DR},\alpha_t} \beta = -\frac{3h_t^2}{32\pi^2} s_\beta c_\beta \left[\frac{1}{\epsilon} + \log\left(\frac{Q^2}{{\mu_R^{\alpha_t}}^2}\right)\right], \qquad \delta^{\overline{\rm DR},\alpha_t} \mu = \frac{3h_t^2}{32\pi^2} \mu \left[\frac{1}{\epsilon} + \log\left(\frac{Q^2}{{\mu_R^{\alpha_t}}^2}\right)\right]. \tag{D.6.6}$$

Appendix E

The Higgs Sector in the Standard Model

E.1 The Standard Model Higgs Sector at Tree-Level

To discuss the decoupling limit of the MSSM, we want to do a small digression on the SM Higgs sector. The tree-level potential is given by

$$V^{0,\mathrm{SM}}(\phi) = \frac{\lambda}{2}(\phi^\dagger\phi)^2 - \mu^2\phi^\dagger\phi, \qquad \phi = \frac{1}{\sqrt{2}}\begin{pmatrix} 0 \\ v+\eta \end{pmatrix}. \tag{E.1.1}$$

There are two unknown parameters μ and λ. The VEV v is known from the experiments. In order to incorporate EWSB we need $\mu^2 < 0$. Minimizing the potential yields

$$\left.\frac{\partial V^{0,\mathrm{SM}}}{\partial\eta}\right|_{\min} = 0 \quad \Rightarrow \quad \lambda = \frac{2\mu^2}{v^2}. \tag{E.1.2}$$

This means that there is only one unconstrained parameter μ, which is further related to the SM Higgs mass

$$(m_{h,0}^{\mathrm{SM}})^2 = \left.\frac{\partial^2 V^{0,\mathrm{SM}}}{\partial\eta^2}\right|_{\min} = 2\mu^2, \quad \Rightarrow \quad \lambda = \frac{(m_{h,0}^{\mathrm{SM}})^2}{v^2}. \tag{E.1.3}$$

This means that the whole SM Higgs sector at tree-level is determined by the Higgs mass $m_{h,0}^{\mathrm{SM}}$, which is so far the only unmeasured quantity in the SM. The trilinear and quartic Higgs couplings are

$$\lambda_{hhh}^{0,\mathrm{SM}} = \left.\frac{\partial^3 V^{0,\mathrm{SM}}}{\partial\eta^3}\right|_{\min} = 3\frac{(m_{h,0}^{\mathrm{SM}})^2}{v}, \tag{E.1.4}$$

$$\lambda_{hhhh}^{0,\mathrm{SM}} = \left.\frac{\partial^4 V^{0,\mathrm{SM}}}{\partial\eta^4}\right|_{\min} = 3\frac{(m_{h,0}^{\mathrm{SM}})^2}{v^2}. \tag{E.1.5}$$

In the SM loop-corrections to the Higgs sector modify the relation between m_h, λ_{hhh} and λ_{hhhh}. Compared to the MSSM calculating the effective potential up to $\mathcal{O}(\alpha_t)$, $\mathcal{O}(\alpha_t\alpha_s)$ and $\mathcal{O}(\alpha_t^2)$ in the SM is much easier, especially if one can recycle the techniques and tools used in the MSSM.

E.2 The Standard Model Higgs Sector at One-Loop $\mathcal{O}(\alpha_t)$

From Eq. (C.2.54) we know that the one-loop $\mathcal{O}(\alpha_t)$ correction to the effective potential in the SM is only due to top loops

$$\Delta V^{\mathcal{O}(\alpha_t),\mathrm{SM}}(\bar{m}_t^2) = \frac{3}{16\pi^2}(\bar{m}_t^2)^2\left(\frac{1}{\epsilon} - \log\frac{\bar{m}_t^2}{Q^2} + \frac{3}{2}\right). \tag{E.2.1}$$

The only field-dependence is in the top mass. By using $\bar{m}_t^2 \to y_t(v+\eta)/\sqrt{2}$ we can find the one-loop-corrected Higgs mass and self-coupling by taking derivatives with respect to η. Note also that the top-Yukawa coupling in the SM y_t is related to the top-Yukawa coupling in the MSSM h_t by $h_t = y_t \sin\beta$. The minimization condition at one-loop level yields

$$\left.\frac{\partial V^{\mathcal{O}(\alpha_t),\mathrm{SM}}}{\partial\eta}\right|_{\min} \equiv \left.\frac{\partial V^{0,\mathrm{SM}}}{\partial\eta}\right|_{\min} + \left.\frac{\partial \Delta V^{\mathcal{O}(\alpha_t),\mathrm{SM}}}{\partial\eta}\right|_{\min} = 0, \tag{E.2.2}$$

$$\Rightarrow \quad 0 = \frac{1}{4}\lambda v^3 - \mu^2 v + \frac{3}{16\pi^2}y_t^4 v^3\left(\frac{1}{\epsilon} - \log\frac{m_t^2}{Q^2} + 1\right). \tag{E.2.3}$$

Using this constraint for the one-loop-corrected Higgs mass, we can eliminate μ to get

$$\left(m^{SM}_{h,\mathcal{O}(\alpha_t)}\right)^2 = \left.\frac{\partial^2 V^{\mathcal{O}(\alpha_t),\mathrm{SM}}}{\partial\eta^2}\right|_{\min} = 2\mu^2 - \frac{3}{8\pi^2}y_t^4 v^2 = \left(m^{\mathrm{SM}}_{h,0}\right)^2 + \left(\Delta m^{\mathrm{SM}}_{h,\mathcal{O}(\alpha_t)}\right)^2. \tag{E.2.4}$$

This means that also in the SM the Higgs boson gets a mass correction that goes like m_t^4. Moreover, we can in the same manner calculate the one-loop-corrected trilinear and quartic Higgs couplings

$$\lambda^{\mathcal{O}(\alpha_t),\mathrm{SM}}_{hhh} = \left.\frac{\partial^3 V^{\mathcal{O}(\alpha_t),\mathrm{SM}}}{\partial\eta\partial\eta\partial\eta}\right|_{\min} = \frac{3\left(m^{\mathrm{SM}}_{h,\mathcal{O}(\alpha_t)}\right)^2}{v} - \frac{3}{\pi^2 v^3}m_t^4, \tag{E.2.5}$$

$$\lambda^{\mathcal{O}(\alpha_t),\mathrm{SM}}_{hhhh,1} = \left.\frac{\partial^4 V^{\mathcal{O}(\alpha_t),\mathrm{SM}}}{\partial\eta\partial\eta\partial\eta\partial\eta}\right|_{\min} = \frac{3\left(m^{\mathrm{SM}}_{h,\mathcal{O}(\alpha_t)}\right)^2}{v^2} - \frac{12}{\pi^2 v^4}m_t^4. \tag{E.2.6}$$

Appendix F

Analytical Results

F.1 $\mathcal{O}(\epsilon)$-Terms for Trilinear Couplings at $\mathcal{O}(\alpha_t)$

In the following we list the $\mathcal{O}(\epsilon)$-terms for the trilinear Couplings at $\mathcal{O}(\alpha_t)$ which are used to calculate the WFR counter terms for the self-couplings at $\mathcal{O}(\alpha_t^2)$, see Eq. (2.5.49 - 2.5.58)

$$\begin{aligned}\Delta\lambda_{hhh}^{\mathcal{O}(\alpha_t)}|_{\mathcal{O}(\epsilon)} = \frac{3c_\alpha^3}{16\pi^2 v_2^3} m_t^3 \Bigg\{ & 12\frac{c_{2\theta}^2 W_t^3 s_{2\theta}}{m_{\tilde{t}_1}^2 - m_{\tilde{t}_2}^2} + 4m_t\left(4 + 3\log\frac{m_t^2}{Q^2}\right)\log\frac{m_t^2}{Q^2} \\ & + \Bigg[\frac{1}{m_{\tilde{t}_1}^2}\left(- W_t^3 s_{2\theta}^3 - 12W_t^3 s_{2\theta} c_{2\theta}^2 \frac{m_{\tilde{t}_1}^4}{(m_{\tilde{t}_1}^2 - m_{\tilde{t}_2}^2)^2} - 6m_t W_t^2 s_{2\theta}^2 - 12m_t^2 W_t s_{2\theta} - 8m_t^3\right)\log\frac{m_{\tilde{t}_1}^2}{Q^2} \\ & + \left(- 3W_t s_{2\theta} + 3W_t^3 c_{2\theta}^2 s_{2\theta}\frac{m_{\tilde{t}_1}^2 + m_{\tilde{t}_2}^2}{(m_{\tilde{t}_1}^2 - m_{\tilde{t}_2}^2)^2} - 6m_t - \frac{6m_t W_t^2 c_{2\theta}^2}{m_{\tilde{t}_1}^2 - m_{\tilde{t}_2}^2}\right)\log^2\frac{m_{\tilde{t}_1}^2}{Q^2} \\ & + \left(m_{\tilde{t}_1}^2 \leftrightarrow m_{\tilde{t}_2}^2, s_{2\theta} \to -s_{2\theta}\right)\Bigg]\Bigg\}, \end{aligned} \tag{F.1.1}$$

$$\begin{aligned}\Delta\lambda_{HHH}^{\mathcal{O}(\alpha_t)}|_{\mathcal{O}(\epsilon)} = \frac{3s_\alpha^3}{16\pi^2 v_2^3} m_t^3 \Bigg\{ & 12c_{2\theta}^2 s_{2\theta}\frac{Z_t^3}{m_{\tilde{t}_1}^2 - m_{\tilde{t}_2}^2} + 4m_t\left(4 + 3\log\frac{m_t^2}{Q^2}\right)\log\frac{m_t^2}{Q^2} \\ & + \Bigg[\frac{1}{m_{\tilde{t}_1}^2}\left(- Z_t^3 s_{2\theta}^3 - 12Z_t^3 s_{2\theta} c_{2\theta}^2 \frac{m_{\tilde{t}_1}^4}{(m_{\tilde{t}_1}^2 - m_{\tilde{t}_2}^2)^2} - 6m_t Z_t^2 s_{2\theta}^2 - 12m_t^2 Z_t s_{2\theta} - 8m_t^3\right)\log\frac{m_{\tilde{t}_1}^2}{Q^2} \\ & + \left(- 3Z_t s_{2\theta} + 3Z_t^3 c_{2\theta}^2 s_{2\theta}\frac{m_{\tilde{t}_1}^2 + m_{\tilde{t}_2}^2}{(m_{\tilde{t}_1}^2 - m_{\tilde{t}_2}^2)^2} - 6m_t - \frac{6m_t Z_t^2 c_{2\theta}^2}{m_{\tilde{t}_1}^2 - m_{\tilde{t}_2}^2}\right)\log^2\frac{m_{\tilde{t}_1}^2}{Q^2} \\ & + \left(m_{\tilde{t}_1}^2 \leftrightarrow m_{\tilde{t}_2}^2, s_{2\theta} \to -s_{2\theta}\right)\Bigg]\Bigg\}, \end{aligned} \tag{F.1.2}$$

$$\Delta\lambda_{hhH}^{\mathcal{O}(\alpha_t)}|_{\mathcal{O}(\epsilon)} = \frac{3c_\alpha^2 s_\alpha}{16\pi^2 v_2^3} m_t^3 \Bigg\{ 12 c_{2\theta}^2 s_{2\theta} \frac{W_t^2 Z_t}{m_{\tilde{t}_1}^2 - m_{\tilde{t}_2}^2} + 4 m_t \left(4 + 3\log\frac{m_t^2}{Q^2}\right)\log\frac{m_t^2}{Q^2}$$
$$+ \Bigg[\Bigg(-2W_t s_{2\theta} - s_{2\theta} Z_t + 3 W_t^2 Z_t c_{2\theta}^2 s_{2\theta} \frac{m_{\tilde{t}_1}^2 + m_{\tilde{t}_2}^2}{(m_{\tilde{t}_1}^2 - m_{\tilde{t}_2}^2)^2} - 6m_t - 2\frac{m_t c_{2\theta}^2 W_t}{m_{\tilde{t}_1}^2 - m_{\tilde{t}_2}^2}(W_t + 2Z_t) \Bigg) \log^2\frac{m_{\tilde{t}_1}^2}{Q^2}$$
$$+ \frac{1}{m_{\tilde{t}_1}^2} \Bigg(- Z_t W_t^2 s_{2\theta}^3 - 12 Z_t W_t^2 s_{2\theta} c_{2\theta}^2 \frac{m_{\tilde{t}_1}^4}{(m_{\tilde{t}_1}^2 - m_{\tilde{t}_2}^2)^2} - 2W_t m_t s_{2\theta}^2 (W_t + 2Z_t)$$
$$- 4 m_t^2 s_{2\theta}(2W_t + Z_t) - 8 m_t^3 \Bigg) \log\frac{m_{\tilde{t}_1}^2}{Q^2} + \left(m_{\tilde{t}_1}^2 \leftrightarrow m_{\tilde{t}_2}^2, s_{2\theta} \to -s_{2\theta}\right) \Bigg] \Bigg\}, \tag{F.1.3}$$

$$\Delta\lambda_{hHH}^{\mathcal{O}(\alpha_t)}|_{\mathcal{O}(\epsilon)} = \frac{3s_\alpha^2 c_\alpha}{16\pi^2 v_2^3} m_t^3 \Bigg\{ 12 c_{2\theta}^2 s_{2\theta} \frac{W_t Z_t^2}{m_{\tilde{t}_1}^2 - m_{\tilde{t}_2}^2} + 4 m_t \left(4 + 3\log\frac{m_t^2}{Q^2}\right)\log\frac{m_t^2}{Q^2}$$
$$+ \Bigg[\Bigg(- W_t s_{2\theta} - 2Z_t s_{2\theta} + 3 Z_t^2 W_t c_{2\theta}^2 s_{2\theta} \frac{m_{\tilde{t}_1}^2 + m_{\tilde{t}_2}^2}{(m_{\tilde{t}_1}^2 - m_{\tilde{t}_2}^2)^2} - 6m_t - 2\frac{m_t c_{2\theta}^2 Z_t}{m_{\tilde{t}_1}^2 - m_{\tilde{t}_2}^2}(2W_t + Z_t) \Bigg) \log^2\frac{m_{\tilde{t}_1}^2}{Q^2}$$
$$+ \frac{1}{m_{\tilde{t}_1}^2} \Bigg(- Z_t^2 W_t s_{2\theta}^3 - 12 Z_t^2 W_t s_{2\theta} c_{2\theta}^2 \frac{m_{\tilde{t}_1}^4}{(m_{\tilde{t}_1}^2 - m_{\tilde{t}_2}^2)^2} - 2m_t Z_t s_{2\theta}^2 (2W_t + Z_t)$$
$$- 4 m_t^2 s_{2\theta}(W_t + 2Z_t) - 8 m_t^3 \Bigg) \log\frac{m_{\tilde{t}_1}^2}{Q^2} + \left(m_{\tilde{t}_1}^2 \leftrightarrow m_{\tilde{t}_2}^2, s_{2\theta} \to -s_{2\theta}\right) \Bigg] \Bigg\}, \tag{F.1.4}$$

$$\Delta\lambda_{hAA}^{\mathcal{O}(\alpha_t)}|_{\mathcal{O}(\epsilon)} = \frac{3c_\alpha c_\beta^2}{16\pi^2 v_2^3} m_t^3 \Bigg\{ 4 W_t s_{2\theta} \frac{Y_t^2}{m_{\tilde{t}_1}^2 - m_{\tilde{t}_2}^2} + 4 m_t \log^2\frac{m_t^2}{Q^2}$$
$$+ \Bigg[\Bigg(- W_t s_{2\theta} + Y_t^2 W_t s_{2\theta} \frac{m_{\tilde{t}_1}^2 + m_{\tilde{t}_2}^2}{(m_{\tilde{t}_1}^2 - m_{\tilde{t}_2}^2)^2} - 2m_t - \frac{2m_t Y_t^2}{m_{\tilde{t}_1}^2 - m_{\tilde{t}_2}^2} \Bigg) \log^2\frac{m_{\tilde{t}_1}^2}{Q^2}$$
$$- 4 s_{2\theta} \frac{Y_t^2 W_t m_{\tilde{t}_1}^2}{(m_{\tilde{t}_1}^2 - m_{\tilde{t}_2}^2)^2} \log\frac{m_{\tilde{t}_1}^2}{Q^2} + \left(m_{\tilde{t}_1}^2 \leftrightarrow m_{\tilde{t}_2}^2, s_{2\theta} \to -s_{2\theta}\right) \Bigg] \Bigg\}, \tag{F.1.5}$$

$$\Delta\lambda_{HAA}^{\mathcal{O}(\alpha_t)}|_{\mathcal{O}(\epsilon)} = \frac{3c_\beta^2 s_\alpha}{16\pi^2 v_2^3} m_t^3 \Bigg\{ 4 s_{2\theta} \frac{Y_t^2 Z_t}{m_{\tilde{t}_1}^2 - m_{\tilde{t}_2}^2} + 4 m_t \log^2\frac{m_t^2}{Q^2}$$
$$+ \Bigg[\Bigg(- Z_t s_{2\theta} + Y_t^2 Z_t s_{2\theta} \frac{m_{\tilde{t}_1}^2 + m_{\tilde{t}_2}^2}{(m_{\tilde{t}_1}^2 - m_{\tilde{t}_2}^2)^2} - 2m_t - \frac{2m_t Y_t^2}{(m_{\tilde{t}_1}^2 - m_{\tilde{t}_2}^2)} \Bigg) \log^2\frac{m_{\tilde{t}_1}^2}{Q^2}$$
$$- 4 s_{2\theta} \frac{m_{\tilde{t}_1}^2 Y_t^2 Z_t}{(m_{\tilde{t}_1}^2 - m_{\tilde{t}_2}^2)^2} \log\frac{m_{\tilde{t}_1}^2}{Q^2} + \left(m_{\tilde{t}_1}^2 \leftrightarrow m_{\tilde{t}_2}^2, s_{2\theta} \to -s_{2\theta}\right) \Bigg] \Bigg\}, \tag{F.1.6}$$

$$\Delta\lambda_{hAG}^{\mathcal{O}(\alpha_t)}|_{\mathcal{O}(\epsilon)} = \frac{3s_\beta c_\beta c_\alpha}{16\pi^2 v_2^3} m_t^3 \Bigg\{ -4s_{2\theta}\frac{W_t Y_t X_t}{m_{\tilde{t}_1}^2 - m_{\tilde{t}_2}^2} - 4m_t \log^2\frac{m_t^2}{Q^2} + \Bigg[\Bigg(W_t s_{2\theta} - s_{2\theta} Y_t W_t X_t \frac{m_{\tilde{t}_1}^2 + m_{\tilde{t}_2}^2}{(m_{\tilde{t}_1}^2 - m_{\tilde{t}_2}^2)^2} + 2m_t + \frac{2m_t Y_t X_t}{m_{\tilde{t}_1}^2 - m_{\tilde{t}_2}^2}\Bigg)\log^2\frac{m_{\tilde{t}_1}^2}{Q^2} + 4s_{2\theta}\frac{W_t Y_t X_t m_{\tilde{t}_1}^2}{(m_{\tilde{t}_1}^2 - m_{\tilde{t}_2}^2)^2}\log\frac{m_{\tilde{t}_1}^2}{Q^2} + \Big(m_{\tilde{t}_1}^2 \leftrightarrow m_{\tilde{t}_2}^2, s_{2\theta} \to -s_{2\theta}\Big)\Bigg]\Bigg\}, \tag{F.1.7}$$

$$\Delta\lambda_{HAG}^{\mathcal{O}(\alpha_t)}|_{\mathcal{O}(\epsilon)} = \frac{3s_\alpha s_\beta c_\beta}{16\pi^2 v_2^3} m_t^3 \Bigg\{ -4s_{2\theta}\frac{Z_t Y_t X_t}{m_{\tilde{t}_1}^2 - m_{\tilde{t}_2}^2} - 4m_t \log^2\frac{m_t^2}{Q^2} + \Bigg[\Bigg(Z_t s_{2\theta} - Y_t Z_t s_{2\theta} X_t \frac{m_{\tilde{t}_1}^2 + m_{\tilde{t}_2}^2}{(m_{\tilde{t}_1}^2 - m_{\tilde{t}_2}^2)^2} + 2m_t + \frac{2m_t Y_t X_t}{(m_{\tilde{t}_1}^2 - m_{\tilde{t}_2}^2)}\Bigg)\log^2\frac{m_{\tilde{t}_1}^2}{Q^2} + 4s_{2\theta}\frac{Z_t Y_t X_t m_{\tilde{t}_1}^2}{(m_{\tilde{t}_1}^2 - m_{\tilde{t}_2}^2)^2}\log\frac{m_{\tilde{t}_1}^2}{Q^2} + \Big(m_{\tilde{t}_1}^2 \leftrightarrow m_{\tilde{t}_2}^2, s_{2\theta} \to -s_{2\theta}\Big)\Bigg]\Bigg\}, \tag{F.1.8}$$

$$\Delta\lambda_{hGG}^{\mathcal{O}(\alpha_t)}|_{\mathcal{O}(\epsilon)} = \frac{3c_\alpha s_\beta^2}{16\pi^2 v_2^3} m_t^3 \Bigg\{ 4s_{2\theta}\frac{W_t X_t^2}{m_{\tilde{t}_1}^2 - m_{\tilde{t}_2}^2} + 4m_t \log^2\frac{m_t^2}{Q^2} + \Bigg[\Bigg(-W_t s_{2\theta} + s_{2\theta} W_t X_t^2 \frac{m_{\tilde{t}_1}^2 + m_{\tilde{t}_2}^2}{(m_{\tilde{t}_1}^2 - m_{\tilde{t}_2}^2)^2} - 2m_t - \frac{2m_t X_t^2}{m_{\tilde{t}_1}^2 - m_{\tilde{t}_2}^2}\Bigg)\log^2\frac{m_{\tilde{t}_1}^2}{Q^2} - 4s_{2\theta}\frac{W_t X_t^2 m_{\tilde{t}_1}^2}{(m_{\tilde{t}_1}^2 - m_{\tilde{t}_2}^2)^2}\log\frac{m_{\tilde{t}_1}^2}{Q^2} + \Big(m_{\tilde{t}_1}^2 \leftrightarrow m_{\tilde{t}_2}^2, s_{2\theta} \to -s_{2\theta}\Big)\Bigg]\Bigg\}, \tag{F.1.9}$$

$$\Delta\lambda_{HGG}^{\mathcal{O}(\alpha_t)}|_{\mathcal{O}(\epsilon)} = \frac{3s_\alpha s_\beta^2}{16\pi^2 v_2^3} m_t^3 \Bigg\{ 4Z_t s_{2\theta}\frac{X_t^2}{m_{\tilde{t}_1}^2 - m_{\tilde{t}_2}^2} + 4m_t \log^2\frac{m_t^2}{Q^2} + \Bigg[\Bigg(-Z_t s_{2\theta} + s_{2\theta} Z_t X_t^2 \frac{m_{\tilde{t}_1}^2 + m_{\tilde{t}_2}^2}{(m_{\tilde{t}_1}^2 - m_{\tilde{t}_2}^2)^2} - 2m_t - \frac{2m_t X_t^2}{m_{\tilde{t}_1}^2 - m_{\tilde{t}_2}^2})\Bigg)\log^2\frac{m_{\tilde{t}_1}^2}{Q^2} - 4s_{2\theta}\frac{Z_t X_t^2 m_{\tilde{t}_1}^2}{(m_{\tilde{t}_1}^2 - m_{\tilde{t}_2}^2)^2}\log\frac{m_{\tilde{t}_1}^2}{Q^2} + (m_{\tilde{t}_1}^2 \leftrightarrow m_{\tilde{t}_2}^2, s_{2\theta} \to -s_{2\theta})\Bigg]\Bigg\}. \tag{F.1.10}$$

Bibliography

[1] G. Aad *et al.* [ATLAS Collaboration], Phys. Lett. B [arXiv:1207.7214 [hep-ex]];
S. Chatrchyan *et al.* [CMS Collaboration], Phys. Lett. B [arXiv:1207.7235 [hep-ex]].

[2] S. L. Glashow, Nucl. Phys. **22** (1961) 579;
S. Weinberg, Phys. Rev. Lett. **19** (1967) 1264;
A. Salam, in Elementary Particle Theory ed. N. Svaratholm, Amquist and Wiksells, Stockholm (1968), p. 376.

[3] G. 't Hooft, Rev. Mod. Phys. **72** (2000) 333 [Erratum-ibid. **74** (2002) 1343].

[4] P. W. Higgs, Phys. Rev. Lett. **13** (1964) 508;
P. W. Higgs, Phys. Lett. **12** (1964) 132;
P. W. Higgs, Phys. Rev. **145** (1966) 1156.

[5] F. Englert and R. Brout, Phys. Rev. Lett. **13** (1964) 321.

[6] G. S. Guralnik, C. R. Hagen and T. W. B. Kibble, Phys. Rev. Lett. **13** (1964) 585.

[7] C. H. Llewellyn Smith, Phys. Lett. B **46** (1973) 233;
J. M. Cornwall, D. N. Levin and G. Tiktopoulos, Phys. Rev. Lett. **30** (1973) 1268 [Erratum-ibid. **31** (1973) 572];
J. M. Cornwall, D. N. Levin and G. Tiktopoulos, Phys. Rev. D **10** (1974) 1145 [Erratum-ibid. D **11** (1975) 972].

[8] S. R. Coleman and J. Mandula, Phys. Rev. **159** (1967) 1251.

[9] P. Ramond, Phys. Rev. D **3** (1971) 2415;
A. Neveu and J. H. Schwarz, Nucl. Phys. B **31** (1971) 86;
J. -L. Gervais and B. Sakita, Nucl. Phys. B **34** (1971) 632.

[10] Y. .A. Golfand and E. P. Likhtman, JETP Lett. **13** (1971) 323 [Pisma Zh. Eksp. Teor. Fiz. **13** (1971) 452];
D. V. Volkov and V. P. Akulov, Phys. Lett. B **46** (1973) 109.

[11] J. Wess and B. Zumino, Phys. Lett. B **37** (1973) 95;
A. Salam and J. A. Strathdee, Nucl. Phys. B **76** (1974) 477.

[12] R. Haag, J. T. Lopuszanski and M. Sohnius, Nucl. Phys. B **88** (1975) 257.

[13] J. Wess and B. Zumino, Phys. Lett. B **49** (1974) 52;
J. Iliopoulos and B. Zumino, Nucl. Phys. B **76** (1974) 310;
S. Ferrara, J. Iliopoulos and B. Zumino, Nucl. Phys. B **77** (1974) 413;
B. Zumino, Nucl. Phys. B **89** (1975) 535;
M. T. Grisaru, W. Siegel and M. Rocek, Nucl. Phys. B **159** (1979) 429.

[14] P. Fayet, Nucl. Phys. B **90** (1975) 104.
P. Fayet, Phys. Lett. B **64** (1976) 159.
P. Fayet, Phys. Lett. B **69** (1977) 489.
Two of the first reviews on the MSSM are H. E. Haber and G. L. Kane, Phys. Rept. **117** (1985) 75 and H. P. Nilles, Phys. Rept. **110** (1984) 1;
A review on the phenomenology of the MSSM without introducing the superspace formalism is S. P. Martin, In * Kane, G.L. (ed.): Perspectives on supersymmetry II* 1-153 [hep-ph/9709356];
A complete and very modern textbook about the MSSM is M. Drees, R. Godbole and P. Roy, Hackensack, USA: World Scientific (2004) 555 p.

[15] S. L. Adler, Phys. Rev. **177** (1969) 2426;
J. S. Bell and R. Jackiw, Nuovo Cim. A **60** (1969) 47.

[16] V. Tishchenko [MuLan Collaboration], Nucl. Phys. Proc. Suppl. **225-227** (2012) 232.

[17] S. Chatrchyan *et al.* [CMS Collaboration], Phys. Lett. B **713** (2012) 68 [arXiv:1202.4083 [hep-ex]].

[18] S. Schael *et al.* [ALEPH and DELPHI and L3 and OPAL and LEP Working Group for Higgs Boson Searches Collaborations], Eur. Phys. J. C **47** (2006) 547 [hep-ex/0602042].

[19] T. Appelquist and J. Carazzone, Phys. Rev. D **11** (1975) 2856.

[20] J. R. Ellis, G. Ridolfi and F. Zwirner, Phys. Lett. B **257** (1991) 83;
Y. Okada, M. Yamaguchi and T. Yanagida, Prog. Theor. Phys. **85** (1991) 1;
H. E. Haber and R. Hempfling, Phys. Rev. Lett. **66** (1991) 1815.

[21] J. R. Ellis, G. Ridolfi and F. Zwirner, Phys. Lett. B **262** (1991) 477.

[22] A. Brignole, Phys. Lett. B **281** (1992) 284.

[23] P. H. Chankowski, S. Pokorski and J. Rosiek, Nucl. Phys. B **423** (1994) 437 [hep-ph/9303309];
A. Dabelstein, Z. Phys. C **67** (1995) 495 [hep-ph/9409375]; D. M. Pierce, J. A. Bagger, K. T. Matchev and R. -J. Zhang, Nucl. Phys. B **491** (1997) 3 [hep-ph/9606211].

[24] V. D. Barger, M. S. Berger, A. L. Stange and R. J. N. Phillips, Phys. Rev. D **45** (1992) 4128.

[25] R. Barbieri, M. Frigeni and F. Caravaglios, Phys. Lett. B **258** (1991) 167;
Y. Okada, M. Yamaguchi and T. Yanagida, Phys. Lett. B **262** (1991) 54;
J. R. Espinosa and M. Quiros, Phys. Lett. B **266** (1991) 389;
H. E. Haber and R. Hempfling, Phys. Rev. D **48** (1993) 4280 [hep-ph/9307201].

[26] M. S. Carena, J. R. Espinosa, M. Quiros and C. E. M. Wagner, Phys. Lett. B **355** (1995) 209 [hep-ph/9504316];
M. S. Carena, M. Quiros and C. E. M. Wagner, Nucl. Phys. B **461** (1996) 407 [hep-ph/9508343];
H. E. Haber, R. Hempfling and A. H. Hoang, Z. Phys. C **75** (1997) 539 [hep-ph/9609331];
J. R. Espinosa and I. Navarro, Nucl. Phys. B **615** (2001) 82 [hep-ph/0104047].

[27] R. Hempfling and A. H. Hoang, Phys. Lett. B **331** (1994) 99 [hep-ph/9401219].

[28] R. -J. Zhang, Phys. Lett. B **447** (1999) 89 [hep-ph/9808299].

[29] J. R. Espinosa and R. -J. Zhang, JHEP **0003** (2000) 026 [hep-ph/9912236].

[30] J. R. Espinosa and R. -J. Zhang, Nucl. Phys. B **586** (2000) 3 [hep-ph/0003246].

[31] P. Slavich, PhD thesis, UNIVERSITÀ DEGLI STUDI DI PADOVA, DIPARTIMENTO DI FISICA (2001).

[32] G. Degrassi, P. Slavich and F. Zwirner, Nucl. Phys. B **611** (2001) 403 [hep-ph/0105096].

[33] A. Brignole, G. Degrassi, P. Slavich and F. Zwirner, Nucl. Phys. B **631** (2002) 195 [hep-ph/0112177].

[34] S. Heinemeyer, W. Hollik and G. Weiglein, Phys. Rev. D **58** (1998) 091701 [hep-ph/9803277];
S. Heinemeyer, W. Hollik and G. Weiglein, Phys. Lett. B **440** (1998) 296 [hep-ph/9807423];
S. Heinemeyer, W. Hollik and G. Weiglein, Phys. Lett. B **455** (1999) 179 [hep-ph/9903404];
S. Heinemeyer, W. Hollik and G. Weiglein, Comput. Phys. Commun. **124** (2000) 76 [hep-ph/9812320].

[35] S. Heinemeyer, W. Hollik, H. Rzehak and G. Weiglein, Eur. Phys. J. C **39** (2005) 465 [hep-ph/0411114];
A. Dedes, G. Degrassi and P. Slavich, Nucl. Phys. B **672** (2003) 144 [hep-ph/0305127].

[36] B. C. Allanach, A. Djouadi, J. L. Kneur, W. Porod and P. Slavich, JHEP **0409** (2004) 044 [hep-ph/0406166].

[37] S. P. Martin, Phys. Rev. D **66** (2002) 096001 [hep-ph/0206136];
S. P. Martin, Phys. Rev. D **67** (2003) 095012 [hep-ph/0211366].

[38] S. P. Martin, Phys. Rev. D **75** (2007) 055005 [hep-ph/0701051].

[39] P. Kant, R. V. Harlander, L. Mihaila and M. Steinhauser, JHEP **1008** (2010) 104 [arXiv:1005.5709 [hep-ph]].

[40] Y. P. Philippov, Phys. Atom. Nucl. **70** (2007) 1288 [hep-ph/0611260];
M. V. Dolgopolov and Y. P. Philippov, hep-ph/0310018.

[41] A. Dobado, M. J. Herrero, W. Hollik and S. Penaranda, Phys. Rev. D **66** (2002) 095016 [hep-ph/0208014].

[42] F. Boudjema and A. Semenov, Phys. Rev. D **66** (2002) 095007 [hep-ph/0201219].

[43] U. Baur, T. Plehn and D. L. Rainwater, Phys. Rev. Lett. **89** (2002) 151801 [hep-ph/0206024].

[44] A. Djouadi, W. Kilian, M. Muhlleitner and P. M. Zerwas, Eur. Phys. J. C **10** (1999) 27 [hep-ph/9903229].

[45] C. Castanier, P. Gay, P. Lutz and J. Orloff, In *2nd ECFA/DESY Study 1998-2001* 1362-1372 [hep-ex/0101028].

[46] S. R. Coleman and E. J. Weinberg, Phys. Rev. D **7** (1973) 1888.

[47] R. Jackiw, Phys. Rev. D **9** (1974) 1686.

[48] T. P. Cheng and L. F. Li, Oxford, UK: Clarendon (1984) (Oxford Science Publications)

[49] S. Weinberg, Phys. Rev. D **7** (1973) 2887.

[50] A. I. Davydychev and J. B. Tausk, Nucl. Phys. B **397** (1993) 123.

[51] C. Ford, I. Jack and D. R. T. Jones, Nucl. Phys. B **387** (1992) 373 [Erratum-ibid. B **504** (1997) 551] [hep-ph/0111190].

[52] F. Bloch and A. Nordsieck, Phys. Rev. **52** (1937) 54.

[53] T. Kinoshita, J. Math. Phys. **3** (1962) 650;
T. D. Lee and M. Nauenberg, Phys. Rev. **133** (1964) B1549.

[54] G. 't Hooft, Nucl. Phys. B **33** (1971) 173;
G. 't Hooft, Nucl. Phys. B **35** (1971) 167;
G. 't Hooft and M. J. G. Veltman, Nucl. Phys. B **50** (1972) 318.

[55] W. Pauli and F. Villars, Rev. Mod. Phys. **21** (1949) 434.

[56] G. 't Hooft and M. J. G. Veltman, Nucl. Phys. B **44** (1972) 189.

[57] J. C. Ward, Phys. Rev. **78** (1950) 182;
Y. Takahashi, Nuovo Cim. **6** (1957) 371.

[58] A. A. Slavnov, Theor. Math. Phys. **10** (1972) 99 [Teor. Mat. Fiz. **10** (1972) 153];
J. C. Taylor, Nucl. Phys. B **33** (1971) 436.

[59] W. Siegel, Phys. Lett. B **84** (1979) 193;
D. M. Capper, D. R. T. Jones and P. van Nieuwenhuizen, Nucl. Phys. B **167** (1980) 479.

[60] I. Jack, D. R. T. Jones, S. P. Martin, M. T. Vaughn and Y. Yamada, Phys. Rev. D **50** (1994) 5481 [hep-ph/9407291].

[61] D. J. Gross and F. Wilczek, Phys. Rev. Lett. **30** (1973) 1343.
H. D. Politzer, Phys. Rev. Lett. **30** (1973) 1346.

[62] J. Beringer et al. (Particle Data Group), Phys. Rev. D86, 010001 (2012).

[63] K. Nakamura et al. (Particle Data Group), JP G 37, 075021 (2010) and 2011 partial update for the 2012 edition (URL: http://pdg.lbl.gov).

[64] D. B. Chitwood *et al.* [MuLan Collaboration], Phys. Rev. Lett. **99** (2007) 032001 [arXiv:0704.1981 [hep-ex]].

[65] M. S. Carena, S. Heinemeyer, C. E. M. Wagner and G. Weiglein, Eur. Phys. J. C **26** (2003) 601 [hep-ph/0202167].

[66] E. Accomando, G. Chachamis, F. Fugel, M. Spira and M. Walser, Phys. Rev. D **85** (2012) 015004 [arXiv:1103.4283 [hep-ph]].

[67] M. S. Carena, H. E. Haber, S. Heinemeyer, W. Hollik, C. E. M. Wagner and G. Weiglein, Nucl. Phys. B **580** (2000) 29 [hep-ph/0001002].

[68] J. M. Frere, D. R. T. Jones and S. Raby, Nucl. Phys. B **222** (1983) 11.

[69] G. Degrassi and A. Sirlin, Phys. Rev. D **46** (1992) 3104.

[70] H. Eberl, A. Bartl and W. Majerotto, Nucl. Phys. B **472** (1996) 481 [hep-ph/9603206];
W. Beenakker, R. Hopker, T. Plehn and P. M. Zerwas, Z. Phys. C **75** (1997) 349 [hep-ph/9610313].

Acknowledgements

At this point I would like to thank all the people who directly and indirectly contributed to the success of this work.
First of all there is Babis who took care of my affiliation with the official side of the ETH. Through his outstanding teaching back in the days of my Master studies and the supervision of my Master thesis, he played a crucial role in awaking my interests for the field of theoretical particle physics.
I am especially grateful to Michael who accepted me as his Ph.D. student after knowing me for ten minutes. Following his explanations about all sorts of conceptual and technical aspects of high energy physics was always a pleasure for me. His patience and expertise in answering all my questions (even the very silly ones and those that I asked for the third time) impressed meevery time again.
Moreover I would like to thank all the people in the groups of Babis and Aude Gehrmann at the ETH for their company during the last three and a half years. I am especially grateful to Stephan Bühler, Franz Herzog and Gabriel Abelof, not only for helping me with all the minor problems that showed up in the *very* end of my thesis.
My Thursday memories of the time of my Ph.D. will always be connected to my stays at PSI. I am especially grateful to all the people there for the relaxed atmosphere and all the interesting anecdotes during the extended lunch time breaks.
I would also like to thank P. Slavich for giving me access to his Ph.D. thesis. His complete and very correct work laid the basis for my thesis and made my life a lot easier.
Last but not least I would like to thank all the people who supported me privately during this period, especially my girlfriend Claudia, my parents Martin & Brigitte and my brothers Christian, Stefan & Anton.
This Work was supported by the Swiss National Science Foundation (SNSF).

Curriculum Vitae

Personal Data

Name:	Mathias Brucherseifer
Place of birth:	Aachen, Germany
Date of birth:	March 13, 1985
Nationality:	German

Education and Employment

August 2004	Matura at Kantonsschule Wattwil (Switzerland)
September 2004 – September 2007	Bachelor studies in Physics at ETH Zürich
September 2007 – February 2009	Master studies in Physics at ETH Zürich
February 2009	Master of Science ETH in Physics (MSc ETH Physics) Master's thesis supervised by C. Anastasiou Title: *"Gluon fusion in realistic composite Higgs models"*
April 2009 – September 2012	Ph.D. studies at ETH Zürich and PSI Villigen supervised by C. Anastasiou and M. Spira Topic: *"Two-loop corrections to Higgs self-couplings in the MSSM"*